



HAL
open science

Chemical and microbial effects of macroalgae on coral holobionts and reef ecosystems

Chloé Pozas-Schacre

► **To cite this version:**

Chloé Pozas-Schacre. Chemical and microbial effects of macroalgae on coral holobionts and reef ecosystems. Ecology, environment. Université Paris sciences et lettres, 2024. English. NNT : 2024UP-SLP015 . tel-04679900

HAL Id: tel-04679900

<https://theses.hal.science/tel-04679900v1>

Submitted on 28 Aug 2024

HAL is a multi-disciplinary open access archive for the deposit and dissemination of scientific research documents, whether they are published or not. The documents may come from teaching and research institutions in France or abroad, or from public or private research centers.

L'archive ouverte pluridisciplinaire **HAL**, est destinée au dépôt et à la diffusion de documents scientifiques de niveau recherche, publiés ou non, émanant des établissements d'enseignement et de recherche français ou étrangers, des laboratoires publics ou privés.



THÈSE DE DOCTORAT

DE L'UNIVERSITÉ PSL

Préparée à l'École Pratique des Hautes Études

Effets chimiques et microbiens des macroalgues sur les holobiontes et écosystèmes coralliens

Chemical and microbial effects of macroalgae on coral holobionts and reef ecosystems

Soutenue par

Chloé Pozas-Schacre

Le 12 avril 2024

École doctorale n° 472

**École doctorale de l'École
Pratique des Hautes Études**

Spécialité

**Connaissance et gestion des
milieux coralliens littoraux et
océaniques**

Composition du jury :

Valeriano PARRAVICINI

Directeur d'Études, EPHE

Président

Maren ZIEGLER

Prof., Justus Liebig University Giessen

Rapporteuse

Andreas HAAS

Senior Scientist, Royal Netherlands Institute of Sea Research

Rapporteur

Miriam REVERTER

Lecturer, University of Plymouth

Examinatrice

Valérie STIGER

Pr., Université de Bretagne Occidentale

Examinatrice

Maggy NUGUES

Maître de conférences - HDR, EPHE

Directrice de thèse



It's not the Destination, it's the journey –
Ralph Waldo Emerson

Acknowledgments

First, I would like to express my gratitude to Maren Ziegler, Andreas Haas, Valérie Stiger, Miriam Reverter and Valeriano Parravicini for agreeing to evaluate my work. I know more than ever how busy research can be and how time is precious.

This PhD would not have been possible without the great support and engagement of my supervisor Maggy Nugues. I am sincerely grateful for the opportunity you gave me to work on a subject that meant a lot to me. You trusted my abilities even though I had never worked with metabarcoding and metabolomics data before. Thank you so much for your availability, encouragements and thorough guidance throughout this PhD journey.

I also want to extend my deepest gratitude to my collaborators. Isabelle Bonnard, Delphine Raviglione and Slimane Chaib, have been amazing in introducing metabolomics to the newbie I was. Isa and Delphine, thank you so much for your commitment to my research. I remember us staying late at the lab to prepare the injection sequences and ensure everything was right for the run; it meant a lot. Slimane, thank you for all your help on MZmine and molecular networking, it has been so valuable. Camille Clérissi, thank you very much for your help throughout my PhD from protocols to analysis and writings. You all have been an essential part in the scientific development of this work. Many thanks for your time, patience and expertise, it has been great to work with you all. I also would like to thank Valeriano, as you did a play a role in this PhD, indirect but significant. By accepting me in your team as an intern back in 2019, you offered me the chance to be part of the CRIOBE. Working in your team, where kindness and support prevailed, confirmed my decision to return to academia.

Research is definitely one of the best examples that “Alone we can do so little, together we can do so much – Helen Keller”. I cannot say how much grateful I am for the help I got from so many people during my field work. Although my dives could be laborious, I always had people offering their help by simple altruism. Thank you, Hugo Bischoff, Alexandre Mercière, Pierrick Harnay, Kim Eustache, Jules Schligler, Yann Lacube, Mathieu Reynaud, Camille Gache and Camille Vizon. I also thank all the staff from the CRIOBE in Mo’orea for their support, Yannick Chancerelle, Marie-Christine Michelle, Gilles Siu, Pascal Ung, Benoit Espiau, Anne Haguenaur, Frederic Zuberer, Frank Lerouvreur and Elina Burns. In Perpignan, I am so thankful for Fabien Morat, Nathalie Toulou, Emilie Boissin, Aurélie Mariotti and Edouard Jobet for their kindness and for their encouragements up until the very end of this PhD. I also want to thank Peter Esteve for allowing me to pop up in his office for my tech issues, always available and kind, despite how busy he was.

Every destination is marked by new friendships and this PhD adventure was no exception. Alex, Mo’orea would not have been the same without our acroyoga and kitesurf sessions, thank you for your friendship, kindness and constant support. A special mention to Pierrick, Camille. G and Yann for the barbecues and the “Coinche” parties, damn I miss those late card games by the ocean. I am also immensely thankful for Caroline Dubé—thank you for bringing my DNA samples to sequencing, for your time and mentorship, it meant a lot. Marie-

Céline Piednoir, you have been such a good friend, I still miss our sunset yoga classes. To all my CRIOBE lab-mates from Mo'orea and Perpignan for the moments shared at the lab and outside, Hugo Bishoff, Jules Schligler, Mathieu Reynaud, Gonzalo Perez-Rosales, Jason Vii, Aurélie Aqua, Jessica Tran, Laura-Li Jannot, Valentin Teillard, Claire Peyran, Clara Mouronvalle, Gaëlle Quéré, Mathieu Adgé, Charles Loiseau, Céline Tardy, Titouan Morage, Thomas Guttierrez, Hendrickje Jorissen, Zoé Delecambre, Camille V., Camille Léonard, Jeremy Carlot, Nina Schiettekatte, and Jeremy Wicquart. A special thanks to my dear friends, Kim Eustache and Irene Salinas-Akhmadeeva, who have always been here. You were the best emotional support and outdoor buddies. It was so nice to have you all around and you all have been essential in maintaining a healthy life, thank you.

Finally, I am immensely grateful to my family and friends, who have always encouraged me in every way possible and who have always been here despite the distance. Annabelle, Barbara, Morgan, Rémy, Richard, Thomas and Mathieu, seeing you on the weekends when I was heading back to Toulouse meant so much every time. Of course, a special thanks to my Mum, Catherine, for her unconditional love and understanding. You have always supported my endeavors and never doubted my choice in this carrier path. You were a constant source of strength and love that helped me to successfully complete this thesis. A few words for my feline and canine buddies, Paco, Harry, Fiji, James, Corail, Cannelle, Prana, Jodie and Tuki, as their presence always filled my heart with comfort and happiness.

I acknowledge the scholarship and funding that supported this PhD research: the Ecole Pratique des Hautes Etudes (EPHE) and the Agence National pour la Recherche (ANR).

Long live the corals

Table of Contents

Chapter 1. Introduction and thesis outline	15
1. Coral reef ecosystems and their threats.....	17
2. Coral-macroalgal phase-shifts.....	19
3. The main competitors: corals vs. algae	21
3.1. Coral holobionts and recruitment process	21
3.1.1. Corals and their microbial symbionts.....	21
3.1.2. Microbiome of early coral life stages.....	24
3.2. Macroalgae: their ecological success	26
4. Coral-algal competition: chemical and microbial effects.....	29
4.1. Contact-mediated mechanisms.....	29
4.2. Water-mediated mechanisms	30
4.3. Rupture of coral recruitment success by macroalgae.....	33
5. PhD overview.....	35
5.1. Lagoons of Mo’orea: a case study.....	35
5.2. Reef “omics”, the new paradigm in reef ecology.....	37
5.3. Thesis aims and chapter outlines.....	39
Chapter 2. Invasive macroalgae shape chemical and microbial waterscapes on coral reefs.....	41
Abstract	42
1. Introduction	43
2. Result.....	45
2.1. Experimental design and benthic community composition	45
2.2. Microbial and chemical diversity of reef waters	46
2.3. Compositional differences among reef water microbiomes and metabolomes.....	47
2.4. Dominant microbial taxa across boundary layers and algal treatments	48
2.5. Diffusion pattern of macroalgal metabolites across boundary layers	51
2.6. Broad molecular classification of diffusing algal-derived metabolites.....	53
2.7. Co-variation of algal-associated metabolites and microorganisms.....	57
3. Discussion	58
4. Materials and Methods overview	65
5. Supplementary Information.....	67
5.1. Supplementary Methods.....	67
5.2. Supplementary Figures.....	78
5.3. Supplementary Tables	90
Chapter 3. Negative parental and environmental effects of macroalgae on coral recruitment are linked with alterations in the coral larval microbiome.....	99
Abstract	100
1. Introduction	101
2. Materials and methods	103
2.1. Experimental field set-up	103

2.2. Benthic surveys	104
2.3. Microbiome sampling	105
2.4. Sequencing of the 16S rRNA gene and metabarcoding data processing	105
2.5. Coral recruitment experiments	106
2.6. Statistical analysis	107
2.6.1. Benthos data	107
2.6.2. Microbiome data	108
2.6.3. Coral recruitment experiment data	109
3. Results	109
3.1. Benthic community composition	109
3.2. Coral microbiome composition	110
3.3. Substrate microbiome composition	112
3.4. Differential abundance analysis of ASVs between algal treatments	112
3.5. Coral recruitment experiments	114
4. Discussion	116
5. Conclusion.....	120
6. Supplementary Information.....	122
6.1. Supplementary Figures.....	122
6.2. Supplementary Tables	132
Chapter 4. Contact- and water-mediated interactions with an allelopathic macroalga affect the coral microbiome and metabolome.....	141
Abstract	142
1. Introduction	143
2. Results	145
2.1. Visual assessment of coral health.....	145
2.2. Variation in coral and CSW microbiome and metabolome composition across interaction types	145
2.3. Changes in specific microbial taxa relative to control	148
2.4. Changes in specific molecular classes relative to control	150
2.5. Identifying correlation between microbes and metabolites within the coral holobiont	152
2.6. Metabolites stoichiometry and energetics	153
3. Discussion	154
4. Materials and Methods	159
4.1. Experimental design.....	159
4.2. Sampling.....	159
4.3. 16S rDNA gene sequencing and metabarcoding data acquisition.....	160
4.4. Metabolites recovery and mass spectrometry analysis	161
4.5. Metabolomic data acquisition	162
4.6. Statistical analysis	163
5. Supplementary Information.....	165
5.1. Supplementary Methods.....	165
5.2. Supplementary Figures.....	170
5.3. Supplementary Tables	180

Chapter 5. General discussion and research perspectives	189
1. Summary of main results.....	191
2. Understanding water-mediated interactions through hydrodynamics.....	193
3. Ecological relevance of water-mediated competition	196
4. From “who is there?” to “what are they doing?”	199
4.1. Notable microbes and metabolites patterns.....	199
4.2. Linking patterns to mechanisms through experimental and multiomic research....	201
5. Perspectives on future macroalgal-dominated reefs.....	204
6. Conclusion.....	206
References	207
Résumé substantiel (French)	255
Substantial abstract.....	261
Appendices	267
Appendix 1: Manuscript “Congruent trophic pathways underpin global coral reef food webs”	267
Appendix 2: Manuscript « Delineating reef fish trophic guilds with global gut content data synthesis and phylogeny”	268
Appendix 3: Manuscript « Compounded effects of sea urchin grazing and physical disturbance on macroalgal canopies in the lagoon of Moorea, French Polynesia”.....	269
Appendix 4: Scientific vulgarization on the chemical and microbial effects of macroalgae on coral recruitment (text in French).....	270

List of Figures

Figure 1.1 | Conceptual diagram of forces leading to alternative ecological states on coral reefs. Coral- (bottom-left) and macroalgal-dominated states (bottom-right) are two alternative stable states. After large disturbances causing massive coral loss (i.e., destabilizing feedback processes), healthy coral reefs have good chance to recover (i.e., staying in their “coral valley”). The coral ball may shift in the “algal valley” if pulse disturbances (e.g., cyclones) are much greater or if the resilience of the system has been eroded, for example if overfishing exceed a certain threshold (i.e., lowering the ridge between the two valleys). The macroalgal-dominated state may be a persistent basin of attraction locking the system into its new state due to strong reinforcing feedback processes (algal valley lower than the coral valley)..... 21

Figure 1.2 | Model of the coral holobiont, comprising the coral host, its obligate algal symbionts (Symbiodiniaceae) and diverse other microorganisms such as Bacteria, Archaea, viruses, fungi and other protists. All members interact together to sustain holobiont health and homeostasis. From Peixoto et al., 2021 23

Figure 1.3 | Coral recruitment and bacterial acquisition across life stages. Recruitment is a process involving a pelagic and a benthic phase connected by the key step of larval settlement and metamorphosis. Broadcast spawners release eggs bundles and sperm in the water column surrounded by bacteria-rich mucus. Mucus bacteria can be primed by the parents or acquired rapidly after larval release in the water column. Brooders directly transmit bacteria to their offspring (i.e., vertical transmission) and release fully developed larvae. Bacteria uptake occurs via the environment at all life stages (i.e., horizontal transmission). Adapted from van Oppen & Blackall, 2019..... 25

Figure 1.4 | Model of reef waterscapes. (A) Waterscapes are the combination of three boundary layers whose thickness and composition vary with the distance from the benthos. Inspired by Barott & Rowher, 2012. (B) Summary of the in-situ studies investigating their microbial and chemical composition..... 32

Figure 1.5 | Map of Mo'orea, island of French Polynesia. Field experiments were conducted in a fringing reef on the north coast. Map acquired with the help of Charles Loiseau 36

Figure 1.6 | Untargeted metabolomics and metabarcoding workflows in this PhD. (A) Metabolomic profiles were acquired by LC-MS/MS on an Orbitrap Q-Exactive in positive and negative ionization modes. MS data were analyzed in MZmine. Feature tables were uploaded in the GNPS platform for construction of Feature-Based Molecular Networks (FBMN), library searches and molecular classification with the MolNetEnhancer extended workflow. Compounds were annotated from SIRIUS putative molecular formulas and manual library searches. (B) Metabarcoding consisted in 16S rDNA gene sequencing on an Illumina NovaSeq platform. Sequencing data were processed using the DADA2 for ASV inference (amplicon sequence variant) and genus-level assignation (Silva database). (C) For multiomic analysis, data were integrated with DIABLO algorithm (mixOmics R package). Statistical analysis were conducted on R and networks were visualized on Cytoscape. Logos were obtained from the official websites and icons from the BioRender website. Inspired by Mannocho-Russo et al., 2023. 39

Figure 2.1 | Multiomic composition of reef boundary layers. Score plots of the multi-block PLS-DA (DIABLO) performed on metabarcoding and metabolomic data between (A) benthic boundary layers, (B) momentum boundary layers, (C) algal-removed waters and (D) algal-dominated waters. Analyses were validated by a permutation test based on cross-model validation, the CER represents the proportion of misclassification and a $P < 0.05$ indicates that the clustering was not obtained by chance alone. Ellipses are 95% data ellipses. Reef water types are abbreviated and colored as in the experimental design figure (Fig. S2). Individual PLS-DA are shown in Fig. S5. 48

Figure 2.2 | Reef waters-associated discriminant microbial taxa. Benthic boundary layers (BBL) were collected above algal-dominated and algal-removed bommies. Momentum boundary layers (MBL) were associated to algal-removed substrate or above macro-algal species: *Dictyota bartayresiana* and *Turbinaria ornata*. Microbial ASVs are at the genus-level and labeled at the family and genus level when possible or at the lowest level achievable (e.g., order, phylum). ASVs are colored according to their microbial class and clustered according their mean CLR transformed abundances across the five water types using Euclidian distances and Ward's minimum variance method. Data was scaled by mean-centering and dividing by the standard deviation. 50

Figure 2.3 | Analysis of algal metabolites diffusion into the water column for (i) *Dictyota bartayresiana* and (ii) *Turbinaria ornata*. (A) PLS-DA score plots of MS1 features with ESI+ MS/MS fragmentation spectra ($n = 2214$ features) showing metabolomic profiles clustered according to algal whole tissues, surfaces, MBLs and BBL. Metabolites relative peak areas were CLR-transformed and mean-centered. CER and associated p-values were obtained by cross-model validation and permutation tests. Ellipses are 95% data ellipses. (B) Venn diagrams of MS1 features in whole tissues, surfaces and MBLs of *Dictyota* ($n = 3444$) and *Turbinaria* ($n = 3224$) and algal-dominated BBL ($n = 1661$). (C) Mean (\pm standard error) retention time in minutes using UHPLC reverse phase column of MS1 features. Lettering indicates significantly difference using Dunn test's posthoc, $P < 0.05$) 52

Figure 2.4 | Molecular classification of subnetworks with discriminant features found in the algal metabolomes and associated waters. (A) Molecular network of all MS1 features (nodes) with MS/MS fragmentation linked by a cosine score > 0.7 (edges). Nodes are colored by the sample type in which their relative abundance was the highest. Examples of subnetworks of interest with discriminant features found in whole tissue & surface samples and boundary layers (BBL – benthic & MBL – momentum) of the two algal species *Dictyota bartayresiana* and *Turbinaria ornata* are boxed 1 to 8. (B) Boxed subnetworks details in which nodes are colored by their mean relative intensities (i.e., peak areas) in each sample type. (C) Mean of summed features relative intensities of subnetworks of interest across sample types according to their consensus Classyfire ontology derived from MolNetEnhancer (GNPS) and CANOPUS (SIRIUS)..... 56

Figure 2.5 | Co-variation of discriminant microbial ASV and molecular features in algal momentum boundary layers. Bipartite correlation network obtained from DIABLO analysis and visualized on Cytoscape. A correlation threshold was set to 0.7 resulting in three clusters A, B and C. Nodes are contoured according to their type (i.e., ASVs in purple and metabolites in grey) and colored by their mean relative intensities (i.e., peak areas) in the MBL of *Dictyota bartayresiana* and *Turbinaria ornata*. 58

Figure 3.1 | Microbiome diversity and composition. Alpha diversity of (a) coral adults and larvae and of (b) cryptic and exposed surfaces from algal-removed and algal-dominated bommies. Effects of coral life stage/surface and algal treatment on diversity were tested using linear mixed effect models with details in the electronic supplementary material, table S2. Beta diversity of (c) coral adults and larvae and (d) cryptic and exposed surfaces from algal-removed and algal-dominated bommies. Variations of microbiome composition were tested by PERMANOVA (nperm = 999). PCA were run on CLR-transformed ASV abundances with Euclidian distances. Ellipses correspond to 95% data ellipses. Top 20 most abundant microbial families across (e) coral adults and larvae and (f) cryptic and exposed surfaces from algal-removed and algal-dominated bommies. 111

Figure 3.2 | Microbial ASVs associated with algal removal treatment (a) Random Forest accuracy for classifying samples relative to the algal-removal treatment. Significantly differentially abundant ASVs (ANCOMBC, p.adj < 0.05) between algal-dominated vs algal-removed bommies within (b) coral adult and larvae samples and (c) exposed and cryptic surfaces. Fold changes were calculated relative to the mean changes in the algal-removed treatment. For the surface microbiomes, only ASVs with a log-fold change > 2 or < -2 are included. ASVs are grouped by family, genus and class..... 114

Figure 3.3 | Coral recruitment experiments. (a) Survival (mean ± se, n = 12) of larvae brooded by corals from algal-removed and algal-dominated bommies after 6 days in seawater from each algal treatment. (b) Settlement (mean ± se, n = 12) of larvae brooded by corals from algal-removed and algal-dominated bommies on tiles from algal-removed and algal-dominated bommies after 24h. (c) Post-settlement survival (mean ± se, n = 12) of coral settlers produced by corals from algal-removed and algal-dominated bommies 7 and 21 days after out-planting on algal-removed and algal-dominated bommies. Statistical significance was assessed with GLME using binomial distribution, detailed results can be found in electronic supplementary material, table S8..... 115

Figure 4.1 | Diversity patterns of coral and near-surface coral seawater (CSW) microbial communities and metabolomes. Richness (Shannon diversity index) of **a.** microbiome and **c.** metabolome (MS1 chemical features) as well as beta dispersion (within-group variability) of **b.** microbiome and **d.** metabolome. Differences were assessed between interaction type (i.e., Int; contact vs close proximity vs control), sampling location (i.e., Loc; apex vs. side fragments) and colony position (i.e., Pos; up vs. downstream). Statistical significance was determined by ANOVA on coral and coral seawater samples, respectively. Only fixed effects are shown here. Interaction effects were not significant and detailed results can be found in Supplementary Tables 2, 3. N = 48 coral samples and N = 24 CSW samples for metabolomics, but N = 46 coral and N = 18 CSW samples for metabarcoding due to sample loss..... 147

Figure 4.2 | Microbial and chemical composition of coral and near-surface coral seawater samples. PCA score plots of microbiome (**a.** coral and **b.** coral seawater) and metabolome (**c.** coral and **d.** coral seawater) samples. Metabarcoding and metabolomic relative abundance data was CLR transformed and auto-scaled (mean-centered & scaled). Differences on compositional variability were assessed between interaction type (i.e., Int; contact vs close proximity vs control), sampling location (i.e., Loc; apex vs. side fragments) and colony position (i.e., Pos; up vs. downstream). Significance of explaining variables and their interaction was tested by PERMANOVA (N = 999 permutations; Supplementary Table 4)..... 148

Figure 4.3 | Relative abundance fold changes (mean ± se) of specific microbial taxa and molecular subnetworks in corals and near-surface coral seawater (CSW). Top 20 most discriminant and significantly differentially abundant ASVs in **a.** corals and **b.** CSWs. Selected molecular subnetworks with at least 3 discriminant features and/or one of the top 20 features in **c.** corals and **d.** CSWs. ASVs and networks at the far right were not detected in controls. Fold changes were calculated relative to the mean changes in the control condition and log10 transformed. Significantly differentially abundant ASVs (only in side fragments; see Result section for details) and subnetworks across interaction types are indicated in bold. Fold changes were calculated relative to the mean changes in the control condition and log10 transformed. Relative abundances of discriminant features were summed within each sample across molecular subnetworks. Discriminant ASVs and metabolites were determined by the PLS-DA shown in Supplementary Figure 4..... 150

Figure 4.4 | Molecular subnetworks and putative annotations of coral metabolites varying across interaction types. Each node in the networks represents a unique feature with its associated MS/MS spectra labelled by its precursor mass. Nodes are linked by a cosine score > 0.7 (edges). Black circled nodes are discriminant features (i.e., VIP score > 1). Pie charts represent the mean relative abundances (i.e., peak areas) of each node in either control (blue), close proximity (2 cm; orange) or direct (green) interaction. Node are sized relative to the total feature abundance in all coral samples. Putative subnetwork molecular classes were derived from Classyfire ontology via MolNetEnhancer (GNPS) and CANOPUS (SIRIUS). Feature identities and putative formulas were obtained through GNPS and SIRIUS. Exact positions of desaturations are uncertain. 152

Figure 4.5 | Correlation network of ASVs and metabolites across algal interaction types in coral holobionts. Bipartite network resulted from multiblock DIABLO analysis et generated two clusters **a.** and **b.** A threshold on correlation value was set to 0.7, thereby selecting 25 ASVs and 44 metabolites. Nodes are colored by the ASV/metabolite mean relative abundance in either control (blue), close proximity (2 cm; orange) or direct contact (green) treatment in coral samples. Node contour represents the type of variable: ASV (purple) or metabolite (grey). Metabolite putative formulas and annotations can be found in Supplementary Table 6c..... 153

Figure 5.1 | Summary of thesis chapters. This PhD investigated the extent to which algal-associated metabolites and microbes could play a role in water-mediated competition against corals. Chapter 2 focused on the microbial and chemical composition of macroalgae-associated waterscapes. Chapter 3 investigated whether these waterscapes disrupt coral larval and adult microbiomes and recruitment success. Chapter 4 tested the influence of contact-mediated vs. water-mediated effects of *Dictyota bartayresiana* on the coral microbiome and metabolome. 192

Figure 5.2 | Key research perspectives highlighted in this PhD research to further understand the roles of algal-associated microbes and metabolites on reef metabolism and resilience. These include: 1. Better understanding the movement of algal-derived metabolites and microbes across boundary layers with ambient hydrodynamics, and how these interact together. It is also important 2. To assess how these waterborne substances affect coral holobionts across life stages and 3. To establish the causal links between microbial dynamics and holobiont health. 203

List of Tables

Table 1.1 | Life-history strategies and ecological traits of brown macroalgae, specifically *Turbinaria ornata* and *Dictyota bartayresiana*, contributing to their proliferation and persistence on degraded reefs. Adapted from Stewart, 2008. Traits 1 to 6, 8 and 9 are specific to *Turbinaria*.
..... 28

Chapter 1

Introduction and thesis outline

1. Coral reef ecosystems and their threats

Iconic ecosystems of our tropical oceans, coral reefs are among some of the most productive and diverse ecosystems on Earth where biodiversity estimates range from 1 to 9 million species constituting about 25% of all marine species (Hatcher, 1988; Knowlton, 2001; Knowlton et al., 2010; Spalding et al., 2001). These species inhabit the highly complex tridimensional structure built by calcifying benthic organisms such as scleractinian corals, keystone species of these ecosystems (Stella et al., 2010; Graham & Nash, 2013; Coker et al., 2014). However, such rich diversity has been daunting for coral reef scientists as tropical reefs thrive in oligotrophic conditions where essential nutrients like nitrogen and phosphorous are scarce (Lewis, 1977; Hatcher, 1997). In fact, their paradoxical persistence lies in a rapid and efficient nutrient recycling in which the tiniest reef inhabitants play a central role, the microbes (Gast et al., 1998; Silveira et al., 2017a). Primary producers, such as stony corals and algae, release significant amounts of their photosynthates as dissolved organic matter (DOM) in seawater. These small organic molecules or “metabolites” are then rapidly transformed by microbial communities. They are either directly utilized as growth substrates for biomass production or remineralized for primary production, tunneling energy through coral reef food webs (Wild et al., 2004; Haas et al., 2011; Wegley Kelly et al., 2022; Nelson et al., 2023). Reef taxa metabolites can also act as important signaling cues for communication and defense structuring reef communities (Paul et al., 2011; Ochsenkühn et al., 2018; Wichard & Beemelmans, 2018). Therefore, reef waters harbor a tremendous diversity of chemicals and microorganisms supporting the functions of coral reef ecosystems.

The value of coral reefs extends to human populations, which heavily depend on them for food security, income earnings, coastal production as well as cultural richness (Moberg & Folke, 1999; Woodhead et al., 2019). Through extensive biomass production, corals reefs support the livelihoods of over 500 million people worldwide (Hicks & Cinner, 2014). Despite their invaluable ecological services, coral reefs are disproportionally threatened by a combination of local (e.g., pollution, overfishing, habitat destruction) and global (e.g., marine heatwave, ocean acidification) stressors which stems largely from human activities (Hoegh-Guldberg et al., 2007; Bruckner et al., 2008; Burke et al., 2011; Hughes et al., 2017). Above all, global warming, leading to massive coral mortality through bleaching, is now recognized a major driver of reef decline (Graham et al., 2015; Hughes et al., 2018). In the past few decades, accumulated stress on coral reefs has resulted in a ~50% decline in coral cover globally accompanied with a 63% loss of coral reef-associated biodiversity (Eddy et al., 2021). For

example, in the Indo-Pacific reefs, coral cover has declined from 42.5 % in the early 1980s to 22.1 % in 2003 (Bruno & Selig, 2007). Future climate projections seriously question the persistence of reefs by 2100 due to the intensification of marine heatwaves as well as ocean acidification (Hoegh-Guldberg et al., 2007; Frölicher et al. 2018). The additive effects of local and global stressors can considerably reduce the timeframe of environmental suitability for coral reefs, calling for urgent actions to tackle greenhouse emissions and prevent local reef degradation (Setter et al., 2022; Voolstra et al., 2023).

Following coral loss, benthic community structure can shift from coral dominance to the dominance of another sessile taxa, such as macroalgae, sponges or soft corals (Norström et al., 2009; Crisp et al., 2022; Reverter et al., 2022). Unidirectional phase-shifts from corals to algae have, by far, been the most documented. Constituting a dramatic manifestation of reef degradation, these shifts have become one of the main paradigms of coral reef research (Bellwood et al., 2004; Hughes et al., 2007; Mumby & Steneck, 2008; Crisp et al., 2022). After mass coral mortality, many reefs worldwide have recovered in a few years or decades without transitioning to a macroalgal-dominated state (Adjeroud et al., 2009, 2018; Graham et al., 2015). Yet, when reef transitions occur, they constitute a great concern for the scientific community as little evidence exists regarding their reversal due to the existence of reinforcing feedback processes perpetuating these phase-shifts over time (Mumby et al., 2007; Mumby & Steneck 2008; Schmitt et al., 2019). One of these processes imply macroalgal competition against corals (Barott et al., 2012; van de Leemput et al., 2016; Schmitt et al., 2021). The negative effects of macroalgae on corals are now well established and involve a range of physical, microbial and chemical mechanisms (McCook et al., 2001; Birrell et al., 2008a; Rasher et al., 2011; Clements & Hay, 2023). Nevertheless, the extent to which macroalgae effectively damages corals and the mechanisms driving these competitive interactions, including both contact- and water-mediated interactions, are important knowledge gaps in reef ecology and coral resilience research.

In the following sections, I will further introduce the ecology of transitioned reefs from coral to macroalgal dominance and will present the main competitors, the coral and macroalgal holobionts. I will, then, describe in more details the contact *vs.* water-mediated mechanisms by which macroalgae compete with corals and limit reef recovery. Finally, I will expose my case study, the lagoonal reefs of Mo'orea in French Polynesia, the value of "omics" in reef ecology, and will provide an overview of the chapters of this dissertation.

2. Coral-macroalgal phase-shifts

The first evidence of stable coral-algal phase-shifts was reported on the Great Barrier Reef in 1984 (Hatcher, 1984). Best-documented case studies occurred in Jamaica where baseline coral cover in the 1970s decreased from 52% to 3% in twenty years concurrently with an increase in macroalgal cover from 4% to 92% (Hughes et al., 1987; Hughes, 1994). Establishing baseline levels for macroalgal abundance has been challenging due to a lack of consensus attributed to limited historical records and habitat specificities (Bruno et al., 2009, 2014; Hughes et al., 2010). However, scientist interviews suggest that 5-15% of macroalgae cover is perceived as natural (Bruno et al., 2014). Historical records have revealed a baseline macroalgal cover of 2% in the Caribbean (Hughes et al., 1987; Côté et al., 2005). Importantly, macroalgal cover alone is a poor indicator of reef health as even macroalgal cover as low as 20% can be detrimental to coral recovery (Hughes et al., 2010; Cannon et al., 2023).

Inshore or fringing reefs have been particularly susceptible to transition towards macroalgal dominance (Schmitt et al., 2019; Crisp et al., 2022; Fabricius et al., 2023) However, the focus on specific benthic groups (coral and algae), the over-representation of Caribbean studies and the lack of clear definitions (e.g., dominance, phase-shift) have challenged our assessment of the magnitude of this phenomenon (Bruno et al., 2009; Norström et al., 2009; Roff & Mumby, 2012; Crisp et al., 2022; Reverter et al., 2022) Therefore, a phase-shift has been defined as “a transition between dominant (i.e., most abundant) benthic groups, with the two phases of dominance persisting at least for three years before and three years after the shift” (Crisp et al., 2022). While coral-algal phase-shifts are more frequent in the Western Atlantic region, they do occur in other reef regions, such as in the Eastern Pacific (Polynesian and Hawaiian reefs) where 30% of algal-dominated reefs have been reported (Roff & Mumby, 2012; Reverter et al., 2022).

Besides changes in benthic assemblages, macroalgal dominance bear consequences on other biological compartments. For example, macroalgal-dominated reefs are associated with a lower fish diversity than coral-dominated reefs (Chong-Seng et al., 2012). Even the smallest biological scales can be altered by the proliferation of macroalgae, from microbial community structure to water biochemistry. Lower DOC and oxygen concentrations, higher microbial abundances and shift in the trophic structure of microbial communities are symptomatic of algal-dominated reefs (Dinsdale et al., 2008; Haas et al., 2010, 2016; Wegley Kelly et al., 2014; Frade et al., 2020). This phenomenon called “microbialization” refers to the enrichment of bacterial copiotroph as the availability of algal-induced DOM increases which in turn depletes

organic carbon stocks and shunts down trophic transfer (Dinsdale et al., 2008; Haas et al., 2016; Wegley Kelly et al., 2022; Nelson et al., 2023).

The dynamic of phase-shifts is governed by interacting external (i.e., destabilizing processes as chronic or acute disturbances) and internal forces (i.e., reinforcing feedback processes) where forces initiating the shift might be different from those maintaining the system in its alternative state (Scheffer et al., 2001; Nyström et al., 2012). On coral reefs, large scale disturbances (e.g., cyclones, corallivores outbreaks or massive bleaching events) can lead to drastic reductions in coral cover freeing space for opportunistic colonization (Hughes, 1994; Aronson & Precht, 2006; Kayal et al., 2012; Adjeroud et al., 2018). Whether reefs can recover to near pre-disturbance levels or transition towards an altered state is attributed to top-down forces and bottom-up forces controlling algal proliferation. Both modelling and experimental approaches have identified herbivory loss (Hughes et al., 2007; Mumby et al., 2007; Mumby & Steneck, 2008; Smith et al., 2010; Adam et al., 2011; Holbrook et al., 2016; Schmitt et al., 2021) and nutrient enrichment (Smith et al., 2010; Johnson et al., 2018; Adam et al., 2021) as key reinforcing feedback processes locking reefs into algal-dominated states.

Reducing these feedback processes to or beyond the threshold at which the phase-shift occurred does not simply enable the system to shift back to its original state, although very few examples exist (Idjadi et al., 2010). Instead, coral reefs have exemplified the concept of “hysteresis” where two states can exist under the same environmental conditions (i.e., bistability) leading to distinct forward and reverse trajectories of the system (Scheffer et al., 2001; Beisner et al., 2003; Mumby et al., 2007). This property makes the return of a coral-dominated state extremely difficult and the strength of reinforcing and destabilizing feedbacks will define how easily the shift can be reversed, if at all possible (Schmitt et al., 2019; Bulleri et al., 2022). In addition, the strength of attraction towards the macroalgal-dominated state can differ between reef habitats (Adam et al., 2011; Schmitt et al., 2019). For example, in Mo’orea (French Polynesia), herbivores in the lagoon were unable to control for macroalgal abundance in contrast to the fore reef, suggesting that, due to hysteresis, the lagoonal system would need a substantially higher level of herbivory to revert to a non-macroalgal state (Schmitt et al., 2019). Therefore, by altering key ecosystem processes, human-driven stressors have decreased the resilience of coral reefs, thereby lowering the tipping point under which reefs transition towards alternative stable states (Scheffer et al., 2001; Bellwood et al., 2004; Hughes et al., 2010; Fig. 1.1).

Besides top-down and bottom-up forces, macroalgae and corals can also exert reinforcing feedback processes. Macroalgae are fast colonizers, growing much faster than corals, and can become space holders in just a few months (Payri & Naim, 1982; Adam et al., 2011; Roff & Mumby, 2012). Once established, they can maintain their dominance and prevent coral recovery not only through space preemption, but also through competitive ecological traits and strategies (McCook et al., 2001; Stewart, 2008; Schmitt et al., 2021)

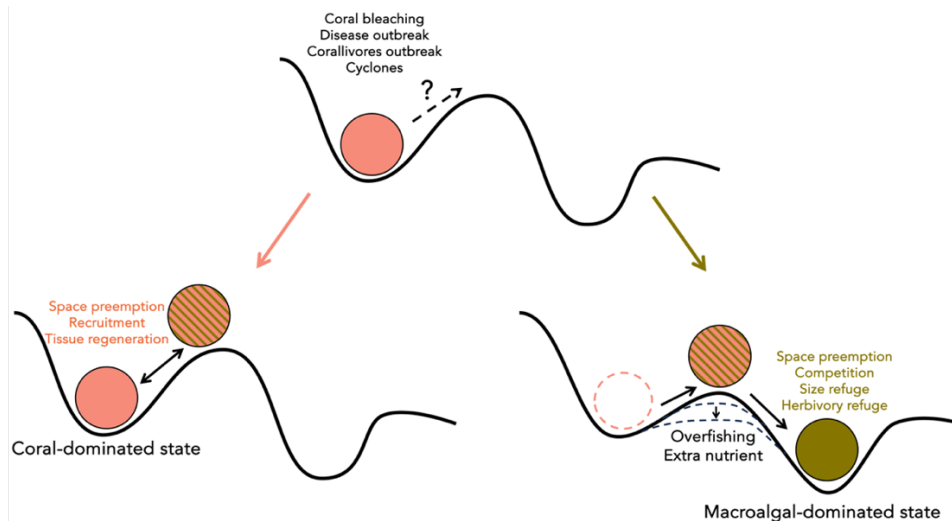


Figure 1.1 | Conceptual diagram of forces leading to alternative ecological states on coral reefs. Coral- (bottom-left) and macroalgal-dominated states (bottom-right) are two alternative stable states. After large disturbances causing massive coral loss (i.e., destabilizing feedback processes), healthy coral reefs have good chance to recover (i.e., staying in their “coral valley”). The coral ball may shift in the “algal valley” if pulse disturbances (e.g., cyclones) are much greater or if the resilience of the system has been eroded, for example if overfishing exceed a certain threshold (i.e., lowering the ridge between the two valleys). The macroalgal-dominated state may be a persistent basin of attraction locking the system into its new state due to strong reinforcing feedback processes (algal valley lower than the coral valley).

3. The main competitors: corals vs. algae

3.1. Coral holobionts and recruitment process

3.1.1. Corals and their microbial symbionts

Scleractinian corals, colonial animals from the Anthozoa class and Cnidaria phylum, are the main organisms responsible for reef formation; a task they share with other sessile organisms such as octocorals (e.g., *Heliopora*), hydrozoans (e.g., *Millepora*) or calcifying coralline algae (CCA). Coral polyps, individuals of coral colonies, deposit calcium carbonate at their base participating in reef accretion. They live in symbiosis with a multitude of microorganisms, representatives of all three kingdoms Bacteria, Archaea, Eukarya as well as virus and fungi, in a consortium named “holobiont” (Rohwer et al., 2002; Rosenberg et al., 2007). The concept has been broadened to other reef taxa as sponges or macroalgae harboring their own microbial communities (hereafter “microbiome”; Barott et al., 2011; Pita et al., 2018). The

first described and best-known symbionts are dinoflagellates from the genus *Symbiodinium* (Symbiodiniaceae, commonly referred as zooxanthellae) providing nearly 90% of the coral energetic requirements in the form of sugars, lipids and nitrogen compounds (Muscatine & Porter, 1977; Falkowski et al., 1984; Davy et al., 2012). Besides these obligate photosymbionts, corals are associated with a great diversity of prokaryotes spanning across 39 bacterial and 2 archaeal phyla (Blackall et al., 2015; Huggett & Apprill, 2019)

First investigations of the coral microbiome composition have been based on culturing techniques and have demonstrated abundant bacterial communities within the mucus layer (Mitchell & Ducklow, 1979). The advent of DNA-based culture-free techniques at the beginning of the 21st century has enabled to dig into the tremendous diversity of microbes and further investigate their putative roles (Rohwer et al., 2002; Kellogg, 2004; Lesser et al., 2004; Wegley et al., 2004; Vega Thurber et al., 2009). Decades of research have now revealed some general patterns in microbiome diversity, abundance, and dynamics. The most commonly detected coral-associated bacteria belong to the classes Gammaproteobacteria, Alphaproteobacteria, Bacteroidetes and Firmicutes (Huggett & Apprill, 2019). In addition, the different coral compartments (i.e., skeleton, tissue and mucus) constitute micro-habitats, each harboring distinct microbial communities (Sweet et al., 2011; Bourne et al., 2016; Pollock et al., 2018). Particularly, the surface mucus layer (SML) is a very dynamic habitat due to its constant interaction with the environment. It likely constitutes the first line of defense against pathogenic infection by producing antibiotics and occupying niche entries (Ritchie, 2006; Tremblay et al., 2011; Bourne et al., 2016; Glasl et al., 2016). Some bacterial taxa have demonstrated a strong ubiquity to coral microbiomes constituting core members, such as *Endozoicomonas* and *Ruegeria* (Ainsworth et al., 2015; Huggett & Apprill, 2019; McCauley et al., 2022; Hochart et al., 2023).

Microbial symbionts have been associated with various roles underpinning holobiont health and homeostasis from nutrient recycling (Raina et al., 2010; Räddecker et al., 2015; Silveira et al., 2017a), defense against pathogens (e.g., antimicrobial compounds, competitive niche exclusion, inhibition of quorum sensing; (Rosenberg et al., 2007; Krediet et al., 2013; Raina et al., 2016; Modolon et al., 2020), provision of essential metabolites (Bourne et al., 2016; Pereira et al., 2017; Pogoreutz et al., 2022; Villela et al., 2023) and stress mitigation (Ziegler et al., 2017; Rosado et al., 2019; Peixoto et al., 2021; Santoro et al., 2021; Fig. 1.2). Investigating how the abundance of microbes change in stressed holobionts has given further insights into the nature of coral-bacteria associations, particularly whether they are beneficial, neutral or detrimental. In this respect, *Endozoicomonas*, an abundant genus in healthy coral microbiomes,

often strongly decreases when coral holobionts are exposed to heat-stress, diseases, unsuitable environmental conditions or competition, suggesting a beneficial role (Morrow et al., 2013; Ziegler et al., 2016; McDevitt-Irwin et al., 2017; Gignoux-Wolfsohn et al., 2017; Meyer et al., 2019) These bacteria have been observed in aggregates deep into gastrovascular tissues (Neave et al., 2017a; Wada et al., 2022; Maire et al., 2023). Genomic analyses have revealed that they may be important for amino acid and vitamin biosynthesis (Pogoreutz et al., 2022), sulfur cycle (Robbins et al., 2019; Tandon et al., 2020), phosphate cycle (Wada et al., 2022), as well as protein and carbohydrate transports (Neave et al., 2017b). Comparatively, Vibrionaceae, Rhodobacteraceae, Alteromonadaceae and Pseudoalteromonadaceae are bacterial families that often increase in the microbiome of compromised coral holobionts (Zaneveld et al., 2016; Ziegler et al., 2016; McDevitt-Irwin et al., 2017). Although, bacteria belonging to these families are now flagged as opportunist and/or putative pathogens, the extent to which they affect coral health is still poorly known. Recently, the coral pathogen *Vibrio coralliilyticus* induced the lytic cycle of prophage to compete with coral-associated bacteria (Wang et al., 2022). In addition, some symbionts are particularly unknown as Archaea, fungi and endolithic members (Bourne et al., 2016; Pernice et al., 2020; Roik et al., 2022). Overall, while it is certain that bacterial symbionts play critical roles in holobiont health, we still strongly lack functional insights into coral-microbes interactions.

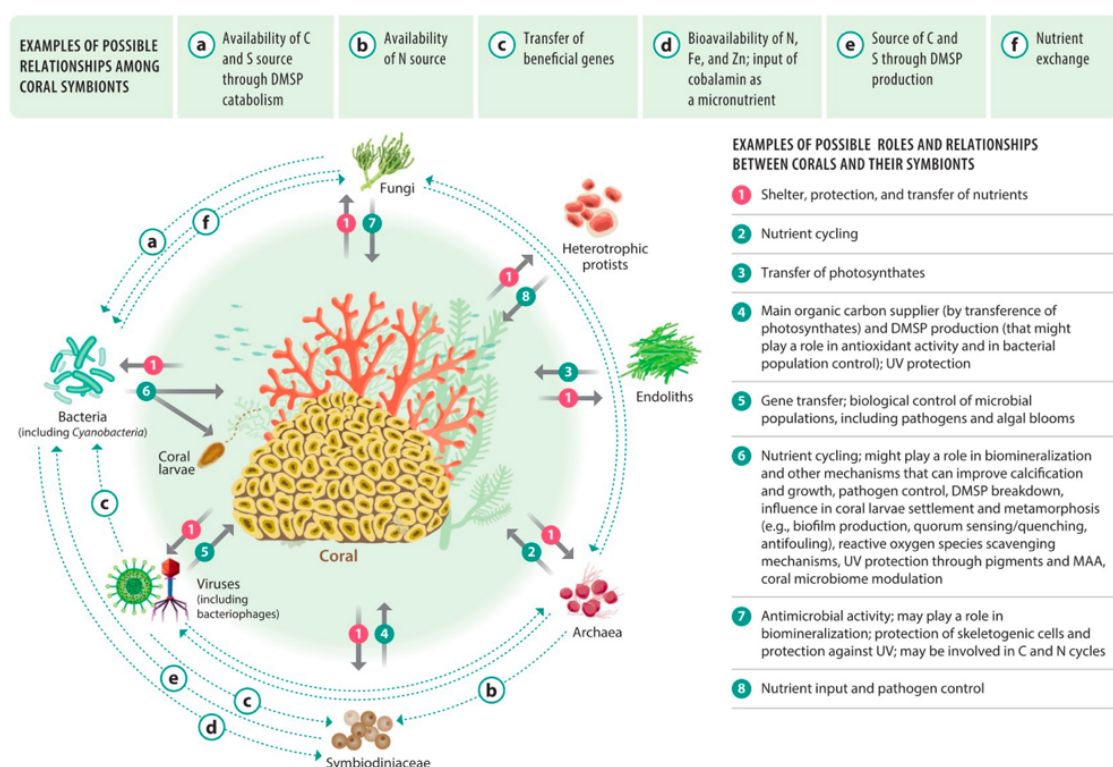


Figure 1.2 | Model of the coral holobiont, comprising the coral host, its obligate algal symbionts (Symbiodiniaceae) and diverse other microorganisms such as Bacteria, Archaea, viruses, fungi and other protists. All members interact together to sustain holobiont health and homeostasis. From Peixoto et al., 2021

3.1.2. Microbiome of early coral life stages

The onset of coral-bacterial associations occurs at the earliest life stages and is closely related to the coral reproductive strategy (Thompson et al., 2015; van Oppen & Blackall, 2019; Fig. 1.3). Broadcast spawners release eggs and sperm in the water column where external fertilization and embryonic development take place. In contrast, brooders release sperm in the water which will fertilize eggs inside the polyps; larvae are then internally brooded and released once mature (Ritson-Williams et al., 2009). For spawners, studies have documented an absence of bacterial cells in the gametes and an acquisition of bacteria once the planula is fully developed, suggesting horizontal transmission (i.e., uptake from the environment; Apprill et al., 2009; Sharp et al., 2010). For brooders, bacteria have been observed in the ectodermis and surface of newly released larvae, suggesting vertical transmission (e.g., from parents to offspring; (Sharp et al., 2012). In addition, a mixed strategy has been proposed for both brooding (e.g., *Pocillopora damicornis* and *P. acuta*; Epstein et al., 2019a; Damjanovic et al., 2020) and spawning (e.g., *Acropora digitifera*; Bernasconi et al., 2019) corals. In fact, mucus surrounding the gametes may favor the transmission of symbionts from the parents to their offspring after their release (Ceh et al., 2013a; Leite et al., 2017; Bernasconi et al., 2019).

Planula larvae can remain pelagic for days to months before settling to their substrate of choice and undergoing metamorphosis (Ritson-Williams et al., 2009; Gleason & Hofmann, 2011; Fig. 1.3). Bacteria are critical in the success of these steps. For example, rates of settlement vary with the age and composition of microbial biofilms (Webster et al., 2004; Erwin et al., 2008; Bulleri et al., 2018; Padayhag et al., 2023). Some specific bacterial strains can induce larval settlement and metamorphosis, including *Pseudoalteromonas*, *Thalassomonas* and *Alteromonas* (Negri et al., 2001; Tran & Hadfield, 2011; Sneed et al., 2014; Freire et al., 2019; Petersen et al., 2021). In fact, these bacteria have often been associated with the surface microbiome of crustose coralline algae (CCA), known to induce high rates of coral settlement (Price, 2010; Siboni et al., 2020; Jorissen et al., 2021; Yang et al., 2021). Metabolites produced by bacteria could also induce settlement. Specific strains of *Pseudoalteromonas* produce settlement-inducing compounds, such as the Tetrabromopyrrole (TMB) and cycloprodigiosin (Tebben et al., 2015; Petersen et al., 2021)

Microbial communities of early coral life stages change throughout ontogeny. The microbiomes of larvae and recruits are more diverse and variable than those of adult corals (Lema et al., 2014; Leite et al., 2017; Bernasconi et al., 2019; Damjanovic et al., 2020). This “winnowing process” is thought to allow the microbiome composition to be fine-tuned to a

certain environment (Nyholm & McFall-Ngai, 2004). While adult corals are dominated by *Endozoicomonas*, microbiomes of early coral life stages harbor abundant bacteria affiliated to *Alteromonas*, *Roseobacter* and *Vibrio* (Sharp et al., 2012; Lema et al. 2014; Williams et al., 2015; Bernasconi et al., 2019). These genera may be involved in nitrogen acquisition (Ceh et al., 2013; Lema et al., 2014), sulfur cycling as well as larval development and defense (Thompson et al., 2015; Bernasconi et al., 2019; Freire et al., 2019). In contrast to adults, very few studies have investigated the extent to which microbial communities associated with coral offspring are affected by environmental conditions and disturbances, hindering our understanding of their roles throughout coral ontogeny (Beatty et al., 2018; Epstein et al., 2019a; Zhou et al., 2021)

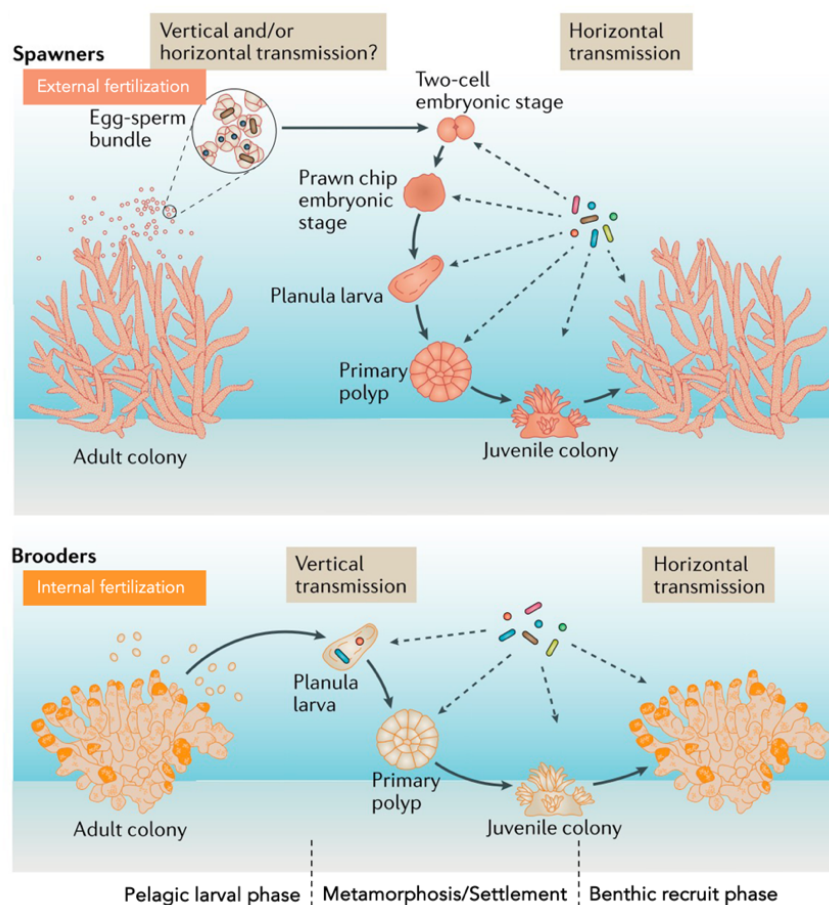


Figure 1.3 | Coral recruitment and bacterial acquisition across life stages. Recruitment is a process involving a pelagic and a benthic phase connected by the key step of larval settlement and metamorphosis. Broadcast spawners release eggs bundles and sperm in the water column surrounded by bacteria-rich mucus. Mucus bacteria can be primed by the parents or acquired rapidly after larval release in the water column. Brooders directly transmit bacteria to their offspring (i.e., vertical transmission) and release fully developed larvae. Bacteria uptake occurs via the environment at all life stages (i.e., horizontal transmission). Adapted from van Oppen & Blackall, 2019.

3.2. Macroalgae: their ecological success

Despite their proliferation in the last decades, macroalgae are natural members of benthic communities on coral reefs, supporting essential ecological functions (Fong & Paul, 2011; Ceccarelli et al., 2018; Diaz-Pulido, 2019). Reef-associated macroalgae constitute a complex polyphyletic group comprising members of 3 phyla: the Rhodophyta (red algae), Ochrophyta (class Phaeophyceae or brown algae), Chlorophyta (green algae). In this thesis, I will focus on brown macroalgae defined as fleshy erect macroalgae including erect calcifying species, hereafter referred to as “macroalgae”. They are important members of the coral reef food web by acting as primary producers (Diaz-Pulido, 2019) and serving as primary food sources for several herbivores (e.g., fishes, turtles, invertebrates; Choat et al., 2002; Fong & Paul, 2011). By accumulating epibionts on their surfaces and sheltering understory algal communities, they also act as trophic support (Fong et al., 2018; Bittick et al., 2019). Consequently, they participate in nutrient cycling on reefs through organic matter release and biomass transfer to higher trophic levels (Fong & Paul, 2011; Wegley Kelly et al., 2022; Dunne et al., 2023). Several reef-associated species, especially juvenile fishes (e.g., lethrinids, scarids, labrids) and small macro-invertebrates, use macroalgae as refuge habitat sometimes even exclusively (Cunha et al., 2013; Evans et al., 2014; Eggertsen et al., 2017; Sambrook et al., 2019). For example, 15 % of recruiting fish species are specifically observed in macroalgal-dominated areas (Evans et al., 2014).

The success of macroalgae on reefs lies in the combination of life-history traits and defense strategies (Table 1.1; Stewart, 2008; Zubia et al., 2020). In this respect, *Turbinaria ornata* (family Sargassaceae, hereafter *Turbinaria*) has several characteristics that make it a foundational species of macroalgal-dominated state (Bittick et al., 2019; Schmitt et al., 2019, 2021). For example, in the lagoons of Mo’orea (French Polynesia), this species largely contributes to the hysteresis by forming dense aggregation of nearly 100 individuals/m² on top of coral bommies (Stewart et al., 2007) Distinct morphotypes can emerge from different reef habitats and this spatial phenotypic plasticity has enabled this alga to be very effective in thriving under various environmental conditions (Stewart, 2006, 2008; Martinez et al., 2007). Specifically, morphotypes from the backreef bear pneumatocysts in their blades allowing them to stay close to the water surface. This granted buoyancy results in greater mass transfer rates and light accessibility (Stewart, 2006; Stewart et al., 2007). In contrast, fore reef morphs tend to be shorter and stiffer due to high wave energy (Stewart, 2008). *Turbinaria* has also a very effective reproductive mode, capable of producing propagules throughout the year (Stiger &

Payri, 1999a, 2004). In addition, when they detach from the substrate, buoyant fronds create rafts that can remain fertile for 3 months which allow them to colonize islands and archipelagos over very large distances (Stiger & Payri, 1999b; Stewart, 2008; Martinez et al., 2007).

Herbivory pressure is a significant driver of algal community structure and plays a pivotal role in the evolution of ecological, structural and chemical defenses in macroalgae (Duffy & Hay, 1990; Steneck et al., 2017). As an example, *Turbinaria* thalli are particularly unpalatable to browsers; they have a rough texture with rows of sharp blades and produce high quantity of phenolic compounds (Stiger et al., 2004). By forming dense patches, macroalgae may exclude herbivores from algal aggregations, potentially avoiding a greater predation risk or abrasion by algal blades (Hoey & Bellwood, 2011; Davis, 2018). Spatial refuges from herbivory can occur on a much smaller spatial scale where algal germlings settle in micro-refuges within reef cracks (Brandl et al., 2014). In addition, palatable young germlings settle in the vicinity of adult thalli (< 1 m distance) (Stiger & Payri, 1999b; Zubia et al., 2020) benefitting from their chemical and structural protections (Stiger et al., 2004; Davis, 2018). In fact, size-related immunity to herbivory for *Turbinaria* has been observed for thalli taller than 2 cm (i.e., less than 1 month old; Davis, 2018), offering a short window for herbivores. *Turbinaria* can also create a refuge from herbivory for understory algal species contributing to the establishment of diverse algal communities (Bittick et al., 2010, 2019).

Members of the genera *Dictyota* are additional prominent members of algal communities and can represent up to 10% of the benthic cover (e.g., Polynesian reefs; Theophilus et al., 2020). They have a thin thallus with dichotomous branching and typically form small, 10-15 cm wide patches. These algae are chemically defended throughout their successive life stages by the production of a great diversity of secondary metabolites, mostly diterpenoids and sesquiterpenoids (Cronin & Hay, 1996; Pereira et al., 2000; Bogaert et al., 2020). Canopy-forming algae, such as *Turbinaria* and *Sargassum*, are often associated with *Dictyota* which settles as epiphytes or understory algae (Bittick et al., 2010; Pereira et al., 2010). In an herbivory assay, the alga *Sargassum furcatum* was less predated by the urchin *Lytechinus variegatus* when associated with *Dictyota* sp, suggesting a chemically-mediated beneficial association (Pereira et al., 2010). In addition, *Dictyota* can sustain high herbivory levels thanks to a fast branch regeneration (Rasher et al., 2013; Fong et al., 2016; Tanaka et al., 2017). Fish feeding and physical disturbances can result in algal fragments that can easily get entangled and re-attach to the substrates or as epiphytes, a trait that likely contributed to their fast proliferation on reefs (Herren et al., 2006; Table 1.1).

The ecological characteristics of macroalgae have enabled them to exploit the degraded conditions of certain reefs. Their extensive self-replenishment capacities appear as key forces favoring hysteresis. With increasing algal abundance, the interaction between corals and algae have become more frequent at the expense of corals (Hughes, 1994; Haas et al., 2010; Barott et al., 2012; Barott & Rohwer, 2012; Brown et al., 2018). For example, in non-marine protected areas (non-MPAs) with ~30% of macroalgal cover, coral-algal interactions are 5-15 fold more frequent and 23-67 fold more extensive (i.e., % of colony margin in contact with macroalgae) than in MPAs (Bonaldo & Hay, 2014). In hyper-diverse ecosystems such as coral reefs, competition is a prevalent and fundamental process shaping the composition of benthic assemblages, where sessile organisms engage in competition for space and light (Knowlton & Jackson, 2001). The increasing frequency of coral-algal interactions intensifies competition between these primary reef taxa. Therefore, it is paramount to better understand how macroalgae effectively compete with corals and at which scale the different mechanisms of competition occurs.

Table 1.1 | Life-history strategies and ecological traits of brown macroalgae, specifically *Turbinaria ornata* and *Dictyota bartayresiana*, contributing to their proliferation and persistence on degraded reefs. Adapted from Stewart, 2008. Traits 1 to 6, 8 and 9 are specific to *Turbinaria*.

Ecological traits	Roles	Reference
1. Spatial phenotypic plasticity	Acclimatization to different reef habitats (i.e., low-flow and high-flow)	Stiger & Payri, 1999a; Stewart, 2006, 2008
2. Pneumatocystes and flexible thalli of backreef morphotypes	Increase mass transfer, prevent desiccation, and optimize light accessibility	Stewart et al., 2007
3. Reproductive cycle and gynodioecy	High rates of fertility and quasi-continuous production of propagules in the close vicinity of mature thalli	Stiger & Payri, 1999a, 2005
4. Ontogenetic changes in morphology and fertility	Creating floating rafts with fertile thalli	Stewart, 2006
5. Buoyancy and reproductive capacity maintained 3 months after detachment	Long-distance dispersal	Stiger & Payri, 1999b ; Martinez et al., 2007 ; Stewart, 2008
6. Tough texture with hard spines	Structural defenses against herbivory	Stewart, 2008
7. Production of deterrent secondary metabolites	Chemical defenses against herbivory	Cronin & Hay, 1996 ; Stiger et al., 2004 ; Pereira et al., 2000, 2010
8. Size-structured vulnerability to herbivory	Escape from herbivory	Davis, 2018; Briggs et al., 2018
9. Intraspecific associational refuge	Escape from herbivory	Dell et al., 2016; Davis, 2018
10. Spatial refuge	Escape from herbivory	Hoey & Bellwood, 2011; Brandl et al., 2014
11. Interspecific associational refuge	Escape from herbivory, promote algal community diversity	Bittick et al., 2010, 2019 ; Pereira et al., 2010
12. Vegetation fragmentation	Enhance dispersal	Herren et al., 2006 ; Stewart, 2008

4. Coral-algal competition: chemical and microbial effects

4.1. Contact-mediated mechanisms

Coral-algal interactions have been considered competitive with the compelling evidence that macroalgal contact has negative effects on coral fitness (McCook et al., 2001; Barott & Rohwer, 2012; Clements & Hay, 2023). Field experiments manipulating macroalgal abundance have demonstrated that macroalgal contact decreases coral growth (Tanner, 1995; Lirman, 2001; River & Edmunds, 2001; Box et al., 2007; Clements et al., 2018, 2020) and fecundity (Tanner, 1995; Foster et al., 2008; Monteil et al., 2020). To distinguish between the confounding effects of physical abrasion by algal thalli from its associated microbial and chemical effects, inert algal mimics have been widely used. For example, contact with *Lobophora variageta* and *Dictyota pulchella* thalli or their algal mimics cause similar reduction in growth of the coral *Agaricia* (Box & Mumby, 2007). Similarly, the reduction in growth and photosynthetic activity of *Acropora millepora* is equivalent whether corals are in contact with *Galaxaura rugosa* and *Sargassum polycystum* or fake algae (Clements et al., 2020). In contrast, several studies found that plastic algal mimics produce fewer effects on corals than live organisms (Rasher & Hay, 2010; Rasher et al., 2011; Andras et al., 2012). While these studies suggest that physical effects, such as shading and abrasion, are an important competitive mechanism, it is likely that they actually act in concert with microbial effects and allelopathy depending on algal species.

Chemical potency against corals is variable among algal species and has been negatively correlated with their structural defenses (Rasher & Hay, 2010; Morrow et al., 2011; Rasher et al., 2011; Longo & Hay, 2017). For example, *Sargassum* and *Turbinaria* or their chemical extracts have little effect on coral health compared to other species, such as *Lobophora*, *Dictyota*, and *Chlorodesmis* (Rasher & Hay, 2010; Rasher et al., 2011; Shearer et al., 2012; Vieira et al., 2016a; Longo & Hay, 2017). Some of the extracted lipid-soluble allelochemicals have been characterized as diterpenes (Rasher et al., 2011) and polyunsaturated alcohols (Vieira et al., 2016a). The hydrophobicity of these compounds suggests a transfer via contact with algal surfaces (Rasher & Hay, 2010; Vieira et al., 2016a; Longo & Hay, 2017). In addition, even among algal genera, including *Dictyota* and *Galaxaura*, allelopathy levels vary across species (Box & Mumby, 2007; Rasher et al., 2011; Clements et al., 2020). Beyond hydrophobic allelochemicals, macroalgae could transfer coral pathogens promoting diseases (Nugues et al., 2004; Sweet et al., 2013), and harmful bacteria causing severe bleaching and decrease of photosynthetic activity (Vieira et al., 2016b).

Further evidence for the detrimental stress caused by macroalgal contact has been demonstrated with investigations of the coral transcriptome and metabolome (Shearer et al., 2012, 2014; Quinn et al., 2016; Roach et al., 2020; Little et al., 2021). For example, alterations in gene expression in corals exposed to macroalgal chemical extracts may mitigate oxidative stress (Shearer et al., 2012). Other studies have revealed intracellular production of specific lipids, such as the PAF-C16 or the ceramide 18:1/16:0, at the interface between corals and algae (e.g., turf, *Halimeda*) suggesting anti-inflammatory responses (Quinn et al., 2016; Roach et al., 2020). In addition, algal contact can impact coral holobionts down to microbial scales by altering the microbiome community structure (Zaneveld et al., 2016). An extensive body of research has now established that contact with live algae (Morrow et al., 2013; Pratte et al., 2018; Lu et al., 2022; van Duyl et al., 2023) or their chemical extracts (Morrow et al., 2012, 2017) increase microbiome richness, variability and composition, with an enrichment of opportunistic/potential pathogens and a loss of beneficial microbes, this last symptom being defined as “dysbiosis” (Vega Thurber et al., 2012; Zaneveld et al., 2016, 2017). Reduction in coral health (e.g., tissue necrosis, mortality, bleaching) can pair with microbiome alterations (Vega Thurber et al., 2012; Zaneveld et al., 2016), although not systematically (Clements et al., 2020; Fong et al., 2023). To conclude, the extent to which macroalgae negatively affects corals through physical effects, direct toxicity of compounds, microbial infection, or a combination of all is highly dependent on the species involved. It is now recognized that macroalgae can effectively compete with corals through several contact-mediated stressors in which chemical and microbial mechanisms are prevalent. However, it is still unclear whether algal-associated compounds and microbes can negatively impact coral fitness at a distance *via* water transport.

4.2. Water-mediated mechanisms

Water-mediated effects in coral-macroalgal competition have first been demonstrated using laboratory experiments and grounded the interactive role of metabolites and microbes in damaging corals. In earlier studies, corals incubated with high concentrations of organic carbon suffered higher mortality than corals incubated with inorganic nutrients (Kuntz et al., 2005; Kline et al., 2006). Smith et al., 2006 linked this observation to algal exudates and microbial activity. When putting coral and algae in two individual compartments separated by a 0.2 μm filter in no flow experimental chambers, the addition of antibiotics suppressed the hypoxic zones and extensive coral mortality which were observed in the treatment without antibiotics. Further research showed that macroalgae and turf exude high amount of photosynthetically-

derived DOC which stimulates rapid bacterial growth and leads to oxygen depletion (Barott et al., 2009; Haas et al., 2010, 2011, 2013a, 2013b; Wangpraseurt et al., 2012) that can be detrimental to corals (Smith et al., 2006; Haas et al. 2014). In fact, microbial communities thriving on algal exudates are less diverse and functionally distinct, shifting towards copiotroph and potentially pathogenic communities (Haas et al., 2013a; Nelson et al., 2013; Roach et al., 2017). For example, *Turbinaria* exudates select for microbial communities with the highest mean abundance of pathogenic genes and are enriched in taxa belonging to the family Rhodobacteraceae, Flavobacteriaceae, Cryomorphaceae and Vibrionaceae compared to coral exudates (Nelson et al., 2013). Altogether, these studies have led to the conceptualization of the DDAM (dissolved organic matter, disease, algae, microbes) model stipulating that algae release high amount of labile organic matter feeding abundant and detrimental microbial communities which in turn cause coral mortality through hypoxia and pathogenic invasion (Barott & Rohwer, 2012).

This model proposes that algae harm corals without contact, particularly when corals are located downstream (Barott & Rohwer, 2012). Close proximity with macroalgae can affect coral productivity and microbiome composition, yet reported effects are highly dependent on the identities of interacting species. For example, the coral microbiome of only one species (*Montipora stellata*) out of three is disrupted when corals were placed 5 cm away from *Lobophora* sp. and *Hypnea pannosa*, while physiological damages require direct contact (Fong et al., 2020). Water incubated with *Caulerpa* sp. and *Halimeda cnidata* modulates coral productivity, either positively (i.e., *Pocillopora verrucosa*) or negatively (i.e., *Porites rus*) depending on coral species (Engelhardt et al., 2023). Flow dynamic is another paramount factor determining the extent of water-mediated competition. For example, hypoxia at coral-turf interface is facilitated under low flow conditions, unless corals are placed downstream, suggesting enhanced retention of organic matter and microbes (Jorissen et al., 2016). While it is clear from these studies that secondary metabolites and associated microbes can affect coral holobionts over short distances (< 5 cm), whether similar mechanisms occur under natural flow conditions needs to be determined.

On reefs, the water column is structured in boundary layers due to alterations in flow conditions (e.g., drag forces, frictions, turbulences) as water flows over hard benthic structures (Shashar et al., 1996; Reidenbach et al., 2006; Hench & Rosman, 2013; Rogers et al., 2018). Three boundary layers of variable thickness have been described: the benthic boundary layer (BBL – m to cm scale) influenced by the overall shape of the reef and main currents; the momentum boundary layer (MBL – cm to mm scale) receiving organic matter from the benthos

through advection; and the diffusive boundary layer (DBL – mm to μm scale) essentially formed by the diffusion and accumulation of benthic products (Shashar et al., 1996; Barott & Rohwer, 2012; Fig. 1.4 A). Together, they form complex and dynamic waterscapes influenced by flow velocity and benthos complexity causing variation in organic matter transfer within and between boundary layers (Davis et al., 2021).

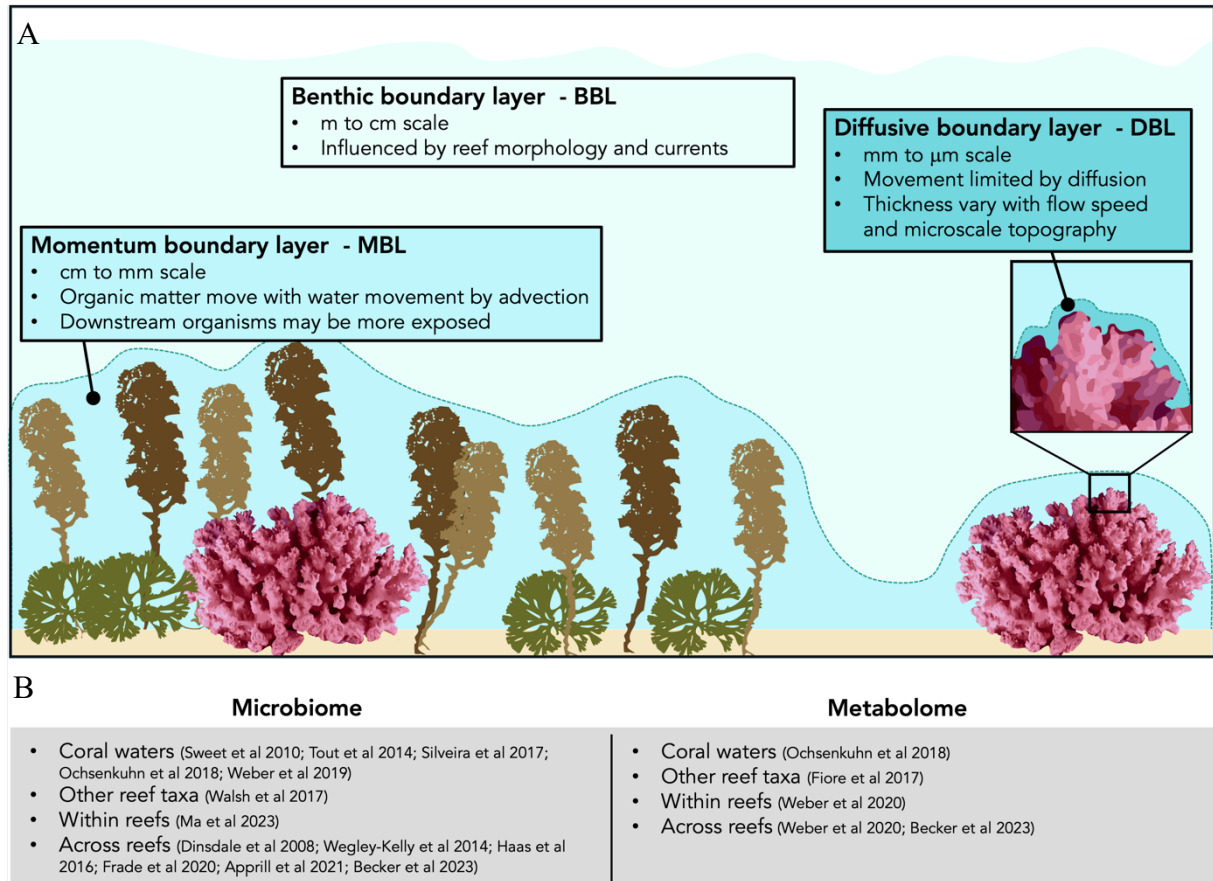


Figure 1.4 | Model of reef waterscapes. (A) Waterscapes are the combination of three boundary layers whose thickness and composition vary with the distance from the benthos. Inspired by Barott & Rowher, 2012. (B) Summary of the *in-situ* studies investigating their microbial and chemical composition.

The composition of reef waterscapes has essentially been investigated from a microbial perspective and has been linked with benthic community composition. Specifically, macroalgal-dominated reefs are enriched in opportunist microbes and potential pathogens compared to coral-dominated reefs (Dinsdale et al., 2008; Wegley Kelly et al., 2014; Haas et al., 2016; Frade et al., 2020). In addition, macroalgae can influence pelagic microbial communities at the organismal scale. For example, turf and macroalgal MBLs are enriched in microbes and genes, suggestive of low oxygen conditions and pathogenetic pathways (Walsh et al., 2017). However, some studies have contradicted these patterns, such as Ma et al., 2022 who observed a weak

correlation between benthic assemblages and microbiome composition within a single reef or (Silveira et al., 2017b) who have not been able to distinguish the MBL from the BBL.

Comparatively, reef exometabolomes (i.e., pools of reef taxa exometabolites) have only been investigated in recent years with scarce *in-situ* studies (Fig. 1.4 B). A recent aquarium-based study showed that corals, algae and CCA release specific chemicals that differ in their elemental stoichiometry and macronutrient content, where energy-rich algal exometabolites may explain the enhanced activity of microbes growing on these compounds (Wegley Kelly et al., 2022). Surprisingly, other studies could not distinguish surface from reef bottom waters and relate reef exometabolomes with benthic composition across reef habitats (Weber et al., 2020; Becker et al., 2023). Such results are puzzling due to the tight microbe-metabolite coupling induced by benthic taxa that exist in reef waters (Haas et al., 2013a; Ochsenkühn et al., 2018; Nelson et al., 2023). Therefore, there are considerable knowledge gaps in the identity and distribution of reef exometabolites and the organisms that released them.

Furthermore, how reef waterscapes influence coral holobionts is largely unknown. Corals from algal-dominated reefs harbor a more diverse and variable microbiome than those from algal-dominated reefs, although without drastic changes in composition (Beatty et al., 2018, 2019). However, none of these studies specified whether contact occurred and the distances separating corals from algae. In fact, only one field study found that, in the absence of algal contact, the coral microbiome increases in richness and variability as macroalgal cover increases (Briggs et al., 2021). This work revealed that contact and macroalgal cover have antagonistic effects on the coral microbiome structure challenging our understanding of holobiont response to macroalgal dominance. In addition, the effects of water-mediated competition are closely related to ambient hydrodynamics and the underlying mechanisms are even more difficult to apprehend under natural flow conditions (Hench & Rosman, 2013; Brown & Carpenter, 2015; Jorissen et al., 2016; Rogers et al., 2018; Candy et al., 2023). Therefore, to fully grasp the complexity of water-mediated competition, it is necessary to investigate the context-dependencies under which they occur *in-situ*.

4.3. Rupture of coral recruitment success by macroalgae

Coral recruitment comprises several successive stages where each stage determines the capacity of coral populations to recover from mortality events. Recruitment success depends on larval availability and survival, settlement on suitable substrates, post-settlement survival and growth of juveniles (Ritson-Williams et al., 2009). Larvae hinge on multiple biotic (e.g.,

microbes, metabolites, benthic taxa) and abiotic cues (e.g., light) to find optimum settlement locations (Gleason & Hofmann, 2011; Randall et al., 2020). Typically, they will select low-light, low-sediment microhabitats that will protect them from predation without benthic competitors (Price, 2010; Doropoulos et al., 2016; Evensen et al., 2021).

Macroalgal cover often correlates negatively with coral recruitment (Birrell et al., 2008a; Arnold et al., 2010; Chong-Seng et al., 2014; Webster et al., 2015; Mumby et al., 2016; Evensen et al., 2019a). Several processes could lead to negative interactions between macroalgae and coral recruitment. For example, Chong-Seng et al., 2014 found similar settlement rates between coral- and algal-dominated reefs, while juvenile densities strongly decreased in algal-dominated reefs, suggesting that degraded reefs cannot support post-settlement survivorship despite the availability of coral larvae. Indeed, larvae may not avoid algal-dominated reefs and rather suffer from macroalgal competition on a local scale (Gleason et al., 2009; Beatty et al., 2018). The presence of macroalgae can inhibit larval settlement, despite the presence of suitable cues (e.g., CCA chips; (Baird & Morse 2004; Kuffner et al., 2006; Gleason et al., 2009; Diaz-Pulido et al., 2010; Beatty et al., 2018). For example, in an experiment demonstrating small-scale inhibition of settlement, larvae preferentially settled away from *Lobophora* sp. patches compared to inert mimics (Evensen et al., 2019b). Strong bottleneck on post-settlement mortality preceded by low larval settlement can have a dramatic additive effect that can considerably jeopardize recruitment success as a whole (Webster et al., 2015; Evensen et al., 2019a).

To investigate microbial and chemical effects, several studies have tested macroalgal-associated waters using either incubation or *in-situ* sampling, yet results vary greatly (Maypa & Raymundo, 2004; Birrell et al., 2008b; Denis et al., 2014). Water from macroalgal-dominated reefs increase larval mortality when compared to water of coral-dominated reefs (Beatty et al., 2018). Likewise, leachates from *Sargassum* sp. trigger a stress-like swimming behavior of coral larvae (Antonio-Martínez et al., 2020). In contrast, *Lobophora*-water enhances larval settlement compared to *Padina*-water (Birrell et al., 2008b), while *Padina*- and *Sargassum*-water rather induces metamorphosis (Maypa & Remundo, 2004; Denis et al., 2014).

Laboratory-based studies have demonstrated that macroalgal allelopathy could effectively deter recruitment by killing larvae and inhibiting their settlement (Paul et al., 2011; Morrow et al., 2017; Evensen et al., 2019b; Fong et al., 2019; Page et al., 2023). When comparing aqueous (i.e., hydrophilic) and organic extracts (i.e., lipid-soluble), these studies found a stronger effect of the former (Morrow et al., 2017; Evensen et al., 2019b; Page et al., 2023). While such results suggest effective water mediation of allelochemicals, it is counterintuitive with the idea that allelopathy correlates negatively with compound polarity (Vieira et al., 2016a). Besides, the

miscibility of aqueous extracts and high extraction yields may have led to an overestimation of water-mediated effects of algal allelochemicals in these studies (Evensen et al., 2019b; Page et al., 2023).

Microbially-mediated inhibition of recruitment has also been proposed. For example, echoing the work of Smith et al., 2006, the addition of antibiotics limits the negative effects of the green algae *Ulva* on larval survivorship, suggesting that algal exudates foster higher microbial concentrations and/or compromised larval defense against pathogens (Vermeij et al., 2009). In addition, macroalgae can modify epilithic microbial communities which in turn could deter recruitment (Kegler et al., 2017; Bulleri et al., 2018). The removal of algal canopy alone does not necessarily promote recruitment, suggesting that abrasion from algal fronds is not the only mechanism (Bulleri et al., 2018). In fact, macroalgal whole thalli influence microbial biofilms and taxa such as Cyanobacteria, Sphingomonadaceae and Verrucomicrobia negatively correlate with recruit density (Bulleri et al., 2018). To conclude, while macroalgae can be detrimental to coral recruitment success, we still have difficulties to detangle the specific stages impacted by macroalgae and the inhibitory mechanisms.

5. PhD overview

5.1. Lagoons of Mo'orea: a case study

The island of Mo'orea in French Polynesia (17° 31' S, 149° 49' W; Fig. 1.5) has been a hub for coral reef sciences. The history of perturbations and community composition of the reefs around this island are perhaps some of the best documented worldwide. Since the 1970s, benthic communities have been shaped by major disturbances: a) two crown of thorns (COTs) starfish outbreaks in 1979 and 2007-2009, b) seven coral bleaching events between 1983 and 2019, and c) two cyclones in 1991 and 2010 (Adjeroud et al., 2009, 2018; Trapon et al., 2011; Kayal et al., 2012; Speare et al., 2022). These perturbations have differentially impacted Polynesian reefs (Trapon et al., 2011; Pérez-Rosales et al., 2021) The fore reefs have shown great recovery thanks to high coral recruitment (Adjeroud et al., 2009, 2018; Holbrook et al., 2018; Kayal et al., 2018) and herbivore control on macroalgal growth (Adam et al., 2011; Holbrook et al., 2016; Schmitt et al., 2019). Comparatively, the lagoons have not escaped phase-shifts. Algal proliferation, mainly driven by *Turbinaria ornata*, has been reported in the early 1980s and 1990s. For example, *Turbinaria* biomass represented < 1% to 84% of the total algal biomass between 1971 and 1980 (Payri & Naim, 1982), and *Turbinaria* and *Sargassum* constituted up to 20-53% of the benthic community in some inshore reefs in 1987-1989 (Done et al., 1991).

More recently, macroalgal community on certain backreefs could represent 30-50% of the benthic cover compared to a coral cover as low as $< 5\%$ (Adam et al., 2021). These algal assemblages are mostly represented by the species, *Turbinaria ornata*, *Sargassum pacificum*, *Dictyota bartayresiana* and *Amansia rhodantha* (Bittick et al., 2010; Adam et al., 2021). The macroalgal-dominated state in the lagoons has now become a strong basin of attraction that has been favored by the loss of key herbivores (e.g., browsers, urchins; Schmitt et al. 2019, 2021; Bulleri et al. 2022), chronic nutrient enrichment (Adam et al., 2021), as well as the ecological traits of these algae, as discussed earlier (Duff & Hay, 1990; Stewart, 2008; Steneck et al., 2017; Bittick et al., 2019). Contact-mediated competition against corals has likely favored hysteresis on these algal-dominated reefs (McCook et al., 2001; Ritson-Williams et al., 2009; Clements & Hay, 2023). However, we still have little knowledge on the extent to which macroalgae negatively impact the coral holobiont and its recruitment success through water-mediated mechanisms. Facing their dramatic proliferation on inshore reefs, such knowledge constitutes critical gaps in our understanding of coral resilience capacity.

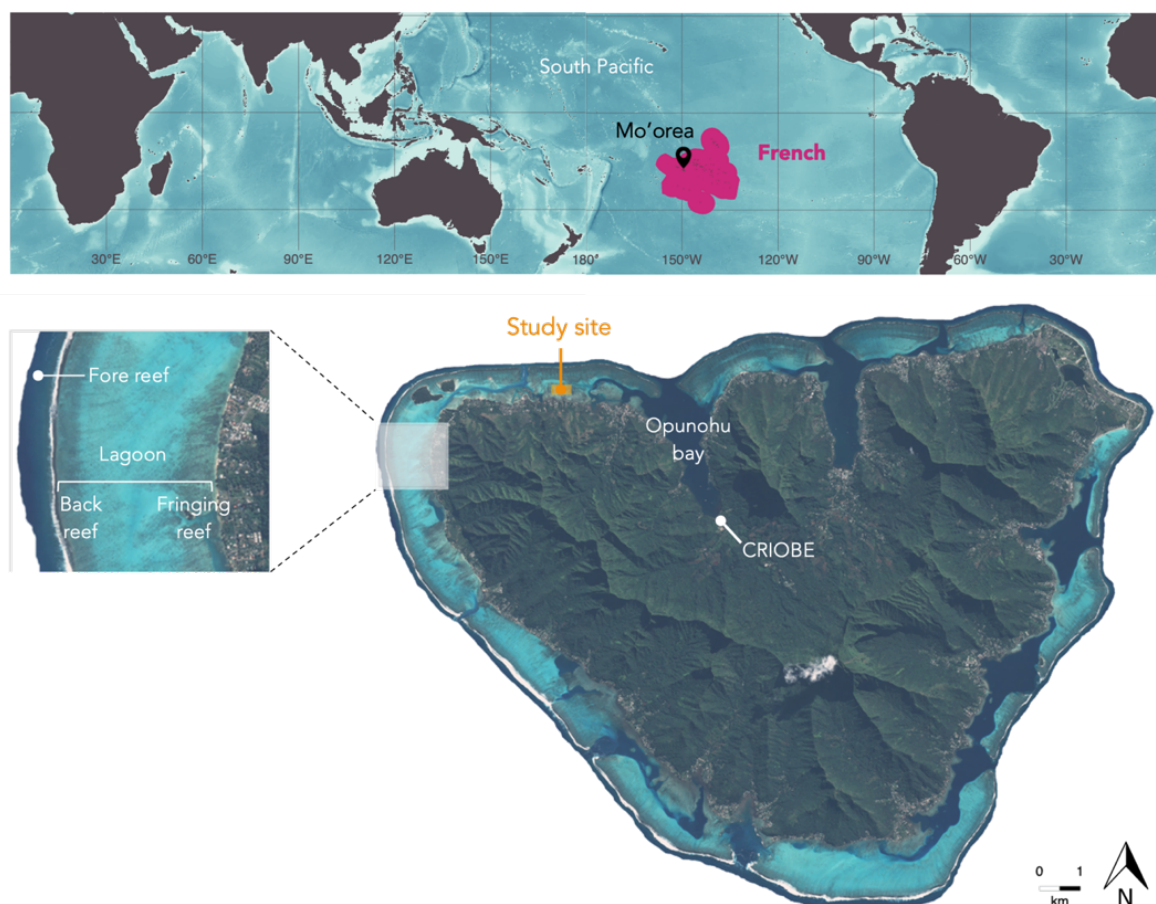


Figure 1.5 | Map of Mo'orea, island of French Polynesia. Field experiments were conducted in a fringing reef on the north coast. Map acquired with the help of Charles Loiseau

5.2. Reef “omics”, the new paradigm in reef ecology

“Omic” sciences encompasses a set of disciplines aiming to describe and quantify biological molecules from DNA sequences to metabolites. In coral reef research, they have often been applied independently tackling only one molecular level at a time (Mohamed et al., 2023). Composition and dynamics of microbial communities have been described by amplicon sequencing of the 16S rDNA marker gene (i.e., metabarcoding). While it has been a first step in investigating who is there, taxonomic assignments remain limited to the genus level and gives little information on their roles in holobionts and reef ecosystems (Johnson et al., 2019). Other gene-based methods, such as metagenomics (i.e., shotgun sequencing) and metatranscriptomics (i.e., RNA sequencing), can provide further information by providing a more complete picture of the genomic diversity and which genes are transcribed in a given context (Wright et al., 2015; Glasl et al., 2020; Mohamed et al., 2023). The last “omic” getting increasing traction in reef sciences is metabolomics. Metabolomics is the study of low-weight molecules either present in tissues (i.e., intracellular metabolites) of living organisms or the environment (i.e., extracellular metabolites). Metabolites are end products of cellular processes. Since they are involved in metabolism and signaling pathways, they are invaluable tools in chemical ecology. Liqui-chromatography coupled with mass-spectrometry (LC-MS) is one of the preferred methods in metabolomics where both targeted and untargeted approaches can be applied (Kido Soule et al., 2015; Petras et al., 2017). While targeted method aims at specifically quantifying known metabolites, untargeted metabolomics is a semi-quantitative method that can detect thousands of compounds to comprehensively describe metabolomic profiles across samples. Tandem-mass spectra (MS² or MS/MS) can be acquired in LC-MS/MS runs providing molecular fingerprints of the metabolites which can then be searched in databases and processed for putative formulas and annotations. However, the biggest challenge in metabolomics is this annotation step which require extensive analytical tools, manual verifications and comparisons to known standards, leaving many compounds unknown despite the advancement of promising computational methods (da Silva et al., 2015; Steen et al., 2020).

Being in its infancy, marine metabolomics has gained a growing interest in the fields of coral biology and microbial ecology (Kido Soule et al., 2015; Garg, 2021; Wegley Kelly et al., 2021; Mohamed et al., 2023). Recent efforts have started to unveil the chemical diversity of coral holobionts (Reddy et al., 2023) and reef exometabolites (Fiore et al., 2017; Ochsenkühn et al., 2018; Weber et al., 2019; Wegley Kelly et al., 2022), as well as their link with microbial communities (Ochsenkühn et al., 2018; Weber et al., 2022). For example, coral exometabolites

structure microbial communities at the coral interface and across boundary layers (Ochsenkühn et al., 2018). By comparing coral metabolomic profiles exposed to various conditions, studies have highlighted specific compounds potentially involved in heat stress response (Roach et al., 2021; Williams et al., 2021a; Haydon et al., 2023), ocean acidification (Sogin et al., 2016), disease (Ochsenkühn et al., 2018) and immunity in coral-algal interactions (Quinn et al., 2016). More recently, untargeted metabolomics have been applied to investigate CCA-derived metabolites that might play a role in larval settlement (Quinlan et al., 2023).

Coral holobiont metabolism and reef processes (e.g., coral recruitment, nutrient cycling) are inherently linked to a tight metabolite-microbe coupling, and a single “omic” may not be sufficient to apprehend the complexities of such biological systems. Integrative or “multiomic” frameworks are, therefore, a remarkable opportunity to generate hypotheses and to gain functional insights at several scales within coral reef ecosystems: holobionts, holobiont-water interfaces and reef waterscapes (Wegley-Kelly et al., 2021). A handful of studies have integrated multiomic data in coral research (Mohamed et al., 2023), and these have demonstrated that linking the microbiome structure to gene expression and/or metabolome composition can provide useful insights into the role of each holobiont members in stress mitigation (Santoro et al., 2021; Williams et al., 2021b), competition with algae (Roach et al., 2020; Little et al., 2021) and chemical cross-talk within holobionts (Pogoreutz et al., 2022; Mannocho-Russo et al., 2023). In this context, I have applied metabarcoding (i.e., 16S rDNA amplicon sequencing) and untargeted metabolomics (i.e., liquid chromatography coupled to tandem mass spectrometry – LC-MS/MS) workflows to investigate the microbes and metabolites involved in coral-algal competition and reveal their co-variation patterns (Fig. 1.6).

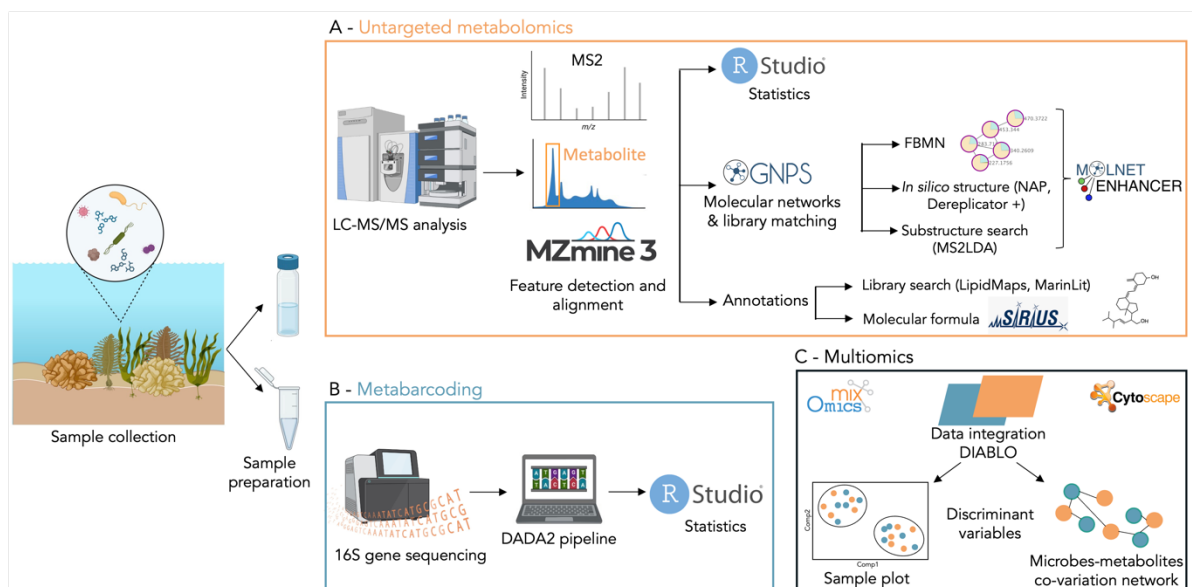


Figure 1.6 | Untargeted metabolomics and metabarcoding workflows in this PhD. (A) Metabolomic profiles were acquired by LC-MS/MS on an Orbitrap Q-Exactive in positive and negative ionization modes. MS data were analyzed in MZmine. Feature tables were uploaded in the GNPS platform for construction of Feature-Based Molecular Networks (FBMN), library searches and molecular classification with the MolNetEnhancer extended workflow. Compounds were annotated from SIRIUS putative molecular formulas and manual library searches. (B) Metabarcoding consisted in 16S rDNA gene sequencing on an Illumina NovaSeq platform. Sequencing data were processed using the DADA2 for ASV inference (amplicon sequence variant) and genus-level assignment (Silva database). (C) For multiomic analysis, data were integrated with DIABLO algorithm (*mixOmics* R package). Statistical analysis were conducted on R and networks were visualized on Cytoscape. Logos were obtained from the official websites and icons from the BioRender website. Inspired by Mannocho-Russo et al., 2023.

5.3. Thesis aims and chapter outlines

In this thesis, I aimed to contribute to our knowledge of the mechanisms by which macroalgal competition against corals constitutes a reinforcing feedback process of reef degradation. By using the lagoon of Mo’orea as an ecological model and the current advancement in marine multiomics, I specifically investigated microbial communities and metabolites involved in coral-algal competition to further decipher their identities and potential roles in water-mediated interactions. I focused my research on the coral species *Pocillopora acuta* because of its abundance in the lagoonal reefs and the availability of its brooded larvae. Two macroalgal species were specifically studied, *Turbinaria ornata* and *Dictyota bartayresiana*, constituting prominent members of macroalgal assemblages on Polynesian lagoons (Bittick et al., 2010; Schmitt et al., 2019; Theophilus et al., 2020) and showing distinct chemical and structural defenses (Rasher et al., 2011). By the means of two *in-situ* experiments, this thesis aimed to answer three overarching questions:

1. How macroalgae modify chemical and microbial reef waterscapes? (Chapter 2)
2. How these waterscapes impact coral microbiome and recruitment success? (Chapter 3)
3. What is the relative influence of contact *vs.* water-mediated competition on coral microbiome and metabolome? (Chapter 4)

These questions are addressed in the three following chapters in the form of scientific articles. Chapters have either been submitted to peer-reviewed international journals or are under preparation; their status is specified in the title page of each chapter. In addition, throughout my PhD, I engaged in the publication of three manuscripts for which I have included the 1st page at the end of this thesis.

In Chapter 2, I specifically tested the influence of macroalgal assemblages on the microbial and chemical composition of reef waterscapes using an algal removal experiment. I aimed at identifying algal-associated metabolites and microbes and describing their spatial distribution across boundary layers (i.e., BBL and MBL). Using an integrative approach, I was able to reveal co-variation patterns of metabolites and microbes within algal MBLs. Such information is paramount to decipher the consequences of macroalgal dominance down to the smallest scales which may be relevant not only for coral-algal competition dynamics, but also to reef metabolism.

Based on the same experimental settings as the precedent chapter, Chapter 3 investigated whether these waterscapes disturb the microbiome of coral adults, larvae and benthic substrates. By performing a series of experiment on the successive stages of coral recruitment, I aimed at identifying which stages are the most impacted by water-mediated effects of macroalgae. As coral colonies originated from algal-removed and algal-dominated bommies, I was able to explore the relative influence of parental and environmental effects on coral recruitment.

In Chapter 4, I performed a manipulative experiment to specifically compare the effects of contact *vs.* water-mediated interactions with the allopathic macroalga *Dictyota bartayresiana*, on coral metabolome and microbiome responses. By placing corals upstream and downstream the algae and by investigating the composition of near-surface coral waters, I aimed at testing whether downstream corals are more impacted than upstream corals. I used the same integrative framework, as Chapter 2, to investigate the links between coral microbes and metabolites to get further insights into the biological responses of coral holobiont to algal competition.

Chapter 2

Invasive macroalgae shape microbial and chemical waterscapes on coral reefs

Chloé Pozas-Schacre^{1*}, Hugo Bischoff², Delphine Raviglione^{1,3}, Slimane Chaib¹, Camille Clerissi^{1,4}, Isabelle Bonnard^{1,3,4}, Maggy M. Nugues¹,

¹ PSL Université Paris : EPHE-UPVD-CNRS, UAR 3278 CRIOBE, Université de Perpignan, 66860 Perpignan, France

² PSL Université Paris: EPHE-UPVD-CNRS, USR 3278 CRIOBE BP 1013, 98729 Papetoai, Moorea, French Polynesia

³ Plateau MSXM plateforme Bio2Mar, Université de Perpignan, 66860 Perpignan, France

⁴ Laboratoire d'Excellence "CORAIL", Perpignan, France

*Chloé Pozas-Schacre

Email: pozaschloe@gmail.com

Abstract

The coral reef ecosystem is a dynamic assemblage of living organisms whose interactions are largely modulated by chemical and microbial mediators. Over the past decades, human impacts have changed the structure of these assemblages, with coral dominance and diminutive algae giving way to coral depletion and macroalgae flourishing. However, how these changes have modified chemical and microbial waterscapes is poorly known. We assessed how the experimental removal of erect macroalgal assemblages influenced the chemical and microbial composition of two reef boundary layers, the benthic and the momentum, surrounding coral bommies in Mo'orea, French Polynesia. The data demonstrate that the multiomic signature of coral reef waters is spatially structured, both vertically and horizontally, according to boundary layers and macroalgal dominance. Microbes typically associated with reef degradation were enriched in the boundary layers surrounding macroalgal-dominated bommies. To explore the origin and diffusion of waterborne chemicals, we extracted macroalgal surface- and endo-metabolomes and compared them with those of the boundary layers. Macroalgae were surrounded by a distinct sphere of infochemicals and labile organic matter, some of which showing a diffusion gradient. Covariations of algal-associated metabolites and microbes suggest that these algal-derived metabolites structure planktonic bacterial communities. Together these results pinpoint a macroalgal-specific influence on metabolite pools which in turn shape microbial community structure in the water column. Our study illustrates that, while benthic communities physically mark underwater landscapes, they also generate complex chemical and microbial waterscapes, which play essential roles in the function and resilience of coral reefs.

Significance Statement

On coral reefs, the tight coupling between microorganisms and metabolites drives reef biogeochemical processes and mediates ecological interactions. In the wake of the widespread shift from coral to macroalgal dominance, deciphering the unseen diversity of microbes and chemicals and their spatial distribution is paramount to understand the consequences of benthic community changes on coral reef ecosystem function and resilience. This study demonstrates that macroalgal assemblages modify the multiomic signature of reef boundary layers. It reveals a spatial structuration of planktonic microbial communities and identifies specific classes of compounds characterizing two invasive macroalgal species and their surrounding waters. Results support that macroalgae release chemicals which select for specific planktonic microbial communities, thereby influencing the functioning and structure of coral reefs.

1. Introduction

Coral reefs are among the most productive and diverse ecosystems on the planet. Their high productivity in oligotrophic tropical seas is dependent on a tight benthic-pelagic coupling and key microbial processes (O'Neil & Capone, 2008; Silveira et al., 2017a; Nelson et al., 2023). Benthic organisms, like stony corals, macroalgae or turf, release an extensive amount of dissolved and particulate organic matter underpinning reef community metabolism. For example, photosynthates and coral mucus constitute labile organic matter consumed by microbial assemblages tunneling essential nutrients through the coral reef food web (Wild et al., 2004; Nelson et al., 2013, 2023). Part of this chemical diversity can act as powerful cues involved in communication or defense structuring reef communities (Paul et al., 2011; Wichard & Beemelmans, 2018). As such, the chemical pool in which sessile organisms bath mediates both positive (e.g., settlement cues, metabolites exchange) and negative (e.g., allelopathy, competition) biotic interactions between reef members (Dennison & Barnes, 1988; Paul et al., 2011; Ochsenkühn et al., 2018). The combination of molecular exchanges and microbial processes within reef waters results in complex chemical and microbial waterscapes which are just starting to be deciphered (Walsh et al., 2017; Weber et al., 2020; Wegley Kelly et al., 2022; Becker et al., 2023).

Water masses of variable thickness are formed from drag forces as water flows over the reef geomorphology, resulting in a physical stratification of reef waterscapes (Shashar et al., 1996; Reidenbach et al., 2006). Three boundary layers have been described: the benthic boundary layer (BBL – m to cm scale) influenced by the overall shape of the reef and main currents; the momentum boundary layer (MBL – cm to mm scale) receiving organic matter from the benthos through advection; and the diffusive boundary layer (DBL – mm to μm scale) essentially formed by the diffusion and accumulation of benthic products. These water masses are dynamic, influenced by flow velocity and benthos complexity, causing variation in the transfer of organic matter within and between boundary layers (Davis et al., 2021). Therefore, each boundary layer may have distinct biological and chemical characteristics, reflecting both benthic member identities and physical processes.

Accumulating anthropogenic pressures, such as ocean warming, pollution and overuse, have drastically altered the sessile community structure of the reef benthos, inducing phase shifts from coral to macroalgal dominance with cascading effects down to microbial scale (Wegley Kelly et al., 2014; Haas et al., 2016; Smith et al., 2016). Large-scale studies, across reefs and ocean basins, have demonstrated that the pelagic microbiome reflects the underlying

benthos of shifted reefs. Specifically, reefs that transitioned towards macroalgal dominance tend to harbor higher microbial density and abundance of copiotrophic, potentially pathogenic, microbial taxa than coral-dominated reefs (Wegley Kelly et al., 2014; Haas et al., 2016; Frade et al., 2020). Reef taxa actually exert a strong organismal influence on microbial assemblages, although limited to their immediate vicinity. Benthic primary producers, such as corals, macroalgae or turf algae, exhibit highly distinct microbial community composition in their MBLs which also differs from that of the upper water layer (Tout et al., 2014; Walsh et al., 2017; Weber et al., 2019). These microbial shifts are likely driven by concurrent changes in benthic-derived organic matter, yet its composition and small-scale spatial variation across boundary layers and benthic organisms remain inadequately understood.

In the last two decades, several studies have provided essential groundwork for unveiling the differential influence of benthic communities on chemical diversity and the link with microbial processes (Haas et al., 2011; Nelson et al., 2013; Weber et al., 2022; Wegley Kelly et al., 2022). Coral and macroalgal exudates have specific chemical signatures and select for taxonomically and functionally distinct microbial communities. Specifically, carbon-rich algal exudates select for copiotrophic bacteria with more potential virulence factors compared to coral exudates (Nelson et al., 2013). Yet, it is only recently, with the advancement in marine untargeted metabolomics and chemoinformatics (da Silva et al., 2015; Petras et al., 2017), that these metabolite pools have been shown to differ in their elemental stoichiometry and macronutrient content (Wegley Kelly et al., 2022). However, *in-situ* investigations of the chemical composition of reef waters, as well as their sources, remain scarce (Ochsenkühn et al., 2018; Weber et al., 2020; Becker et al., 2023). For example, molecular gradients from coral surface to overlying boundary layers have been described, comprising infochemicals, such as quorum sensing and antibacterial compounds, that may structure microbial communities surrounding the coral holobiont (Ochsenkühn et al., 2018). Conversely, in two recent studies, untargeted chemical composition of reef exometabolomes did not vary across depths (Weber et al., 2020) and did not reflect benthic composition across habitats (Becker et al., 2023).

Linking changes in metabolite pools and microbiome structure induced by macroalgal dominance is paramount to understand the ecology of transitioning reefs. Dominance of macroalgae may alter reef biogeochemical cycles through changes in microbe-metabolite interactions (Haas et al., 2016; Glasl et al., 2020). Additionally, water-mediated effects are thought to be involved in coral-algal competition, from waterborne allelochemicals to microbially-mediated processes (Smith et al., 2006; Paul et al., 2011; Barott & Rohwer, 2012; Jorissen et al., 2016). If algal-associated microbial and chemical waterscapes drive the demise

of coral reefs, they could create a feedback loop that reinforces macroalgal dominance (Barott & Rohwer, 2012). In the light of accelerating coral reef degradation, a better comprehension of the effects of macroalgal assemblages on chemical and microbial signatures across reef boundary layers, as well as the origin and diffusion of algal-derived metabolites, is needed.

Here we describe an *in-situ* manipulative experiment in Mo'orea, French Polynesia designed to assess how macroalgal assemblages simultaneously influence the chemical and microbial composition of two reef boundary layers: the MBL and BBL. We compared reef waters surrounding macroalgal-dominated and macroalgal-removed coral bommies and investigated algal-derived metabolites and microbes using untargeted metabolomics tandem mass spectrometry (LC-MS/MS) and 16S rDNA metabarcoding. Our integrative analysis reveals a spatial structuration of the chemical and microbial waterscapes according to macroalgal dominance and boundary layers, with an enrichment of opportunist copiotrophic bacteria in algal-associated waters along with diffusion gradients of distinct compound classes produced by two invasive macroalgal species. This study contributes to unveil the identity of metabolites and microbes and their covariations within reef waterscapes constituting a starting point to further investigate their complex roles in coral reef functioning and resilience.

2. Result

2.1. Experimental design and benthic community composition

This *in-situ* experiment took place in the lagoon of Mo'orea, French Polynesia, between June 2020 and June 2021 (*SI Appendix*, Fig. S1 A and B). Six coral bommies were randomly selected and assigned to one of two algal treatments: i) algal-removed or ii) algal-dominated (*SI Appendix*, Fig. S2 A and B). Algal-removed bommies were created by removal of all macroalgae, including canopy-forming holdfasts and understory species. Macroalgal-dominated bommies were left untouched. Before algal removal, benthic communities did not differ between treatments (PERMANOVA, Algal removal treatment: $R^2 = 0.08$, $P > 0.05$). After algal removal, communities varied significantly between treatments and remained distinct throughout the experiment (PERMANOVA, Algal removal treatment: $R^2 = 0.61$, $P < 0.001$; Month: $R^2 = 0.03$, $P > 0.05$; Treatment x Month: $R^2 = 0.05$, $P > 0.05$; *SI Appendix*, Fig. S3 A). Algal-removed bommies were dominated by bare substrate (~44% cover) and turf (~28% cover), while algal-dominated bommies were dominated by macroalgae (~68% cover), with the brown macroalgae *Turbinaria ornata* (~35% cover) & *Dictyota bartayresiana* (~14% cover) as

the two most abundant species (*SI Appendix*, Fig. S3 B and C). Six-month after algal removal, we sampled the BBL (~50 cm above the substrate) of each bommie and the MBL (~5 cm above the substrate) of bare substrate on each algal-removed bommie, as well as of substrates dominated by *T. ornata* or *D. bartayresiana* on each algal-dominated bommie, to investigate their microbial and chemical composition (n = 12 samples per reef water type; *SI Appendix*, Fig. S2 C to E). Measurements by Shashar et al., 1996 were used to define sampling heights above the substratum for each boundary layer. To explore the origin and diffusion of algal-derived metabolites, we extracted surface- (n = 12 samples per species) and endo-metabolomes (n = 3 samples per species) from each of the two macroalgal species. Metabolomic samples were processed over two injection sequences: 1) all water samples in MS1 only and 2) algal whole tissues, surfaces and water samples in tandem mass spectrometry (MS2). Chemical class identification was obtained for surface- and endo-metabolomes and compared with those of the boundary layers of algal-dominated bommies. See *SI Appendix* Supplementary Methods for detailed methodology.

2.2. Microbial and chemical diversity of reef waters

A total of 5517 ASVs and 975 MS1 features were obtained after data filtration (see *SI Appendix* Supplementary Methods; Tab. S1). Nearly half (42%) of all ASVs were common to all five reef water types (*SI Appendix*, Fig. S4 A). Algal-dominated waters had the highest percentage of unique ASVs (12%) compared to algal-removed waters (3%; *SI Appendix*, Fig. S4 A). Particularly, *Dictyota* and *Turbinaria* MBLs comprised together 8% of all detected ASVs as opposed to 3% for the algal-removed MBL. The algal-dominated BBL shared most of its ASVs with *Dictyota* MBL and algal-removed BBL, and 4% of all ASVs were unique to both BBLs. Microbiome alpha-diversity (Shannon index) varied significantly between reef waters (ANOVA, $P < 0.05$; *SI Appendix*, Fig. S4 C). Specifically, it was higher in *Dictyota* MBL than in algal-removed MBL (Tukey HSD test's $P < 0.05$). In the metabolomic data, a large majority (65%) of metabolites were detected across all five reef water types (*SI Appendix*, Fig. S4 B). As for the microbiome, *Dictyota* MBL had the highest number of unique chemical features. Features were mostly shared between the two algal-dominated MBLs (9%) and between all MBLs (6%). BBLs and algal-removed MBL had particularly low percentages of unique chemical features (1.1% and 0.3%, respectively). Chemical alpha-diversity varied significantly between reef waters (ANOVA, $P < 0.01$; *SI Appendix*, Fig. S4 D), with algal-dominated MBLs being more diverse than algal-removed BBL (Tukey HSD test's $P < 0.05$).

2.3. Compositional differences among reef water microbiomes and metabolomes

Differences in the chemical and microbial composition between reef waters were analyzed with PLS-DA, a supervised method to reduce data dimensionality and to discriminate known groups of samples. Both MS1 feature (*SI Appendix*, Fig. S5 A to D) and genus-level ASV (*SI Appendix*, Fig. S5 E to H) transformed abundances revealed compositional differences between the five reef water types. To investigate covariation between the microbiome and metabolome, data were integrated using the multi-block PLS-DA analysis, DIABLO (Singh et al., 2019; see *SI Appendix* Supplementary Methods). The first two components of the two ordinations were highly correlated (correlation coefficient > 0.8), showing a strong covariation between both datasets. BBLs significantly clustered apart according to the algal treatment (Fig. 2.1 A; CER = 0.14, $P < 0.01$). Similarly, the multiomic composition of all three MBLs significantly differed from each other (Fig. 2.1 B; CER = 0.20, $P < 0.001$). Additionally, boundary layers were vertically structured regardless of the algal treatment (Fig. 2.1 C and D). The BBL significantly differed from the MBL on both algal-removed (Fig. 2.1 C; CER = 0.05, $P < 0.001$) and algal-dominated (Fig. 2.1 D; CER = 0.19, $P < 0.001$) bommies. Interestingly, samples collected during the rainy season (December and March) clustered apart from those of the dry season (May and June) (*SI Appendix*, Fig. S6). This pattern might illustrate a global temporality in reef water composition. While the investigation of this hypothesis is out of the scope of this study, it contextualizes promising avenues for future research (Glasl et al., 2020).

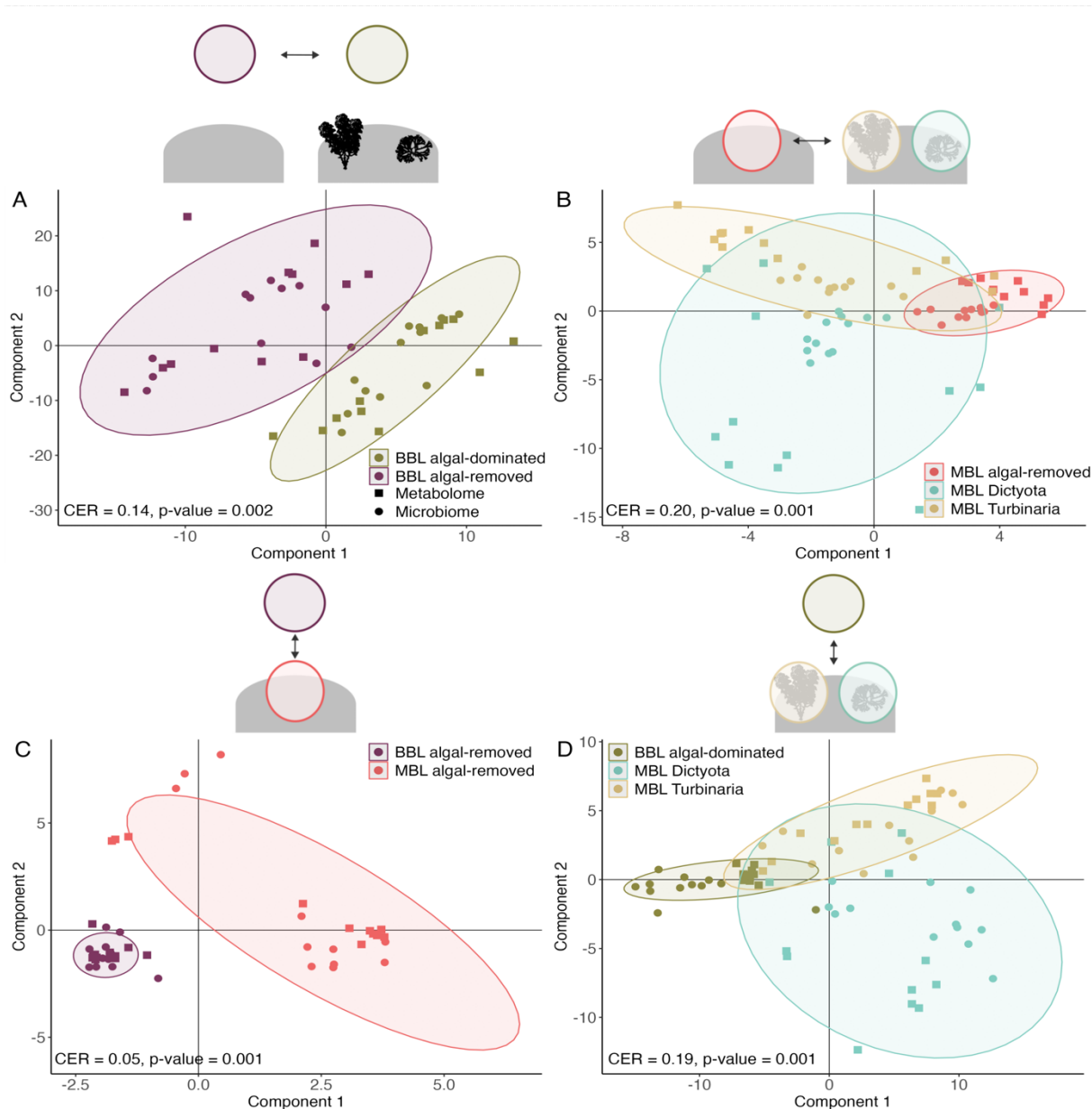


Figure 2.1 | Multiomic composition of reef boundary layers. Score plots of the multi-block PLS-DA (DIABLO) performed on metabarcoding and metabolomic data between (A) benthic boundary layers, (B) momentum boundary layers, (C) algal-removed waters and (D) algal-dominated waters. Analyses were validated by a permutation test based on cross-model validation, the CER represents the proportion of misclassification and a $P < 0.05$ indicates that the clustering was not obtained by chance alone. Ellipses are 95% data ellipses. Reef water types are abbreviated and colored as in the experimental design figure (Fig. S2). Individual PLS-DA are shown in Fig. S5.

2.4. Dominant microbial taxa across boundary layers and algal treatments

Planktonic microbial communities comprised 38 phyla, of which 3 belonged to the Archaea, 235 families and 457 genera. The family Cyanobiaceae (e.g., *Prochlorococcus*) was, by far, the most abundant, followed by the Actinomarinaceae (e.g., *Candidatus Actinomarina*), Alteromonadaceae (e.g., *Alteromonas*), Flavobacteriaceae (NS4 and NS5 marine groups), as well

as the AEGEAN-169 marine group and the SAR86 and SAR116 clades (*SI Appendix*, Fig. S7 *A* and *B*). To identify which genera best explained the microbial composition of the five reef water types, we investigated the VIP scores obtained in the former PLS-DA (*SI Appendix*, Fig. S5 *A* to *D*). A total of 409 genus-level ASVs discriminated the reef water types. We focused on the top 50 ASVs obtaining the highest sum of VIP scores across the four PLS-DA (Fig. 2.2; *SI Appendix* Supplementary Methods). Among them, 32 ASVs belonged to the class Alphaproteobacteria, 10 to the Gammaproteobacteria and 2 to the Bacteroidia. Within the 24 highlighted families, the Rhodobacteraceae alone comprised 10 genera, followed by the Spingomonadaceae and the Rhizobiaceae with 6 and 4 genera, respectively. The two BBLs and the algal-removed MBL comprised a distinct set of discriminant ASVs, while the two algal-dominated MBLs shared a substantial number of ASVs. Algal-dominated BBL and MBLs were enriched in the Gammaproteobacteria *Legionella*, two Bacteroidia *Leeuwenhoekiella* (family Flavobacteriaceae) and *Owenseekia* (Cryomorphaceae) and some Alphaproteobacteria, such as *Epibacterium* (Rhodobacteraceae). Several ASVs belonging to the genera *Pseudobacteriovorax* (class Oligoflexia), *Sphingobium* (Alphaproteobacteria) and *Spongiispira* (Gammaproteobacteria) were characteristic of both BBLs. In the algal-removed BBL, the discriminant ASVs were mostly affiliated to the class Alphaproteobacteria (e.g., the genera *Nitratireductor* and *Oricola* from the family Rhizobiaceae). Several ASVs were characteristic of both the algal-removed BBL and the algal-dominated MBLs, among them five genera from the family Rhodobacteraceae (e.g., *Nautella*, *Roseovarius*), an unclassified Nitriliruptoraceae *Gimesia* (phylum Planctomycetes) and the Polyangial *Sandaracinus*. *Dictyota* MBL was particularly enriched in ASVs belonging to the Gammaproteobacteria (*Legionella*, *Oceanococcus*) and in one Candidatus *Urbacteria* (ABY1). Comparatively, the most discriminant ASVs of *Turbinaria* MBL belonged essentially to the Alphaproteobacteria (e.g., the Rhodobacteraceae *Aestuariicoccus*, *Nautella* and *Sagittula*) and Gammaproteobacteria (e.g., the Alteromonadeaceae *XY-R5*) classes. Numerous ASVs from the Alphaproteobacteria class were enriched in the two algal-dominated MBLs including the genera *Croceicoccus* (Spingomonadaceae), *Henriciella*, *Maricaulis*, (Hyphomonadaceae) and *Pelagibaca* (Rhodobacteraceae). These MBLs also harbored a high abundance of ASVs belonging to the Gammaproteobacteria class, such as the genera *Alcanivorax*, *Halomonas*, *Idiomarina* and *Marinobacter*. Finally, fewer ASVs characterized the algal-removed MBL. These were affiliated with the genera *Aestuariicoccus*, *Mameliella*, *Roseitalea* and *Sagittula* from the Alphaproteobacteria class and *Trichodesmium* from the Cyanobacteria (Fig. 2.2).

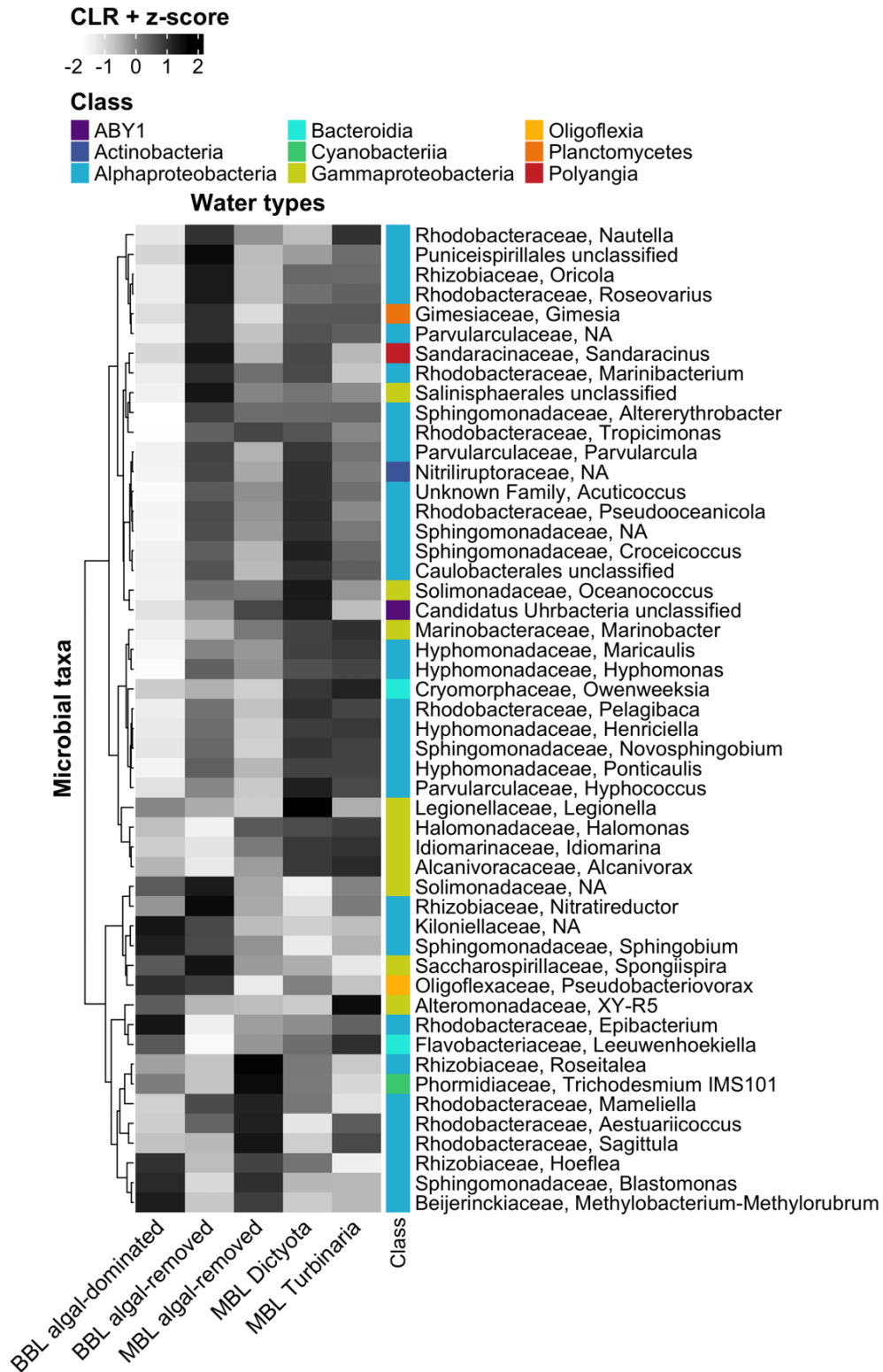


Figure 2.2 | Reef waters-associated discriminant microbial taxa. Benthic boundary layers (BBL) were collected above algal-dominated and algal-removed bommies. Momentum boundary layers (MBL) were associated to algal-removed substrate or above macro-algal species: *Dictyota bartayresiana* and *Turbinaria ornata*. Microbial ASVs are at the genus-level and labeled at the family and genus level when possible or at the lowest level achievable (e.g., order, phylum). ASVs are colored according to their microbial class and clustered according their mean CLR transformed abundances across the five water types using Euclidian distances and Ward's minimum variance method. Data was scaled by mean-centering and dividing by the standard deviation.

2.5. Diffusion pattern of macroalgal metabolites across boundary layers

To explore the diffusion of algal-derived metabolites into the algal boundary layers, we built a quantitative table including the 3943 MS1 features after data filtration from algal whole tissue, surface and water (i.e., algal-dominated BBL, *Dictyota* and *Turbinaria* MBLs) samples. PLS-DA indicated that both species exhibited relatively similar metabolomic differences among sample types (Fig. 2.3 A and B; *Dictyota*: CER = 0.11, $P < 0.001$; *Turbinaria*: CER = 0.13, $P < 0.001$). On the 1st component, metabolite features from algal surfaces and whole tissues clearly clustered apart from the water samples, while the 2nd component separated the algal surface and water samples from the whole tissue samples. Whole tissue and surface specific chemical signatures were confirmed by a substantial number of unique metabolites detected in each sample type (Fig. 2.3 B). Interestingly, a substantial proportion (~30%) of metabolites were shared across all sample types for both algal species. Molecular gradients have been demonstrated in coral-associated boundary layers (Ochsenkühn et al., 2018). We hypothesized that algal compounds would diffuse across boundary layers according to their polarity, with hydrophobic compounds more likely to be retained close to producing organisms and polar compounds more likely to move across boundary layers. By using compounds chromatographic retention time through the HPLC column, as a proxy for their polarity (i.e., in reverse phase column more polar compounds tend to be eluted first) and as far as extraction methods can be compared, we found a progressive decrease in retention time from the algal whole tissue to the algal-dominated BBL, supporting our hypothesis (Fig. 2.3 C, Kruskal-Wallis test, $P < 0.05$; Dunn post-hoc test, $P < 0.05$).

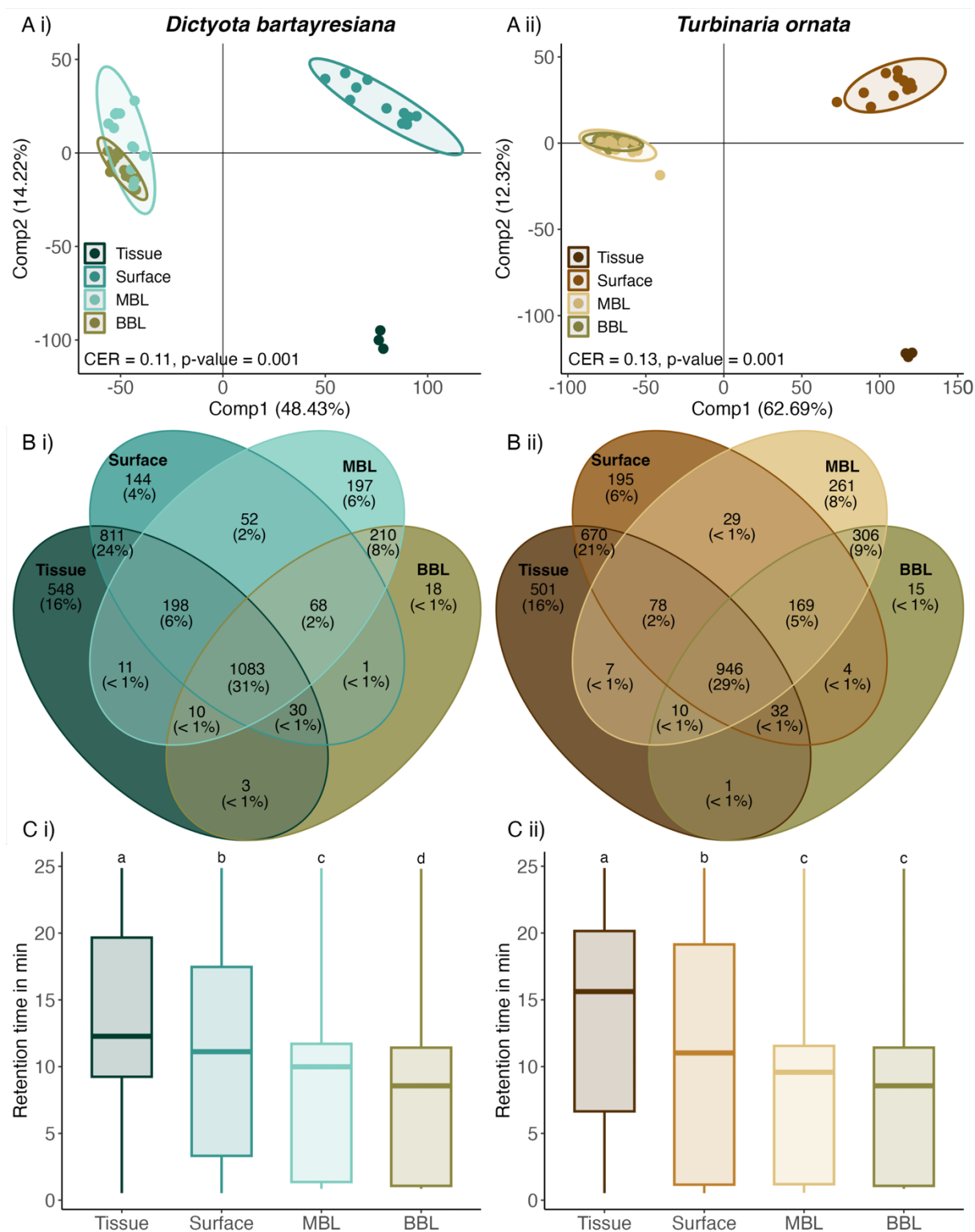


Figure 2.3 | Analysis of algal metabolites diffusion into the water column for (i) *Dictyota bartayresiana* and (ii) *Turbinaria ornata*. (A) PLS-DA score plots of MS1 features with ESI+ MS/MS fragmentation spectra (n = 2214 features) showing metabolomic profiles clustered according to algal whole tissues, surfaces, MBLs and BBL. Metabolites relative peak areas were CLR-transformed and mean-centered. CER and associated p-values were obtained by cross-model validation and permutation tests. Ellipses are 95% data ellipses. (B) Venn diagrams of MS1 features in whole tissues, surfaces and MBLs of *Dictyota* (n = 3444) and *Turbinaria* (n = 3224) and algal-dominated BBL (n = 1661). (C) Mean (\pm standard error) retention time in minutes using UHPLC reverse phase column of MS1 features. Lettering indicates significantly difference using Dunn test's posthoc, $P < 0.05$

2.6. Broad molecular classification of diffusing algal-derived metabolites

The Feature-Based Molecular Network analysis on GNPS (Wang et al., 2016; Nothias et al., 2020) grouped the 4585 initial MS1 features with MS2 fragmentation spectra into 436 subnetworks based on their spectral similarity (i.e., molecular clusters of alike features; Fig. 2.4 A), of which 2214 clustered into 256 subnetworks after filtration (*SI Appendix* Supplementary Methods). To highlight relevant subnetworks of diffusing algal-derived metabolites, we hypothesized that molecules are produced in algal whole tissue and/or surface and gradually diffuse in the upper water layers (i.e., presence in the MBL and, possibly, the BBL). Therefore, we selected, for each algal species, subnetworks that had at least 3 discriminant features (i.e., VIP score > 1), or at least 1 feature with a VIP score superior to the median (for subnetworks with less than 3 features or features without any affiliated subnetwork), that were at least detected in either or both whole tissue or surface and in the MBL (*SI Appendix*, Supplementary Methods). Out of 58 subnetworks obtained, 20 and 13 were exclusively associated to *Dictyota* and *Turbinaria*, respectively (Fig. 2.4 A; *SI Appendix*, Tab. S2). Each subnetwork was broadly classified using the ClassyFire ontology (Feunang et al., 2016) via MolNetEnhancer on GNPS (Ernst et al., 2019) and CANOPUS on SIRIUS (Dührkop et al., 2019, 2021).

Across all samples, benzenoid-related subnetworks were the most abundant comprising about half of the total peak area (Fig. 2.4 C; *SI Appendix*, Fig. S8 A, Tab. S2). Two of them were particularly abundant in both algal-dominated MBLs and BBL (subnetworks 13 & 143 – benzenes derivatives), while subnetwork 26 (phenols) was characteristic of *Turbinaria* surface (*SI Appendix*, Fig. S8 A). Diterpenoids were the most prominent metabolites in *Dictyota*-associated samples (Fig. 2.4 A and C; *SI Appendix*, Fig. S8 B). Their affiliated subnetworks (e.g., subnetworks 115, 103 and 170; Fig. 2.4 B1-3) collectively summed to 16.7%, 7.5%, 4.3% of the total peak areas in *Dictyota* whole tissue, surface and MBL, respectively. Comparatively, they were rare in *Turbinaria* whole tissue and surface (< 0.02% of the total peak areas), but present in *Turbinaria* MBL (1%; *SI Appendix*, Fig. S8). These diterpenoids may be related to spatane and secospatane derivatives with variations in their acetylation and hydroxylation levels: subnetwork 115 (e.g., C₂₆H₃₆O₇, C₂₄H₃₄O₆; Fig. 2.4 B1; *SI Appendix*, Tab. S3 A), subnetwork 103 (e.g., C₁₉H₂₈, Fig. 2.4 B2; *SI Appendix*, Tab. S3 A) and subnetwork 170 (e.g., C₂₀H₂₄O₂, Fig. 2.4 B2; *SI Appendix*, Tab. S3 A). Despite not being flagged as discriminant features, we detected two features with masses and putative formulas very closely matching known allelopathic diterpenoids isolated from *Dictyota* (Schmitt et al., 1998; Takikawa et al., 1998): Crenulacetal C (C₂₄H₃₈O₅, subnetwork 115, Fig. 2.4 B1) and Pachydictyol A (C₂₀H₃₂O,

subnetwork 103, Fig. 2.4 B2; *SI Appendix*, Tab. S3 A). However, we cannot rule out that these features are isomers with different chemical and biological properties. Another subclass of prenol lipids characteristic to *Dictyota* whole tissue and surface was affiliated with sesquiterpenoids (subnetwork 493; *SI Appendix*, Fig. S8 C, Tab. S2). For *Turbinaria*, discriminant terpenoids were rather related to carotenoids (e.g., subnetwork 214; Tab. S3 A), summing to 0.3% of the total peak areas. In general, terpenoids showed a diffusion-like pattern with decreasing relative areas from whole tissue to the water (Fig. 2.4 C; *SI Appendix*, Fig. S8 B-C, Tab. S2).

Fatty acyls and glycerolipids in whole tissue and surface samples were three times more abundant in *Turbinaria* compared to *Dictyota*, summing up to 4.6% and 1.5% of the total peak areas, respectively (Fig. 2.4 C; *SI Appendix*, Tab. S2). Subnetwork 51 was the most prominent in *Turbinaria* whole tissue and surface and was related to glyceroglycolipids (*SI Appendix*, Fig. S8 D, Tab. S2) followed by the subnetworks 187 and 89 (Fig. 2.4 B4 and B5; *SI Appendix*, Fig. S8 B, Tab. S2). Subnetwork 187 was composed of monoacylglycerols and diacylglycerols (e.g., DAG (16:0/14:0), $C_{33}H_{62}O_4$), while subnetwork 89 consisted of monogalactosyl diacylglycerol (e.g., MGDG (18:1/16:0), $C_{43}H_{80}O_{10}$; Fig. 2.4 B4; *SI Appendix*, Tab. S3 A). Interestingly, two features from subnetwork 89 were annotated as sulfoquinovosyl diacylglycerol (e.g., SQDG (34:2), $C_{43}H_{78}O_{12}S$; *SI Appendix*, Tab. S3 A). In contrast, three subnetworks of these classes were noticeably more abundant in algal-dominated MBLs and BBL than in whole tissue and surface (subnetworks 67, 131, 137; *SI Appendix*, Fig. S8 D, Tab. S2). For example, subnetwork 137 was associated to lyso-betaine lipids (e.g., Lyso DGCC (22:6), $C_{32}H_{51}NO_7$; Fig. 2.4 B6; *SI Appendix*, Tab. S3 A). Discriminant features of glycerophospholipids were detected in four subnetworks and were less prominent in algal whole tissue and surface than the previously discussed lipid classes, making up to 0.1% and 0.04% of total peak areas for *Turbinaria* and *Dictyota*, respectively (Fig. 2.4 C; *SI Appendix*, Fig. S8 E, Tab. S2). Subnetworks 138 (phosphatidylcholines) and 336 (phosphatidylglycerols) displayed a diffusion-like pattern, while subnetworks 350 and 570 (phosphatidylcholines) were relatively more abundant in the algal-dominated MBLs and BBL (Fig. 2.4 B7; *SI Appendix* Fig. S8 D). Subnetwork 350 was affiliated to the lysophosphatidylcholines (e.g., Lyso-PC (20:5), $C_{28}H_{48}NO_7P$; Tab. S3 A). Features annotated as organooxygen compounds, organonitrogen compounds, carboxylic acids (e.g., subnetwork 717; Fig. 2.4 B8; Tab. S3 A) and piperidines were generally more abundant in algal-dominated MBLs and BBL than in whole tissue and surface, though some variation among subnetworks occurred (Fig. 2.4 C; *SI Appendix*, Fig. S8 G-I, Tab. S2). Indoles (subnetwork 369; Fig. 2.4 C; *SI Appendix*, Fig. S8 J) were represented within a single

subnetwork characterizing the surface of *Dictyota* and *Turbinaria*.

Additionally, we investigated the subnetworks in negative ionization mode. The dataset was less than half the size of the dataset in positive mode with 1029 features and 83 subnetworks after filtration. A total of 22 and 18 subnetworks were selected for *Dictyota* and *Turbinaria*-associated samples, respectively. Fewer molecular classes could be resolved and only 8 subnetworks could be annotated. Features identified as organooxygen compounds (subnetworks 55 and 126; e.g., Mannitol library match; *SI Appendix*, Tab. S3 A) were the most prominent in the algal whole tissue and surface samples with peaked intensities in the latter. Summed together, these features comprised 38.2% and 41.4% of the total peak areas for *Dictyota* and *Turbinaria*, respectively (*SI Appendix*, Fig. S9). Globally, compound class identities and their diffusion pattern mirrored what had been previously observed in positive ionization mode.

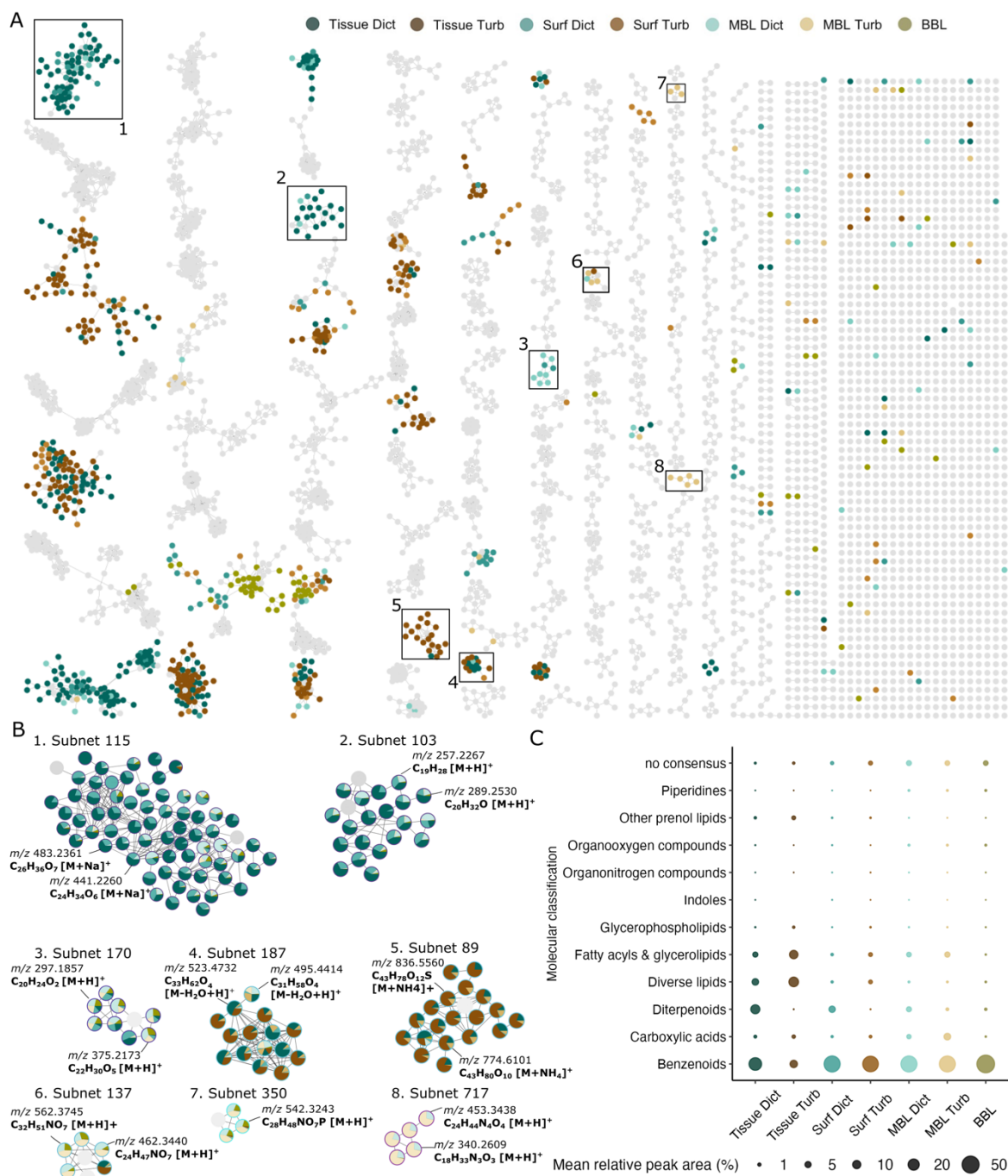


Figure 2.4 | Molecular classification of subnetworks with discriminant features found in the algal metabolomes and associated waters. (A) Molecular network of all MS1 features (nodes) with MS/MS fragmentation linked by a cosine score > 0.7 (edges). Nodes are colored by the sample type in which their relative abundance was the highest. Examples of subnetworks of interest with discriminant features found in whole tissue & surface layers (BBL – benthic & MBL – momentum) of the two algal species *Dictyota bartayresiana* and *Turbinaria ornata* are boxed 1 to 8. (B) Boxed subnetworks details in which nodes are colored by their mean relative intensities (i.e., peak areas) in each sample type. (C) Mean of summed features relative intensities of subnetworks of interest across sample types according to their consensus Classyfire ontology derived from MolNetEnhancer (GNPS) and CANOPUS (SIRIUS).

2.7. Co-variation of algal-associated metabolites and microorganisms

To further investigate the association between previously identified discriminant metabolites ($n = 316$ features) and microorganisms ($n = 207$ genera), we integrated metabolomic and metabarcoding data from both algal MBLs using the multi-block PLS-DA analysis DIABLO (Singh et al., 2019). We excluded the algal-dominated BBL to address species-specific differences within the same boundary layer and avoid confounding factors. DIABLO revealed a strong association between the metabolome and the microbiome of algal MBLs with a distinct cluster for each algal species (correlation coefficient > 0.95 ; *SI Appendix*, Fig. S10). The analysis selected 26 metabolites and 27 ASVs with a strong correlation coefficient (< -0.7 or > 0.7) and resulted in a bipartite network comprising three clusters (Fig. 5). In the first cluster (Fig. 2.5 A), 22 ASVs were involved in relationships with various metabolites. Two diterpenoids (*SI Appendix*, Tab. S3 B), an organonitrogen compound, an organooxygen compound, a piperidine ($C_{14}H_{18}N_2O$), a carboxylic acid ($C_{11}H_{22}N_2O$) and the Lyso-PC (20:5) were negatively correlated with diverse ASVs including the genera *Alistipes*, *Eilatimonas*, *Rikenella*, and *Roseibacterium*, and two unclassified taxa from the Desulfovibrionaceae and Victivallaceae families. These ASVs were also involved in positive relationships with a peptide ($C_{18}H_{33}N_3O_3$, subnetwork 717), that might be related halolitoralin, and a glycerophospholipid. Another diterpenoid was negatively correlated with ASVs belonging to the genera *Ketobacter*, *Mycobacterium* and *Pseudoceanicola* which were positively correlated to organonitrogen and organooxygen compounds and the carboxylic acid. These compounds interacted also positively with ASVs belonging to the genera *Acanthopleuribacter* and *Hyphomonas*. *Tropicibacter* was negatively correlated with an organonitrogen compound and an unknown metabolite connecting a second part of the cluster comprising ASVs belonging to the genera *Roseovarius*, *Ponticaulis* and a Patescibacteria (JGI 0000069-P22). The second cluster (Fig. 2.5 B) comprised lipids such as the SQDG (14:0/18:4) and the MGDG (16:3/20:5) and an amino acid ($C_6H_{16}N_4O_2$) which interacted negatively with *Citreicella* and *Oleibacter*. A second unclassified Saccharospirillaceae were positively correlated with SQDGs. The third cluster (Fig. 2.5 C) included only negative correlations between diterpenoids and XY-R5. Two of these diterpenoids belonged to the subnetwork 115: $C_{26}H_{34}O_6$ and $C_{26}H_{36}O_7$ (*SI Appendix*, Tab. S3 A and B). These metabolites were more abundant in *Dictyota* MBL, while XY-R5 was more abundant in *Turbinaria* MBL. In contrast, *Calorithrix* was positively correlated with two of these metabolites and was enriched in *Dictyota* MBL.

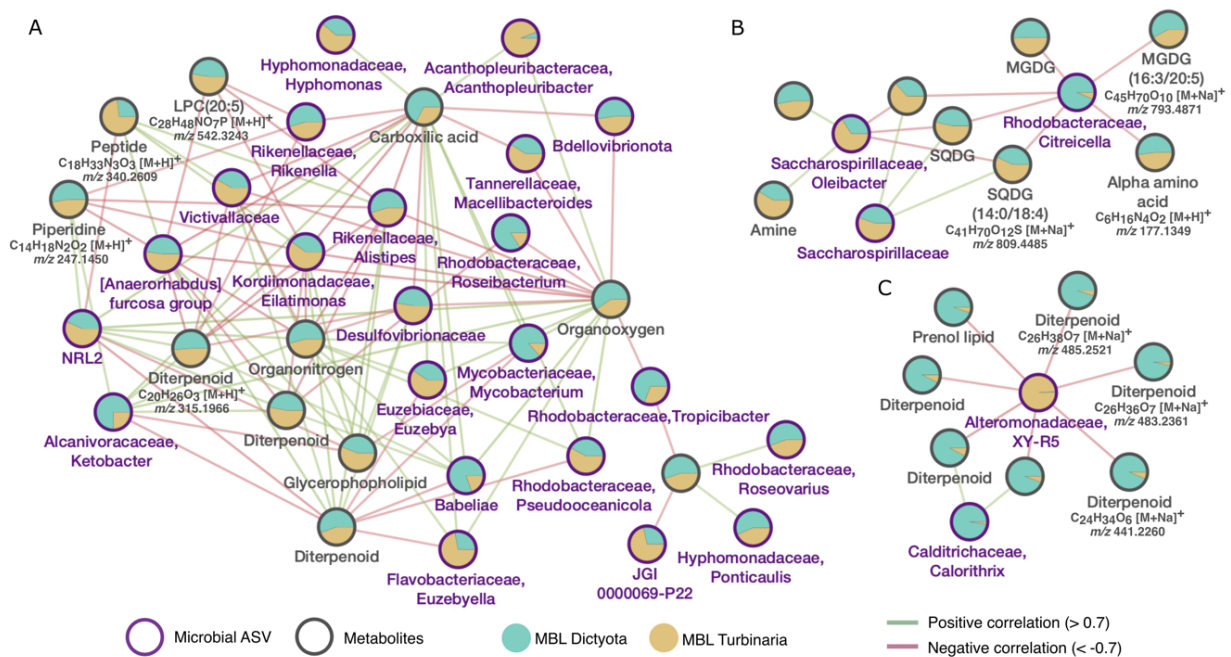


Figure 2.5 | Co-variation of discriminant microbial ASV and molecular features in algal momentum boundary layers. Bipartite correlation network obtained from DIABLO analysis and visualized on Cytoscape. A correlation threshold was set to 0.7 resulting in three clusters A, B and C. Nodes are contoured according to their type (i.e., ASVs in purple and metabolites in grey) and colored by their mean relative intensities (i.e., peak areas) in the MBL of *Dictyota bartayresiana* and *Turbinaria ornata*.

3. Discussion

The data presented herein contribute to further unveil the identity and distribution of metabolites and microbes in reef waters. Our results demonstrate that chemical and microbial waterscapes around coral bommies are spatially structured, both vertically and horizontally, according to macroalgal dominance and boundary layers. Pelagic microbial communities were taxonomically structured with an enrichment of copiotrophic bacteria in algal-dominated waters. The resolution of compound class identities revealed that macroalgae are surrounded by a distinct chemical pool of diverse lipids classes (e.g., prenol lipids and glycerolipids) and labile organic matter (e.g., organooxygen compounds and carboxylic acids). Several of these compounds showed a diffusion profile, with decreasing relative abundance from the whole tissue to the BBL. Data were consistent with the hypothesis that hydrophobic compounds remain close to emitters, while polar compounds move across boundary layers. In addition, microbiome-metabolome data integration highlighted strong co-variations of algal-associated metabolites and microbes, overall suggesting that macroalgae release chemicals which select for specific planktonic microbial communities.

Multiomic signature of coral reef waters: an interplay between benthic-driven water biogeochemistry and hydrodynamics. Microbial assemblages differed between underlying benthic members in both MBL and BBL (Fig. 2.1). Similar results have been observed at the organismal (Tout et al., 2014; Walsh et al., 2017; Weber et al., 2019) and reef (Wegley Kelly et al., 2014; Haas et al., 2016; Frade et al., 2020; Becker et al., 2023) scales. We observed concurrent changes in the metabolomic composition of MBL and BBL, supporting that microbial communities respond to benthos-derived chemical pools (Nelson et al., 2013; Quinlan et al., 2019; Weber et al., 2022). Specifically, differences between *Turbinaria* and *Dictyota* MBLs provide evidence of a strong species-specificity in the interaction between macro- and microorganisms. Algal exudates are characterized by high DOC quantity, dissolved sugar content, lability, as well as distinct elemental stoichiometry and nutrient contents (Haas et al., 2011; Nelson et al., 2013; Wegley Kelly et al., 2022). While incubation and mesocosm experiments have experimentally demonstrated the selective pressure of benthic-derived exudates on microbial growth (Nelson et al., 2013; Weber et al., 2022), our integrative approach shows that this tight microbe-chemical coupling occurs within each boundary layer under real flow condition. Each boundary layer had its own multiomic signature whether sampled above algal-dominated or algal-removed bommies (Fig. 2.1). This spatial structuration has previously been observed in microbial communities (Tout et al., 2014; Walsh et al., 2017; Weber et al., 2019). However, some studies did not detect differences between surface and benthic waters in microbial assemblages (Silveira et al., 2017b) and chemistry (Weber et al., 2020), possibly due to differences in sampling location and/or volume. The vertical separation between BBL and MBL was likely driven by water movement over benthic surfaces and by concentration gradients of benthic organic matter (Shashar et al., 1996; Ochsenkühn et al., 2018; Davis et al., 2021). The difference in the multiomic signature of the BBL between algal-dominated and algal-removed bommies suggests that, although reef currents are expected to homogenize upper water layers, the presence of canopy-forming macroalgae, such as *Turbinaria* and *Sargassum*, could reduce flow velocity and increase turbulence leading to the retention of molecules and bacteria within the algal-dominated BBL (Shashar et al., 1996; Ghisalberti & Nepf, 2006). Together, our results show a high specificity in the interaction between benthic-derived organic matter and microbes that is strongly modulated by ambient hydrodynamics, resulting in a remarkable small-scale spatial heterogeneity of microbial and chemical waterscapes.

Spatial structuration of planktonic microbial communities: implications for reef biogeochemical processes. Microbial activity underpins reef functioning through the recycling

and remineralization of organic matter (O'Neil & Capone, 2008; Silveira et al., 2017a; Nelson et al., 2023). In our study, microbial assemblages were dominated by the autotrophic Cyanobiaceae family (e.g., *Prochlorococcus*) and several heterotrophic taxa, such as the Actinomarinaceae family, SAR11 and SAR86 clades, AEGEAN-169 marine group, all ubiquitous taxa of reef waters optimized for oligotrophic lifestyles (Swan et al., 2013; Brown et al., 2014; Frade et al., 2020; Glasl et al., 2020; Apprill et al., 2021). Additionally, we detected several copiotroph families characteristic of inshore reefs, including Alteromonadaceae, Cryomorphaceae, Flavobacteriaceae, Hyphomonadaceae, Rhodobacteraceae and Sphingomonadaceae (Wegley Kelly et al., 2014; Haas et al., 2016; Frade et al., 2020; Apprill et al., 2021). Particularly, the enrichment of Flavobacteriaceae and Cryomorphaceae (Bacteriodia) have often been described as indicative of high macroalgal cover and signs of reef microbialization (Haas et al., 2016; Frade et al., 2020; Glasl et al., 2020). The high energy gained from algal-derived organic matter may have enhanced the growth of these copiotrophs, which may disrupt nutrient fluxes throughout the coral reef food web (Haas et al., 2016; Wegley Kelly et al., 2022; Nelson et al., 2023). Furthermore, our results show that the microbial assemblages characterizing the different reef waters were taxonomically structured (Fig. 2.2), suggesting some metabolic specializations to the available chemical pools (Nelson et al., 2013; Tout et al., 2014; Walsh et al., 2017; Weber et al., 2019). Indeed, most of the discriminant taxa were aerobic chemoorganoheterotrophs requiring organic substrates for growth and energy. For example, the genera *Croceicoccus* and *Hoeflea* abundant the algal-dominated MBL and BBL, respectively, can metabolize mannitol as their carbon source (Jung et al., 2013; Wu et al., 2016). Algal-dominated MBLs and BBL were discriminated by the abundance of several copiotrophic bacteria capable of degrading complex OM, such as *Idiomarina*, *Leeuwenhoekiella*, *Owenweeksia* and *XY-R5* (Alteromonadaceae). These genera or their families have been associated with algal DOM and reefs with high nutrient loads and macroalgal cover (Nelson et al., 2013; Wegley Kelly et al., 2014; Frade et al., 2020). Additionally, several DMSP-degrading bacteria were enriched in algal-removed (e.g., *Sagittula* and *Mameliella*) and algal-dominated MBLs (e.g., *Marinobacter* and *Idiomarina*). DMSP is a significant substrate for bacterioplankton (Fernandez et al., 2021), which is produced by coral and algal-associated bacteria (Broadbent et al., 2002; Raina et al., 2010), as well as free living taxa, including *Pelagibaca* and *Pseudoceanicola* (Liu et al., 2021), two Rhodobacteraceae enriched in MBLs. Nitrogen transformation on coral reefs is complex and largely mediated by microbial activity (O'Neil & Capone, 2008) and some of the detected taxa may be involved in these processes, such as *Nitratireductor* and *Aceticoccus* (Cai et al., 2018). While our results would have

benefited from metagenomic or metatranscriptomic data, they suggest that reef boundary layers harbor taxa with wide metabolic strategies playing pivotal roles in reef biogeochemical cycles.

Macroalgal-dominated waterscapes are enriched with microbes associated to reef degradation. Our results support that fleshy macroalgae disrupt planktonic microbial communities at the scale of coral bommies within a single reef. An extensive body of literature has demonstrated that macroalgal-dominated reefs harbor microbial communities with opportunist copiotrophic taxa encoding for virulence genes, including members of the Gammaproteobacteria and Bacteroidia classes (Nelson et al., 2013; Wegley Kelly et al., 2014; Haas et al., 2016; Frade et al., 2020). Concurrently with these studies, genera from these two classes were essentially enriched in algal-dominated MBLs and BBL, including *Legionella*, previously associated with diseased coral holobionts or reefs exposed to sewage (Chiou et al., 2010; Ziegler et al., 2016; Gignoux-Wolfsohn et al., 2017). Several taxa characteristic of algal-dominated MBLs are suspected to be coral (Sunagawa et al., 2009; Godwin et al., 2012; Morrow et al., 2017; MacKnight et al., 2021) and algal (Wang et al., 2008; Fernandes et al., 2011; Zozoya-Valdès et al., 2017) pathogens and opportunistic bacteria, as well as abundant members of disturbed reefs (Wegley Kelly et al., 2014; Zaneveld et al., 2016; Ziegler et al., 2016; Bulleri et al., 2018), among them *Halomonas*, *Leeuwenhoekiella*, *Maricaulis* and *Nautella* (Fig. 2.2). However, some taxa (e.g., *Halomonas*) can be beneficial bacteria (Rosado et al., 2019), which calls for cautious interpretation based solely on taxonomic affiliations. Comparatively, microbial communities in the algal-removed MBL were enriched in *Roseitalea* and *Mameliella*, two probiotic bacteria of corals and Symbiodiniaceae (Maire et al., 2021; Zhang et al., 2021). As such, boundary layers surrounding macroalgal-dominated bommies support microbes associated to reef degradation and coral demise. However, the extent to which these algal-associated microbes are detrimental to neighboring corals requires further investigation.

Resolving the chemistry of algae and their boundary layers. The observed differences between the surface- and endo-metabolome of *Turbinaria* and *Dictyota* are consistent with previous studies demonstrating metabolomic variation within algal thallus (Parrot et al., 2019). Specifically, the surface metabolome lied between the endometabolome and the two boundary layers (i.e., the MBL and BBL) for both algal species (Fig. 2.3 A and B), highlighting holobiont surfaces as key interaction zones between the host, its epibiont community and its surrounding environment (Ochsenkühn et al., 2018; Wichard & Beemelmanns, 2018). These zones are the

first line of defense where holobiont-derived metabolites mediate biofilm formation, prevent microbial colonization, and intervene in allelopathic interactions (Lachnit et al., 2013; Othmani et al., 2016; Longo & Hay, 2017). Produced metabolites can diffuse away in the water column (Ochsenkühn et al., 2018). In our study, patterns of molecular abundance and chromatographic retention times from the algal endometabolome to upper water layers indicate the diffusion of algal-derived metabolites into the water column according to their polarity. This finding supports that lipophilic compounds will act on contact or diffuse at a very short distance, while medium polar or hydrophilic compounds will have a wider range of detection and potential activities.

Using spectral library matches and *in silico* annotations, we attempted to resolve the molecular classification of detected metabolites, improving our knowledge about the composition and distribution of OM on coral reefs. Specifically, we detected several subnetworks with limited diffusion in the water column, which were more abundant in the tissues and surfaces of *Dictyota* and *Turbinaria* than in the boundary layers. These include putative defense metabolites, such as sesquiterpenoids (subnetwork 493) and carotenoids (subnetwork 214), known to inhibit bacterial settlement (Lachnit et al., 2013; Othmani et al., 2016), as well as indoles (subnetwork 369), phosphatidylcholines (subnetwork 138) and sulfolipids (SQDG – subnetwork 89) identified as antibacterial (Guschina & Harwood, 2006; Heavisides et al., 2018; Wibowo et al., 2022) and cytotoxic compounds (Slattery & Lesser, 2014). As expected, diterpenoids constituted a prominent group of metabolites associated with *Dictyota* (Fig. 2.4; Chen et al., 2018). Macroalgal diterpenes display various bioactivities, including cytotoxic potency against corals and invertebrate larvae and herbivore deterrence (Schmitt et al., 1998; Barbosa et al., 2004; Rasher et al., 2011). While their toxicity could be constrained to surface-mediated interactions due to the additive effect of multiple compounds and limited water solubility (Rasher et al., 2011; Slattery & Lesser, 2014), we detected them in both boundary layers surrounding macroalgal-dominated bommies and their abundance negatively correlated with several bacteria in the MBL (Figs. 2.4 C and 2.5). These results support that macroalgal diterpenes could significantly structure microbial communities in the water column. Surprisingly, they were also abundant in the MBL of *Turbinaria*, likely due to the presence of epiphytic *Dictyota* on *Turbinaria* thalli, supporting a chemically-mediated associational benefit between both species to escape predation (Pereira et al., 2010). Benzenoids dominated the chemical pool of water samples (Fig. 2.4 C). They represent major volatile compounds produced by diverse organisms such as phytoplankton (Zuo, 2019) and are abundant in turf and coral exometabolomes (Wegley Kelly et al., 2022), which may explain

their high abundance in the boundary layers. Benzenoids can act as defense molecules against grazers, pathogens or epiphytes (Amsler & Fairhead, 2005). We abundantly detected betain lipids and glycerophospholipids in their lyso forms (lyso DGCC - subnetwork 137 and lysoPC – subnetwork 350) in the MBLs and BBL, potentially due to their structural property (e.g., a single fatty acid with a polar head) making them more hydrophilic (Heringdorf, 2008). Organooxygen compounds made up a significant proportion of algal exometabolomes and may represent important growth substrates for microbial life (Nelson et al., 2013).

Despite a broad classification system, our results demonstrate that coral reef macroalgae release a variety of compounds potentially involved in defensive and competitive interactions, as well as in microbial energetics (Schmitt et al., 1998; Rasher et al., 2011; Wegley Kelly et al., 2022). However, minor modifications in the structure of compounds can change their bioactivity, making the prediction of their effects solely based on their class identities ambitious (Dworjanyn et al., 1999). Future research should encompass the specific isolation of these compounds and bioassays to understand their role in microbial processes and interspecific interactions. Importantly, only a fraction of the chemical pool can be successfully retrieved as the successive steps of extraction, ionization, fragmentation and annotation narrow down the diversity of compounds that can be studied, leaving an immense unknown “dark” fraction (da Silva et al., 2015). Although marine DOM has often been characterized using Bond Elute PPL cartridges (Varian Bond Elut, Agilent Technologies, USA; Dittmar et al., 2008; Petras et al., 2017), we have used Strata XL (Phenomenex, USA) resin for its capacity to retain a wide range of compounds and its previously reported ability to recover metabolites from reef aquaria and marine algae *in-situ* (Zendong et al., 2014; Guibert et al., 2019). While the recent advent of *in silico* tools have revolutionized compound dereplication, achieving a confident annotation, even at a broad level, remains highly challenging. In the marine environment, spectral libraries are particularly scarce, leaving many compounds unidentifiable (da Silva et al., 2015; Petras et al., 2017). Multiomics will be greatly improved once the scientific community will alleviate this major restriction of marine metabolomics.

Co-variation of metabolites and microorganisms within the algal MBL. Through the integration of metabarcoding and metabolomic data in a bipartite network, we were able to identify covariation patterns between metabolites and microbes within the MBL of two macroalgal species (Fig. 2.5). As we favored compounds that were algal-derived, the observed interactions may be indicative of defensive interactions (e.g., antifouling; Othmani et al., 2016), microbial metabolism (Nelson et al., 2013) or chemotaxis (Tout et al., 2015; Wichard &

Beemelmans, 2018). Utilization of compounds by planktonic bacteria may be expressed as positive correlations. For example, in our first cluster (Fig. 2.5 A), organooxygen and organonitrogen compounds and carboxylic acids can be used as growth and energy sources (Lory, 2014; Pujalte et al., 2014). Chemotaxis is a microbial behavior which has been previously demonstrated in coral reef bacteria (Tout et al., 2015) and which is essential in mediating ecological interactions between bacteria and alga (Wichard & Beemelmans, 2018). Hyphomonadaceae, Rhodobacteraceae and Flavobacteriaceae are families known to display positive chemotaxis with carboxylic acids (e.g., amino acids, peptides) which may explain the positive correlations observed. In addition, metabolites may be of bacterial origin such as the cyclopeptide positively correlated with four bacterial genera. This compound could be related to halolitoralin, an antifungal cyclopeptide produced by marine bacteria (Yang et al 2002). In the second cluster, the negative correlations with SQDG could reflect their degradation by bacteria (Wei et al., 2022), although those lipids are also known to inhibit microbial growth (Furukawa et al., 2007). In the 1st and third clusters (Fig. 2.5 A and C), negative correlations with diterpenoids could indicate anti-adhesion and antibacterial properties (Othmani et al., 2016; Chen et al., 2018). Nevertheless, we cannot rule out that these correlations are not causal. Without a better annotation of unknown compounds and improved knowledge of coral reef microbes, it will remain challenging to determine the nature of microbe-metabolite interactions.

Conclusion. Capturing the chemical and microbial signatures of coral reef waters is an important step towards understanding microbe-metabolite interactions and how benthic communities mediate these interactions. This study demonstrates that macroalgal assemblages can modify chemical and microbial waterscapes within a single reef. The taxonomic composition of the microbial communities gave insights into the spatialization of reef biogeochemical processes and revealed an enrichment of copiotrophic bacteria characteristic of stressed corals and altered reef states in two boundary layers overlying macroalgal-dominated bommies. By characterizing the broad molecular classification of algal-derived metabolites, this work participates in the description of the chemodiversity on coral reefs and improves our understanding of water-mediated transport of chemical compounds and their roles as structuring and functioning elements. While our results remain preliminary in deciphering the microbial and chemical pools on reefs, they provide leads for more targeted research to assess the scale at which coral reef macroalgae compete with neighboring organisms through waterborne mediators.

4. Materials and Methods overview

This study took place in the fringing reef of Mo'orea, French Polynesia. Six coral bommies were assigned randomly to either one of the two treatments: i) algal-removed or ii) algal-dominated (*SI Appendix*, Fig. S1). After a six-month acclimation period following macroalgal removal, we sampled the BBL (~50 cm above the substrate) of each bommie and the MBL (~5 cm above the substrate) of bare substrate on each algal-removed bommie, as well as of substrates dominated by either *D. bartayresiana* or *T. ornata* on each algal-dominated bommie (*SI Appendix*, Fig. S2). Samples were collected in duplicate for a total of 12 samples for each water type to concurrently analyze their microbiome and chemical composition. To investigate whether compounds detected in algal-associated waters were algal-derived, we sampled surfaces (n = 12 samples) and whole tissues (n = 3 samples) of each algal species on algal-dominated bommies. Sampling was repeated four times: December 2020, March 2021, May 2021 & June 2021, at the exception of whole tissues which were sampled once in February 2021. Taxonomy of microorganisms was characterized by the sequencing of the 16S rDNA marker gene on a NovaSeq platform. Chemical extracts were processed for untargeted metabolomics via liquid chromatography-tandem mass spectrometry (LC-MS/MS) and metabolomics data were processed on MZmine 2.53 software (Pluskal et al., 2010). Features annotations were retrieved from network analysis and *in silico* tools via GNPS (da Silva et al., 2018; Nothias et al., 2020) and SIRIUS (Dührkop et al., 2019, 2021). We built a consensus classification between the GNPS and SIRIUS outputs in a conservative approach motivated by a concern of accuracy. Generally, metabolite annotations were achieved at the levels 2/3 of the Metabolomics Standards Initiative (Sumner et al., 2007). Supervised discriminant analysis (PLS-DA) were performed to identify the microorganisms (genus-level ASVs) and metabolites (MS1 features with MS2 fragmentation spectra) best explaining compositional differences between water types and between algal whole tissues, surfaces, MBLs and BBLs. All analyses were performed with positive ionization mode data, except molecular networks which were also investigated in negative ionization mode. We sought to describe the multiomic signature of boundary layers as well as to investigate the relationship between microbes and metabolites within algal MBLs in an integrative data-driven approach using DIABLO (Singh et al., 2019). Detailed methodological descriptions can be found in the *SI Appendix*, Supplementary Methods.

Data and code sharing. Data and R scripts can be downloaded from a Zenodo repository with restricted access: <https://zenodo.org/records/8422550>. Metabarcoding sequence data have been

deposited in the Sequence Read Archive under the accession code PRJNA941779. MS data are all publicly available in the Mass Spectrometry Interactive Virtual Environment (MassIVE) repository [MSV000091424](https://massive.ucsd.edu/MSV000091424). FBMN workflows can be accessed in GNPS with the following links :

<https://gnps.ucsd.edu/ProteoSAFe/status.jsp?task=b9813b77629a4d44994e70febc96d82b;>
<https://gnps.ucsd.edu/ProteoSAFe/status.jsp?task=55e170b22fd84e5ca890c75420566140;>
<https://gnps.ucsd.edu/ProteoSAFe/status.jsp?task=8772ad1163da4a5eab30177b41e39722;>
<https://gnps.ucsd.edu/ProteoSAFe/status.jsp?task=b0086676f483460bbb7f4d7a9b2145fe>

Author contributions. C.P.S and M.M.N designed the research. C.P.S and H.B performed the experiment. C.P.S, D.R and I.B carried out the microbial and chemical lab work. C.P.S and I.B analyzed the data. D.R, S.C, C.C, I.B and M.M.N contributed to instrumentalization and analytical tools. C.P.S and M.M.N drafted the manuscript. All authors contributed to revisions thereafter and gave final approval for submission.

Competing Interest Statement. We declare we have no competing interest.

Acknowledgments. This work was supported with by the French National Research Agency through the project CORALMATES (ANR-18-CE02-0009-01) lead by M.M.N and by a PhD grant from the Ecole Pratique des Hautes Etudes to C.P.S. The authors are grateful to the French Polynesian government and the Papeto'ai district for collection and research permits. We thank the CRIOBE station staff for their assistance on DNA extractions and fieldwork. We also thank Génome Québec Innovation Centre for the preparation and sequencing of the 16S rRNA amplicon library and the MSXM/Bio2Mar technical facilities for the mass spectrometry data acquisition. We are thankful for the assistance of Benjamin J. Callahan on the DADA2 workflow.

5. Supplementary Information

5.1. Supplementary Methods

Study site and experimental set-up

The experiment took place in a shallow fringing reef lagoon (~2 m deep) off the North coast of Mo'orea, French Polynesia (17°29'14.86"S 149°53'0.76"O). In June 2020, six coral bommies with a diameter of 1-2 m were randomly selected within an area of ~2400 750 m² (i.e., 50120 m long x 1520 m wide; Fig S1). Bommies were randomly assigned to one of the two treatments: i) macroalgae present (thereafter referred as "algal-dominated") and ii) macroalgae removed (i.e., including all holdfasts, thereafter, referred as "algal-removed"). Macroalgae were removed from their substratum manually and with wire brushes taking care not to damage other benthic organisms (e.g., sponges, CCA) or to modify the microtopography (e.g., creating cracks). The experimental treatment was maintained through monthly macroalgal removal. Monthly pictures were taken with an Olympus TG4 camera fixed to a 20 x 20 cm quadrat to track benthic cover change over time (n = 5 photographs per bommie per month). Benthic categories included: bare substrate (i.e., no algae or other organisms discernible from the photographs but presumably colonized by microalgae), crustose coralline algae (CCA), cyanobacteria, living hard coral, algal turf (mixed species assemblages of diminutive and filamentous algae < 1 cm in height) and macroalgae (more upright and anatomically complex algae with canopy height > 1 cm). Within the macroalgae group, 8 genera or species were recorded separately: *Amansia rhodantha*, *Chnoospora* spp., *Dictyota bartayresiana*, *Halimeda* spp., *Lobophora* spp., *Padina boryana*, *Sargassum pacificum* and *Turbinaria ornata*. Photographs were analyzed with PhotoQuad (Trygonis & Sini, 2012) and the percent cover of each category was calculated as the number of points identified of that was calculated for each quadrat from 25 random point. category divided by the total number of points in the quadrat (i.e., 25 points). Percent cover was calculated relative to the number of identifiable points (i.e., excluding points falling into cracks, shaded areas).

Following a six-month acclimation period, we sampled the BBL (~50 cm above the substrate) of each bommie, as well as the MBL (~5 cm above the substrate) of bare substrate on each algal-removed bommie, and of substrates dominated by *T. ornata* or *D. bartayresiana* on each algal-dominated bommie (Fig. S2). Water samples were collected in duplicate to concurrently analyze both their microbiome and metabolome composition. Algal surfaces and whole tissues were collected for each algal species on algal-dominated bommie for characterization of their metabolome and comparison with algal boundary layers. Sampling

spanned over 9 days and was repeated four times: December 2020, March 2021, May 2021 & June 2021; except whole tissues which were sampled once in February 2021. The first two samplings were conducted during the Austral summer (November - April), while the last two were done at the beginning of the Austral winter (May – October).

BBL and MBL water collection and processing

BBL samples were collected using 10 L plastic pouches, rinsed 3 times with reef site water prior sampling, ~50 cm above the substrate on top of the bommies. Pouches were emptied of air and opened underwater generating a water inflow. MBL samples were collected using a modified version of the *in-situ* benthic chamber used by Kubanek et al., 2002. We located a patch of macroalgae and placed a 5 L plastic bottle with the bottom removed over it while avoiding contact between the bottle and the macroalgae. The top end of the bottle was connected to a hose leading to a manual bilge pump resting on the boat pouring the pumped water into a 10 L pouch. The inlet of the hose was at ~5 cm distance from the macroalgal thallus in the chamber. Five minutes after placing the chamber over the macroalgae, seawater was pumped for 3 min to rinse the hose and 10 L pouch approximately three times. Water was then pumped during 10 min to obtain 7 L of seawater (~1 L/90 s). To collect algal-removed MBL seawater, the same procedure was applied placing the chamber over bare substrate on the algal-removed bommies. For each water type, two samples were collected successively so that one would be processed for metabolomics and one for metabarcoding. We sampled the same patches over each of the four sampling months. Pouches were kept in a cool box with ice during transport (~15-20 min) back to the laboratory. 5 L samples were processed maximum one hour upon collection and indifferently selected for the type of processing (metabolomics or metabarcoding).

For metabarcoding, 5 L of collected seawater was pre-filtered with 47 mm GF/D glass filters (Whatman) to remove large particles and then filtered on 47 mm 0.2 µm polyethersulfone filters (Sigma). Filters were cut in small pieces with sterile scalpels and petri dishes and stored into 2 mL cryotubes tubes with 1 mL of DNA/RNA Shield (Zymo Research, USA). Samples were left overnight at room temperature and stored at -20 °C until DNA extraction. Prior to filtration, glass jars were sterilized with 10% javel, 90% EtOH and MilliQ and rinsed three times with the water sample to be processed. For metabolomics, 5 L of collected seawater were directly loaded onto Strata-XL solid-phase extraction (SPE) cartridges (2 g/20 mL, Phenomenex, USA) previously conditioned with 20 mL distilled water. Cartridges were fitted onto a vacuum manifold (Supelco) connected to a vacuum pump (Laboport N820, KNF). After

sample loading, cartridges were rinsed with 20 mL distilled water, dried on the vacuum manifold, lyophilized and stored at -20 °C until elution. Additionally, three experimental blank samples were prepared without samples (i.e., only collecting materials) using distilled water to remove contaminants from the data later on. Cartridges of 2 g with loaded BBL and MBL samples were eluted with 13 mL 100% MeOH (HPLC-MS grade) into pre-weighed glass tubes. MeOH were removed by evaporation with a Genevac centrifugal evaporator EZ-2 serie (SP Industrie, Royaume-Uni) and extracts were stored at -20° C until injection.

Algal surface metabolites collection and extraction

Algal thalli were collected in the vicinity of the algal-dominated bommies to avoid impacting the experimental treatment. Ten thalli of *Turbinaria ornata* and a single large patch of *Dictyota bartayresiana* (about 20-25 cm side length) were collected during each of the four sampling periods. Immediately after collection, algae were placed into large zip bags filled with surrounding water and transported into a cool box back to the laboratory. Surface metabolites from each macroalga were extracted within 2 h following collection using a dipping method with MeOH as the extraction solvent (Othmani et al., 2016). Only healthy algal pieces with no biofouling or lesions were selected to avoid the extraction of non-algal and intracellular compounds. *Turbinaria* thalli were gently spin-dried in a salad spinner for 3 x ~20 s (~70 rpm), while *Dictyota* patches were left to dry for a few minutes prior to extraction. Extraction consisted in dipping algal pieces in a watch glass with 10 mL MeOH during 15 s for *Turbinaria* and 10 s for *Dictyota* (Othmani et al., 2016). For repeatability, we choose arbitrary to extract a standard surface of 21.5 cm² corresponding to the surface of a 6 cm diameter Petri dish. Blades from several *Turbinaria* thalli were successively extracted until total covering of the Petri dish surface. For *Dictyota*, we estimated the wet weight of 21.5 cm² of thalli over 10 repeated measures and used the averaged weight (3.538 g) instead of deploying directly *Dictyota* thalli in the Petri dish. Extraction was performed three times and the solvent was pooled into a 50 mL flask. Samples were dried under a rotary evaporator (35 °C - 100 rpm) (RC600, KNF) then stored at -20 °C until preparation for injection. Blank samples were also prepared using only solvent and glassware, one at each of the four sampling sessions. Surface metabolites were then resolubilized in 100% MeOH (HPLC-MS grade) and transferred to pre-weighed glass tubes.

Algal whole tissue collection and extraction

Algal collection was carried out on the 23rd and 24th February 2021. We collected two 1 L zip bags per species in the vicinity of each algal-dominated bommie. On the boat, algae were

rinsed several times (3-4 baths) with ambient seawater to remove sand, microfauna and epiphytes before being flash frozen into carbonic ice. Back in the laboratory, samples were stored at -80 °C. They were freeze-dried and stored at -20 °C until metabolites extraction. Algae whole tissues were extracted from 250 mg of algal powder after fine grinding with a TissueLyser II (20 s at 20 Hz - Qiagen). A solvent mixture of methanol/dichloromethane (10 mL, v/v, 1:1) was added into glass tubes with the sample matrix. The resulting mixture was vortexed for 60 s and sonicated (ultrasonic bath, 2 min). Extracts were then centrifuged 20 min (3500 rpm at 4 °C) and the supernatants were transferred to pre-weighted glass tubes. The methanol and dichloromethane were removed by evaporation with a Genevac centrifugal evaporator EZ-2 serie (SP Industrie, Royaume-Uni) and samples were stored at -20° C until injection.

Mass spectrometry analysis

Before injection, extracts were resolubilized with 100% MeOH (HPLC-MS grade) at a concentration of 0.5 mg/mL for whole tissue extracts and of 1 mg/mL for algal surface and water extracts. Pooled Quality control (QC) samples were prepared to verify data reproducibility and quality by ensuring the absence of analytical drift and batch effects (Broadhurst et al., 2018). Due to distinct sample matrix composition, QC samples were prepared for each sample type (i.e., whole tissue, surface and water) by pooling all respective samples at equimolar concentrations and equally divided into individual HPLC vials. Samples were injected throughout two analytical sequences to avoid analytical drift and computational limitation. The first sequence with water extracts was processed in MS1 full scan MS in positive and negative ionization mode. The second sequence, including the algal whole tissue and surface extracts as well as a QC with algal MBLs and BBLs, was analyzed in full scan MS and data dependent MS2 in positive and negative ionization modes. Water extracts were not processed in MS/MS for budget constraints. All samples were injected randomly to avoid systematic bias. Experimental blanks (i.e., only MeOH for system suitability and extraction blanks for contaminant detection; n = 12) and QC samples were injected at the beginning and at the end of each analytical sequence to condition the column, assess carry-over effect and detect contaminants. Additionally, QC of each sample type were injected every 8 samples to track analytical repeatability (Fig. S11). Sample metabolomic profiles were acquired from 2 µL injection with a UHPLC system (Vanquish Thermo Scientific, MA, USA) coupled to a Q-Exactive Plus Orbitrap mass spectrometer (Thermo Scientific, MA, USA) with a HESI source. Acquisitions were controlled by the Xcalibur software (Thermo Scientific). The

chromatographic separation was carried out on a Luna Omega 1.6 μm Polar C18 column 100x2.1 mm (Phenomenex, Torrance, CA, USA) and consisted of $\text{H}_2\text{O} + 1\%$ formic acid (mobile phase A) and acetonitrile/isopropanol (50/50) + 1% formic acid (mobile phase B). A linear gradient was used with a flow rate of 0.250 mL/min: 0 to 2 min, at 2% B; 2 to 8 min, from 2 to 65% B; 8 to 25 min, from 65 to 100% B; 25 to 27 min, from 100 to 2% B, 27 to 31 min, at 2% B. Mass spectrometer settings were as follows: sheath, auxiliary and sweep gas 35, 10 and 0 AU, respectively; capillary voltage, 3500V in positive mode and 2500V in negative mode; capillary temperature, 320 °C; ESI probe heater temperature, 200 °C and S-lens RF level, 50. For the 1st sequence, full scan mass spectra (MS1) were acquired in both positive and negative ionization mode with a full scan MS window of 100-1500 m/z and a resolution of 35 000. The maximum injection time was set to 100 ms and automatic gain control (AGC) target set at 3×10^6 . For the 2nd sequence, full scan MS resolution was set at 70 000 and MS/MS spectra were acquired in data dependent mode with an isolation window of 1.5 m/z ; MS2 resolution 17 500; AGC target 3×10^5 ; maximum injection time 100 ms. Up to 5 of most intense selected ions per scan were fragmented with a stepped normalized collision energy of 25-35-45 eV. Dynamic exclusion was set to 5 s and isotope peaks were excluded.

Metabolomics data processing

Mass spectral data acquisition. Raw MS datafiles were converted into .mzML files in centroid mode using MSConvert (Chambers et al., 2012) and then imported into MZmine software (2.53 version – 6) for LC-MS preprocessing. We processed two datasets separately due to distinct MS acquisition modes and computational limitations. The 1st dataset included the samples from the five water types (MS1 data only) for characterization of their metabolomic signatures. The 2nd dataset included algal whole tissues, surfaces and algal MBLs and BBLs (MS1 features and MS/MS fragmentation spectra) to further investigate the origin and diffusion of algal-derived metabolites. While we could not acquire MS/MS of all water samples due to budget constraints, processing the QC of algal water samples (i.e., MBL and BBL), algal whole tissue and surface samples together with the algal water samples enabled us to retrieve the MS/MS data from these samples. Masses were detected in centroid mode at a minimal intensity threshold of 10^4 for MS1 level and 10^2 for MS2 level. Automated data analysis pipeline (ADAP) module (Myers et al., 2017) was used to build chromatograms with a minimum number of 4 scans for group size, minimum peak height of 10^5 and m/z tolerance of 10 ppm. For chromatogram deconvolution using ADAP algorithm, a signal-to-noise ratio of 10 was set, peak duration range 0.01 to 0.5 min, RT wavelet range 0.01 to 0.05 min, and m/z center calculation in Median mode. MS2 scans

were paired with a m/z range of 0.01 Da and a RT range of 0.1 min. Isotopes were removed using the isotopic peak grouper with m/z range tolerance 10 ppm, RT tolerance 0.1 min, maximum charge of 2 and selection of the most intense monoisotopic ions. Chromatograms were then aligned with a m/z tolerance of 10 ppm and a RT tolerance of 0.1 min. Weights for m/z and RT were both set to 1. Isotope pattern comparison was used with these thresholds: 10 ppm isotope m/z tolerance, 10 minimum intensity and 90% minimum score. The obtained list of aligned chromatograms was then filtered to remove duplicate peaks with a m/z tolerance of 5 ppm and RT tolerance of 0.1 min. A selection was applied to keep only isotopes with at least two peaks in an isotopic pattern and that occurred in at least 2 samples. Finally, gap filling was conducted using the Peak finder algorithm with an intensity of tolerance of 10%, m/z tolerance 10 ppm and RT tolerance 0.1 min alongside an RT correction. MS1 peak intensities (i.e., peak areas) of each of the two datasets were exported into a .csv file for statistical analysis. From the 2nd dataset with algal-associated features, we also exported a table comprising the peak intensities of MS1 features with MS2 data only as well as a .mgf file with consensus MS/MS spectra for network analysis and annotation purposes on the GNPS web platform (Wang et al., 2016) and SIRIUS software (Dührkop et al., 2019).

Molecular networking. Molecular networks were generated using the Feature-Based Molecular Networking (FBMN) workflow on the GNPS web platform (Wang et al., 2016; Nothias et al., 2020). FBMN enables to connect ion features based on their spectral similarity in networks and to annotate chemical features. Networks were created with a minimum cosine score of 0.7 and a minimum of 6 matched peaks. For each pair of nodes (i.e., molecular features), only the top 15 edges were kept. Spectra were annotated through search against the GNPS spectral library (e.g., contaminants, MassIVE databases), dereplication, Network Annotation Propagation and MS2LDA extensions (van der Hooft et al., 2016; da Silva et al., 2018; Mohimani et al., 2018). In addition, a search for analogs was defined with a maximum mass difference of 100 m/z from the mass of the precursor ion. Result outputs were combined in the MolNetEnhancer workflow (Ernst et al., 2019) on GNPS and provided compounds chemical putative classification from the Classyfire ontology (e.g., Superclass = Lipids and lipid-like molecules, Class = Prenol lipids, Subclass = Diterpenoids; 15). To improve metabolites classification and verify putative *in silico* annotation, standard International Chemical Identifiers (InChI) were retrieved from compound library matches and converted into InChIkey using the webchem R package (Szöcs et al., 2020) to obtain their hierarchical classification using the Classyfire R package (Feunang et al., 2016). Single-node features

without subnetwork affiliation were given the molecular class of their library or analog match. Library hits of discussed networks were manually verified. Networks were then all visualized in the Cytoscape software 3.9.1 (Shannon et al., 2003).

Putative formula assignation with SIRIUS and annotation strategy. The .mgf file with MS/MS spectra was uploaded into SIRIUS (version 5.6.2; 9). First, *de novo* molecular formulas were obtained with the Sirius module via isotope pattern analysis (Böcker et al., 2009) and fragmentation trees (Böcker & Dührkop, 2016). MS2 *m/z* deviation was set to 5 ppm and maximum 10 potential results were considered. Molecular formulas were obtained considering all possible ionizations and without database search. The ZODIAC module was used to increase the confidence of putative formula (Ludwig et al., 2020). ZODIAC parameters were kept as default. We only considered proposed formulas with a ZODIAC score > 0.95, explaining at least 4 peaks and at least 85% of the spectral intensity. CSI:FingerID predicted a molecular fingerprint for each compound based on its spectrum and fragmentation tree (Dührkop et al., 2015). Fingerprints were then compared against databases. CANOPUS module was used to retrieve the compound classification from its predicted molecular fingerprint (Dührkop et al., 2021). CANOPUS has the advantage to not rely on databases and to predict classification at the level of metabolites. Comparing MolNetEnhancer and CANOPUS outputs allowed us to find a consensus at the superclass or class levels. For most networks, similar results were found between both tools. When this was not the case, CANOPUS results were preferred when most compounds in the subnetwork belonged to the same class and if that class had a probability > 0.9. If no consensus at the class level could be achieved, subnetworks were classified according to their superclass (e.g., lipids-like molecules). To keep a conservative approach, networks composed of many superclasses were classified as “no consensus”. Fatty Acyls & Glycerolipids were commonly found in the same networks as well as Diterpenoids & Steroids. In these cases, a mixed category was created. We manually verified the library hits of discussed networks and compared the putative formula given by SIRIUS using the MarinLit online database for marine natural products (<https://marinlit.rsc.org>) and Lipidmaps (<https://www.lipidmaps.org>).

Microbiome data acquisition and processing

DNA extraction and microbial 16S rDNA gene sequencing. Filter fragments were transferred into ZR Bashing Beads Lysis Tubes (Zymo Research, USA) and lysed by bead beating using a FastPrep-24 5G (MP Biomedicals, USA) for 5 cycles of 1 min at 6 m/s and 1 min rest in-between each cycle. DNA was extracted using the ZymoBIOMICS DNA Miniprep kit (Zymo

Research, USA, D4300) according to manufacturer instructions for samples stored and lysed into DNA/RNA Shield. DNA extracts were then stored at -20 °C and dried with a centrifugal evaporator (EZ-2 serie, Genevac) for shipping. Additionally, several blank extractions were performed to remove later on sequences flagged as contaminants from the data (i.e., filters, extraction kits, Genevac & PCR). The hypervariable region V3-V4 of the 16S rDNA gene was amplified using the universal primers 341F (5'-CCTACGGGNGGCWGCAG- 3') and 805R (3'-GACTACHVGGGTATCTAATCC- 5') suggested for marine bacteria and some archaea (Klindworth et al., 2013; Wear et al., 2018). Amplicons were paired-end (2 x 250 bp) sequenced using an Illumina NovaSeq 6000 sequencer by Genome Quebec (Montréal, Canada).

Metabarcoding data processing. 16S rDNA gene reads were processed using the DADA2 workflow on R (Callahan et al., 2016). DADA2 enables to infer ASVs (i.e., amplicon sequence variants) and to distinguish sequences at the level of the nucleotides, therefore avoiding to group sequences based on a similarity threshold (i.e., OTUs). Sequence qualities were checked with FastQC (Andrew, 2010). Primers were removed with Cutadapt, after having removed reads with ambiguous N bases (Martin, 2011). Only sequences with a minimum length of 200 bp and a maximum length of 250 bp were further processed for the estimation of the error rates. Due to the binned quality score from NovaSeq sequencing, the error rate function was modified, as proposed by the DADA2 community on GitHub, by altering loess function arguments (i.e., weights & span) and enforcing the monotonicity (see : https://github.com/ErnakovichLab/dada2_ernakovichlab/tree/split_for_premise, <https://github.com/benjineb/dada2/issues/1307>). NovaSeq provided very high sequencing depth, with a total of 236 689 ASVs at the end of the processing workflow. Hence, only ASVs detected in at least 2 samples were kept, after having verified that these accounted for a low fraction of the total reads, as well as non-chimeric sequences. To assign taxonomy at the genus level, we used the Silva reference database (v138.1). The count table, taxonomy table & the metadata table were then imported into the phyloseq R package (McMurdie & Holmes, 2013).

Data pre-processing and statistical analysis

Benthos data. Benthic community composition across bommies were visualized using Principal Coordinate Analysis (PCoA) on Bray-Curtis dissimilarities of untransformed data. Variations in these benthic assemblages were assessed by Permutational Multivariate Analysis of Variance (PERMANOVA, *vegan* package v.2.6.4, “adonis2” function and 999 permutations; Oksanen et al., 2022) using, as fixed factors, algal treatment (algal-dominated vs. algal-removal

bommies) before removal of macroalgae, and algal treatment and month after the removal of macroalgae.

Metabarcoding data. Before analyzing microbial communities, we removed mitochondrial or chloroplast sequences. Contaminant sequences (i.e., 91 ASVs) were removed using the prevalence method with the *decontam* R package (Davis et al., 2018) as well as ASVs that were in less than three samples per water type. Processed and cleaned data resulted in 5517 ASVs and 12 693 8111 reads (Tab. S3). For alpha-diversity measure (Shannon index, microbial counts were rarefied (*phyloseq* package function “rarefy_even_depth”; McMurdie & Holmes, 2013) based on the smallest library size (i.e., 45 657 reads) resulting in 2 693 763 reads and 5493 ASVs. Beta-diversity analysis were performed on non-rarefied data with ASV agglomerated at the genus level due to the very high number of ASVs provided by NovaSeq. CLR transformation was used to account for the compositional nature of the metabarcoding data (Gloor et al., 2017; Quinn et al., 2018).

Metabolomic data. Quantitative tables of MS1 peak areas were imported and analyzed in the R environment (version 4.2.2) and cleaned from an in-house R script. All analyses were performed on positive ionization mode data, except molecular subnetworks which were investigated in positive and negative ionization modes. Potential contaminants (e.g., pumps, elution, extraction, solvent) were removed from the data if their mean intensity was at least 4 times higher in the blanks compared to samples. Additionally, we filtered out low quality features (i.e., D-ratio < 0.5 defined in Broadhurst et al., 2018) and transient features (i.e., present in less than three samples per water type). The dataset with water samples (i.e., dataset 1) included 14 131 MS1 features reduced to 975 features after filtration. The dataset with algal samples (i.e., dataset 2 in positive ionization mode) included 16 532 MS1 features, of which 4585 features with MS2 fragmentation spectra, reduced to 3943 MS1 features, of which 2214 with MS2, after filtration. In negative ionization mode, 1640 MS1 features had MS2 of which 1029 passed the filtration steps. MS1 peak intensities from water samples only (i.e., dataset 1) were $\log_{10}(x+1)$ transformed and mean-centered. In the table with algal-associated MS1 features (i.e., dataset 2), each feature intensity was divided by the sum of intensities within each sample to control for the potential bias introduced by different sample injection concentration. Relative intensities were then transformed by center-log ratio (CLR) with the addition of a constant equal to half the minimum value and mean-centered.

Diversity and composition analysis of microbiome and metabolome. Alpha-diversity (Shannon diversity) was compared using one-way ANOVA ($P < 0.05$) followed by a post-hoc Tukey HSD test. Multivariate analyses were performed on CLR-transformed microbiome (i.e., counts) and metabolomic (i.e., relative peak areas) data. We examined inter-group variability using principal component analysis (PCA) and tested group compositional differences with a Permutational Multivariate Analysis of Variance (PERMANOVA 999 permutations; *vegan* package function “adonis2”). To discriminate groups of samples (i.e., water types and algal sample types) and identify the ASVs and metabolites explaining compositional differences, we used partial least squares - discriminant analysis (PLS-DA) from the *mixOmics* R package (Rohart et al., 2017). PLS-DA have been successfully used on compositional metabolomics and metabarcoding datasets (Kalivodová et al., 2015; Cao et al., 2016;). It enables to reduce the dimensionality of the data and to classify the samples into *a priori* known groups. Data was mean-centered, and the variability associated to repeated measures on bommies was accounted for with the argument ‘withinVariation’ in the *mixOmics* R package (Rohart et al., 2017). PLS-DA were validated by cross-model validation (7-fold outer loop CV2 and 6-fold inner loop CV1) to estimate a classification error rate (CER) using the *RVAideMemoire* R package (Hervé, 2023). With a permutation test (999 permutations), the null distribution of CER was tested against the observed CER to assess if clusters were indeed statistically different or if their separations resulted from chance alone. For water types, we performed four PLS-DA for each data type: A) comparing BBLs (i.e., BBL control vs. BBL algae), B) comparing MBLs (i.e., MBL control vs., MBL *Dictyota* vs. MBL *Turbinaria*), C) comparing algal-free boundary layers (i.e., BBL control vs. MBL control) and D) comparing algal-dominated boundary layers (i.e., BBL algae vs., MBL *Dictyota* vs. MBL *Turbinaria*). We performed two additional PLS-DA per algal species to discriminate the sample type: whole tissue, surface, MBL and BBL. For the analysis, we used MS1 features with MS/MS fragmentation spectra for annotation purposes of the identified discriminant features.

Discriminant ASVs and metabolites. The importance of a variable in discriminating groups is defined by its VIP (variable importance in projection) score. Conventionally, a variable is considered discriminant if its score is > 1 , and the higher the score, the better the variable explains the group separation (Cocchi et al., 2018). We identified which ASVs were the most discriminant of the five water types by summing the VIP scores across the four PLS-DA and retained the 50 highest. Heatmaps were used to represent the enrichment of these 50 most discriminating ASVs in the different water types. ASVs were clustered according to their mean

CLR transformed abundances across each water type using Ward's minimum variance method, and data was standardized by mean-centering and scaling by the standard deviation (z-score). VIP scores resulting from the PLS-DA on algal samples were used in our network analysis to select subnetworks of interest by applying a threshold of minimum 3 discriminant features (VIP > 1) and a VIP score > to the median.

Integration of metabarcoding and metabolomic data. To investigate if compositional differences in water types were related across metabarcoding and metabolomic, we used the multiblock PLS-DA (DIABLO - Data Integration Analysis for Biomarker discovery using Latent variable approaches for Omics studies) analysis available in the *mixOmics* R package using the function “block.splsda” (Rohart et al., 2017; Hervé et al., 2018; Singh et al., 2019). DIABLO seeks for correlated variables between pair of datasets that also discriminate sample groups. Prior to run DIABLO, the level of association between the metabarcoding and metabolomic datasets was verified with a Mantel test ($P < 0.05$) on distance matrices and by the correlation of components obtained from PLS regression (correlation coefficient > 0.8). We set a weight of 1 for the association between datasets to favor the covariance between datasets over model's discriminative ability. The optimal number of components and variables were estimated by cross validation with 7 folds using the functions “tune.block.splsda”. DIABLO outputs were validated by a permutation test based on cross-model validation as described above for the PLS-DA analysis using the *RVAideMemoire* package (Hervé, 2023). Specifically, we performed this analysis on the five water types and on algal MBLs only. To test whether all five water types could be discriminated according to their multi-omic signature, we integrated all MS1 metabolomic and metabarcoding data. On algal MBLs, we used DIABLO to identify the key variables reflecting species-related changes and investigate their relationships into an integrative network. We decided to focus solely on algal MBLs as incorporating the algal BBL would have added a confounding source of variation due to change of boundary layer, thereby complicating interpretations. Only previously identified discriminant ASVs ($n = 292$) and features from the selected subnetworks were considered ($n = 309$) to specifically highlight to covariation of the already discussed variables. Only variables with high positive (>0.7) and high negative (<0.7) correlations were further selected and analyzed as a bipartite correlation network on Cytoscape (Shannon et al., 2003)

5.2. Supplementary Figures

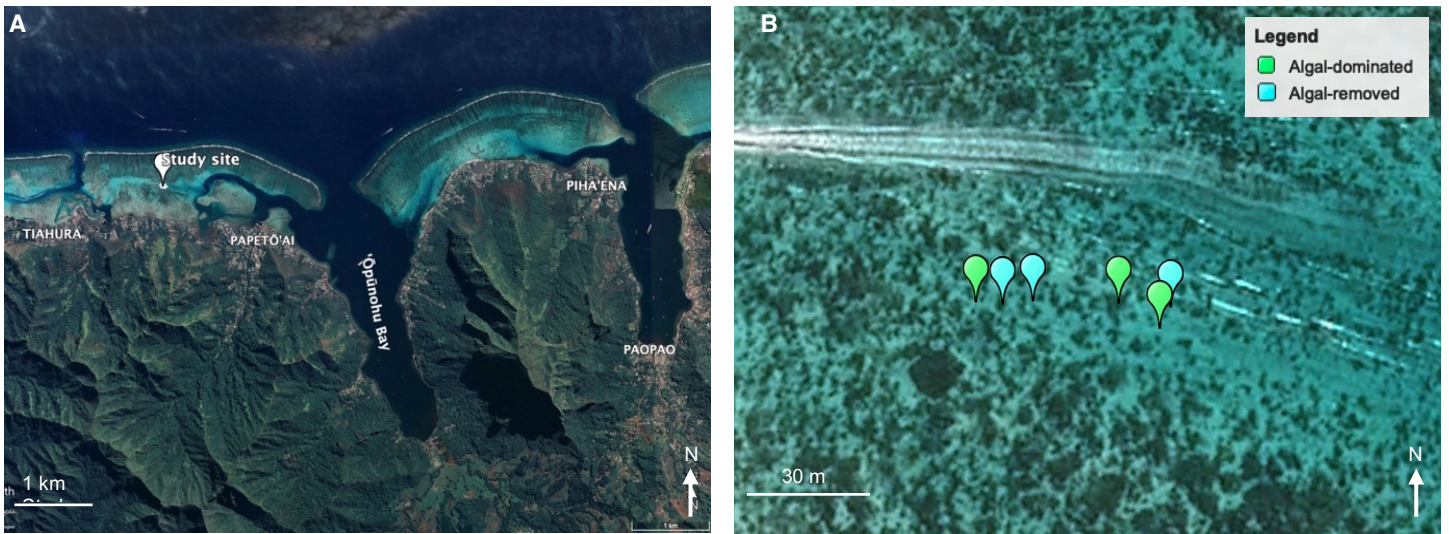


Fig. S1. Satellite images of Mo'orea showing (A) the study site on the north coast of the island ($17^{\circ}29'14.86''\text{S}$ $149^{\circ}53'0.76''\text{W}$) and (B) the locations of the coral bommies assigned to two algal treatments : algal-removed and algal-dominated.

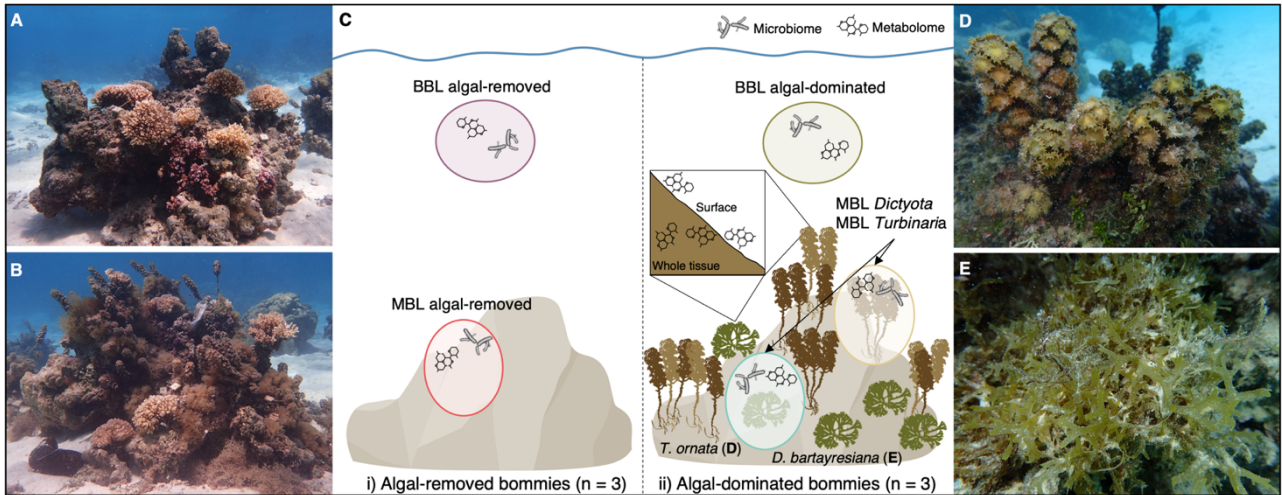


Fig. S2. Experimental design. Bommies were assigned randomly to two algal treatments: (A) and (C i) algal-removed and (B) and (C ii) algal-dominated. Three sample types were collected: water samples (i.e., BBL – Benthic Boundary Layer & MBL – Momentum Boundary Layer), algal surfaces and algal whole tissues of each of the two macroalgal species: *Turbinaria ornata* (D) and *Dictyota bartayresiana* (E). Both the microbiome and metabolome of BBL and MBL were analyzed while only the metabolome of algal samples was considered.

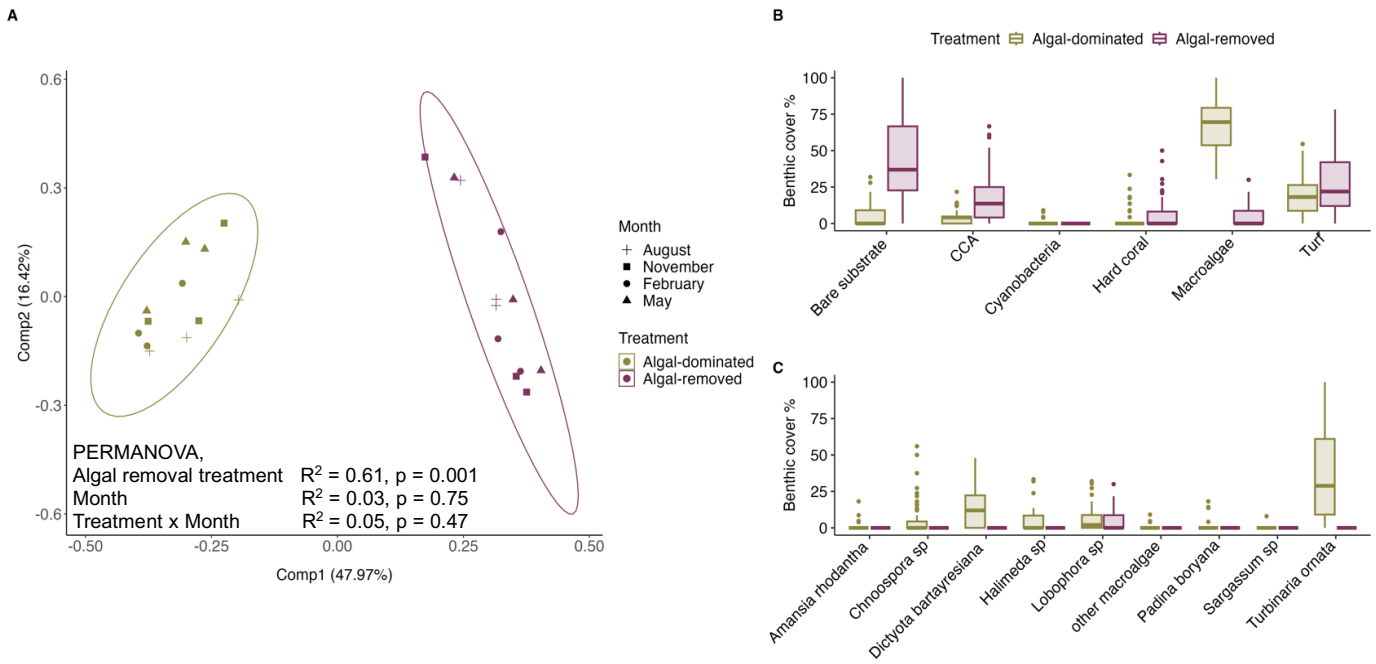


Fig. S3. Benthic community composition on experimental bommies. (A) Score plot of the principal coordinate analysis on Bray-Curtis dissimilarities comparing benthic community composition of algal-dominated and algal-removed bommies during the experiment. The effects of treatment, month and their interaction were tested using a two-way PERMANOVA ($n_{perm} = 999$). Box plots represent cover of (B) main benthic categories and (C) macroalgal species/genera.

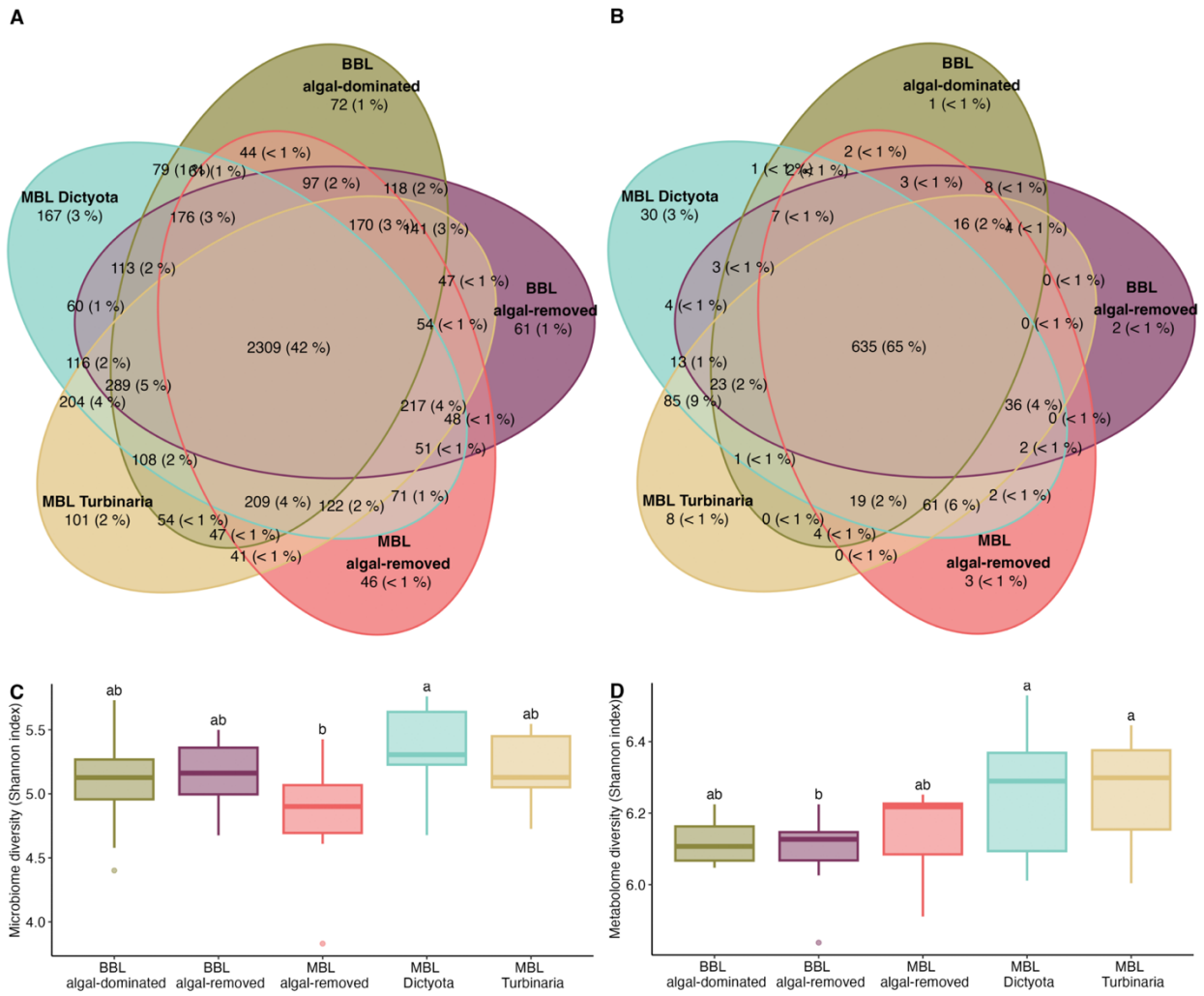


Fig. S4. Microbial & chemical alpha-diversity across the five reef waters. Number of ASVs (A) and chemical features (B) detected in all samples ($n = 59$ metabarcoding samples and $n = 60$ metabolomic samples). Richness (Shannon diversity index by sample) of ASVs (C) and chemical features (D). Reef water types are abbreviated and colored as in the experimental design figure (Fig. S2).

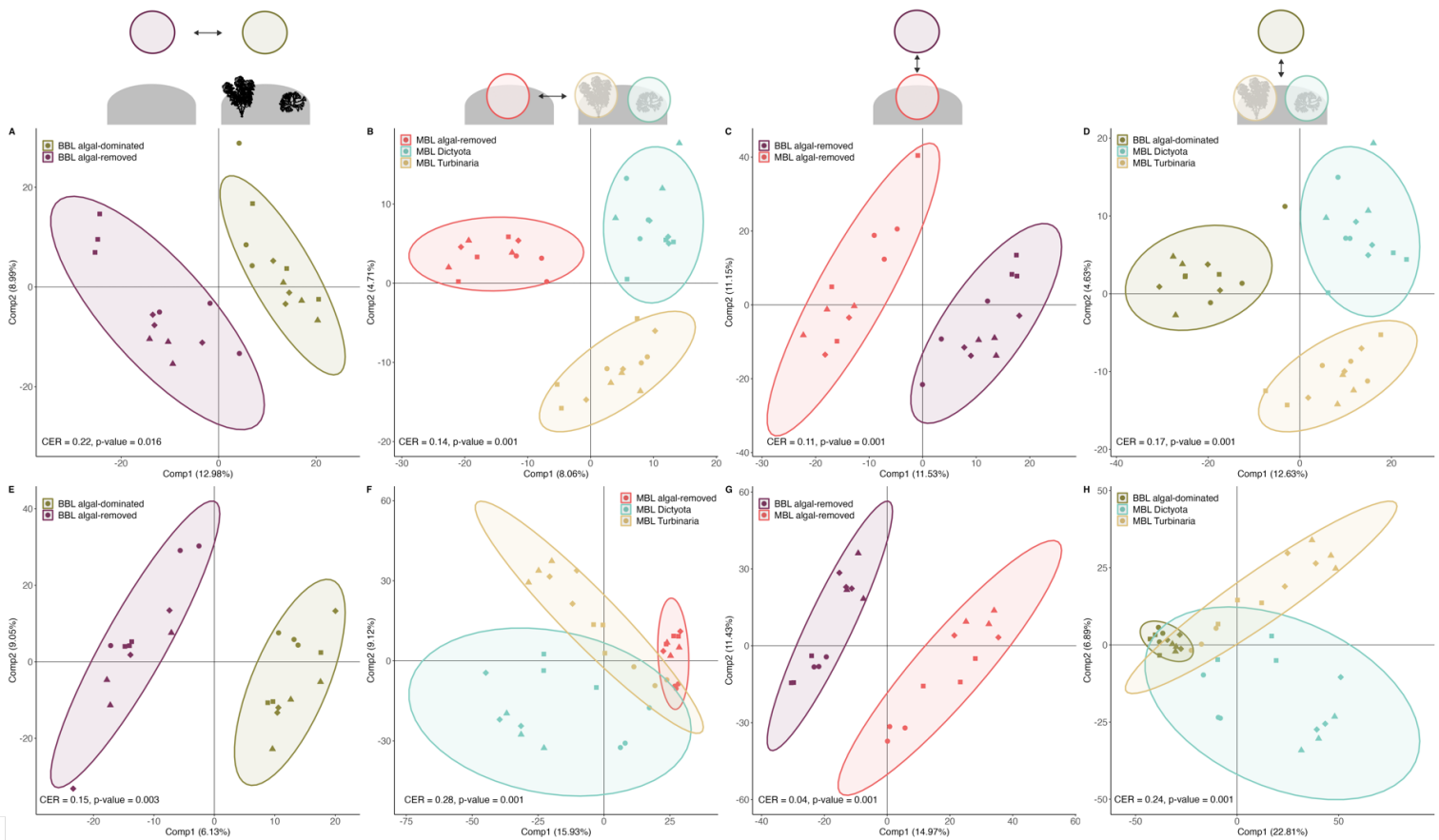


Fig. S5. Microbial and chemical compositional differences of reef waters. PLS-DA (constrained ordination) score plots performed on metabarcoding (A to D) and metabolomic MS1 data (E to H) between boundary layers (A, E), momentum boundary layers (B, F), algal-removed waters (C, G) and algal-dominated waters (D, H). Analyses were validated by a permutation test based on cross-model validation, the CER represents the proportion of misclassification and a $P < 0.05$ indicates that the clustering was not obtained by chance alone. Ellipses are 95% data ellipses. $N = 59$ metabarcoding samples and $N = 60$ metabolomic samples.

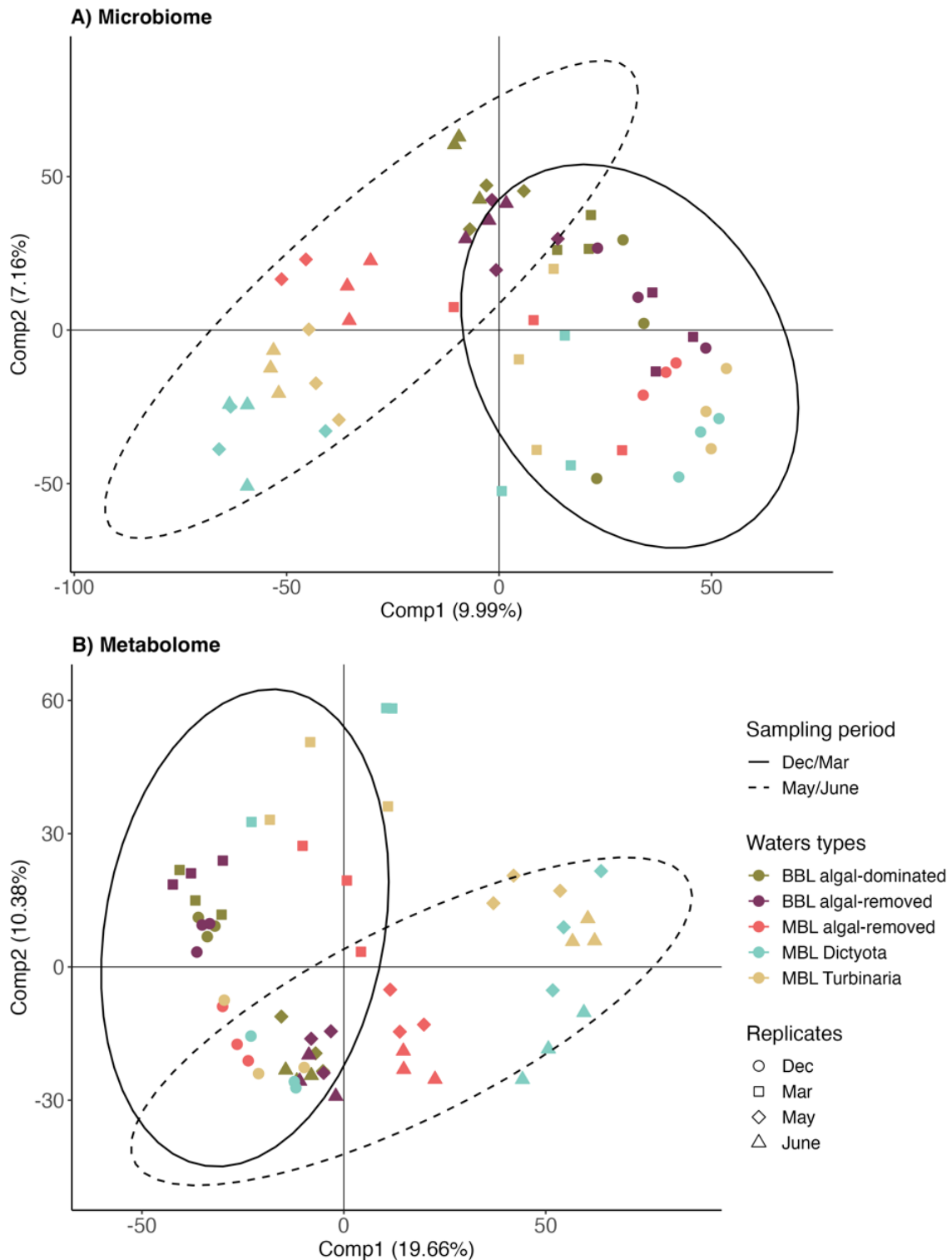


Fig. S6. Unconstrained ordination (PCA) of microbial communities and metabolite pools of the different water types. Score plots principal component analysis performed on metabarcoding (A) and metabolomic MS1 data (B). Metabarcoding abundance data was CLR transformed and metabolomic feature intensities were log10 transformed. Both datasets were mean centered before the ordination. N = 59 metabarcoding samples and N = 60 metabolomic samples. Ellipses are 95% data ellipses.

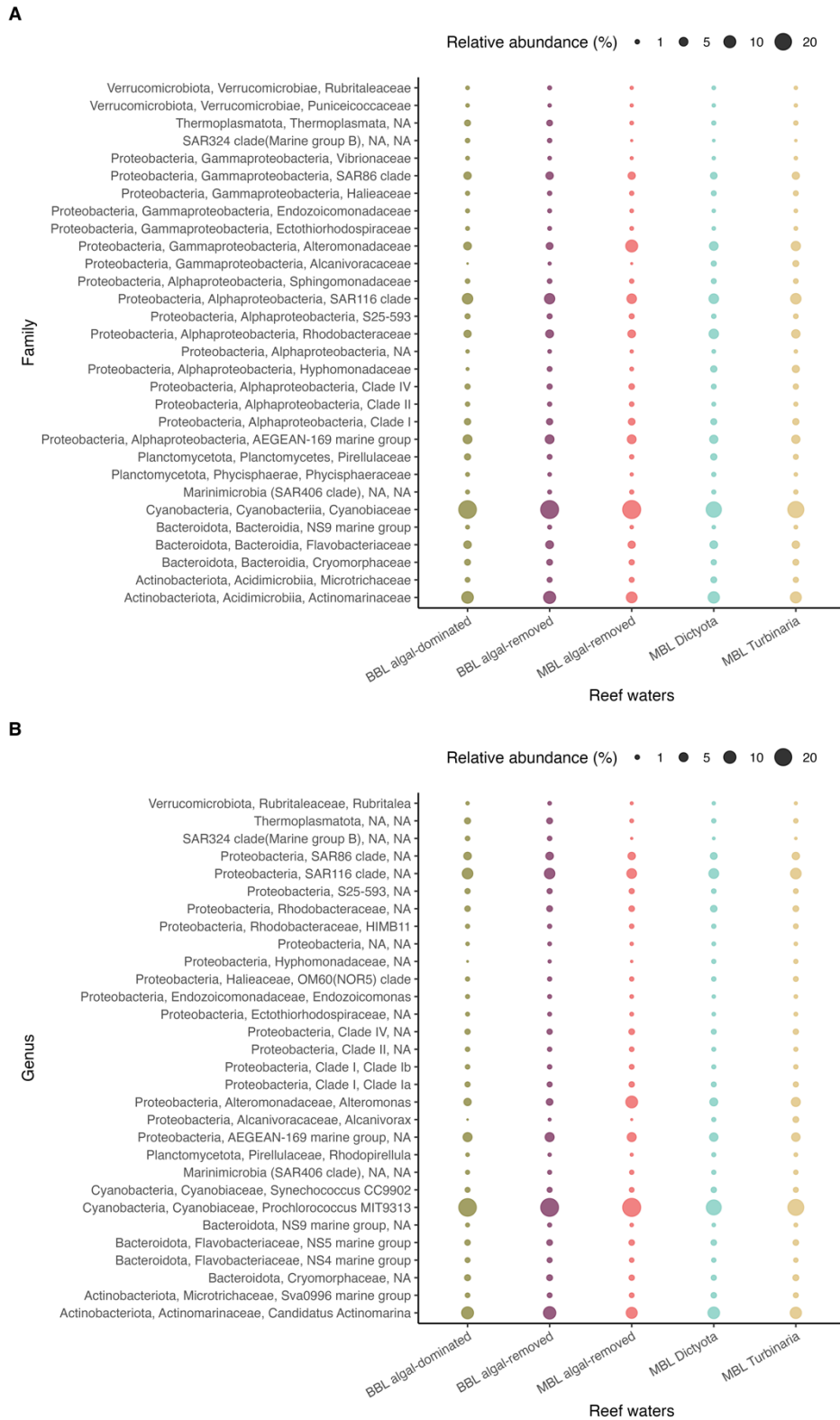
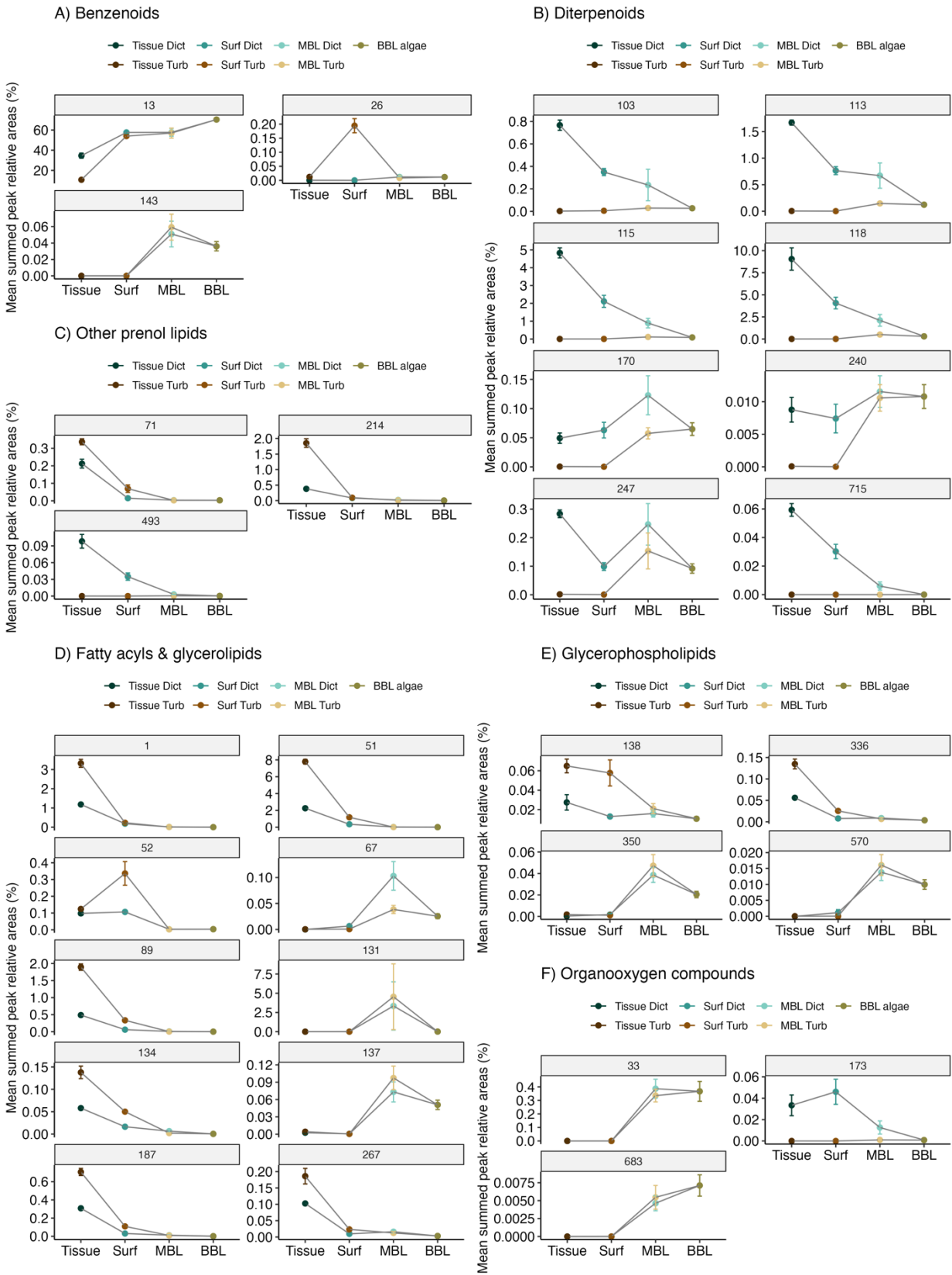


Fig. S7. Distribution of dominant microbial phyla, families and genera across the different seawater types. Relative abundance of the top 30 most abundant microbial (A) families and (B) genera of the 59 seawater 16S rDNA metabarcoding samples.



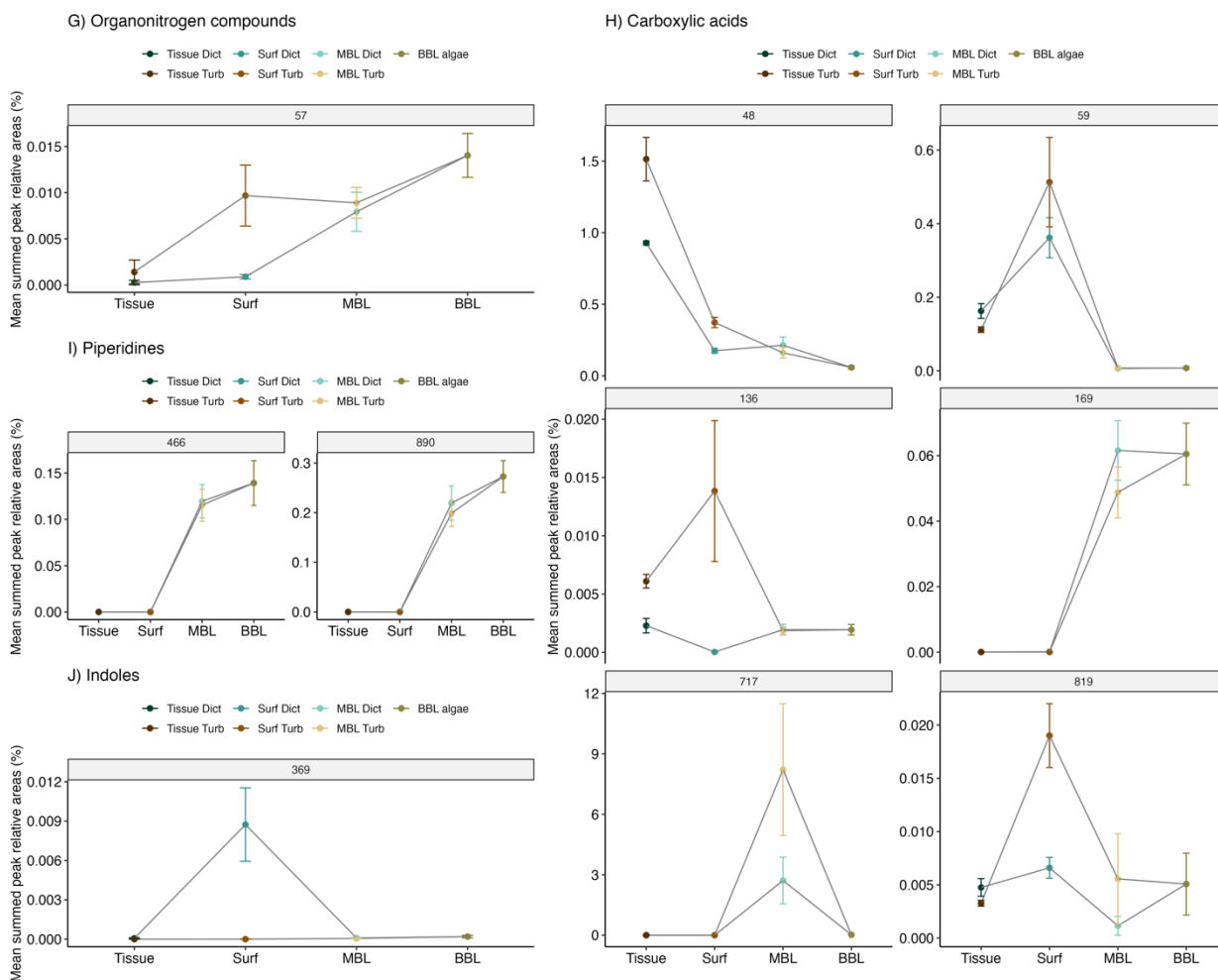


Fig. S8. Selected subnetworks of interest grouped by their molecular putative classification in positive ionization mode. Mean relative feature abundances (% mean \pm SE) for each subnetwork across sample types correspond to the sum of peak areas within each sample for each network and then mean by sample type. Putative classification corresponds to the consensus classification derived from the Classyfire classification via MolNetEnhancer (GNPS) and CANOPUS (SIRIUS).

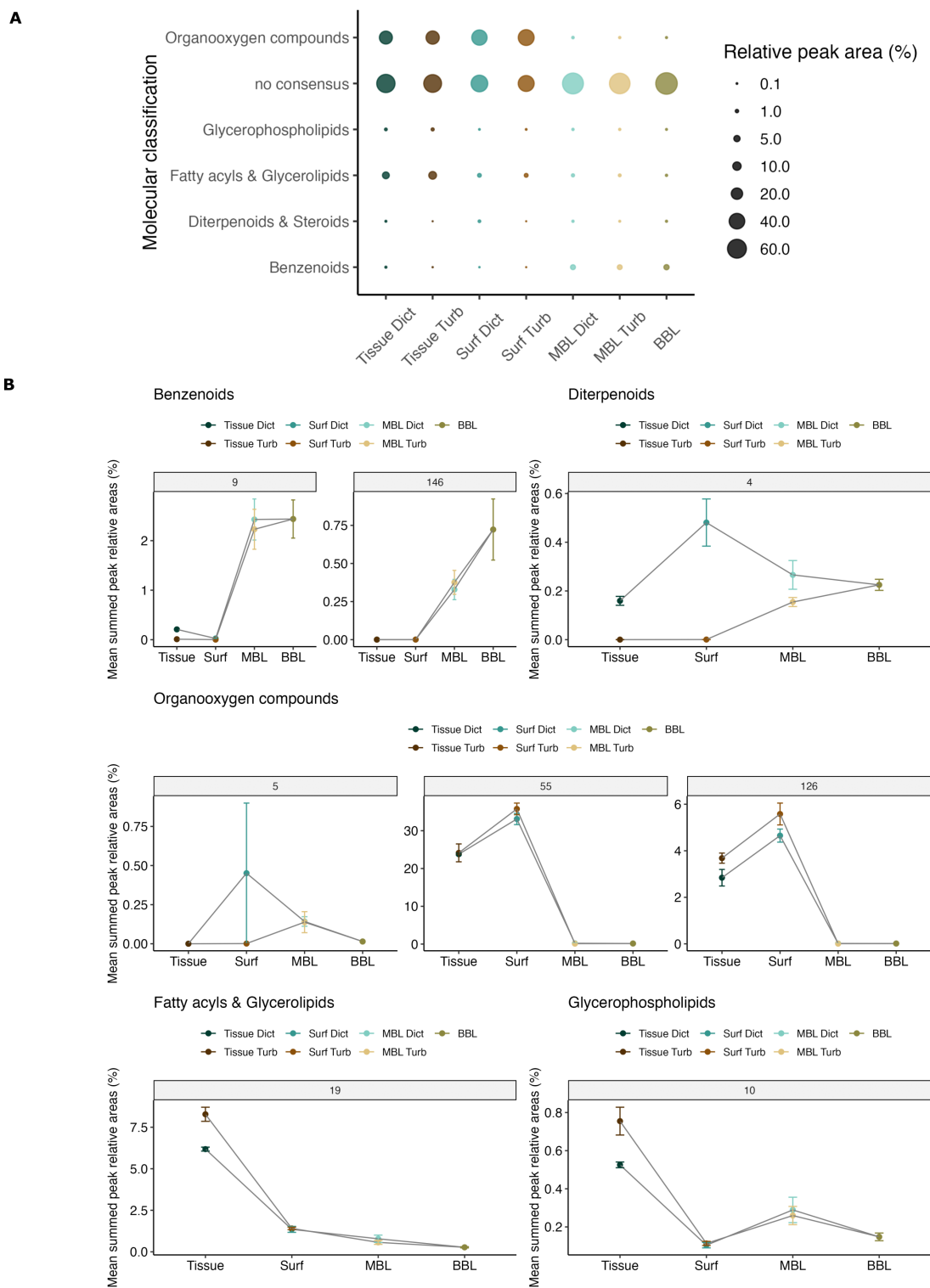


Fig. S9. Selected subnetworks of interest grouped by their molecular putative class and subclass in negative ionization mode. (A) Mean of summed feature relative intensities of broad molecular classification across sample types. (B) Relative feature intensities (% mean \pm SE) detailed for each subnetwork. Putative classification corresponds to the consensus classification derived from the Classyfire classification via MolNetEnhancer (GNPS) and CANOPUS (SIRIUS).

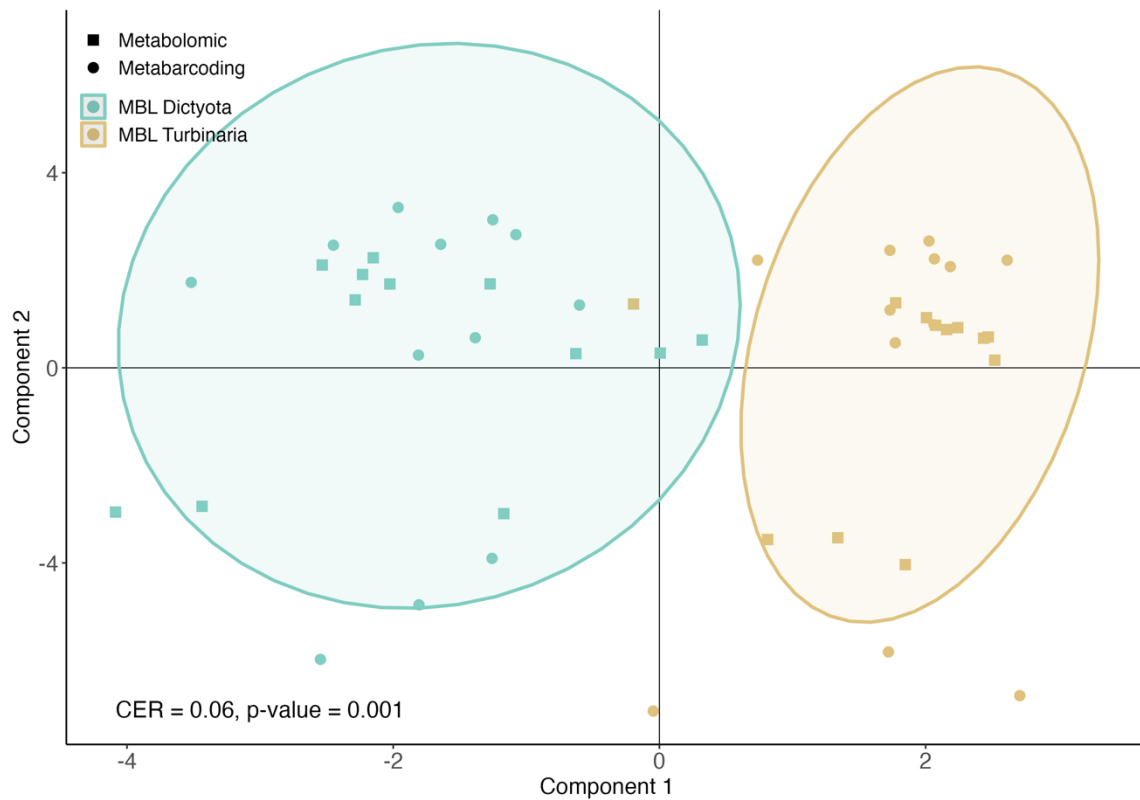


Fig. S10. Multiomic composition of algal MBLs. Score plots of the multi-block PLS-DA (DIABLO) performed on metabarcoding and metabolomic data between the MBL of *Dictyota bartayresiana* and *Turbinaria ornata*. Analysis was validated by a permutation test based on cross-model validation, the CER represents the proportion of misclassification and a $P < 0.05$ indicates that the clustering was not obtained by chance alone. Ellipses are 95% data ellipses.

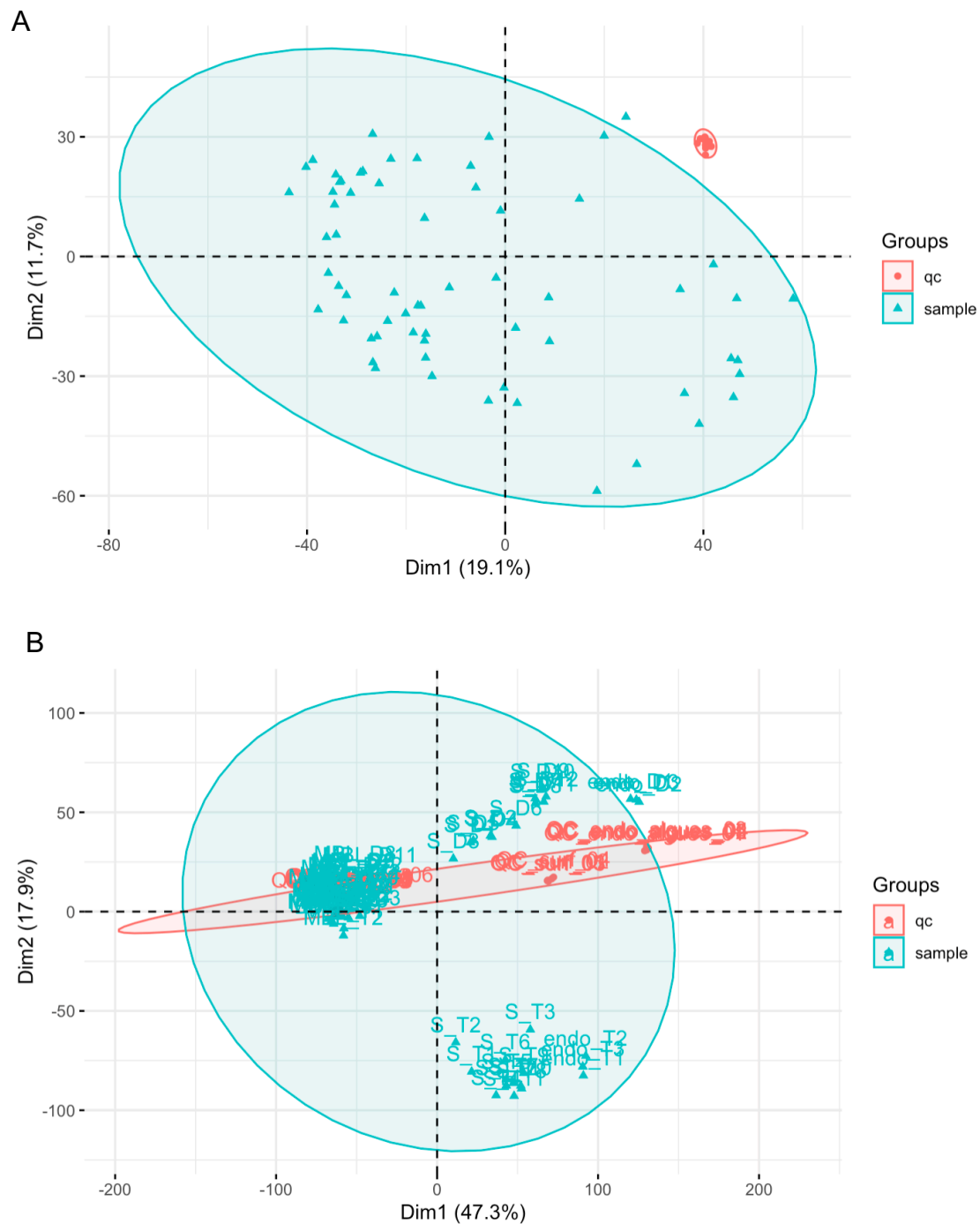


Fig. S11. Metabolomic composition of biological samples and QC samples. PCA score plots performed on raw metabarcoding data after data cleaning (A) water samples and QC samples (i.e., dataset 1) and (B) algal whole tissues, surfaces, MBLs, BBLs and their respective QC samples (i.e., dataset 2). Ellipses are 95% data ellipses. QC samples are grouped together confirming analytical repeatability throughout injection sequences.

5.3. Supplementary Tables

Table S1. Number of ASVs and reads in each water sample of 16S rDNA metabarcoding data processed with DADA2.

Sample	nb_asv	nb_reads	water	type	treatment	replicate	bommie
BBL-A1	1157	271398	bbl_a	bbl	algal-dominated	R1	bom10
BBL-A10	1638	228192	bbl_a	bbl	algal-dominated	R4	bom10
BBL-A11	1811	213815	bbl_a	bbl	algal-dominated	R4	bom4
BBL-A12	1424	145538	bbl_a	bbl	algal-dominated	R4	bom8
BBL-A2	1233	194813	bbl_a	bbl	algal-dominated	R1	bom4
BBL-A3	1809	270523	bbl_a	bbl	algal-dominated	R1	bom8
BBL-A4	1068	156775	bbl_a	bbl	algal-dominated	R2	bom10
BBL-A5	1398	218060	bbl_a	bbl	algal-dominated	R2	bom4
BBL-A6	1667	239596	bbl_a	bbl	algal-dominated	R2	bom8
BBL-A7	1363	182655	bbl_a	bbl	algal-dominated	R3	bom10
BBL-A8	1523	230060	bbl_a	bbl	algal-dominated	R3	bom4
BBL-A9	1602	207253	bbl_a	bbl	algal-dominated	R3	bom8
BBL-C1	1494	274546	bbl	bbl	algal-removed	R1	bom9
BBL-C10	1424	182412	bbl	bbl	algal-removed	R4	bom9
BBL-C11	1655	178852	bbl	bbl	algal-removed	R4	bom3
BBL-C12	1635	185566	bbl	bbl	algal-removed	R4	bom7
BBL-C2	1792	264755	bbl	bbl	algal-removed	R1	bom3
BBL-C3	1314	190358	bbl	bbl	algal-removed	R1	bom7
BBL-C4	1187	178752	bbl	bbl	algal-removed	R2	bom9
BBL-C5	1427	193855	bbl	bbl	algal-removed	R2	bom3
BBL-C6	1689	233836	bbl	bbl	algal-removed	R2	bom7
BBL-C7	1567	205776	bbl	bbl	algal-removed	R3	bom9
BBL-C8	1605	231149	bbl	bbl	algal-removed	R3	bom3
BBL-C9	1540	200667	bbl	bbl	algal-removed	R3	bom7
MBL-C1	879	257739	mbl	mbl	algal-removed	R1	bom9
MBL-C10	1180	167588	mbl	mbl	algal-removed	R4	bom9
MBL-C11	1485	177649	mbl	mbl	algal-removed	R4	bom3
MBL-C12	1755	197774	mbl	mbl	algal-removed	R4	bom7
MBL-C2	1462	244812	mbl	mbl	algal-removed	R1	bom3
MBL-C3	1268	219208	mbl	mbl	algal-removed	R1	bom7
MBL-C4	1030	203435	mbl	mbl	algal-removed	R2	bom9
MBL-C5	390	45657	mbl	mbl	algal-removed	R2	bom3
MBL-C6	1004	162019	mbl	mbl	algal-removed	R2	bom7
MBL-C7	1948	230816	mbl	mbl	algal-removed	R3	bom9
MBL-C8	1685	218700	mbl	mbl	algal-removed	R3	bom3
MBL-D1	1282	219919	mbl_d	mbl	algal-dominated	R1	bom10
MBL-D10	1513	166780	mbl_d	mbl	algal-dominated	R4	bom10
MBL-D11	1764	168519	mbl_d	mbl	algal-dominated	R4	bom4
MBL-D12	2179	275527	mbl_d	mbl	algal-dominated	R4	bom8
MBL-D2	1535	251714	mbl_d	mbl	algal-dominated	R1	bom4

MBL-D3	1450	257343	mbl_d	mbl	algal-dominated	R1	bom8
MBL-D4	1206	204328	mbl_d	mbl	algal-dominated	R2	bom10
MBL-D5	1212	268916	mbl_d	mbl	algal-dominated	R2	bom4
MBL-D6	1425	231207	mbl_d	mbl	algal-dominated	R2	bom8
MBL-D7	1510	201504	mbl_d	mbl	algal-dominated	R3	bom10
MBL-D8	2083	228973	mbl_d	mbl	algal-dominated	R3	bom4
MBL-D9	2062	267375	mbl_d	mbl	algal-dominated	R3	bom8
MBL-T1	1116	221415	mbl_t	mbl	algal-dominated	R1	bom10
MBL-T10	1632	181799	mbl_t	mbl	algal-dominated	R4	bom10
MBL-T11	1930	227974	mbl_t	mbl	algal-dominated	R4	bom4
MBL-T12	1908	347166	mbl_t	mbl	algal-dominated	R4	bom8
MBL-T2	1591	206726	mbl_t	mbl	algal-dominated	R1	bom4
MBL-T3	1787	234914	mbl_t	mbl	algal-dominated	R1	bom8
MBL-T4	1326	231930	mbl_t	mbl	algal-dominated	R2	bom10
MBL-T5	947	170862	mbl_t	mbl	algal-dominated	R2	bom4
MBL-T6	1223	239642	mbl_t	mbl	algal-dominated	R2	bom8
MBL-T7	1687	220904	mbl_t	mbl	algal-dominated	R3	bom10
MBL-T8	1784	239882	mbl_t	mbl	algal-dominated	R3	bom4
MBL-T9	1637	223893	mbl_t	mbl	algal-dominated	R3	bom8

Table S2. List of the subnetworks of interest selected in positive ionization mode. A total of 58 subnetworks with minimum 3 discriminant features and those with at least 1 VIP with a score superior to the median were selected. Mean relative feature abundances (%) for each subnet across metabolome types correspond to the sum of peak areas within each sample for each network and then mean by metabolome type. The number of diffusive features is the number of features at least detected in either or both algal whole tissues and surfaces and in MBLs. Putative classification corresponds to the consensus classification (class and subclass levels) derived from the Classyfire ontology via MolNetEnhancer (GNPS) and CANOPUS (SIRIUS)

Subnetworks	Tissue Dict	Tissue Turb	Surface Dict	Surface Turb	MBL Dict	MBL Turb	BBL algae	Nb feat.	VIP Dict	VIP Turb	Nb diffusive Dict	Nb diffusive Turb	Library or Analogs	Putative classification
1	1.1856	3.3256	0.1878	0.2281	0.0153	0.0122	0.004	74	9	10	21	21	10	Fatty acyls & glycerolipids
10	7.5218	18.4943	0.4252	1.7982	0.004	0.0007	0.0001	80	5	5	8	8	0	Diverse lipids
13	34.6535	10.6757	59.2911	54.4479	52.5043	52.2994	64.0709	43	10	14	41	38	0	Benzenoids
16	0.3167	0.6607	1.2464	2.2208	2.272	2.4073	2.9753	26	12	14	25	25	0	No consensus
20	0	0.0066	0.0045	0.0133	0	0.0008	0	1	0	1	0	1	0	No consensus
21	0.3852	0.7278	0.1201	0.3231	0.1189	0.0834	0.0276	21	4	7	12	12	0	Diverse lipids
26	0.0004	0.0123	0.0001	0.1943	0.0121	0.0085	0.0117	2	2	0	2	2	0	Benzenoids
33	3e-5	0.0001	0.0002	0.0002	0.4371	0.3835	0.4313	4	4	2	4	2	0	Organooxygen compounds
38	3.6e-5	0.0001	0.0001	0.0001	0.002	0.0025	0.0191	1	1	1	1	1	0	No consensus
48	0.9301	1.515	0.1801	0.3757	0.1868	0.1442	0.0517	29	8	9	20	20	0	Carboxylic acids
51	2.2589	7.7951	0.3615	1.1888	0.0231	0.0144	0.0085	65	12	13	29	30	0	Glycerolipids
52	0.0991	0.1263	0.1151	0.3416	0.0444	0.0639	0.0651	10	1	3	7	7	1	Fatty acyls
57	0.0003	0.0014	0.0009	0.0097	0.008	0.0089	0.0140	2	2	1	2	2	2	Organonitrogen compounds
59	0.1628	0.1121	0.3619	0.5130	0.0064	0.0077	0.0076	10	1	3	3	3	0	Carboxylic acids
61	6.6e-5	5.5e-5	0.0475	0.0001	0.0036	0.0036	0.0010	10	3	0	4	1	0	No consensus
67	0.0001	0.0004	0.007	0.0007	0.0899	0.0347	0.0225	2	2	0	2	2	0	Fatty acyls
71	0.2131	0.3854	0.0155	0.07	0.0034	0.0026	0.0028	18	3	3	3	4	0	Other prenol lipids (e.g., tetraterpenoids) & Steroids
89	0.4882	1.8956	0.0623	0.3366	0.0079	0.0035	0.0015	19	4	4	8	8	12	Fatty acyls & glycerolipids
95	0.0001	0.0001	0.0001	0.0001	0.2293	0.2052	0.2161	2	1	2	1	2	0	No consensus
102	0.0292	0	0.0406	2.3e-6	0.0084	0.0004	0.0002	2	2	0	2	1	0	No consensus
103	0.7678	0.0022	0.3582	0.0051	0.2006	0.0261	0.0243	20	2	5	18	16	20	Diterpenoids, retinoids (prenol lipids) & steroids
113	1.6721	0.004	0.7823	0.0022	0.5844	0.1315	0.1086	20	5	4	20	19	3	Diterpenoids
115	4.8343	0.0044	2.1431	0.0047	0.7808	0.1038	0.0795	65	15	9	47	38	27	Diterpenoids & steroids
118	9.065	0.0047	4.1152	0.008	1.8386	0.4469	0.2634	82	11	11	64	53	40	Diterpenoids & steroids
131	0.0001	0.0003	0.0014	0.0004	3.3014	4.46	0.008	7	5	3	5	5	2	Fatty acyls
134	0.0581	0.1426	0.0167	0.0505	0.0057	0.0019	0.0004	18	1	3	3	3	0	Fatty acyls & glycerolipids
136	0.0022	0.0061	3.1406	0.0138	0.0019	0.0018	0.0019	5	1	1	1	1	0	Carboxylic acids
137	0.0026	0.0043	0.0007	0.0006	0.0644	0.0877	0.0454	5	4	3	5	5	0	Glycerolipids
138	0.0279	0.0677	0.0133	0.0587	0.017	0.0227	0.0129	12	2	3	8	8	0	Glycerophospholipides
143	1.0231	7.6959	3.4916	4.0216	0.0509	0.0509	0.0361	2	1	1	1	1	1	Benzenoids
169	4.8e-5	2.2e-5	0.0001	3.5e-5	0.0547	0.0442	0.0536	1	1	1	1	1	0	Carboxylic acids
170	0.0439	0.0005	0.0586	0.0001	0.1061	0.0505	0.0567	8	1	4	8	7	2	Diterpenoids, retinoids (prenol lipids) & steroids
173	0.0334	9.2e-6	0.0469	0	0.0112	0.0009	0.0008	4	3	0	4	1	2	Organooxygen compounds
187	0.3086	0.7071	0.0318	0.1102	0.0108	0.0086	0.0017	15	3	6	12	12	7	Fatty acyls & glycerolipids
214	0.3819	1.8579	0.0873	0.0957	0.0189	0.0107	0.0035	11	1	3	6	5	8	Other prenol lipids (tetraterpenoids) & steroids
240	0.0088	7.3e-5	0.0074	1.9e-5	0.0116	0.0106	0.0108	3	0	3	3	3	0	Diterpenoids, retinoids (prenol lipids) & steroids

243	0.0001	0.0006	0.0005	0.0008	1.375	0.8445	0.1407	2	1	2	1	2	0	No consensus
247	0.2841	0.0016	0.1008	0.0007	0.2152	0.1366	0.0813	5	0	3	5	5	5	Diterpenoids, retinoids (prenol lipids) & steroids
267	0.1027	0.1871	0.0099	0.0235	0.014	0.0111	0.0028	8	3	4	6	6	0	Glycerolipids
336	0.0561	0.1351	0.008	0.0256	0.0076	0.0058	0.003	11	3	3	9	9	3	Glycerophospholipids
348	0.0266	0.0003	0.0524	0.0402	0.0138	0.0129	0.0192	2	1	2	2	2	0	No consensus
350	0.0013	0.0063	0.0034	0.0027	0.0718	0.085	0.0407	3	3	0	3	3	1	Glycerophospholipids
369	0.0001	0	0.0092	3e-6	0.0001	0.0001	0.0002	3	3	0	3	2	0	Indoles
413	0.0002	0.0007	0.0005	0.0012	0.0122	0.0127	0.0041	2	1	1	2	2	0	No consensus
466	7.6e-6	7.2e-6	4.8e-6	2.3e-5	0.1063	0.1039	0.1232	1	1	1	1	1	0	Piperidines
474	0.0153	0.0001	0.0245	0.0244	0.0131	0.0142	0.0208	2	1	2	2	2	0	No consensus
481	0.0053	0.0153	0.0063	0.1669	0.001	0.0007	0.0009	4	1	4	5	5	0	No consensusImidazopyrimidines
493	0.0984	1.9e-5	0.0355	0	0.0026	0.0005	0.0003	4	3	0	3	2	4	Other prenol lipids & steroids
503	0.0001	0.0002	0.0002	0.0002	0.0368	0.0456	0.0693	2	2	1	2	2	0	Diverse lipids
564	0	5.9e-6	9.1e-6	0	0.0066	0.0085	0.0001	1	1	1	1	1	0	Diverse lipids
570	0	2.6e-5	0.004	3.6e-5	0.0122	0.0144	0.0089	2	1	1	1	1	0	Diverse lipids
606	0.0883	0.0041	0.0113	0.0018	0.1302	0.1171	0.1188	2	1	1	2	2	0	Diverse lipids
683	0	0	5.7e-6	0	0.009	0.0112	0.0142	2	1	0	1	0	0	Organoxygen compounds
712	0	0	0.0009	0	0.0006	0.0004	0.0004	1	1	0	1	0	0	No consensus
715	0.0594	0	0.0309	0	0.0053	0	0	2	2	0	2	0	0	Diterpenoids (prenol lipids)
717	4.5e-5	0.0001	0.0001	0.0002	2.4465	7.2823	0.018	5	3	3	3	3	0	Carboxylic acids
819	0.0048	0.0033	0.0068	0.0192	0.001	0.0051	0.0045	2	2	2	2	2	0	Carboxylic acids
890	0.0002	2.3e-5	2.1e-5	4.8e-5	0.1963	0.1802	0.2436	2	2	2	2	2	0	Piperidines

Table S3. Putative annotation of discussed features. Associated to (A) algal metabolomes and water column and (B) bipartite microbe-metabolite network (Algal MBLs). Putative annotations and corresponding spectrum ID are results of the library matches obtained through the GNPS database search. Putative annotation and predicted formula were given by GNPS, MarinLit and LipidMaps databases search and were verified according to the putative formula resulting from SIRIUS (Zodiac score > 90, Number of explained peaks > 4, Explained intensity > 0.85). Characteristic fragments are indicated in **blue**. Neutral losses are indicated in **orange**. Features in bold in (A) are also in the bipartite network and were not re-indicated in (B).

A

[M+H] ⁺ or [M+Na] ⁺ or [M-H] ⁻ m/z	RT (min)	Predicted formula (SIRIUS)	Delta m/z (ppm)	Putative annotation	MS/MS fragmentation spectra	Corresponding subnetwork
483.2361	10.62	C ₂₆ H ₃₆ O ₇	1.6	Triacetylated diterpene with a C8 prenylchain Compatible with a triacetoxy-secospatadienone or a triacetoxy-secospatadienal skeleton (Ravi & Wells, 1982a)	483.2361 [M+Na] ⁺ (1), 423.2147 [C ₂₄ H ₃₂ O ₅ +Na] ⁺ [M-lacetoxy+Na] ⁺ [M-C₂H₄O₂+Na] ⁺ (100), 381.2038 [C ₂₂ H ₃₀ O ₄ +Na] ⁺ [M-acetoxy-acetyl+Na] ⁺ [M-(C₂H₄O₂)-(C₂H₃O)+Na] ⁺ (3), 363.1934 [C ₂₂ H ₂₈ O ₃ +Na] ⁺ [M-2acetoxy+Na] ⁺ [M-2(C₂H₄O₂)+Na] ⁺ (15), 321.1827 [C ₂₀ H ₂₆ O ₂ +Na] ⁺ [M-2acetoxy-lacetyl+Na] ⁺ [M-2(C₂H₄O₂)-1(C₂H₃O)+Na] ⁺ (2), 281.1901 [C ₂₀ H ₂₄ O+H] ⁺ (4), 197.1327 [C ₂₅ H ₁₆ +H] ⁺ (3), 81.0706 [C ₆ H ₈ +H] ⁺ (3), 67.0552 [C ₅ H ₆ +H] ⁺ (1)	115 – Diterpenoids (feature 1861)
441.2260	10.21	C ₂₄ H ₃₄ O ₆	0.3	Diacetylated diterpene with a C8 prenylchain Compatible with a diacetoxy-hydroxy- secospatadienone or a diacetoxy-oxo-secospatadienal skeleton (Ravi & Wells, 1982a)	441.2254 [M+Na] ⁺ (2), 381.2040 [C ₂₂ H ₃₀ O ₄ +Na] ⁺ [M-acetoxy+Na] ⁺ [M-(C₂H₄O₂)+Na] ⁺ (100), 321.1828 [C ₂₀ H ₂₆ O ₂ +Na] ⁺ [M-2acetoxy+Na] ⁺ [M-2(C₂H₄O₂)+Na] ⁺ (25), 109.1018 [C ₈ H ₁₂ +H] ⁺ (C8 prenyl chain) (1), 81.0706 [C ₆ H ₈ +H] ⁺ (1), 69.0707 [C ₅ H ₈ +H] ⁺ (0.5),	115 - Diterpenoids (feature 1690)
501.2823	11.49	C ₂₇ H ₄₂ O ₇	-2.1	Triacetylated diterpene with a C8 prenylchain Compatible with a triacetoxy-secospatadienone skeleton (Ravi & Wells, 1982a)	501.2823 [M+Na] ⁺ (0), 441.2617 [C ₂₅ H ₃₈ O ₅ +Na] ⁺ [M-acetoxy+H] ⁺ (86), 381.2040 [C ₂₂ H ₃₀ O ₄ +Na] ⁺ [M-2acetoxy+H] ⁺ (100), 281.1901 [C ₂₀ H ₂₄ O+H] ⁺ (2), 253.1951 [C ₁₉ H ₂₄ +H] ⁺ (1), 211.1489 [C ₁₆ H ₁₈ +H] ⁺ (1), 197.1326 [C ₁₅ H ₁₆ +H] ⁺ (3), 169.1013 [C ₁₃ H ₁₂ +H] ⁺ (3), 157.1013 [C ₁₂ H ₁₂ +H] ⁺ (3), 145.1014 [C ₁₁ H ₁₂ +H] ⁺ (4), 131.0858 [C ₁₀ H ₁₀ +H] ⁺ (3), 109.1017 [C ₈ H ₁₂ +H] ⁺ (C8 prenyl chain) (11), 95.0863 [C ₇ H ₁₀ +H] ⁺ (3), 81.0706 [C ₆ H ₈ +H] ⁺ (5)	115 - Diterpenoids (feature 4262)
429.2623		C ₂₄ H ₃₈ O ₅	2.7	Acetylated diterpene with 2 methoxy group Compatible with secospatacetal E(Yamase et al., 1999), dictydiacetal (Enoki et al., 1982) and crenulacetal C/D (Takikawa et al., 1998)	429.2623 [M+Na] ⁺ (48), 369.2404 [C ₂₂ H ₃₄ O ₃ +Na] ⁺ [M-acetoxy+H] ⁺ (100), 337.2143 [C ₂₁ H ₃₀ O ₂ +Na] ⁺ [M-acetoxy-methoxy+H] ⁺ (1), 205.1587 [C ₁₄ H ₂₀ O+H] ⁺ (3), 173.1326 [205-methoxy+H] ⁺ [C ₁₃ H ₁₆ +H] ⁺ (6), 131.0859 [C ₁₀ H ₁₀ +H] ⁺ (7), 69.0695 [C ₅ H ₈ +H] ⁺ (8), 55.0541 [C ₄ H ₆ +H] ⁺ (1), 67.0550 [C ₃ H ₆ +H] ⁺ (5)	115 - Diterpenoids (feature 1619)
257.2267	11.85	C ₁₉ H ₂₈	-3.0	Diterpene related with feature 1604 dehydro, demethylated (Rahelivao et al., 2016)	257.2267 [M+H] ⁺ (100), 229.1658 [C ₁₇ H ₂₄ +H] ⁺ (1), 215.1797 [C ₁₆ H ₂₂ +H] ⁺ (7), 201.1641 [C ₁₅ H ₂₀ +H] ⁺ (20), 187.1485 [C ₁₄ H ₁₈ +H] ⁺ (11), 173.1328 [C ₁₃ H ₁₆ +H] ⁺ (12), 161.1327 [C ₁₂ H ₁₆ +H] ⁺ (13), 159.1171 [C ₁₂ H ₁₄ +H] ⁺ (14), 147.1171 [C ₁₁ H ₁₄ +H] ⁺ (16), 135.1171 [C ₁₀ H ₁₄ +H] ⁺ (11), 121.1015 [C ₉ H ₁₂ +H] ⁺ (15), 107.0860 [C ₈ H ₁₀ +H] ⁺ (19), 95.0862 [C ₇ H ₁₀ +H] ⁺ (20), 81.0706 [C ₆ H ₈ +H] ⁺ (30), 69.0707 [C ₅ H ₈ +H] ⁺ (8), 55.0552 [C ₄ H ₆ +H] ⁺ (2) Fragment ions shared with the spatane diterpenoid, gravilin	103 – Diterpenoids (feature 2081)
289.2530	13.21	C ₂₀ H ₃₂ O	1.4	Diterpene with an alcohol function and a C8 prenyl chain Compatible with pachydictyol A (Schmitt et al., 1998), dictyolene (Sun et al., 1977) and spatadienol derivatives (okamurol, okaspatol D, spata-13,17-dien-10-ol) (Cuevas et al., 2023)	289.2530 [M+H] ⁺ (16), 271.2423 [C ₂₀ H ₃₀ +H] ⁺ [M-H₂O+H] ⁺ (100), 229.1956 [C ₁₇ H ₂₄ +H] ⁺ (5), 215.1798 [C ₁₆ H ₂₂ +H] ⁺ (52), 161.1327 [C ₁₂ H ₁₆ +H] ⁺ (54), 135.1171 [C ₁₀ H ₁₄ +H] ⁺ (23), 123.1172 [C ₉ H ₁₄ +H] ⁺ (34), 109.1017 [C ₈ H ₁₂ +H] ⁺ (C8 prenyl chain) (35), 81.0706 [C ₆ H ₈ +H] ⁺ (24), 69.0707 [C ₅ H ₈ +H] ⁺ (12), 55.0552 [C ₄ H ₆ +H] ⁺ (2)	103 - Diterpenoids (feature 1604)
297.1857	9.98	C ₂₀ H ₂₄ O ₂	-1.0	Dihydroxy diterpene related to 4264. Compatible with a didehydro, dehydroxy derivative of rugukamural C (Cuevas et al., 2021)	297.1857 [M+H] ⁺ (100), 279.1742 [C ₂₀ H ₂₂ O+H] ⁺ [M-H₂O+H] ⁺ (17), 269.1902 [C ₁₉ H ₂₄ O+H] ⁺ (44), 261.1645 [C ₂₀ H ₂₀ +H] ⁺ [M-2H₂O+H] ⁺ (2), 251.1797 [C ₁₉ H ₂₂ +H] ⁺ (21), 241.1226 [C ₁₆ H ₁₆ O ₂ +H] ⁺ (2), 195.1171 [C ₁₅ H ₁₄ +H] ⁺ (14), 69.0707 [C ₅ H ₈ +H] ⁺ (20), 57.0706 [C ₄ H ₈ +H] ⁺ (2)	170 – Diterpenoids (feature 1229)

357.2034	9.86	C ₂₀ H ₃₀ O ₄	-3.7	Dihydroxy diterpene related to 4245 Compatible with 4,18-dihydroxydictyolactone (Jongaramruong & Kongkam, 2007), 2,6-cyclohexenane (Ioannou et al., 2009), xenicane (Guella et al., 1994), dichotodione (Ali & Pervez, 2003), dichotenone-A (Ali et al., 2003), rugukamural C (Cuevas et al., 2021) and 5,18,19-trihydroxyspata-13,16E-diene (Gerwick & Fenical, 1981)	357.2034 [M+Na] ⁺ (30), 297.1848 [C ₂₀ H ₂₄ O ₂ +H] ⁺ (90), 279.1741 [C ₂₀ H ₂₂ O+H] ⁺ [297-H ₂ O+H] ⁺ (47), 261.1644 [C ₂₀ H ₂₀ +H] ⁺ [297-2H ₂ O+H] ⁺ (12), 251.1803 [C ₁₉ H ₂₂ +H] ⁺ (86), 214.1225 [C ₁₆ H ₁₆ O ₂ +H] ⁺ (42), 229.1229 [C ₁₅ H ₁₆ O ₂ +H] ⁺ (27), 209.1325 [C ₁₆ H ₁₆ +H] ⁺ (50), 203.1077 [C ₁₃ H ₁₄ O ₂ +H] ⁺ (16), 195.1174 [C ₁₅ H ₁₄ +H] ⁺ (71), 183.1170 [C ₁₄ H ₁₄ +H] ⁺ (43), 173.1328 [C ₁₃ H ₁₆ +H] ⁺ (19), 157.1017 [C ₁₂ H ₁₂ +H] ⁺ (51), 143.0860 [C ₁₁ H ₁₀ +H] ⁺ (36), 131.0856 [C ₁₀ H ₁₀ +H] ⁺ (27), 121.1015 [C ₉ H ₁₂ +H] ⁺ (100), 105.0702 [C ₈ H ₈ +H] ⁺ (34), 95.0859 [C ₇ H ₁₀ +H] ⁺ (32), 81.0705 [C ₆ H ₈ +H] ⁺ (38), 69.0707 [C ₅ H ₈ +H] ⁺ (62), 55.0550 [C ₄ H ₆ +H] ⁺ (14)	170 – Diterpenoids (feature 4264)
375.2173	9.03	C ₂₂ H ₃₀ O ₅	-1.1	Acetylated diterpene Compatible with rugukamural B (hydroxy-oxo-secospatenol skeleton) (Cuevas et al., 2021) or 18-acetoxy-19-oxo-xenicatrien-17,18-olide (Ravi & Wells, 1982b)	375.2173 [M+H] ⁺ (9), 315.1961 [C ₂₀ H ₂₆ O ₃ +H] ⁺ [M-acetoxy+H] ⁺ (33), 287.2009 [C ₁₉ H ₂₆ O ₂ +H] ⁺ (16), 279.1836 [C ₂₀ H ₂₂ O+H] ⁺ (15), 269.1909 [C ₁₉ H ₂₄ O+H] ⁺ (40), 251.1804 [C ₁₉ H ₂₂ +H] ⁺ (18), 251.1225 [C ₁₆ H ₁₆ O ₂ +H] ⁺ (52), 229.1226 [C ₁₅ H ₁₆ O ₂ +H] ⁺ (56), 213.1272 [C ₁₅ H ₁₆ O+H] ⁺ (42), 159.0810 [C ₁₁ H ₁₀ O+H] ⁺ (33), 145.1013 [C ₁₁ H ₁₂ +H] ⁺ (27), 131.0860 [C ₁₀ H ₁₀ +H] ⁺ (41), 121.1015 [C ₉ H ₁₂ +H] ⁺ (15), 105.0702 [C ₈ H ₈ +H] ⁺ (21), 95.0862 [C ₇ H ₁₀ +H] ⁺ (24), 81.0706 [C ₆ H ₈ +H] ⁺ (81), 69.0708 [C ₅ H ₈ +H] ⁺ (100), 55.0550 [C ₄ H ₆ +H] ⁺ (10)	170 – Diterpenoids (feature 4245)
581.4000	14.79	C ₄₀ H ₅₂ O ₃	-0.03	Carotenoid compatible with hydroxyalloxanthin (Azizan et al., 2020)	581.4000 [M+H] ⁺ (10), 411.2687 [C ₃₀ H ₃₄ O+H] ⁺ (3), 355.2425 [C ₂₇ H ₃₀ +H] ⁺ (3), 119.0858 [C ₉ H ₁₀ +H] ⁺ (14), 109.1016 [C ₈ H ₁₂ +H] ⁺ (100), 67.0550 [C ₃ H ₆ +H] ⁺ (13) Fragment ions shared with fucoxanthin	214 – Other Prenol lipids (feature 2411)
425.2695	10.86	C ₂₅ H ₃₈ O ₄	5.1	Unknown carotenoid (Bustamam et al., 2021)	425.2695 [M+Na] ⁺ (0.2), 255.1380 [C ₁₇ H ₁₈ O ₂ +H] ⁺ (4), 237.1269 [C ₁₇ H ₁₆ O+H] ⁺ (2), 227.1421 [C ₁₆ H ₁₈ O+H] ⁺ (5), 179.1069 [C ₁₁ H ₁₄ O ₂ +H] ⁺ (3), 159.0804 [C ₁₁ H ₁₀ O+H] ⁺ (10), 135.0806 [C ₉ H ₁₀ O+H] ⁺ (9), 119.0859 [C ₉ H ₁₀ +H] ⁺ (9), 109.1016 [C ₈ H ₁₂ +H] ⁺ (100), 105.0702 [C ₈ H ₈ +H] ⁺ (10), 95.0500 [C ₆ H ₆ +H] ⁺ (8), 81.0706 [C ₆ H ₈ +H] ⁺ (6), 67.0551 [C ₃ H ₆ +H] ⁺ (9) Fragment ions shared with diatoxanthin	214 – Other Prenol lipids (feature 3154)
562.3745	11.40	C ₃₂ H ₅₁ NO ₇	1.,19	Lyso-DGCC (22:6) ^a	562.3745 [M+H] ⁺ (38), 132.1022 [C ₆ H ₁₃ NO ₂ +H] ⁺ (18), 104.1076 [C ₅ H ₁₃ NO+H] ⁺ (100), 86.0972 [C ₅ H ₁₁ N+H] ⁺ (5), 73.0293 [C ₃ H ₄ O ₂ +H] ⁺ (4), 60.0817 [C ₃ H ₉ N+H] ⁺ (6), 227.1421 [C ₁₆ H ₁₈ O+H] ⁺ (5), 209.1325 [C ₁₆ H ₁₆ +H] ⁺ (3) Fragment ions of carboxyhydroxymethylcholin	137 – Fatty acyls & Glycerolipids (feature 1050)
536.3600	11.00	C ₃₀ H ₅₀ NO ₇	3.,39	Lyso-DGCC (20:5)	536.3600 [M+H] ⁺ (40), 132.1022 [C ₆ H ₁₃ NO ₂ +H] ⁺ (17), 115.0759 [C ₆ H ₁₀ O ₂ +H] ⁺ (3), 104.1076 [C ₅ H ₁₃ NO+H] ⁺ (100), 86.0972 [C ₅ H ₁₁ N+H] ⁺ (5), 73.0293 [C ₃ H ₄ O ₂ +H] ⁺ (4), 60.0817 [C ₃ H ₉ N+H] ⁺ (6) Fragment ions of carboxyhydroxymethylcholin	137 – Fatty acyls & Glycerolipids (feature 1539)
462.3440	10.76	C ₂₄ H ₄₇ NO ₇	3.,18	Lyso-DGCC (14:0)	462.3440 [M+H] ⁺ (54), 252.1448 [C ₁₀ H ₂₁ NO ₆ +H] ⁺ (1), 178.1079 [C ₇ H ₁₅ NO ₄ +H] ⁺ (6), 132.1023 [C ₆ H ₁₃ NO ₂ +H] ⁺ (22), 104.1076 [C ₅ H ₁₃ NO+H] ⁺ (100), 86.0972 [C ₅ H ₁₁ N+H] ⁺ (5), 73.0293 [C ₃ H ₄ O ₂ +H] ⁺ (4), 60.0817 [C ₃ H ₉ N+H] ⁺ (5) Fragment ions of carboxyhydroxymethylcholin	137 – Fatty acyls & Glycerolipids (feature 2029)
523.4732	19.89	C ₃₃ H ₆₂ O ₄	0.3	DAG (16:0/14:0) (dehydroxy) (Paix et al., 2020)	523.4732 [M-H ₂ O+H] ⁺ (61), 239.2374 [C ₁₆ H ₃₀ O+H] ⁺ [FA16:0+H] ⁺ (8), 211.2056 [C ₁₄ H ₂₆ O+H] ⁺ [FA14:0-H ₂ O+H] ⁺ (12), 193.1954 [C ₁₄ H ₂₄ +H] ⁺ (1), 151.1485 [C ₁₁ H ₁₈ +H] ⁺ (2), 137.1326 [C ₁₀ H ₁₆ +H] ⁺ (8), 123.1172 [C ₉ H ₁₄ +H] ⁺ (16), 109.1016 [C ₈ H ₁₂ +H] ⁺ (36), 95.0862 [C ₇ H ₁₀ +H] ⁺ (70), 71.0863 [C ₅ H ₁₀ +H] ⁺ (82), 57.0707 [C ₄ H ₈ +H] ⁺ (100) Characteristic fragment ions	187 -Fatty acyls & Glycerolipids (feature 2871)
495.4414	18.71	C ₃₁ H ₆₀ O ₅₄	0	DAG (14:0/14:0) (dehydroxy) (Paix et al., 2020)	495.4414 [M-H ₂ O+H] ⁺ (62), 211.2059 [C ₁₄ H ₂₆ O+H] ⁺ [FA14:0-H ₂ O+H] ⁺ (28), 193.1954 [C ₁₄ H ₂₄ +H] ⁺ (3), 151.1484 [C ₁₁ H ₁₈ +H] ⁺ (1), 137.1330 [C ₁₀ H ₁₆ +H] ⁺ (9), 123.1171 [C ₉ H ₁₄ +H] ⁺ (18), 109.1017 [C ₈ H ₁₂ +H] ⁺ (38), 95.0862 [C ₇ H ₁₀ +H] ⁺ (72), 71.0864 [C ₅ H ₁₀ +H] ⁺ (90), 57.0708 [C ₄ H ₈ +H] ⁺ (100) Characteristic fragment ions	187 -Fatty acyls & Glycerolipids (feature 4343)
774.6101	21.97	C ₄₃ H ₈₀ O ₁₀	1.45	MGDG (16:0/18:1) ou MGDG (18:1/16:0) (Carriot et al., 2021)	774.6101 [M+NH ₄] ⁺ (0), 577.5197 [C ₃₇ H ₆₈ O ₄ +H] ⁺ [M-Gal+H] ⁺ (55), 339.2897 [C ₂₁ H ₃₈ O ₃ +H] ⁺ [M-Gal-H ₂ O-FA16:0+H] ⁺ (96), 313.2739 [C ₁₉ H ₃₆ O ₃ +H] ⁺ [M-Gal-H ₂ O-FA18:1+H] ⁺ (100), 265.2528 [C ₁₈ H ₃₀ O+H] ⁺ (6), 257.2478 [C ₁₆ H ₃₂ O ₂ +H] ⁺ (4), 247.2422 [C ₁₈ H ₂₈ +H] ⁺ (3), 239.2373 [C ₁₆ H ₃₀ O+H] ⁺ (5), 109.1016 [C ₈ H ₁₂ +H] ⁺ (19), 95.0861 [C ₇ H ₁₀ +H] ⁺ (34), 81.0706 [C ₆ H ₈ +H] ⁺ (25), 57.0708 [C ₄ H ₈ +H] ⁺ (32)	89 – Fatty acyls & Glycerolipids (feature 2369)

836.5560	20.16	C ₄₃ H ₇₈ O ₁₂ S	0.9	SQDG (34:2) (Carriot et al., 2021; Zheng et al., 2017)	836.5560 [M+NH ₄] ⁺ (0), 575.5038 [C ₃₇ H ₆₆ O ₄ +H] ⁺ (36), 337.2740 [C ₂₁ H ₃₆ O ₃ +H] ⁺ (64), 313.2740 [C ₁₉ H ₃₆ O ₃ +H] ⁺ (64), 263.2372 [C ₁₈ H ₃₀ O+H] ⁺ (11), 239.2373 [C ₁₆ H ₃₀ O+H] ⁺ (10), 123.1171 [C ₉ H ₁₄ +H] ⁺ (13), 109.1017 [C ₈ H ₁₂ +H] ⁺ (25), 95.0861 [C ₇ H ₁₀ +H] ⁺ (47), 81.0706 [C ₆ H ₈ +H] ⁺ (40), 57.0702 [C ₄ H ₈ +H] ⁺ (28) Characteristic fragment ions	89 – Fatty acyls & Glycerolipids (feature 2611)
542.3243	11.31	C ₂₈ H ₄₈ NO ₇ P	-0.4	Lyso-PC (20:5) https://www.lipidmaps.org/databases/lmsd/LMGP01050050	542.3243 [M+H] ⁺ (7), 524.3143 [C ₂₈ H ₄₆ NO ₆ P+H] ⁺ (3), 258.1101 [C ₈ H ₂₀ NO ₆ P+H] ⁺ (1), 184.0738 [C ₅ H ₁₄ NO ₄ P+H] ⁺ (100), 125.0003 [C ₂ H ₅ NO ₄ P+H] ⁺ (11), 104.1076 [C ₅ H ₁₃ NO+H] ⁺ (83), 86.0972 [C ₅ H ₁₁ N+H] ⁺ (28), 60.0817 [C ₃ H ₉ N+H] ⁺ (8) Characteristic fragment ions	350 – Glycerophospholipids (feature 1199)
340.2609	6.67	C ₁₈ H ₃₃ N ₃ O ₃	0.9	tripeptide related to feature 1623	340.2609 [M+H] ⁺ (82), 322.2495 [C ₁₈ H ₃₁ N ₃ O ₂ +H] ⁺ (100), 227.1758 [C ₁₂ H ₂₂ N ₂ O ₂ +H] ⁺ [M-Leu/Ile+H] ⁺ (28), 209.1653 [C ₁₂ H ₂₀ N ₂ O+H] ⁺ (65), 114.0919 [C ₆ H ₁₁ NO+H] ⁺ [M-2 Leu/Ile+H] ⁺ (36), 96.0815 [C ₆ H ₉ N+H] ⁺ (28), 86.0605 [C ₄ H ₈ O ₂ +H] ⁺ (13), 69.0708 [C ₃ H ₈ +H] ⁺ (5), 58.0423 [C ₃ H ₅ O+H] ⁺ (1)	717 – Carboxylic acids (feature 1526)
453.3438	7.11	C ₂₄ H ₄₄ N ₄ O ₄	-1.8	Cyclic tetrapeptide, compatible avec with halolitoralin B (cyclo-[Ile-Leu-Ile-Leu]) (Yang et al., 2002)	453.3438 [M+H] ⁺ (100), 435.3338 [C ₂₄ H ₄₂ N ₄ O ₃ +H] ⁺ (76), 340.2598 [C ₁₈ H ₃₃ N ₃ O ₃ +H] ⁺ [M-Leu/Ile+H] ⁺ (7), 322.2495 [C ₁₈ H ₃₁ N ₃ O ₂ +H] ⁺ (46), 227.1759 [C ₁₂ H ₂₂ N ₂ O ₂ +H] ⁺ [M-2 Leu/Ile+H] ⁺ (32), 209.1652 [C ₁₂ H ₂₀ N ₂ O+H] ⁺ (53), 132.1022 [C ₁₆ H ₁₃ NO ₂ +H] ⁺ (1), 114.0919 [C ₆ H ₁₁ NO+H] ⁺ [M-3 Leu/Ile+H] ⁺ (57), 96.0814 [C ₆ H ₉ N+H] ⁺ (18), 89.0604 [C ₄ H ₈ O ₂ +H] ⁺ (2), 86.0608 [C ₄ H ₇ N+H] ⁺ (4), 69.0708 [C ₃ H ₈ +H] ⁺ (3)	717 – Carboxylic acids (feature 1623)
181.0723	1.06	C ₆ H ₁₄ O ₆	2.9	Mannitol https://massbank.eu/MassBank/RecordDisplay?id=MSBNK-RIKEN-PR100904	181.0723 [M-H] ⁻ (100), 163.0616 [C ₆ H ₁₂ O ₅ -H] ⁻ (21), 131.0353 [C ₅ H ₈ O ₄ -H] ⁻ (6), 119.0352 [C ₄ H ₈ O ₄ -H] ⁻ (11), 113.0247 [C ₅ H ₆ O ₃ -H] ⁻ (9), 101.0245 [C ₄ H ₆ O ₃ -H] ⁻ (82), 89.0243 [C ₃ H ₆ O ₃ -H] ⁻ (59), 85.0294 [C ₄ H ₆ O ₂ -H] ⁻ (17), 73.0292 [C ₃ H ₆ O ₂ -H] ⁻ (13), 71.0135 [C ₃ H ₄ O ₂ -H] ⁻ (71), 59.0133 [C ₂ H ₄ O ₂ -H] ⁻ (46)	126 – Organooxygen compounds (feature 843) – Negative ionization

B

[M+H] ⁺ or [M+Na] ⁺ or [M-H] ⁻ m/z	RT (min)	Predicted formula (SIRIUS)	Delta m/z (ppm)	Putative annotation	MS/MS fragmentation spectra	Corresponding subnetwork
247.1450	7.69	C ₁₄ H ₁₈ N ₂ O ₂	-0.8	Unknown	247.1450 [M+H] ⁺ (65), 230.1182 [C ₁₄ H ₁₅ NO ₂ +H] ⁺ [M-NH ₃] ⁺ (29), 212.1072 [C ₁₄ H ₁₃ NO+H] ⁺ (9), 202.1231 [C ₁₃ H ₁₅ NO+H] ⁺ (100), 184.1126 [C ₁₃ H ₁₃ N+H] ⁺ (3), 174.0919 [C ₁₁ H ₁₁ NO+H] ⁺ (16), 162.0913 [C ₁₀ H ₁₁ NO+H] ⁺ (3), 152.1074 [C ₉ H ₁₃ NO+H] ⁺ (4), 134.0965 [C ₉ H ₁₁ N+H] ⁺ (1), 124.0755 [C ₇ H ₉ NO+H] ⁺ (2), 67.0547 [C ₅ H ₆ +H] ⁺ (1)	Single node – Piperidine (feature 803)
315.1966	9.96	C ₂₀ H ₂₆ O ₃	0.1	Unknown	315.1966 [M+H] ⁺ (80), 297.1855 [C ₂₀ H ₂₆ O ₃ +H] ⁺ (100), 287.2010 [C ₁₉ H ₂₆ O ₂ +H] ⁺ (5), 279.1745 [C ₂₀ H ₂₂ O+H] ⁺ (10), 269.1906 [C ₁₉ H ₂₄ O+H] ⁺ (48), 258.1328 [C ₁₆ H ₁₈ O ₃ +H] ⁺ (7), 251.1803 [C ₁₉ H ₂₂ +H] ⁺ (21), 241.1955 [C ₁₈ H ₂₄ +H] ⁺ (12), 227.1434 [C ₁₅ H ₁₈ O+H] ⁺ (7), 213.1273 [C ₁₅ H ₁₆ O+H] ⁺ (17), 197.1327 [C ₁₅ H ₁₆ +H] ⁺ (12), 185.1333 [C ₁₄ H ₁₆ +H] ⁺ (12), 171.1170 [C ₁₃ H ₁₄ +H] ⁺ (12), 159.1170 [C ₁₂ H ₁₄ +H] ⁺ (22), 145.1015 [C ₁₁ H ₁₂ +H] ⁺ (18), 131.0859 [C ₁₀ H ₁₀ +H] ⁺ (16), 119.0861 [C ₉ H ₁₀ +H] ⁺ (22), 107.0861 [C ₈ H ₁₀ +H] ⁺ (17), 95.0862 [C ₇ H ₁₀ +H] ⁺ (19), 81.0705 [C ₆ H ₈ +H] ⁺ (27), 69.0708 [C ₅ H ₈ +H] ⁺ (25), 55.0551 [C ₄ H ₆ +H] ⁺ (6)	Single node - Diterpenoid (feature 1029)
177.1349	1.01	C ₆ H ₁₆ N ₄ O ₂	-4.5	Related to Arginine	177.1349 [M+H] ⁺ (0), 118.0866 [C ₃ H ₁₁ NO ₂ +H] ⁺ [M-guanidyle+H] ⁺ [M-CH ₅ N ₃ +H] ⁺ (100), 60.0565 [CH ₅ N ₃ +H] ⁺ [guanidyle+H] ⁺ [CH ₅ N ₃ +H] ⁺ (2)	59– Carboxylic acid/Amino acid (feature 3051)
793.4871	18.01	C ₄₅ H ₇₀ O ₁₀	-0.1	MGDG (16:3/20:5) (Marcellin-Gros et al., 2020)	793.4871 [M+Na] ⁺ (100), 543.2940 [C ₃₁ H ₄₂ O ₈ +H] ⁺ [M-FA2+Na] ⁺ [M-C ₂₀ H ₃₀ O ₂ +Na] ⁺ (18), 517.2781 [C ₂₉ H ₄₀ O ₈ +H] ⁺ (10), 491.2624 [C ₂₇ H ₃₈ O ₈ +H] ⁺ [M-FA1+Na] ⁺ [M-C ₁₆ H ₂₅ O ₂ +Na] ⁺ (42), 135.1173 [C ₁₀ H ₁₄ +H] ⁺ (4), 85.0292 [C ₄ H ₄ O ₂ +H] ⁺ (10), 61.0293 [C ₂ H ₄ O ₂ +H] ⁺ (8)	51 – Fatty acyls & glycerolipids (feature 2135)
809.4485	17.70	C ₄₁ H ₇₀ O ₁₂ S	-0.7	SQDG (14:0/18:4) or SQDG (18:4/14:0) (Cutignano et al., 2016)	809.4485 [M+Na] ⁺ (0), 583.4338 [C ₃₅ H ₆₀ O ₅ +H] ⁺ (100), 551.2509 [C ₂₃ H ₄₄ O ₁₁ S+H] ⁺ (4), 373.2353 [C ₂₁ H ₃₄ O ₄ +H] ⁺ (10), 355.2242 [C ₂₁ H ₃₂ O ₃ +H] ⁺ (3), 325.2353 [C ₁₇ H ₃₄ O ₄ +H] ⁺ (13), 285.2420 [C ₁₇ H ₃₂ O ₃ +H] ⁺ (3), 230.9942 [C ₆ H ₈ O ₆ S+H] ⁺ (2) Identified in negative ionization mode 785.4526 [M-H] ⁻ (100), 557.2432 (unknown) [M-FA1-H] ⁻ [M-C ₁₄ H ₂₈ O ₂ -H] ⁻ , 509.2428 (unknown) [M-FA2-H] ⁻ [M-C ₁₈ H ₂₈ O ₂ -H] ⁻ , 225.0079 [C ₆ H ₁₀ O ₇ S - H] ⁻ (46), 206.9973 [C ₆ H ₈ O ₆ S - H] ⁻ (5), 164.9865 [C ₄ H ₆ O ₅ S - H] ⁻ (21), 152.9866 [C ₃ H ₆ O ₅ S - H] ⁻ (11), 148.9916 [C ₄ H ₆ O ₄ S - H] ⁻ (10), 134.0759 [C ₃ H ₄ O ₄ S - H] ⁻ (6), 125.0247 [C ₆ H ₆ O ₃ - H] ⁻ (4), 94.9808 [CH ₄ O ₃ S - H] ⁻ (20), 80.9649 [H ₂ O ₃ S - H] ⁻ (77), 71.0134 [C ₃ H ₄ O ₂ - H] ⁻ (9)	1 – Fatty acyls & glycerolipids (feature 2281)
485.2521	10.66	C ₂₆ H ₃₈ O ₇	0.1	Triacetylated diterpene with a C8 prenylchain. Compatible with a triacetoxy- secospatadienone diterpene (ruguloptone A) or a triacetoxy- secospatadienal skeleton (Cuevas et al., 2021) or a hydroazulenoid diterpene (König et al., 1993) or a spatane diterpene (Gerwick & Fenical, 1981)	485.2521 [M+Na] ⁺ (0), 425.2301 [C ₂₄ H ₃₄ O ₅ +Na] ⁺ [M-1acetoxy+Na] ⁺ [M-C ₂ H ₄ O ₂ +Na] ⁺ (99), 365.2093 [C ₂₂ H ₃₀ O ₃ +Na] ⁺ [M-2acetoxy+Na] ⁺ [M-2(C ₂ H ₄ O ₂)+Na] ⁺ (100), 305.1879 [C ₂₄ H ₃₄ O ₅ +Na] ⁺ [M-3acetoxy+Na] ⁺ [M-3(C ₂ H ₄ O ₂)+Na] ⁺ (1), 283.2060 [C ₂₀ H ₂₆ O+H] ⁺ (2), 227.1435 [C ₁₆ H ₁₈ O+H] ⁺ (2), 157.1014 [C ₁₂ H ₁₂ +H] ⁺ (5), 131.0859 [C ₁₀ H ₁₀ +H] ⁺ (3), 119.0859 [C ₉ H ₁₀ +H] ⁺ (5), 81.0707 [C ₆ H ₈ +H] ⁺ (6), 69.0707 [C ₅ H ₈ +H] ⁺ (4), 55.0548 [C ₄ H ₆ +H] ⁺ (1)	115 - Diterpenoids (feature 1870)

^a Abbreviations: DAG: Diacylglycerol, DGCC: diacylglyceryl carboxyhydroxymethylcholine, PC: phoshatidylcholine, MGDG Monogalactosyl diacylglycerol, SQDG: Sulfoquinovosyl diacylglycerol

Chapter 3

Negative parental and environmental effects of macroalgae on coral recruitment are linked with alterations in the coral larval microbiome

Chloé Pozas-Schacre¹, Hugo Bischoff², Camille Clerissi^{1,3}, Maggy M. Nugues^{1,3}

¹PSL Université Paris: EPHE-UPVD-CNRS, UAR 3278 CRIOBE, Université de Perpignan, 66860 Perpignan, France

²PSL Université Paris: EPHE-UPVD-CNRS, UAR 3278 CRIOBE BP 1013, 98729 Papetoai, Moorea, French Polynesia

³Laboratoire d'Excellence "CORAIL," Perpignan, France

*Corresponding author

Email: pozaschloe@gmail.com

Abstract

The persistence of reef-building corals is threatened by macroalgal assemblages which create a major demographic bottleneck in coral recruitment. Whether parental and environmental effects exist under coral-algal competition and whether they influence the offspring performance via effects on the larval microbiome represent major knowledge gaps in the comprehension of the mechanisms by which macroalgae may hinder coral recovery. Here, we describe the diversity and composition of the microbiome of larvae and adults of the coral *Pocillopora acuta* and surrounding benthic substrate on algal-removed and algal-dominated bommies. We then assess the relative influence of parental and environmental effects on coral recruitment processes by reciprocally exposing coral larvae from two parental origins (algal-removed and algal-dominated bommies) to algal-removed and algal-dominated environmental conditions. Dense macroalgal assemblages caused significant alterations in the microbiome composition of coral larvae and benthic substrate. Larvae produced by parents from algal-dominated bommies had a significantly lower survival compared to offspring from algal-removed bommies regardless of environmental conditions. In contrast, algal-induced parental and environmental effects interacted with one another to reduce the survival of coral recruits. Together our results demonstrate negative algal-induced parental and environmental effects on coral recruitment that could be mediated by alterations of the offspring microbiome.

1. Introduction

Corals live with a striking diversity of microbial symbionts (Symbiodiniaceae, bacteria, archaea, virus, fungi) that underpin host health through metabolic and defense functions (Bourne et al., 2016). To establish and maintain associations with microbes across life stages is therefore essential for the holobiont survival. Microbial symbionts can be acquired through the environment (i.e., horizontal transmission; Apprill et al., 2009), the parents (i.e., vertical transmission; Sharp et al., 2012) or a combination of both (i.e., mixed strategy; Epstein et al., 2019a; Damjanovic et al., 2020). A dynamic microbiome structuring occurs throughout coral ontogeny, with juvenile corals harboring a more diverse and variable microbiome than adult microbiomes (Lema et al., 2014; Damjanovic et al., 2020). This “winnowing process” during early life stages of marine invertebrates has been suggested to enable the establishment of fine-tuned microbial associations for a given environment (Nyholm & McFall-Ngai, 2004). Consequently, characterizing how environmental factors shape the coral microbiome at different life stages is critical to identify key host-microbes associations and to assess their stability or flexibility under stressful conditions.

On coral reefs, the cumulative impact of human-driven stressors (e.g., warming ocean temperatures, overfishing, pollution) has resulted in the widespread replacement of dominant benthic members where phase-shifts from coral to macroalgal dominance prevail (Smith et al., 2016). Decades of research have established the negative nature of coral-macroalgae interactions as algae compromise the survival, growth, recruitment and fecundity of corals (Birrell et al., 2008a; Vega Thurber et al., 2012; Webster et al., 2015; Monteil et al., 2020). Microbially-mediated competition is now recognized as one of main driver of coral demise (Barott & Rohwer, 2012; Clements & Hay, 2023) and macroalgae can disrupt the prokaryotic community of coral holobionts (Vega Thurber et al., 2012; Fong et al., 2020; Briggs et al., 2021; Clements & Hay, 2023). Suggested mechanisms involve allelopathy (Rasher et al., 2011; Morrow et al., 2017), transmission of pathogens through direct contact (Nugues et al., 2004), and the release of hydrophilic allelochemicals and dissolved organic carbon (DOC) feeding copiotroph and opportunistic microbes on the benthos and in the water column (i.e., the DDAM model: DOC, disease, algal and microbes (Vermeij et al., 2009; Barott & Rohwer, 2012; Nelson et al., 2013; Haas et al., 2016; Jorissen et al., 2016). Although macroalgal assemblages shape the microbial and chemical composition of reef waterscapes (Haas et al., 2016), their effects on the coral microbiome are inconsistent. For example, the microbiome of *Pocillopora damicornis* did not vary in composition between algal- versus coral-dominated reefs in Fiji (Beatty et al.,

2018, 2019). In another study, coral microbiome diversity and variability increased with increasing site-level algal cover in two islands of French Polynesia, even in the absence of direct contact (Briggs et al., 2021). Given the importance of microorganisms on holobiont health and the variable results produced by current studies, a better understanding of algal effects on the coral microbiome is needed to predict the resilience of coral communities as macroalgae proliferate.

Coral recruitment is a fundamental process for the replenishment of coral communities (Birrell et al., 2008a). Coral larvae can settle in the presence of microbial biofilms, and microbial biofilm composition of distinct age and environment influences the amount of larval settlement (Webster et al., 2004; Bulleri et al., 2018; Padayhag et al., 2023). Macroalgal assemblages can create a major demographic bottleneck in coral recruitment (Birrell et al., 2008; Evensen et al., 2019b; Webster et al., 2015). In particular, an *in-situ* study comparing recruitment success between algal- versus coral-dominated reefs suggest negative algal effects on larval settlement and post-settlement survival (Webster et al., 2015). These effects have been related to alterations in the microbiome of microbenthic communities (Bulleri et al., 2018; Padayhag et al., 2023). However, few studies have investigated relationships between macroalgal abundance, coral recruitment success and the microbiome of coral early life stages. In Fiji, the composition of the larval microbiome of *P. damicornis* between algal- versus coral-dominated reefs remained unchanged despite lower larval survival in algal-dominated seawater (Beatty et al., 2018).

Furthermore, parental effects (i.e., effect of the parental phenotype on the phenotype or performance of the offspring) can influence the survival and growth of coral offspring. Parental effects alone explain up to 17% and 94% of the variance in juvenile survival in spawning and brooding reproductive strategy, respectively (Kenkel et al., 2015; Quigley et al., 2016). In brooding species which internally produce larvae, maternal effects are expected to be stronger than in broadcast spawning species due a greater maternal investment (Richmond & Hunter, 1990) and a vertical transmission of microbial symbionts (Sharp et al., 2012; Damjanovic et al., 2020). The environmental stress experienced by the parents can lead to positive and negative cross-generational effects on offspring performance and has been related to altered maternal provisioning (Michalek-Wagner & Willis, 2001; Ross et al., 2016; Marangon et al., 2023). For example, the transfer of essential metabolites (e.g., lipids, amino acids) is reduced in eggs of heat-stressed parents in soft corals (Michalek-Wagner & Willis, 2001). In addition, parents could differentially invest in their offspring via distinct Symbiodiniaceae (Quigley et al., 2016) and prokaryotic communities (Epstein et al., 2019a; Marangon et al., 2023). So far, most studies

have explored parental effects relative to climate-associated stressors, yet as macroalgae can alter both health and fecundity of corals one might expect that similar effects might jeopardize coral recruitment success. To our knowledge, only one study (Beatty et al., 2018) has suggested algal-induced parental effects on corals. However, those effects were not associated with changes in the offspring microbiome. Thus, whether parental effects exist under coral-algal competition and whether they could influence the offspring performance via effects on the larval microbiome represent major knowledge gaps in our understanding of the mechanisms by which macroalgae may prevent coral recovery.

In this work, we study the effect of dense macroalgal assemblages on the brooding coral *P. acuta*. We hypothesized that macroalgal assemblages may have negative parental and environmental effects on coral recruitment and that these effects may be mediated by alterations in the coral and substrate microbiome. To test these assumptions, we conducted a manipulative field experiment in which we compared coral (i.e., adults and larvae) and microbenthic substrate microbiomes between algal-removed and algal-dominated bommies within a single fringing reef in Mo'orea, French Polynesia, enabling to control for confounding reef-scale effects. Then, we assessed the relative influence of parental and environmental effects on coral recruitment success by reciprocally exposing coral larvae from two parental origins (i.e., colonies originating from algal-removed vs. algal-dominated bommies) to algal-removed and algal-dominated environmental conditions in a series of survival and settlement experiments.

2. Materials and methods

2.1. Experimental field set-up

We conducted the manipulative field experiment between June and December 2020 in a shallow fringing reef lagoon (2-2.5 m deep) off the North coast of Mo'orea, French Polynesia (17°29'14.86"S 149°53'0.76"W). In June 2020, eight coral bommies (1-2 m in diameter) covered by dense macroalgal assemblages were randomly selected within an area of ~1000 m² (distance between adjacent bommies: ~10 m; electronic supplementary material, figure S1a and b). Bommies were randomly allocated to one of two treatments: i) macroalgae present (thereafter referred as "algal-dominated") and ii) macroalgae removed (i.e., including canopy-forming holdfasts and understory species, referred as "algal-removed") (electronic supplementary material, figures S1c-d and S2a). Macroalgae were removed from their substratum manually with wire brushes taking care not to damage other benthic organisms or

to alter the substrate topography. Their absence on algal-removed bommies was maintained on a monthly basis.

After algal removal, six colonies (~12 cm in diameter) of the brooding coral *P. acuta* were transplanted on each experimental bommie and left untouched for 5 to 6 months, a period sufficient for parental effects to occur (Ross et al., 2016). Colonies were chiseled at their base and secured on small (4 x 4 cm) tagged plastic grids with two cable ties. Grids were then attached onto the bommies with releasable cable ties and tagged mounting screws inserted into holes drilled into dead coral substratum using a pneumatic drill. This procedure was used so colonies could be brought to the laboratory facilities for coral larval collection and re-attached onto the bommies at their exact same position. Colonies were placed on substrate predominantly covered by bare substrate, crustose coralline algae (CCA) or thin (< 5 mm) turf communities, without direct contact with macroalgae, although some periodic contact may have occurred due to water movement.

In August 2020, eleven aragonite tiles (3 x 3 x 1 cm) were fixed on each bommie for the sampling of substrate microbiome and the coral recruitment experiments (electronic supplementary material, figure S2a-c). One hole was drilled at the center of each tile for attachment to the dead coral substratum. Each tile was tagged and fixed on the bommies with a cable and a tagged mounting screw inserted into a hole drilled into dead coral substratum using a pneumatic drill. Tiles were placed as corals without direct contact with macroalgae.

2.2. Benthic surveys

Benthic communities were quantified on each bommie by taking photographs of 5 randomly placed, 20 x 20 cm quadrats with an Olympus TG4 camera in June (before algal removal), August and November 2020. Benthic categories included: bare substrate (i.e., absence of macroorganisms but presumably colonized by microalgae), crustose coralline algae (CCA), cyanobacteria, living hard coral, algal turf (i.e., mixed species assemblages of filamentous algae < 1 cm in height) and macroalgae (upright and anatomically complex algae with canopy height > 1 cm). Within the macroalgae category, 8 genera or species were recorded: *Amansia rhodantha*, *Chnoospora* spp., *Dictyota bartayresiana*, *Halimeda* spp., *Lobophora* spp., *Padina boryana*, *Sargassum pacificum* and *Turbinaria ornata*. The percent cover of each category was calculated for each quadrat from 25 random points using the software PhotoQuad (Trygonis & Sini, 2012). For each category, the percent cover corresponded to the number of points of that category divided by the total number of identifiable points in the quadrat.

2.3. Microbiome sampling

In November 2020, 3 fragments of 3 colonies from each bommie were sampled to characterize the microbiome of adult corals (electronic supplementary material, figure S2b). Coral fragments were broken off into 2 mL microtubes underwater and transported back at the laboratory into cool boxes with ice. Larvae brooded by these colonies were sampled on November 19 and 20 (4th and 5th day after the new moon). Two colonies out of the 3 sampled for the adult microbiome were randomly selected on each bommie and brought to the laboratory. They were grouped by each treatment and isolated into individual plastic containers (~25 L) placed inside a large water tank filled with 220 L of seawater collected ~50 cm above the bommies from their respective treatment. Seawater was recirculated in each closed system using one pump (~2000 L/h – EHEIM compact+ 3000 pump) and water temperature was maintained at ~27°C using heaters. Container outflows were covered by a 200 µm mesh net around 11:00 pm to prevent larval escape. Larvae were released throughout the night and, early morning (between 5:00 and 7:00 am), 30 larvae of each colony were collected with sterile pipette tips. One colony of each treatment did not release larvae. Each fragment and larvae of each colony were rinsed three times with 0.22 µm filtered sterilized seawater (FSW), transferred into 2 mL cryotubes with 1 mL of DNA/RNA Shield (Zymo Research). Additionally, one water sample (5 L) from each water tank was filtered onto a 0.22 µm filter. Filters were cut with sterile tools and pieces were transferred into 2 mL cryotubes with 1 mL of DNA/RNA Shield (Zymo Research). In December 2020 (2 days before the settlement experiment), 3 tiles per bommie were randomly sampled to characterize the substrate microbiome. Tiles were placed into individual sterile Whirl-Pak bags underwater and transported in a cool box with ice to the laboratory. Cryptic and exposed surfaces of each tile were sampled independently. After rinsing with FSW, surfaces were sampled first by scraping with a sterile scalpel and second by swabbing with a sterile cotton swab. Scrapings and cotton swab heads of each surface were placed into 2 mL cryotubes with 1 mL of DNA/RNA Shield. DNA/RNA Shield-containing cryotubes were stored at -20°C until DNA extraction.

2.4. Sequencing of the 16S rRNA gene and metabarcoding data processing

DNA was extracted using the ZymoBIOMICS DNA Miniprep kit (Zymo Research, USA, D4300). Both sampled materials and the 1 mL DNASHield were placed in beadtubes. Extractions were then performed from the lysate according to manufacturer instructions for samples stored and lysed into DNA/RNA Shield. After extraction, samples were stored at -20°C

and dried with a centrifugal evaporator (EZ-2 serie, Genevac) for safe shipment to Genome Quebec (Montréal, Canada) for 16S rRNA marker gene amplification by PCR and sequencing. Unfortunately, 4 coral samples were damaged during shipment. The hypervariable region V3-V4 of the 16S rRNA gene was amplified using the universal primers 341F (5'-CCTACGGGNGGCWGCAG- 3') and 805R (3'-GACTACHVGGGTATCTAATCC- 5'), suggested for marine bacteria and some archaea (Klindworth et al., 2013) and amplicons were sequenced on an Illumina NovaSeq 6000 sequencer. Paired-end (2x250bp) reads were processed using DADA2 (Callahan et al., 2016) on R (version 4.2.3) to generate amplicon sequence variants (ASVs). First, reads with ambiguous N bases were discarded and the primers were removed using the Cutadapt program (Martin, 2011). Reads were filtered out if their length was not comprised between 200 and 250bp and if they contained bases with a quality score inferior to 2 or more than 3 expected errors. Sequences were denoised based on a modified error rate estimation function, by altering loess arguments (weights and span) and enforcing monotonicity, more suitable for NovaSeq data. After reads merging and ASVs inference, chimeric sequences and those detected in a single sample were removed. Taxonomy was assigned from phylum to genus levels using the Silva reference database (v138.1). The sequence table, taxa table and metadata were then imported in the *phyloseq* R package (McMurdie & Holmes, 2013). Data were filtered again by removing mitochondria and chloroplast reads, low abundance reads (i.e., at least 20 reads in 5 % of the samples and contaminants with the *decontam* R package (prevalence method) using our blank samples (n = 9) (Davis et al., 2018).

2.5. Coral recruitment experiments

To determine the relative influence of parental and environmental effects on coral recruitment processes, offspring produced by each parental origin were reciprocally exposed to algal-removed and algal-dominated environmental conditions in a series of experiments (electronic supplementary material, figure S2c). In the larval survival experiment, larvae were collected on 18 December 2020 (5th day after the new moon) as described previously, pooled by their parental origin and deployed in a full factorial design into 1L glass jars filled with 400 mL of seawater freshly collected ~50 cm above algal-removed or algal-dominated bommies. Each jar held 10 larvae and there were 12 replicated jars per combination of factors. Jars were randomly interspersed in a heat-regulated water bath. Light was provided by 2 lamps (Viperspectra Aqualight system 165W) set ~45 cm above the jars on a 12:12h photoperiod with

an irradiance of $\sim 60 \mu\text{mol m}^{-2}$. Seawater was changed every 2 days (30% of the jar volume). Temperature was recorded every 15 mins with two HOBO Pendant[®] loggers, while pH, conductivity and O₂ saturation were monitored twice daily in eight randomly selected jars. At Day 6, the number of surviving larvae was counted in each jar using a binocular magnifier. Larvae were considered alive if swimming after gentle pipette aspirations.

In the larval settlement and post-settlement survival experiments, larvae were collected on 20 December 2020 as described previously, pooled by their parental origin and deployed in a full factorial design into 1 L glass jars, each containing 800 mL of seawater and one tile both originating from algal-removed or algal-dominated bommies. A dowel was inserted through the central hole of each tile, so their cryptic (underside) surface was accessible to larvae. Each jar held 10 larvae and there were 12 replicated jars per combination of factors. Jars were maintained in the water bath as described above under the same environmental conditions, and water physiochemical parameters were monitored in the same manner. After 24h, the number of settled larvae were counted on all tile surfaces and individually mapped. After the initial mapping, tiles with settled larvae were returned to their tagged field positions and reexamined at days 7 and 21 to estimate early post-settlement survival. Larval survival and settlement were expressed as percentages of the initial number of larvae added to each jar. Post-settlement survival was expressed as percentage of the number of coral settlers counted after 24h on each tile.

2.6. Statistical analysis

2.6.1. Benthos data

Benthic community composition across bommies were visualized using Principal Coordinate Analysis (PCoA) on Bray-Curtis dissimilarities of untransformed data. Variations in these benthic assemblages were assessed by Permutational Multivariate Analysis of Variance (PERMANOVA, *vegan* package v.2.6.4, “adonis2” function and 999 permutations; (Oksanen et al., 2022) using, as fixed factors, algal treatment (algal-dominated vs. algal-removal bommies) before removal of macroalgae, and algal treatment and time (August vs. November) after the removal of macroalgae.

2.6.2. Microbiome data

Due to obvious differences, coral and substrate microbiomes were analysed separately. We considered the fixed factors coral life stage (adult vs. larvae) and algal treatment for the coral microbiome, and the fixed factors surface (exposed vs. cryptic) and algal treatment for the substrate microbiome. Alpha diversity (Shannon diversity index) was measured on rarefied count data using the *phyloseq* R package (McMurdie & Holmes, 2013) and the “rarefy_even_depth” function. To assess differences between coral life stage (or surface) and algal treatment, data were analysed using linear mixed-effects models (LME) using the *lme4* (v1.1.31) (Bates et al., 2015) and *emmeans* (v1.8.3) R packages (Russell, 2018). As coral fragments were not independent, we added colony as a random factor. Similarly, bommie was added as a random factor in the model on tile surface microbiome. Beta diversity statistics and visualizations were conducted from centered log-ratio (CLR) transformed data with the package *microbiome* (Lahti & Shetty, 2017) and Euclidian similarity matrices. Differences in microbiome composition were visualized by Principal Component Analysis (PCA) and tested using PERMANOVA (999 permutations). Microbiome variability (beta dispersion) was investigated with the “betadisper” function and tested with a permutation test (999 permutations) from the *vegan* package.

To identify the most contributing microbial taxa to microbiome compositional differences, we used the supervised classification algorithm Random Forest with the package *caret* (Kuhn, 2008). Models were trained with 500 trees following a K-folds cross validation scheme (6 folds, “trainControl” function from the *MLmetrics* package (Yan, 2016). Model performance was evaluated by its accuracy score and the “varImp” function was used to retrieve the best predictors by their IncMSE score (increase in mean squared error). We conducted the analysis at the family level to explore broad microbial abundance patterns (coral life stage (or surface) x algal treatment) and selected the 20 most explaining families to build two-way heatmaps from their mean CLR-transformed abundances using Euclidian distances and Ward’s minimum variance method. Then, to specifically identify the ASVs best explaining differences between algal treatments, we ran random forests on the microbiomes of coral adults, coral larvae and cryptic and exposed surfaces independently. *ANCOMBC* (Analysis of Compositions of Microbiomes with Bias Correction) package (Lin & Peddada, 2020) was used for differential abundance analysis on the microbial families and the 100 top-ranked ASVs. Differential abundances were considered significant if adjusted p-values were < 0.05. For cryptic and

exposed surfaces, significant ASVs were only shown if they had a log-fold change > 2 or < -2 due to the high number of significantly different ASVs.

2.6.3. Coral recruitment experiment data

Survival and settlement data were modelled with a binomial distribution using generalized linear mixed-effects models (GLME; “glmer” function from *lme4* package ; Bates et al., 2015). Data were modelled with parental origin (i.e., larvae brooded by parents originating from algal-dominated vs. algal-removed bommies), environment (i.e., environmental conditions experienced in algal-dominated vs. algal-removed bommies, i.e., seawater, substrate and/or bommie depending on specific variables) and time (i.e., Day 7 vs. 21) as fixed factors. The effects of parental origin and environment on settlement rates were first explored pooling all tile surfaces. To assess surface-specific differences, a second model was run adding the fixed factor tile surface nested within the random factor tile. Due to low settlement on exposed and vertical tile surfaces, post-settlement survival data were modelled using data from cryptic surfaces by adding time as a fixed factor and bommie as a random factor. Pairwise comparisons were conducted when fixed effects were significant using the *emmeans* package (function “emmeans”). Model assumptions of homogeneity of variance, normal distribution of the residuals and absence of overdispersion were checked with the *DHARma* package (Hartig, 2017).

3. Results

3.1. Benthic community composition

Benthic community composition did not differ between algal treatments before the start of the experiment (PERMANOVA, Algal treatment: $R^2 = 0.02$, $p > 0.05$). Specifically, community composition varied significantly between algal treatments and remained distinct throughout the experiment (PERMANOVA, Algal treatment: $R^2 = 0.59$, $p < 0.001$; Time: $R^2 = 9e-4$, $p > 0.05$; Treatment x Time: $R^2 = 0.05$, $p > 0.05$; electronic supplementary material, figure S3a). After removal, algal-removed bommies were dominated by bare substrate (~44% cover) and turf (~28% cover), while algal-dominated bommies were dominated by macroalgae (~68% cover), with the brown macroalgae *Turbinaria ornata* (~39% cover) & *Dictyota bartayresiana* (~11% cover) as the two most abundant species (electronic supplementary material, figure S3b-c).

3.2. Coral microbiome composition

The final 16S rRNA gene dataset data resulted in 4474 ASVs and 26 514 802 reads across 132 samples (electronic supplementary material, figure S4, table S1). Alpha diversity of coral microbiomes significantly differed between adults and larvae (LME, $p < 0.001$), but not between algal treatments ($p > 0.05$, figure 3.1a; electronic supplementary material, table S2a). Larval microbiomes (emmean = 3.43 ± 0.09) were nearly three times more diverse than adult microbiomes (emmean = 1.02 ± 0.05). Coral prokaryotic community significantly varied across coral life stages (PERMANOVA, Coral life stage: $p < 0.001$, figure 3.1c), but the effect of coral life stage differed between algal treatments (Coral life stage x Algal treatment: $p < 0.05$). Specifically, the algal treatment significantly structured the larval microbiome (Pairwise PERMANOVA, $p = 0.01$), but not the adult microbiome ($p > 0.05$; electronic supplementary material, table S3a). Microbiome variability was higher in larval compared to adult stages regardless of the algal treatment (PERMDISP, Life stage: $p < 0.001$, Algal treatment: $p > 0.05$; electronic supplementary material, figure S5a, table S4a).

The coral adult microbiome was largely dominated by the Endozoicomonadaceae family (class Gammaproteobacteria), accounting for 88.9% of the microbial sequences (figure 3.1e, electronic supplementary material, figure S6a). Comparatively, the coral larval microbiome harbored a greater diversity of Gammaproteobacterial families, such as Alteromonadaceae (e.g., *Alteromonas*, *Salinimonas*), accounting for nearly half of the bacterial community (45.6%), followed by Marinobacteraceae (1.4%, *Marinobacter*) and Vibrionaceae (1.1%, *Vibrio*; electronic supplementary material, figure S6a). Numerous Alphaproteobacterial families, such as Rhodobacteraceae (33.6%, e.g., *Maribius*, *Limmimaricola*) and Sphingomonadaceae (3.8%, *Erythrobacter*), were also highly abundant in coral larvae. Overall, dominant bacterial families in the adult and larval microbiome displayed little differential abundance between algal treatments (electronic supplementary material, figures S6a and S7a). A single family, the Flavobacteriaceae (class Bacteroidia), significantly increased in the adult microbiome from algal-dominated bommies (ANCOMBC, $p.adj < 0.05$).

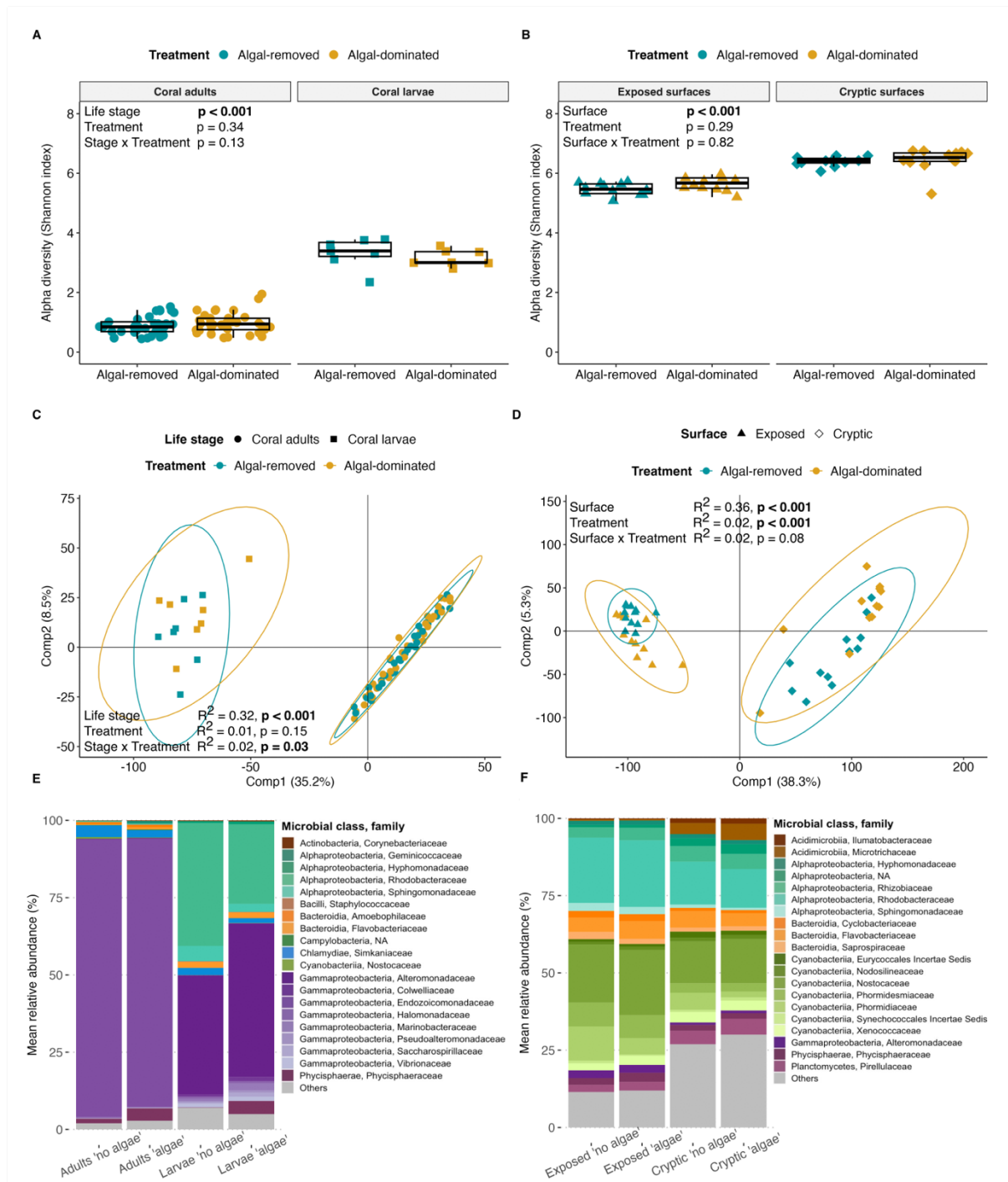


Figure 3.1 | Microbiome diversity and composition. Alpha diversity of (a) coral adults and larvae and of (b) cryptic and exposed surfaces from algal-removed and algal-dominated bommies. Effects of coral life stage/surface and algal treatment on diversity were tested using linear mixed effect models with details in the electronic supplementary material, table S2. Beta diversity of (c) coral adults and larvae and (d) cryptic and exposed surfaces from algal-removed and algal-dominated bommies. Variations of microbiome composition were tested by PERMANOVA (nperm = 999). PCA were run on CLR-transformed ASV abundances with Euclidian distances. Ellipses correspond to 95% data ellipses. Top 20 most abundant microbial families across (e) coral adults and larvae and (f) cryptic and exposed surfaces from algal-removed and algal-dominated bommies.

3.3. Substrate microbiome composition

Substrate microbiome richness did not differ between algal treatments (LME, $p > 0.05$), but significantly differed between exposure ($p < 0.001$; figure 3.1*b*; electronic supplementary material, table S2*b*). The microbiome of the cryptic surface (emmean = 6.78 ± 0.06) was more diverse than that of the exposed surface (emmean = 5.80 ± 0.06). The composition of the substrate microbiome significantly differed between exposure and algal treatment (PERMANOVA, Surface: $p < 0.001$, Algal treatment: $p < 0.001$, Surface x Algal Treatment: $p > 0.05$; figure 3.1*d*; electronic supplementary material, table S3*b*). The substrate microbiome variability did not vary between algal treatments, but significantly differed between exposure (PERMDISP, Surface: $p < 0.001$, Algal treatment: $p > 0.05$; electronic supplementary material, figure S5*b*, table S4*b*). Specifically, the microbiome variability of cryptic surfaces was significantly higher than that of exposed surfaces.

Microbiomes of exposed and cryptic surfaces were dominated by the classes Cyanobacteriia, Alphaproteobacteria and Bacteroidia (figure 3.1*f*). Nostocaceae was the most abundant Cyanobacterial family representing 21.1% and 15.7% of the microbial sequences on exposed and cryptic surfaces, respectively, followed by Phormidiaceae which was also more abundant on exposed surfaces. Rhodobacteraceae (e.g., *Ruegeria*, *Limibaculum*, electronic supplementary material, figure S6*b*) and Rhizobiaceae were dominant families of the Alphaproteobacteria class. The former accounted for 22.1% and 14.3% of the microbial sequences on exposed and cryptic surfaces, respectively. Three families of Bacteroidia, in particular the Flavobacteriaceae (e.g., *Muricauda*), were abundant. Additionally, both exposed and cryptic surfaces contained ASVs belonging to the Planctomycetes, Phycisphaerae and Acidimicrobiia classes. No microbial family was significantly differentially abundant between algal treatments on exposed surfaces (ANCOMBC, $p.adj > 0.05$). On cryptic surfaces, the relative abundance of 14 families significantly varied with algal treatment, including Stappiaceae, Phormidiaceae, Cellvibrionaceae and Tenderiaceae which decreased on algal-dominated bommies relative to algal-removed bommies (ANCOMBC, $p.adj < 0.05$; electronic supplementary material, figure S7*b*).

3.4. Differential abundance analysis of ASVs between algal treatments

Random forests achieved a strong ($> 70\%$) classification accuracy for all sample types (figure 3.2*a*). However, no significantly differentially abundant ASV was detected in the coral adult microbiome. In the coral larval microbiome, 12 ASVs differed significantly between algal

treatments (ANCOMBC, $p_{adj} < 0.05$, figure 3.2b). Most were affiliated to the Alphaproteobacteria. Six belonged to the Rhodobacteraceae, including two *Maribius*, one *Palleronia-Pseudomaribius* and two *Sulfitobacter*, and significantly decreased in larvae brooded by corals from algal-dominated bommies relative to algal-removed bommies. Interestingly, four of these taxa were undetected in the coral adult microbiome, but present in the coral larval collection tank (electronic supplementary material, table S5). Other decreasing ASVs belonged to the genera *Mycobacterium* and *Vibrio*. In contrast, ASVs enriched in larvae brooded by corals from algal-dominated bommies were affiliated to the genera *Erythrobacter*, *Thalassolituus* and *Marinobacterium*. In addition, an ASV which was identified as *Vibrio coralliilyticus* (ASV2412, electronic supplementary material, table S6), a well described coral pathogen (Bourne et al., 2016), was detected in coral larvae microbiomes, but its abundance did not differ between algal treatments.

Comparatively, a high number of ASVs in the substrate microbiomes differed significantly between algal treatments (i.e., 37 and 30 ASVs for exposed and cryptic surfaces, respectively). Therefore, we only showed the significant ASVs with a log-fold change > 2 or < -2 (figure 3.2c). On the exposed surfaces, a majority of ASVs were depleted on algal-dominated bommies relative to algal-removed bommies. These were affiliated to the Acidimicrobiia (e.g., *Illumatobacter*), Alphaproteobacteria (e.g., *Tropicimonas*, *Jannashia*), Gammaproteobacteria (*Granulosicoccus*, *Agaribacter*) and Planctomycetes (*Rubripirelulla*). Among the Bacteroidia, ASVs affiliated to the genera *Portibacter* and *Lewinella* (Sparospiraceae) were significantly enriched on the exposed surface of algal-dominated bommies relative to algal-removed bommies, while *Aquibacter* (Flavobacteriaceae) and *Crocinitomix* (Crocinitominaceae) displayed the opposite trend. ASVs belonging to the Cyanobacteriia were only flagged in the microbiome of the exposed surface. For example, the ASV *Acrophormium* PCC-7375 (Phormidesmiaceae) was significantly depleted while *Rivularia* PCC-7117 (Nostocaceae) was significantly enriched on algal-dominated bommies relative to algal-removed bommies. On the cryptic surface, several ASVs associated to the Alphaproteobacteria and Planctomycetes were significantly enriched in algal-dominated bommies, such as those belonging to the genera *Silicimonas*, *Limibaculum* (Rhodobacteraceae), *Bauldia* (Rhizobiales Incertae Sedis), *Rhodopirelulla* and *Pir4* lineage (Pirellulaceae). In contrast, seven ASVs were depleted on the cryptic surface of algal-dominated bommies. These ASVs belonged to the genera *Marinibacterium* (family Rhodobacteraceae), *Muricauda*, *Aquimarina* (Flavobacteriaceae) and *Blastopirellula* (Pirellulaceae).

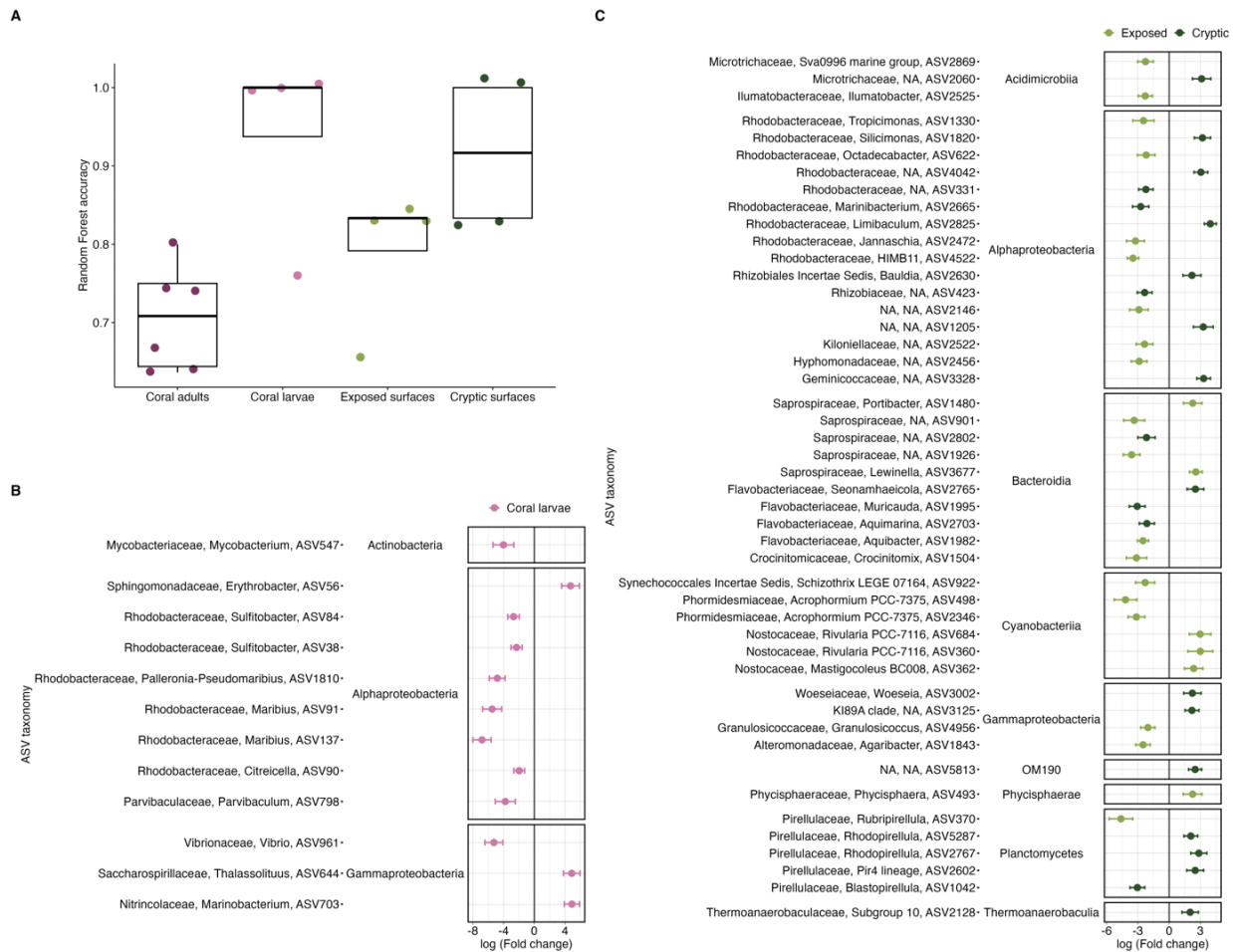


Figure 3.2 | Microbial ASVs associated with algal removal treatment (a) Random Forest accuracy for classifying samples relative to the algal-removal treatment. Significantly differentially abundant ASVs (ANCOMBC, $p_{adj} < 0.05$) between algal-dominated vs algal-removed bommies within (b) coral adult and larvae samples and (c) exposed and cryptic surfaces. Fold changes were calculated relative to the mean changes in the algal-removed treatment. For the surface microbiomes, only ASVs with a log-fold change > 2 or < -2 are included. ASVs are grouped by family, genus and class.

3.5. Coral recruitment experiments

Water physiochemical conditions of larval survival and settlement experiments were similar across algal treatments (electronic supplementary material, table S7; Kruskal-Wallis, $p > 0.05$). Parameters averaged $27.92 \text{ }^\circ\text{C}$ (± 0.63) for temperature, 8.24 (± 0.09) for pH, 29.11 psu (± 1.03) for salinity and 87.34% (± 5.09) for O_2 saturation. The parental origin significantly influenced larval survival (GLME, $p = 0.02$; figure 3.3a, electronic supplementary material, table S8a). Specifically, the percentage of larval survival on all bommies declined from 94.8% (± 1.7) for larvae brooded by parents from algal-removed bommies to 88.8% (± 2.6) for larvae brooded by parents from algal-dominated bommies, representing a reduction of 6.3% . The analysis revealed no significant environmental (i.e., seawater) effect or interaction between the two factors on larval survival.

When considering settlement on whole tiles (i.e., pooling all surfaces), there were no parental or environmental (i.e., seawater and substrate) effects or interaction between these factors on larval settlement, which averaged 63.3% (± 3.7) (figure 3.3b, electronic supplementary material, table S8b). When adding tile surface to the model, there was a significant 3-way interaction parental origin x environment x tile surface (GLME, $p < 0.001$). Post-hoc tests revealed that larvae brooded by corals on algal-dominated bommies settled less on cryptic tile surfaces originating from algal-dominated bommies relative to cryptic tile surfaces originating algal-removed bommies, while the opposite was found for vertical tile surfaces (electronic supplementary material, table S8c, figure S8). Therefore, larvae brooded by corals from algal-dominated bommies preferred to settle on slightly more exposed surfaces of algal-dominated bommies.

There was a significant interaction between parental origin and environmental factors on post-settlement survival (GLME, $p = 0.006$; figure 3.3c, electronic supplementary material, table S8c). Post-hoc tests revealed a significant environmental effect on post-settlement survival for larvae brooded by parents from algal-dominated bommies only. The percent survival of recruits produced by parents from algal-dominated bommies declined from 69.1% (± 4.9) on algal-removed bommies to 34.5% (± 9.6) on algal-dominated bommies at Day 7 and from 61.1% (± 7.5) to 29.8% (± 8.3) at Day 21, representing reductions of 50.1% and 51.2% on days 7 and 21, respectively. In contrast, post-settlement survival of larvae brooded by parents from algal-removed bommies did not vary between algal treatments and averaged 61.5% (± 6.2) and 52.7% (± 6.8) for days 7 and 21, respectively.

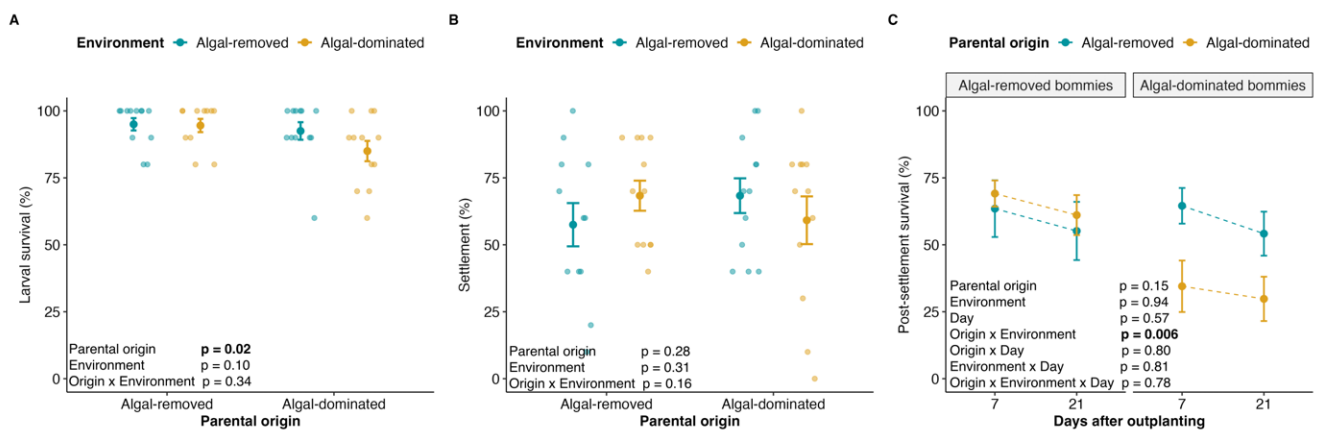


Figure 3.3 | Coral recruitment experiments. (a) Survival (mean \pm se, $n = 12$) of larvae brooded by corals from algal-removed and algal-dominated bommies after 6 days in seawater from each algal treatment. (b) Settlement (mean \pm se, $n = 12$) of larvae brooded by corals from algal-removed and algal-dominated bommies on tiles from algal-removed and algal-dominated bommies after 24h. (c) Post-settlement survival (mean \pm se, $n = 12$) of coral settlers produced by corals from algal-removed and algal-dominated bommies 7 and 21 days after out-planting on algal-removed and algal-dominated bommies. Statistical significance was assessed with GLME using binomial distribution, detailed results can be found in electronic supplementary material, table S8.

4. Discussion

Our work showed that dense macroalgal assemblages did not significantly alter the microbiome of adult corals at the scale of coral bommies within a single fringing reef. Despite the large differences in macroalgal cover between the algal-removed and algal-dominated bommies (i.e., 4% vs. 68%) and the 5-month exposure to each treatment, the diversity, variability and composition of the coral adult microbiome did not significantly vary between the algal treatments. These results disagree with several studies suggesting that macroalgae can alter the coral microbiome (Vega Thurber et al., 2012; Morrow et al., 2017; Briggs et al., 2021). However, they may be explained by the fact that our sampled colonies were initially placed without direct contact with macroalgae. Many of the mechanisms by which algae affect corals, including the release of allelochemicals (Rasher et al., 2011; Morrow et al., 2017) and dissolved organic matter (Vermeij et al., 2009; Jorissen et al., 2016), operate on small-spatial scales. In case of coral pathogen transmission, they are likely to require direct contact (Vu et al., 2009). These results could also be related to the identity of the coral host itself. Pocilloporids have a remarkable capacity to maintain their microbiome under macroalgal competition (Beatty et al., 2018) and abiotic disturbances (Epstein et al., 2019b; Ziegler et al., 2019). Ziegler et al., 2019 proposed that microbiome flexibility is host-specific with Pocilloporids being “microbiome regulators”, capable of some microbial regulations while keeping a constant microbiome. This property may be related to their opportunist life-history strategies characterized by high recruitment rates and fast-growth (Darling et al., 2012). Although a lack of microbiome flexibility may hinder the acclimation potential of corals (Price et al., 2023), a stable microbiome could enhance coral resilience to rapid environmental changes and microbial pathogens (Beatty et al., 2019; Epstein et al., 2019b). For example, microbiome stability was associated with unaltered anti-pathogen activity against *V. coralliilyticus* in adult *P. damicornis* corals from both coral-dominated marine protected areas and macroalgal-dominated fished reefs in Fiji (Beatty et al., 2019). In our study, the relative abundance of Vibrionaceae in adult *P. acuta* corals was not significantly influenced by the algal treatment. In contrast, corals from both algal-removed and algal-dominated bommies were largely dominated (>85% relative abundance) by bacteria from the Endozoicomonadaceae family. This family of bacteria likely plays critical roles in the health and resilience of coral holobionts of different coral species, including Pocilloporids (Neave et al., 2017b; Beatty et al., 2019).

The coral larval microbiome was compositionally distinct and more diverse and variable compared to the adult microbiome. These ontogenetic changes are associated with a

“winnowing process” (Nyholm & McFall-Ngai, 2004) and match with previous studies on corals (Lema et al., 2014; Epstein et al., 2019a; Damjanovic et al., 2020) and other marine invertebrates (Marangon et al., 2023). The coral larval microbiome was dominated by the Rhodobacteraceae and Alteromonadaceae families. These families have been detected in high abundance in larvae of *P. acuta* (Damjanovic et al., 2020) and other coral species (Sharp et al., 2012; Lema et al., 2014). Importantly, our study shows that the composition of the coral larval microbiome differed significantly between larvae brooded by corals from algal-removed and algal-dominated bommies. Our knowledge of the processes by which bacterial communities are acquired during the larval stage is still very limited (Apprill et al., 2009; Sharp et al., 2012; Damjanovic et al., 2020). However, in the closely related brooding coral *P. damicornis*, the establishment of bacterial communities in the offspring is driven by both parental and planulation environments, with the majority of uptake occurring horizontally (Epstein et al., 2019a). Similarly, in *P. acuta*, larvae shared a minority of their ASVs with their parents (Damjanovic et al., 2020). Since our colonies were maintained in seawater from their respective treatment during larval release, the relative importance of parental vs. environmental origins of larval microbes cannot be separated. Larvae were collected less than 8 hours upon emergence and rinsed in FSW three times before preservation. In a similar timeframe, vertical transmission of bacteria can occur in the form of bacterial aggregates in newly released *P. acuta* larvae (Damjanovic et al., 2020). Likewise, in the coral *Porites astreoides*, bacterial cells were detected in the ectoderm of larvae in less than an hour after release constituting the vertically-transmitted microbiome (Sharp et al., 2012). Therefore, in our study, it is likely that both parental and planulation environments drove the differences in coral larval microbiome between algal treatments.

ASVs enriched in larvae brooded by parents from algal-dominated bommies were affiliated to the genera *Erythrobacter*, *Thalassolituus* and *Marinobacterium*. These bacteria have previously been associated with coral disease and coral-algal competition (Fong et al., 2020; Huntley et al., 2022). In contrast, their microbiome was depleted in putative beneficial bacteria. For example, *Sulfitobacter* and *Vibrio* can produce and/or degrade DMSP (Raina et al., 2010). DMSP and its breakdown products (e.g., DMS) play major roles in coral health (e.g., as antioxidant and antibiotic). Rhodobacteraceae and vibrios are also important bacteria which contribute to carbon and nitrogen acquisition (Ceh et al., 2013b; Lema et al., 2014). While vibrios have often been described as potential coral pathogens (Bourne et al., 2016), some species may be mutualistic by preventing bacterial colonization (Jessen et al., 2013). The loss of these beneficial bacteria could compromise larval physiology and defense through a decrease

in their nutritional and protective functions. Remarkably, the relative abundance of the Alteromonadaceae family was not impacted by the algal treatment, demonstrating a strong host-microbe association. Some *Alteromonas* strains provide nitrogen sources (Ceh et al., 2013b; Lema et al., 2014), participate in larval settlement induction (Webster et al., 2004), and prevent pathogenetic invasion (Gil-Turnes et al., 1989).

Macroalgal assemblages significantly structured the substrate microbiome, as previously demonstrated (Bulleri et al., 2018). Microbial communities on algal-dominated bommies likely responded to macroalgal-induced changes in water chemistry. For example, algal-derived dissolved organic matter differs in composition from that of corals influencing the microbial structure of biofilm and pelagic communities (Nelson et al., 2013; Remple et al., 2021). These labile and energy-rich algal exudates typically favor the growth of copiotrophic bacteria potentially detrimental to corals (Nelson et al., 2013; Haas et al., 2016). On exposed surfaces, certain bacteria enriched on algal-dominated bommies have been associated with coral diseases, including the genera *Lewinella* and *Rivularia* and the family Saprospiraceae (Briggs et al., 2021; Huntley et al., 2022). Similarly, cryptic surface microbiomes from algal-dominated bommies harbored bacterial opportunists of corals, such as the genus *Limibaculum* (Rosales et al., 2023), and several bacterial classes enriched on algal-dominated bommies have been negatively correlated with coral settlement, including Thermonanaerobaculia and Planctomycetes (Padayhag et al., 2023). On algal-dominated bommies, several bacterial families and genus decreased relative to algal-removed bommies, potentially due changes in competitive dynamics between microorganisms within microbenthic microbiomes (Guillonneau et al., 2018).

After 6 days of exposure to seawater from algal-removed or algal-dominated bommies, mean larval survival remained high (> 80%) in both algal treatments. Such high survival rates are consistent with previous studies showing that Pocilloporid larvae can survive in the plankton for over 100 days (Richmond, 1987). Nevertheless, we found a significant effect of parental origin on larval survival. Larvae produced by parents from algal-dominated bommies had their survival reduced by ~6% relative to those produced by parents from algal-removed bommies. Similar and even stronger cross-generational effects of algal dominance on larval survival have been demonstrated when comparing larval survival from a coral-dominated MPA and a macroalgal-dominated fished area in Fiji (Beatty et al., 2018). Since the microbiome composition of larvae significantly differed between parental origins, these effects could be due to a compromised larval microbiome. As discussed above, larvae brooded by parents from algal-dominated bommies harbored a microbiome enriched with opportunistic bacteria and

depleted in beneficial bacteria, which could have increased their mortality in the pre-settlement stage. At 6 days old, which corresponds to the duration of larval exposure to the algal treatments, coral larvae also extensively rely on their parental reserves (Richmond, 1981). Reproduction is a costly process (Monteil et al., 2020). Under algal stress, parents may have faced a physiological trade-off in which they reallocated energy for their own metabolism and defense rather than towards larval provisioning, thereby influencing their offspring survival. For example, bleached corals alter the quality and/or quantity of metabolites transferred to their larvae (Michalek-Wagner & Willis, 2001). We failed to detect any effect of the environment (in this case, water origin) on larval survival. Previous lab-based studies found that polar algal compounds (Morrow et al., 2017) and/or algal-associated microbes (Vermeij et al., 2009) could significantly decrease larval survival, contradicting our result. By using seawater, where algal dissolved compounds and microbes occur under natural concentrations, our result rather provides limited evidence of water-mediated effects on larval survival (but see Beatty et al., 2018). However, these effects may have been underestimated as seawater was collected in the upper water column (~50 cm) above the bommies, and not near algal surfaces.

While macroalgae often prevent coral larval settlement in field and laboratory experiments (Bulleri et al., 2018; Evensen et al., 2019b), we found no parental and environmental effects on coral larval settlement. Larvae settled equally on tiles from both algal treatments, although they could escape the enhanced post-settlement mortality by not settling on tiles from algal-dominated bommies. This result occurred in spite of significant differences in substrate microbiome between algal treatments, suggesting that the substrate microbiome was not indicative of the negative environment for the larvae. It is possible that this result is due to the presence of positive cues and/or limited abundance of negative cues on the settlement tiles. After 4 months conditioning, allowing for a mixed benthic community of settlement inducers and inhibitors (Arnold & Steneck, 2011), cryptic surfaces of settlement tiles were covered by crustose coralline algae, a well-known settlement cue, and not densely covered by macroalgae (electronic supplementary material, figure S9). In addition, Pocilloporids settle unselectively (Gouezo et al., 2020). In contrast, algal-induced parental and environmental effects interacted with one another to affect the survival of coral recruits. Interestingly, post-settlement survival was only reduced on algal-dominated bommies for recruits produced by parents from algal-dominated bommies. Such interaction may occur if algal-induced environmental effects coincide with the vulnerable state of recruits due to their (i.e., algal-dominated) parental origin, and/or if negative algal-induced parental effects are offset by the positive effects of the algal-removed environment. Our results do not allow us to distinguish between these two scenarios.

However, the altered microbiome of coral larvae produced by parents from algal-dominated bommies is consistent with an increase in their vulnerability to detrimental (e.g., algal-dominated) environments.

5. Conclusion

As macroalgae proliferate and threaten reef health (Webster et al., 2015; Smith et al., 2016; Clements & Hay, 2023), it is essential to characterize their effects on the microbial dynamics of coral development stages and their habitats to predict future coral community structure. Using 16S rRNA gene sequencing, we show that microbial specificity of two major life stages (i.e., adult and larvae) was maintained whether corals were transplanted on algal-removed or algal-dominated bommies. While our result revealed a remarkable stability of *P. acuta* adult microbiome, parental exposure to dense macroalgal assemblages influenced the microbiome of their larvae and their subsequent performance throughout the recruitment process, thereby indicating cross-generational effects under coral-macroalgae competition. Our data provide an additional mechanism by which macroalgae perpetuate their dominance on degraded reefs. The cumulative impacts of low larval survival and low survival of the juvenile phenotypes brooded by parents exposed to macroalgae in algal-dominated conditions may dramatically disrupt coral recovery trajectories. These results further suggest that algal-induced parental vs. environmental effects can form complex interactions across coral development stages. Deciphering between parental and environmental drivers of offspring success with respect to coral-macroalgal competition confers promising areas to further dig into the cryptic competitive mechanisms of macroalgae. Such knowledge will be paramount for predicting benthic community changes and providing science-based guidelines for reef conservation.

Data accessibility. Metabarcoding data can be publicly accessioned under the NCBI BioProject PRJNA1024906. All data and R scripts can be downloaded from a Dryad repository: https://datadryad.org/stash/share/g0Q55x3CXrksaab4FJxVqbhtgDdYhDR3I_DxTOXV3eI

Authors' contributions. C.P.S and M.M.N designed the research. C.P.S collected and analyzed the data. H.B. collected the data. C.P.S and M.M.N led the writing of the manuscript. C.C provided analytical tools. All authors gave final approval for publication.

Competing interests. We declare we have no competing interests.

Funding. This research was supported by supported with by the French National Research Agency through the project CORALMATES (ANR-18-CE02-0009-01) lead by M.M.N and by a PhD grant from the Ecole Pratique des Hautes Etudes to C.P.S.

Acknowledgments. We thank the French Polynesian government for the research permits and the CRIOBE research station for logistical and technical assistance. Génome Québec Innovation Centre performed the preparation and sequencing of the 16S rRNA amplicon library. We also would like to thank Irene Salinas-Akhmadeeva for her coral and larvae illustrations.

6. Supplementary Information

6.1. Supplementary Figures

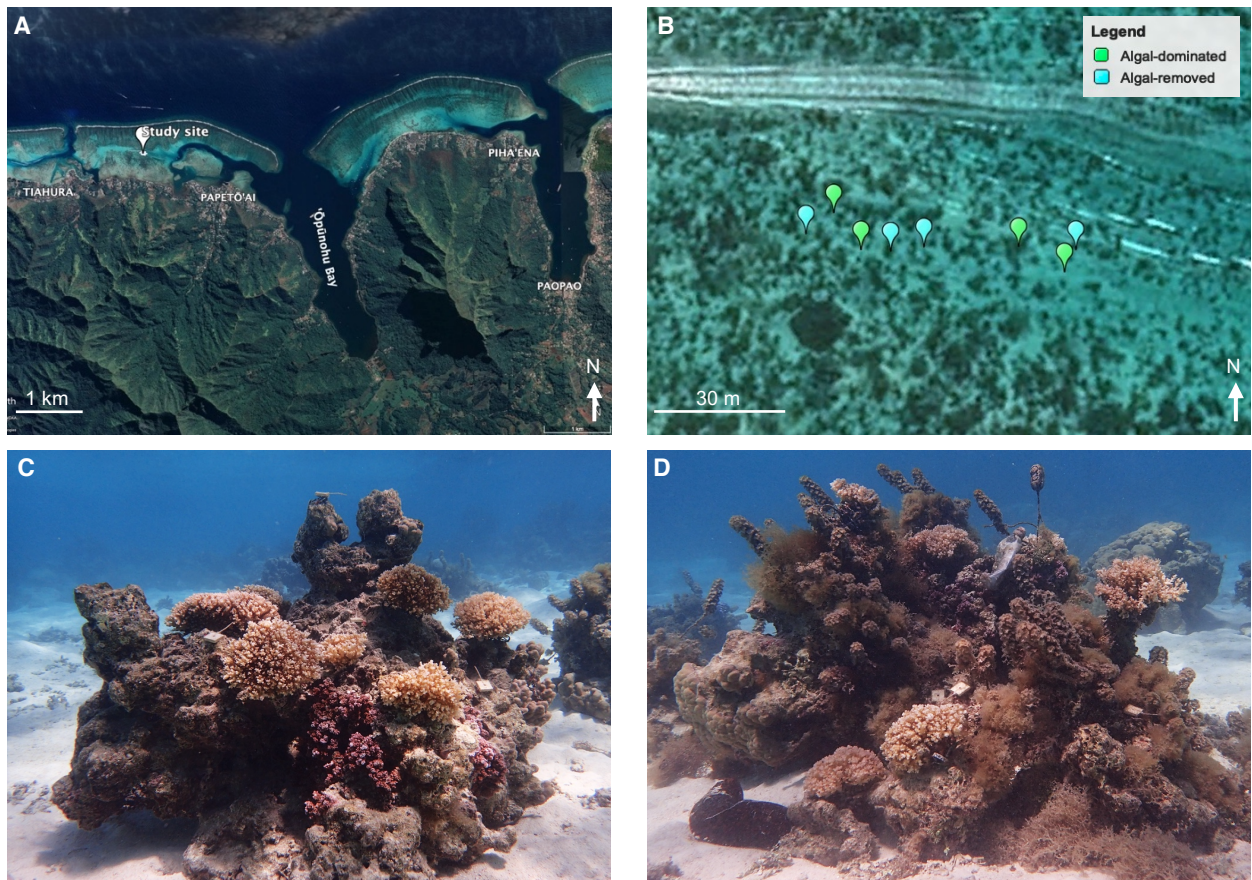


Figure S1 | Satellite images of Mo'orea showing (a) the study site on the north coast of the island ($17^{\circ}29'14.86''S$ $149^{\circ}53'0.76''W$) and (b) the locations of the coral bommies assigned to the two algal treatments : (c) algal-removed and (d) algal-dominated.

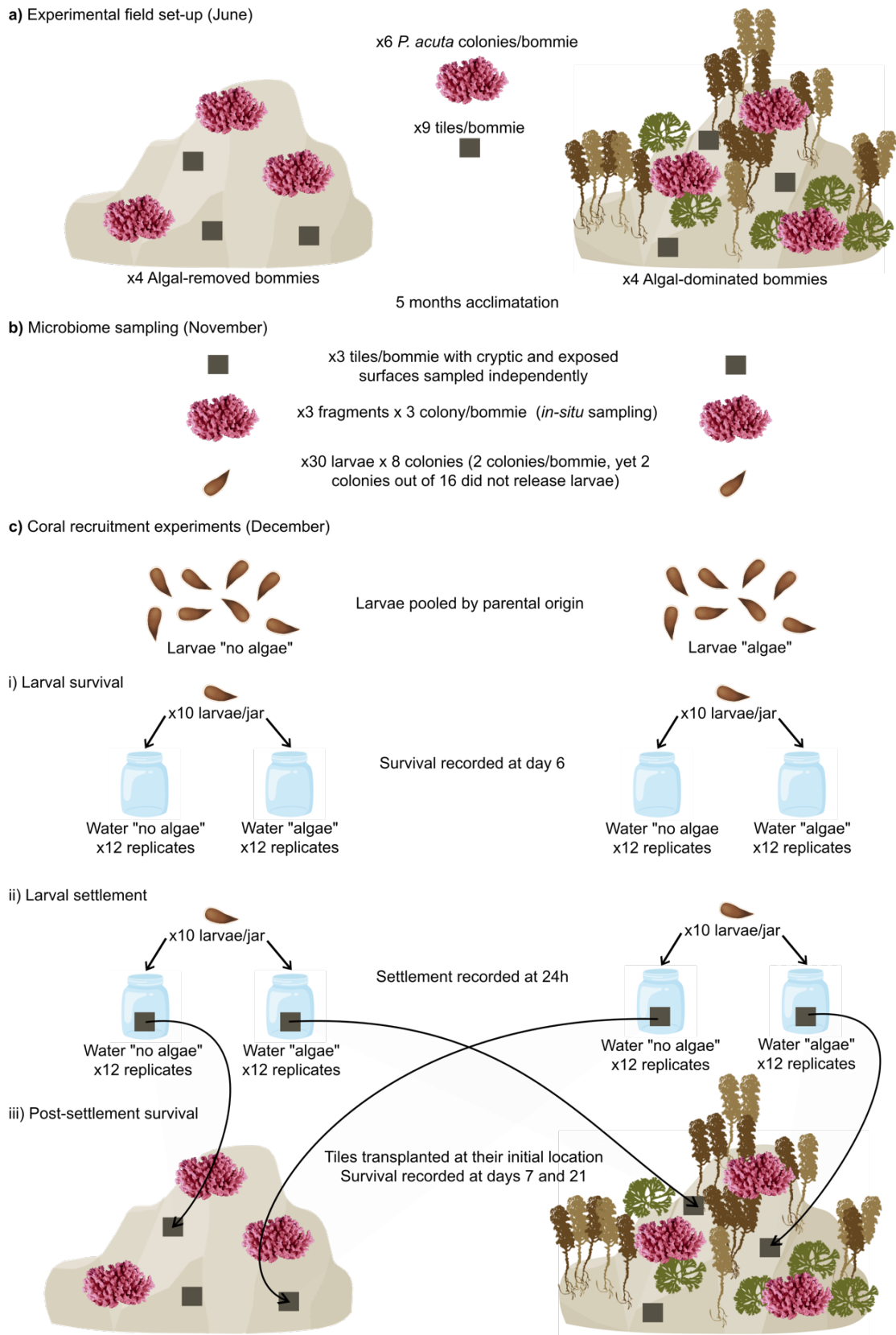


Figure S2 | Experimental design. (a) Coral bommies were assigned to one of the two treatments: algal-removed (i.e., algal communities manually removed) and algal-dominated (i.e., bommies left untouched). (b) Microbiomes of transplanted tiles, corals and their larvae were sampled after 5 to 6 months. (c) Larvae were pooled by their parental origin and used for i) coral larval survival, ii) settlement and iii) early post-settlement survival experiments.

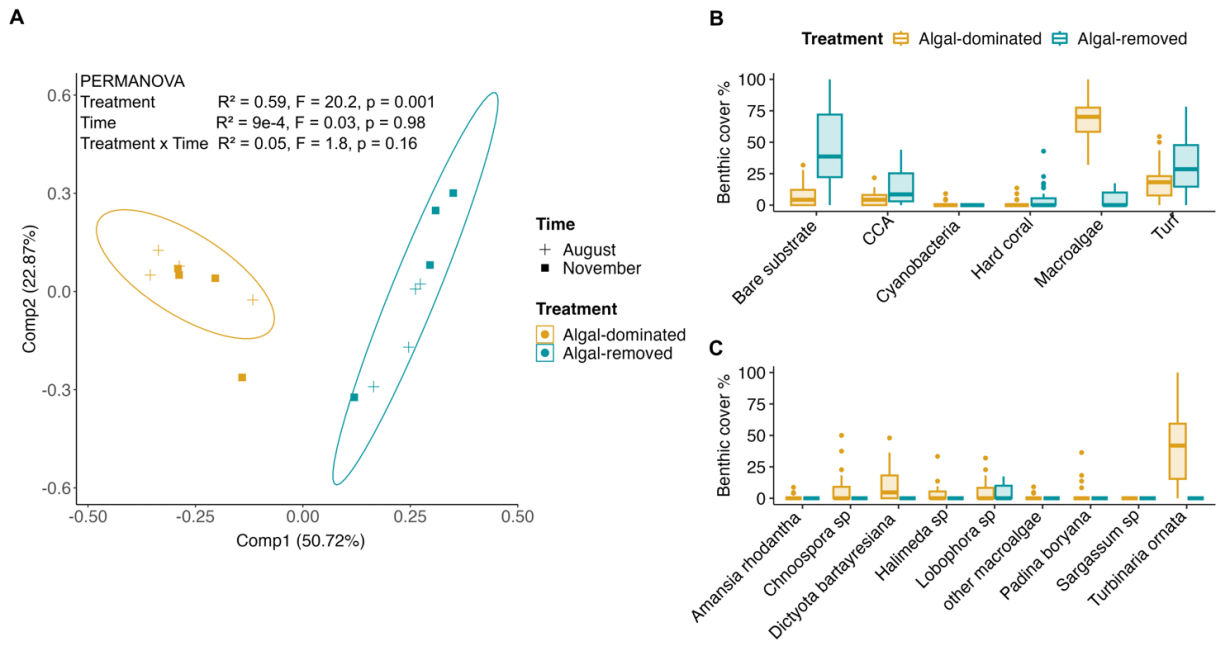


Figure S3 | Benthic community composition on experimental bommies. (a) Score plot of the principal coordinate analysis on Bray-Curtis dissimilarities comparing benthic community composition of algal-removed and algal-dominated bommies during the experiment. Box plots represent cover of (b) main benthic categories and (c) macroalgal species/genera on algal-dominated and algal-removed bommies throughout August and November.

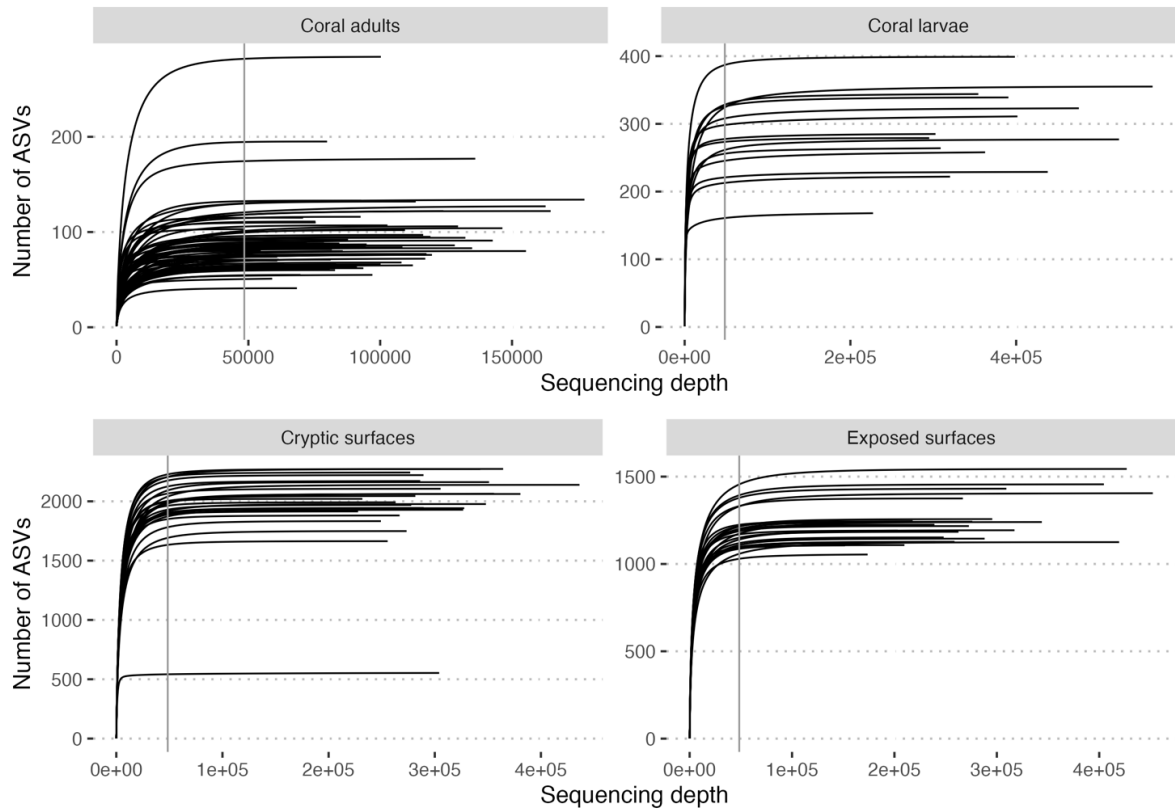


Figure S4 | Rarefaction curves for each sample type of ASV richness relative to the sequencing depth after data filtration. Vertical line corresponds to the minimum library size of 48 457 reads.

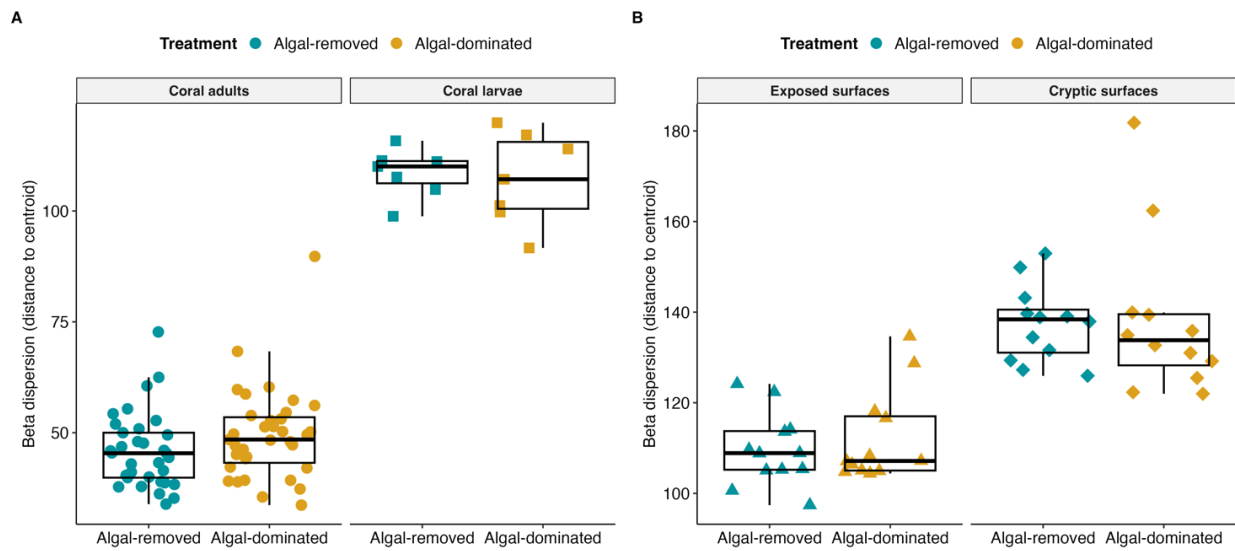


Figure S5 | Microbiome variability. Beta dispersion measured as the distance to centroid from PCA in figure 1c and d. Significance was assessed by a permutation test ($n_{\text{perm}} = 999$).

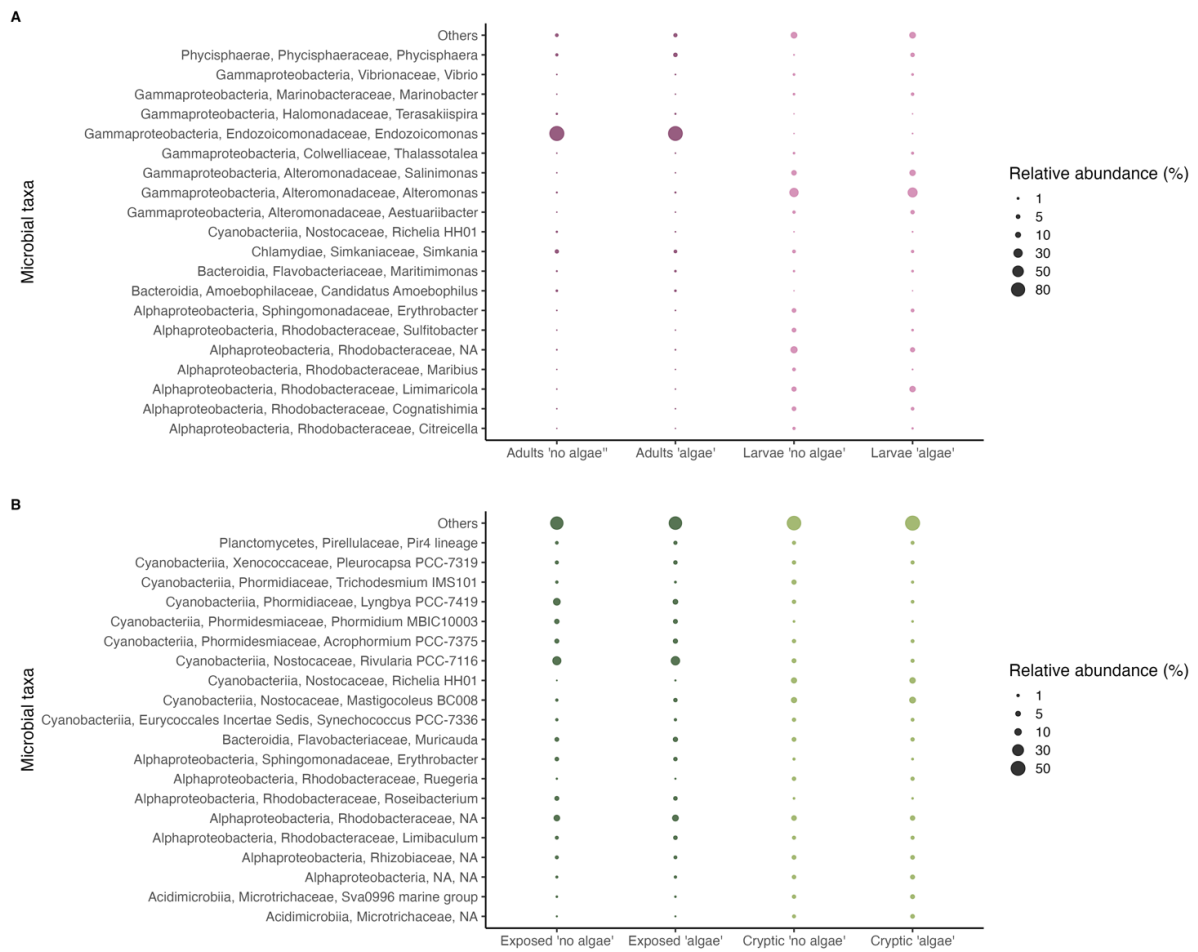
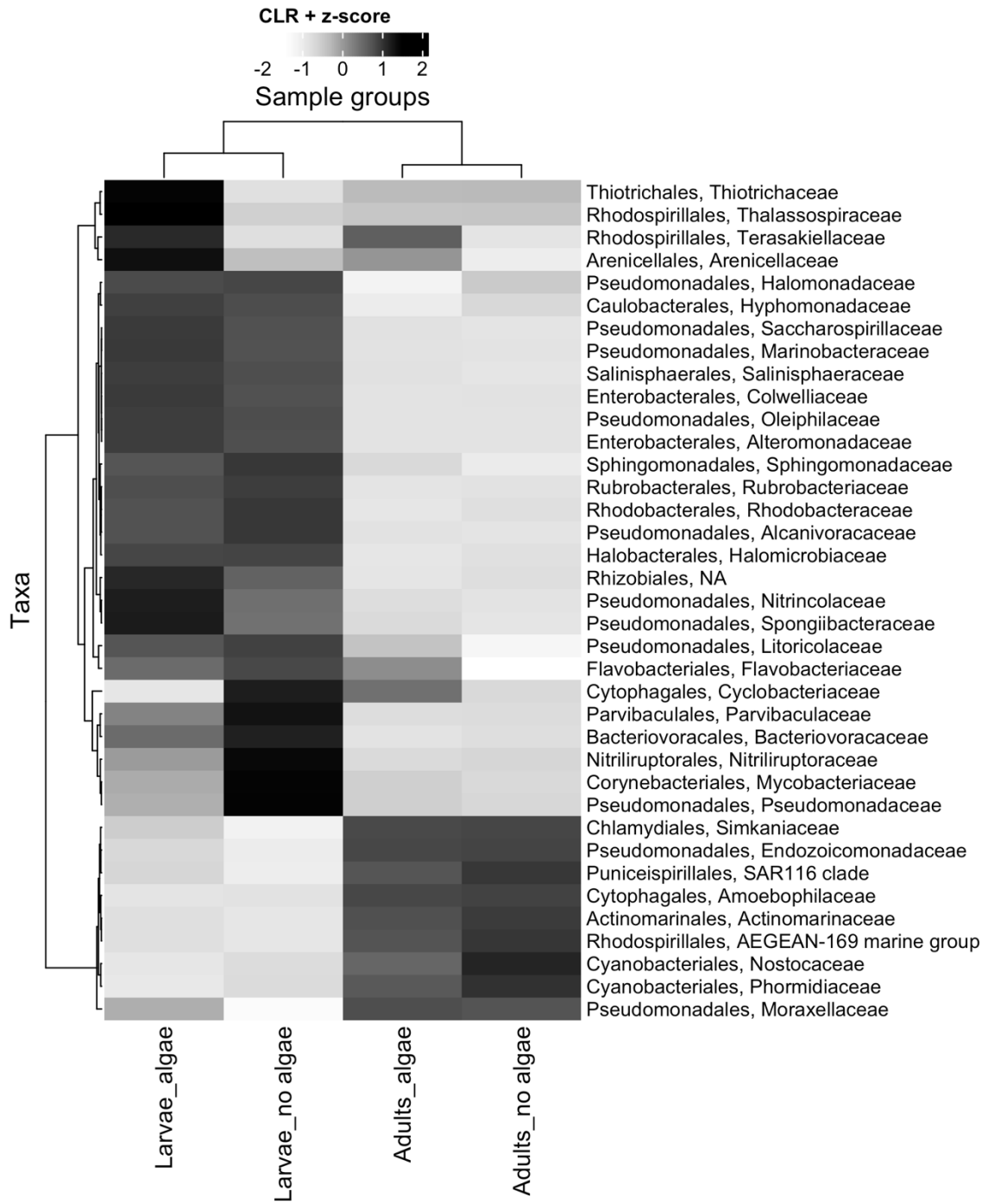


Figure S6 | Dominant microbial genus. Top 20 most abundant microbial genus within (a) coral adult and larval samples and with (b) cryptic and exposed surface samples between algal-removed (“no algae”) and algal-dominated (“algae”) bommies.

A



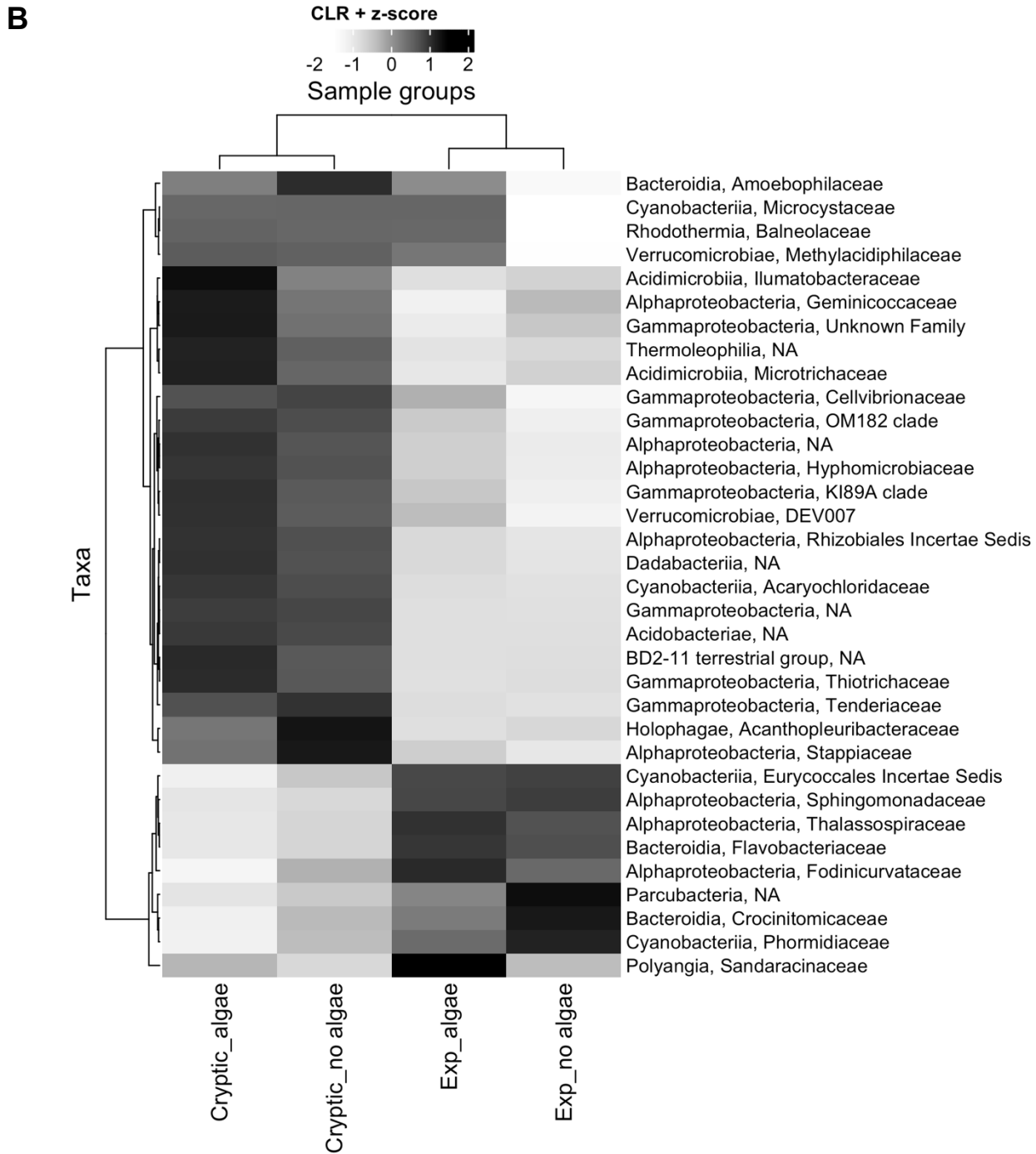


Figure S7 | Microbial families characteristic of sample types and algal-removal treatment. Random Forest analysis were performed on a subset data with (a) Coral and larvae samples and with (b) cryptic and exposed substrates between algal-removed (“no algae”) and algal-dominated (“algae”) bommies. The 20 microbial families best explaining differences between the samples are visualized by a heatmap built from mean CLR-transformed abundances across sample groups using Euclidian distances and Ward’s minimum variance method. Data was scaled by mean-centering and dividing by the standard deviation.

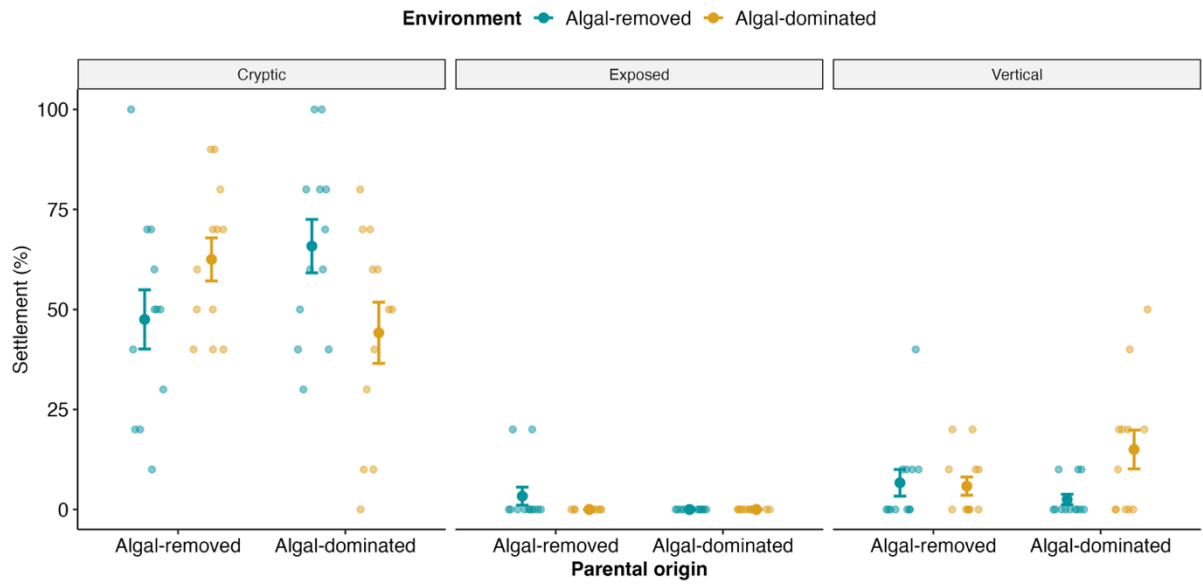


Figure S8 | Larval settlement (mean % \pm se). The number of settled larvae were recorded at the cryptic, exposed and vertical sides after 24h. Tiles were left 5 months on algal-removed and algal-dominated bommies. N = 12 replicates per level for each factor and N = 10 larvae were tested for each replicate.

Algal-removed bommies

Tile 20 – Bommie 2



Tile 91 – Bommie 9



Tile 67 – Bommie 7

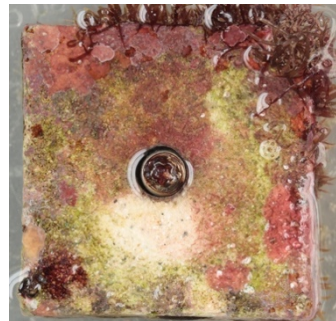


Tile 30 – Bommie 3



Algal-dominated bommies

Tile 108 – Bommie 10



Tile 6 – Bommie 1



Tile 35 – Bommie 4



Tile 79 – Bommie 8

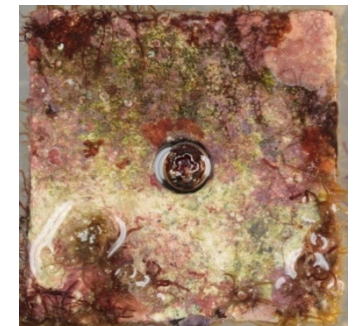


Figure S9 | Representative benthic communities of tiles (exposed and cryptic surfaces) deployed on algal-removed and algal-dominated bommies and used for settlement assay after a conditioning of 4 months.

6.2. Supplementary Tables

Table S1 | Sample size, ASV richness and read depth summary across sample type and algal removal treatment. 4 adult coral samples were lost during shipment of which 3 from algal-removed treatment and 1 from algal-dominated treatment.

<i>Sample type</i>	<i>Tile side</i>	<i>Treatment</i>	<i>Nb samples</i>	<i>Nb ASVs (mean ± sd)</i>	<i>Nb reads (mean ± sd)</i>
Adults		Algal-removed	33	84.0 ± 26.6	90671.6 ± 240044.2
Adults		Algal-dominated	35	96.2 ± 42.9	102729.2 ± 32463.8
Larvae		Algal-removed	7	279.3 ± 68.3	372474.1 ± 113038.2
Larvae		Algal-dominated	7	299.7 ± 55.9	393825.4 ± 53631.3
Substrate	Cryptic	Algal-removed	12	2033.5 ± 133.4	330923.6 ± 53.631.3
Substrate	Cryptic	Algal-dominated	12	1893.8 ± 461.2	278477.8 ± 32097.2
Substrate	Exposed	Algal-removed	12	1232.0 ± 119.3	304546.3 ± 84033.2
Substrate	Exposed	Algal-dominated	12	1227.6 ± 138.1	253391.5 ± 73277.9
Water		Algal-removed	1	258	193177
Water		Algal-dominated	1	258	361777

Table S2 | Results of ANOVA for the fixed effects of linear mixed-effect (LME) models on the alpha diversity (Shannon diversity index) of (a) coral and larvae microbiomes and (b) cryptic and exposed surface microbiomes.

<i>Response</i>	<i>Fixed effects</i>	<i>df</i>	<i>Chisq</i>	<i>p-value</i>
(a) Coral adults and larvae	Intercept	1	147.42	< 0.001
	Life stage	1	335.76	< 0.001
	Algal removal treatment	1	0.90	0.34
	Life stage x Treatment	1	2.27	0.13
(b) Cryptic and exposed surfaces	Intercept	1	6134.3010	< 0.001
	Surface	1	82.20	< 0.001
	Algal removal treatment	1	1.10	0.29
	Surface x Treatment	1	0.05	0.82

Table S3 | Results of PERMANOVA testing variations in the composition of (a) coral adult and larval microbiomes and (b) cryptic and exposed surface microbiomes. Significant p-values (< 0.05) are indicated in bold. N = 12 replicates per combination of factors. Pairwise tests were performed with the function “pairwise.adonis2” from the *pairwiseAdonis* package (Martinez Arbizu, 2020)

	<i>Fixed effects</i>	<i>df</i>	<i>R</i> ²	<i>p-value</i>
(a) Coral adults and larvae	Life stage	1	0.32	< 0.001
	Algal removal treatment	1	0.01	0.15
	Life stage x Treatment	1	0.02	0.03
	Residual	78	0.644	
	<i>Pairwise tests</i>			
	Adults : Algal-dominated vs. removed bommies			0.27
	Larvae : Algal-dominated vs. removed bommies			0.01
(b) Cryptic and exposed surfaces	Surface	1	0.36	< 0.001
	Algal removal treatment	1	0.02	< 0.001
	Surface x Treatment	1	0.02	0.08
	Residual	44	0.59	

Martinez Arbizu, P. 2020 pairwiseAdonis: Pairwise multilevel comparison using adonis. R package version 0.4.
<https://github.com/pmartinezarbizu/pairwiseAdonis>

Table S4 | Results of PERMDISP testing differences in the dispersion of (a) coral adult and larval microbiomes and (b) cryptic and exposed surface microbiomes. Significant p-values (< 0.05) are indicated in bold. N = 12 replicates per combination of factors. To account for group differences across life stage and algal treatment, we calculated dispersions between groups of a new variable combining all levels of factors and used the “pairwise” argument in the “permutest” function.

	<i>Groups</i>	<i>df</i>	<i>F</i>	<i>p-value</i>
(a) Coral adults and larvae	Life stage	1	44.85	< 0.001
	Algal removal treatment	1	0.17	0.66
	<i>Pairwise tests</i>			
	Algal-dominated bommies : Adults vs. larvae			0.002
	Algal-removed bommies : Adults vs. larvae			0.001
	Adults : Algal-dominated vs. removed bommies			0.13
	Larvae : Algal-dominated vs. removed bommies			0.61
(b) Cryptic and exposed surfaces	Surface	1	93.58	< 0.001
	Algal removal treatment	1	1.89	0.20
	<i>Pairwise tests</i>			
	Algal-dominated bommies : Exposed vs. cryptic			0.001
	Algal-removed bommies : Exposed vs. cryptic			0.001
	Exposed : Algal-dominated vs. removed bommies			0.53
	Cryptic : Algal-dominated vs. removed bommies			0.94

Table S5 | Differentially abundant ASVs in coral larval microbiome across coral adult, larval and water samples from algal-removed (“no”) and algal-dominated bommies (“alg”).

ASVs	adults_no	adults_alg	larvae_no	larvae_alg	tank_no	tank_alg
Mycobacteriaceae, Mycobacterium, ASV547	9,1107E-05	9,0757E-05	0,00179598	0,00055237	9,8355E-05	0
Parvibaculaceae, Parvibaculum, ASV798	0	0	0,00160631	0,00012892	0,00305419	5,2519E-05
Rhodobacteraceae, Citreicella, ASV90	0	0	0,01153582	0,00304664	0,00047107	0,00015203
Rhodobacteraceae, Maribius, ASV137	0	2,0882E-06	0,00978877	0,00010537	0,00022777	0
Rhodobacteraceae, Maribius, ASV91	0	0	0,01471323	0,00040648	0,00108191	0
Rhodobacteraceae, Palleronia-Pseudomaribius, ASV1810	0	0	0,00068539	3,3358E-05	0	0
Rhodobacteraceae, Sulfitobacter, ASV38	1,827E-05	5,9833E-06	0,03516942	0,00589859	0,00091108	0,00055006
Rhodobacteraceae, Sulfitobacter, ASV84	0	0	0,01543284	0,00154898	0,00082308	0,00014926
Sphingomonadaceae, Erythrobacter, ASV56	0,00015349	9,2275E-05	0,000242	0,00141552	0	0,00035934
Nitrocolaceae, Marinobacterium, ASV703	0	0	2,4535E-05	0,00183007	0,00012424	0,00100338
Saccharospirillaceae, Thalassolituus, ASV644	0	5,0399E-06	5,6745E-05	0,00185814	0,00033648	0,00064128
Vibrionaceae, Vibrio, ASV961	0	0	0,0014226	9,1367E-05	4,6589E-05	0

Table S6 | Summary of the discussed ASVs in coral larval microbiomes. 16S rDNA sequences were blasted to find matches in the GenBank database. Only putative identities with a sequence similarity > 95% are presented.

ASV	Lowest taxonomic level SILVA	Closest relative (sequence similarity)	Host or environment	Accession number (GenBank)
ASV56	Erythrobacter	Erythrobacter rubeus strain KMU-140 (98%)	Seawater	NR_179343
ASV703	Marinobacterium	Marinobacterium jannaschii strain IFO 15466 (96%)	Type strain	NR_024653
ASV644	Thalassolituus	Thalassolituus oleivorans MIL-1 16S (95.6%)	Seawater sediment	NR_102806
ASV84	Sulfitobacter	Sulfitobacter aestuarii strain hydD52 (100%)	Seawater	NR_179825
ASV38	Sulfitobacter	Sulfitobacter faviae strain S5-53 (100%)	Seawater	NR_152065
ASV91	Maribius	Maribius salinus strain CL-SP27 (100%) or Maribius pelagius	Seawater	NR_043272
ASV798	Parvibaculum	Parvibaculum indicum strain P31 (100%)	Seawater	NR_116565
ASV961	Vibrio	Vibrio parahaemolyticus strain ATCC 17802 (99.3%)	Type strain	NR_114631
ASV2412	Vibrio	Vibrio coralliilyticus strain ATCC BAA-450 (99.8%)	Marine sponge	NR_117892

Table S7 | Summary (mean \pm sd) of water physiochemical parameters for the larval survival and settlement experiments (figures 4a and b). Temperature was recorded by HOBO Pendant loggers, while pH, conductivity and O₂ saturation were measured. Salinity was calculated from conductivity and temperature data (Aminot and K  rouel, 2004).

<i>Experiment</i>	<i>Treatment</i>	<i>Temp (�C)</i>	<i>pH</i>	<i>Conductivity (mS/cm)</i>	<i>Salinity (psu)</i>	<i>O² saturation (%)</i>
Larval survival	Algal-removed	27.65 \pm 0.42	8.21 \pm 0.08	47.84 \pm 1.28	30.49 \pm 0.80	84.00 \pm 4.73
	Algal-dominated	27.48 \pm 0.45	8.19 \pm 0.12	46.95 \pm 1.91	30.67 \pm 0.94	85.67 \pm 2.81
Larval settlement	Algal-removed	27.95 \pm 0.59	8.26 \pm 0.07	47.61 \pm 1.05	28.60 \pm 0.45	90.13 \pm 3.35
	Algal-dominated	28.07 \pm 0.78	8.25 \pm 0.13	47.22 \pm 0.70	28.80 \pm 0.76	92.50 \pm 4.66

Aminot, A. and K  rouel, R., 2004. *Hydrologie des  cosyst mes marins : param tres et analyses*. Editions Quae.

Table S8 | Results of ANOVA for the fixed effects of the binomial GLMEs on (a) larval survival, (b) larval settlement, (c) larval settlement on tile surfaces and (d) post-settlement survival. Significant pvalues (< 0.05) are bold. N = 12 replicates per combination of factors

<i>Response</i>	<i>Fixed effects</i>	<i>df</i>	<i>Chisq</i>	<i>pvalue</i>
(a) Probability of larval survival	Intercept	1	49.42	< 0.001
	Parental origin	1	5.71	0.02
	Environment	1	2.65	0.10
	Origin x Environment	1	0.90	0.32
(b) Probability of larval settlement	Intercept	1	1.09	0.30
	Parental origin	1	1.18	0.28
	Environment	1	1.05	0.31
	Origin x Environment	1	1.99	0.16
(c) Probability of larval settlement on tile surfaces	Intercept	1	0.19	0.66
	Parental origin	1	5.10	0.02
	Environment	1	3.30	0.07
	Tile surface	2	67.10	< 0.001
	Origin x Environment	1	10.10	0.001
	Origin x Surface	2	5.84	0.05
	Environment x Surface	2	1.58	0.45
	Orig. x Env. x Surface	2	15.31	< 0.001
<i>Posthoc on tile surfaces</i>				
Exposed	Larvae “algae”: algal-removed vs. dominated bommies			1.00
	Larvae “no algae”: algal-removed vs. dominated bommies			1.00
Cryptic	Larvae “algae”: algal-removed vs. dominated bommies			0.005
	Larvae “no algae”: algal-removed vs. dominated bommies			0.09
Vertical	Larvae “algae”: algal-removed vs. dominated bommies			0.01
	Larvae “no algae”: algal-removed vs. dominated bommies			0.99
(d) Post-settlement survival probability	Intercept	1	0.68	0.41
	Parental origin	1	2.08	0.15
	Environment	1	0.004	0.95
	Day	1	0.32	0.57
	Origin x Environment	1	7.48	0.006
	Origin x Day	1	0.06	0.80
	Environment x Day	1	0.05	0.82
	Orig. x Env. x Day	1	0.07	0.78
<i>Posthoc</i>				
	Larvae “algae”: algal-removed vs. dominated bommies			0.02
	Larvae “no algae”: algal-removed vs. dominated bommies			1.00

Chapter 4

Contact- and water-mediated interactions with an allelopathic macroalga affect the coral microbiome and metabolome

Chloé Pozas-Schacre^{1*}, Hugo Bischoff², Delphine Raviglione¹, Camille Clerissi^{1,3}, Isabelle Bonnard^{1,3}, Maggy M. Nugues^{1,3}

¹ PSL Université Paris : EPHE-UPVD-CNRS, UAR 3278 CRIOBE, Université de Perpignan, 66860 Perpignan, France

² PSL Université Paris: EPHE-UPVD-CNRS, UAR 3278 CRIOBE BP 1013, 98729 Papetoai, Moorea, French Polynesia

³ Laboratoire d'Excellence "CORAIL," Perpignan, France

*Corresponding author

Email: pozaschloe@gmail.com

Abstract

Macroalgal proliferation constitutes a major threat to coral reef resilience. Macroalgae can affect corals leading to alterations in their microbiome and metabolome. However, our understanding of the spatial scale of these effects and the influence of environmental factors is limited. By using a manipulative field experiment, we show that contact- and water-mediated interactions with an allelopathic macroalga distinctly structured coral microbiome and metabolome. Water-mediated interactions led to a loss of beneficial symbionts and enrichment of opportunists, but to a lesser extent compared to contact-mediated interactions. Additionally, surface seawater near corals in direct contact exhibited an increase in opportunistic microbes and a decrease in phototrophs regardless of flow direction. Differential abundance of coral metabolites in both interaction types suggests an adjustment of lipid metabolism to meet the energetic cost of competition and the production of defense metabolites. These findings contribute to highlight the chemical and microbial mechanisms associated with coral-algal competition.

1. Introduction

In recent decades, anthropogenic disturbances, such as climate change, over-exploitation and eutrophication, have intensified, causing extensive coral loss and macroalgal proliferation worldwide (Crisp et al., 2022; Reverter et al., 2022). Coral reef degradation often involves coral-macroalgal phase-shift, with macroalgae impairing coral health (Rasher & Hay, 2010; Vega Thurber et al., 2012; Clements et al., 2018) and eroding reef resilience (Hughes et al., 2007). As such, macroalgal dominance is not only a consequence of coral loss, but also a driving force due to the existence of feedback processes (Mumby & Steneck, 2008; Schmitt et al., 2019). While physical stress alone can induce coral damage, through abrasion, smothering or shading (McCook et al., 2001; Clements et al., 2018, 2020), it is now widely accepted that chemicals and microbes constitute major players in coral-algal interactions (Nugues et al., 2004; Smith et al., 2006; Rasher & Hay, 2010; Barott & Rohwer, 2012). Upon direct contact, macroalgae may vector harmful bacteria (Nugues et al., 2004; Briggs et al., 2021) and cytotoxic compounds (Rasher et al., 2011; Vieira et al., 2016a; Morrow et al., 2017), causing diseases, necrosis and bleaching. Additionally, water-mediated effects may occur through the release of more hydrophilic compounds, such as allelochemicals (Morrow et al., 2017) or carbon-rich metabolites (e.g., DOC), fostering the growth of potentially virulent bacterial assemblages (Smith et al., 2006; Nelson et al., 2013; Roach et al., 2017) and promoting coral mortality through hypoxia (Smith et al., 2006; Barott et al., 2012; Wangpraseurt et al., 2012; Jorissen et al., 2016). Field and laboratory experiments suggest that water-mediated interactions are spatially constrained within a few centimeters or less from the coral-algal interface (Smith et al., 2006; Wangpraseurt et al., 2012; Jorissen et al., 2016; Clements et al., 2020; Fong et al., 2020). However, water-mediated interactions appear highly context-dependent (e.g., species pairings, water flow dynamics), and the scarcity of *in-situ* investigations have hindered our understanding of these dependencies and their effects on corals (Barott et al., 2012; Brown & Carpenter, 2015; Clements et al., 2020; Briggs et al., 2021; Clements & Hay, 2023).

Coral and algae form entities called holobionts, comprising the host and a complex diversity of symbionts, including bacteria, archaea, fungi, microeukaryotes and viruses (Barott et al., 2011; Bourne et al., 2016). Growing evidence suggests that the microbiome plays critical functions, such as nutrient cycling, production of essential metabolites and protection from bacterial invasion (Krediet et al., 2013; Bourne et al., 2016), thereby contributing to the holobiont homeostasis (Ziegler et al., 2017; Santoro et al., 2021). Contact with whole algal thalli or their chemical extracts can disrupt the diversity, variability and composition of the coral

microbiome (Vega Thurber et al., 2012; McDevitt-Irwin et al., 2017; Morrow et al., 2017), even beyond the contact interface suggesting a systemic response of the holobiont (Morrow et al., 2013; Pratte et al., 2018). Specifically, changes in coral-associated bacterial communities due to coral-algal competition can lead to dysbiosis when opportunists and potential pathogens (e.g., Rhodobacteraceae, Vibrionaceae) are overrepresented concurrently with a loss of symbionts (e.g., *Endozoicomonas*; Vega Thurber et al., 2012; Zaneveld et al., 2016; McDevitt-Irwin et al., 2017).

To mitigate the effects of microbial invasion and tissue damage, holobionts rely on the activation of specific biological pathways, such as the immune response, to maintain homeostasis (Shearer et al., 2012, 2014; Palmer, 2018). In this context, by investigating the pool of small molecules produced by an organism, metabolomics constitutes a promising asset in coral research to decipher the metabolic strategies mitigating the effects of stress exposure (Wegley Kelly et al., 2021). When exposed to benthic algae, corals exhibit differential abundance of intracellular metabolites, with some bioactive lipids potentially involved in coral immunity (Quinn et al., 2016; Roach et al., 2020). This immune response may vary spatially throughout the colony with translocation of compounds to compromised portions and differential activation of molecular mechanisms (Roff et al., 2006; Wright et al., 2015; Smith et al., 2020). For example, the interface between coral and turf harbor distinct chemical changes compared to coral portions away from the competition zone (Roach et al., 2020). Recent advances in coral metabolomics have revealed a remarkable spatial variability of metabolites within coral colonies and even branches (Roach et al., 2023). Therefore, not considering this spatial heterogeneity can hinder our understanding of the biological mechanisms involved in coral resistance to algal competition.

Sessile organisms, such as corals or algae, depend on surrounding seawater for metabolic exchange (Dennison & Barnes, 1988; Mass et al., 2010), chemical signaling (e.g., coral recruitment; Gleason & Hofmann, 2011) and competitive interactions (Barott & Rohwer, 2012). Near-surface water layer could be where most of these processes occur (Barott & Rohwer, 2012; Weber et al., 2019). For example, corals release chemical cues near their surfaces, including chemo-attractants, quorum sensing and antibacterial compounds mediating interactions with planktonic microbial communities (Garren et al., 2014; Ochsenkühn et al., 2018). In coral-algal interactions, the accumulation of metabolic waste and microbes near coral surfaces can be particularly detrimental (Barott & Rohwer, 2012; Wangpraseurt et al., 2012; Jorissen et al., 2016). Thus, investigating the near-surface coral seawater microbial and chemical composition may offer key insights on the mechanisms driving coral-algal

interactions. Furthermore, frameworks integrating several *-omics* data appear now paramount to tackle the complexity of the coral holobiont (Garg, 2021; Mohamed et al., 2023) and mechanisms driving coral-algal interaction outcomes (Roach et al., 2020; Little et al., 2021).

Here, by means of a manipulative experiment in the lagoon of Mo'orea, French Polynesia, we evaluated the relative influence of contact and water-mediated interactions (i.e., close proximity of 2 cm) with the chemically potent macroalga *Dictyota bartayresiana* (Rasher & Hay, 2010; Rasher et al., 2011) on the coral holobiont *Pocillopora acuta* (Supplementary Fig. 1). We combined 16S rDNA metabarcoding and untargeted metabolomic (LC-MS/MS) data to investigate how the interaction type and direction of prevailing current influence the microbiome and metabolome composition of the coral holobiont and its associated near-surface seawater (CSW). In addition, we explored the extent to which coral microbiome and metabolome vary within colonies by comparing apex and side fragments. Our study demonstrates that, while only contact interactions with macroalgae cause coral tissue damage, both contact and water-mediated interactions trigger microbial and chemical changes within the coral holobiont and its CSW. Together, our findings help to clarify the contextual factors under which coral-algal interactions operate, as well as the holobiont responses to algal stress.

2. Results

2.1. Visual assessment of coral health

After three months of algal exposure, all colonies in direct contact with *Dictyota* presented signs of necrosis (binomial test for H0: proportion of necrosed colonies greater than 90%, $p = 0.4305$) and some degree of bleaching and algal overgrowth (Supplementary Fig. 2). These symptoms occurred only over portions of colonies that were in direct contact with the algae and regardless of whether colonies were up or downstream of the algae. Close proximity (i.e., 2 cm) with *Dictyota* did not cause any visible damage.

2.2. Variation in coral and CSW microbiome and metabolome composition across interaction types

The final 16S rDNA metabarcoding data resulted in 4260 amplicon sequence variants (ASVs) across the 64 samples of which 3300 and 1271 ASVs were in corals and CSWs, respectively (Supplementary Table 1). The metabolomic dataset comprised 2143 MS1 features of which 1841 and 767 features belonged to corals and CSWs, respectively (Supplementary

Table 1). Due to the prevailing influence of sample type (i.e., coral vs. CSW) on microbial and chemical composition (Supplementary Fig. 3), coral and CSW datasets were analyzed separately. Coral microbiome alpha-diversity (Shannon index) was significantly influenced by sampling location (i.e., side vs. apex fragments), but not by the type of algal interaction (i.e., contact vs. close proximity vs. control) and colony position (i.e., up vs. downstream) (ANOVA, $p < 0.05$; Fig. 4.1a; Supplementary Table 2). The alpha-diversity of side fragments in direct contact with *Dictyota* was increased by 86 % relative to that of side fragments in the control (1.86 ± 0.83), but this increase was not significant (Supplementary Table 2). Coral metabolome alpha-diversity did not significantly differ between interaction types, sampling locations or colony positions (ANOVA, $p > 0.05$; Fig. 4.1c, Supplementary Table 2). Within the CSW, the microbiome and metabolome alpha-diversity remained fairly stable across interaction types and colony positions (ANOVA, $p > 0.05$; Fig. 4.1a and c; Supplementary Table 2). Beta-diversity was assessed both within- and between-groups. Differences in microbiome and metabolome dispersions (within-group beta-diversity) mirrored those of alpha-diversity (Fig. 4.1b & d; Supplementary Table 3). The interaction type significantly structured the microbiome composition (between-group beta-diversity) of both corals and CSW, as well as the metabolome composition of corals (PERMANOVA, $p < 0.05$; Fig. 4.2a & b). However, the coral microbiome response to interaction types differed between sampling locations (PERMANOVA, $p < 0.05$). Microbial communities of side fragments differed across interaction types, which was not the case for apex fragments (pairwise PERMANOVA, $p < 0.05$; Supplementary Table 4). Specifically, direct contact elicited different compositional changes in side fragments from close proximity and control conditions. For the CSW microbiome, direct contact elicited different compositional changes from control conditions, but not from close proximity, with the latter not different from control conditions. For the coral metabolome, the effect of interaction type depended upon colony position. Upstream colonies showed significant differences among all algal treatments, while downstream colonies showed a significant difference between control and direct contact treatments only (Supplementary Table 4; pairwise PERMANOVA, $p < 0.05$). Comparatively, neither interaction type nor colony position influenced the CSW metabolome composition (PERMANOVA, $p > 0.05$; Fig. 4.2c & d). To identify the ASVs and metabolites best explaining the discrimination between interaction types, we ran supervised PLS-DAs (partial least squares – discriminant analyses). The analyses confirmed that the type of algal interaction significantly structured the coral microbiome and metabolome composition (permutation test, $p < 0.05$; Supplementary Fig. 4). The PLS-DAs revealed that the CSW metabolome varied among interaction types (Supplementary Fig. 4), suggesting that differences

were not pronounced enough to be detected by PERMANOVA. PLS-DA maximizes the separation between samples thereby making it more sensitive to subtle differences. The differential abundances of the identified discriminant ASVs and metabolites (VIP score > 1) were further investigated.

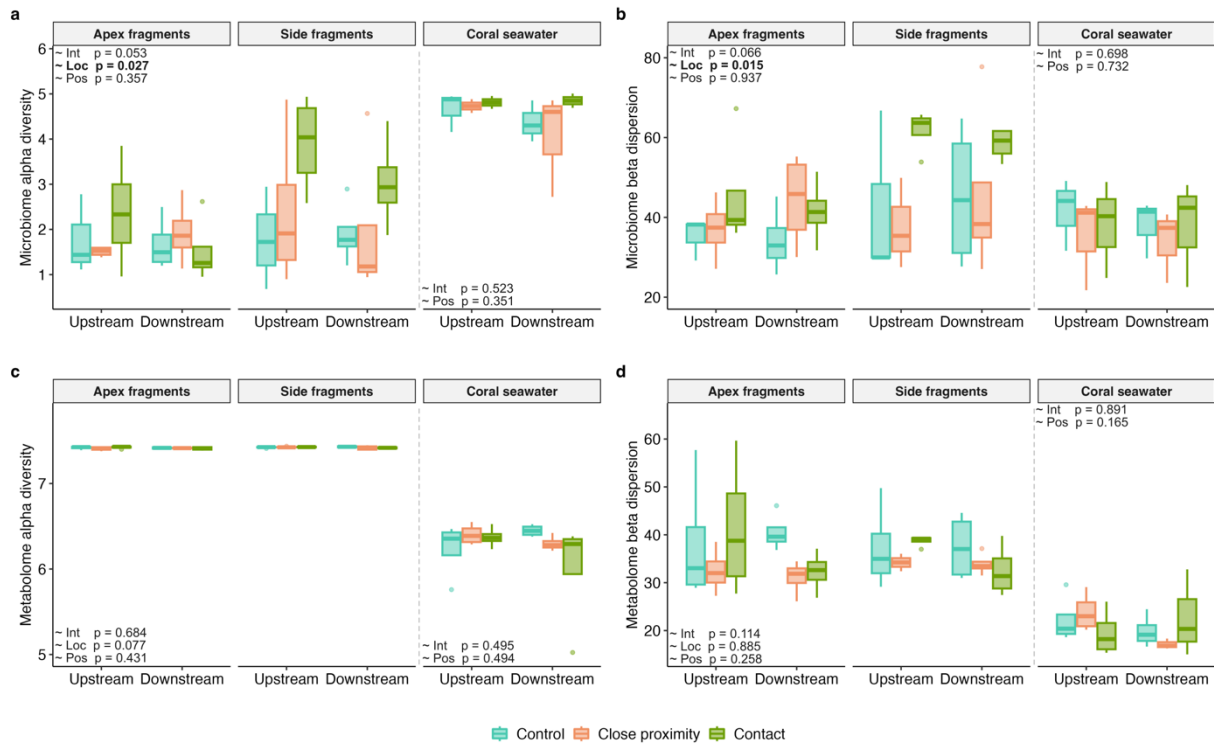


Figure 4.1 | Diversity patterns of coral and near-surface coral seawater (CSW) microbial communities and metabolomes. Richness (Shannon diversity index) of **a.** microbiome and **c.** metabolome (MS1 chemical features) as well as beta dispersion (within-group variability) of **b.** microbiome and **d.** metabolome. Differences were assessed between interaction type (i.e., Int; contact vs close proximity vs control), sampling location (i.e., Loc; apex vs. side fragments) and colony position (i.e., Pos; up vs. downstream). Statistical significance was determined by ANOVA on coral and coral seawater samples, respectively. Only fixed effects are shown here. Interaction effects were not significant and detailed results can be found in Supplementary Tables 2, 3. N = 48 coral samples and N = 24 CSW samples for metabolomics, but N = 46 coral and N = 18 CSW samples for metabarcoding due to sample loss.

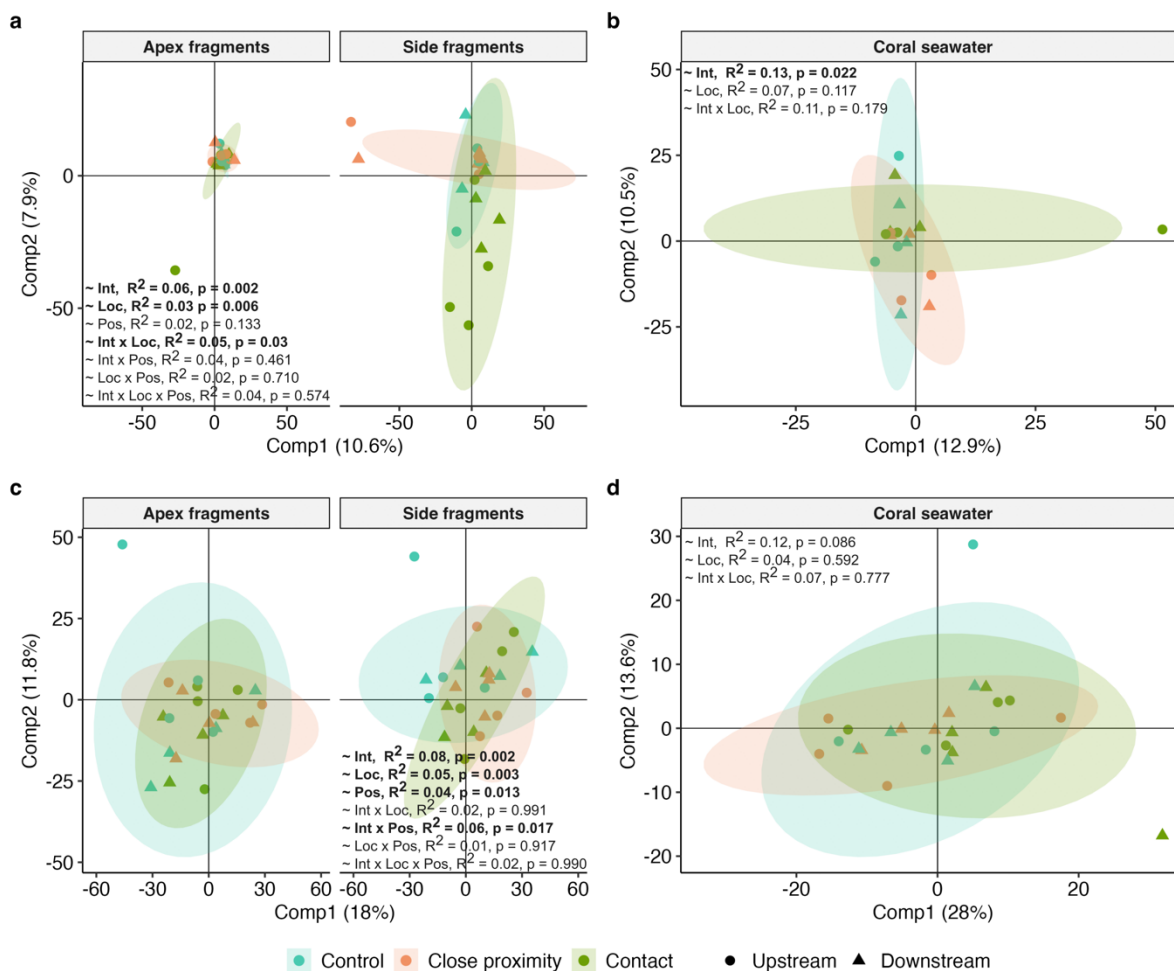


Figure 4.2 | Microbial and chemical composition of coral and near-surface coral seawater samples. PCA score plots of microbiome (**a.** coral and **b.** coral seawater) and metabolome (**c.** coral and **d.** coral seawater) samples. Metabarcoding and metabolomic relative abundance data was CLR transformed and auto-scaled (mean-centered & scaled). Differences in compositional variability were assessed between interaction type (i.e., Int; contact vs close proximity vs control), sampling location (i.e., Loc; apex vs. side fragments) and colony position (i.e., Pos; up vs. downstream). Significance of explaining variables and their interaction was tested by PERMANOVA (N = 999 permutations; Supplementary Table 4).

2.3. Changes in specific microbial taxa relative to control

We identified 1289 and 565 ASVs explaining differences between interaction types in the composition of coral and CSW microbiomes. Among the 20 most represented microbial families (in terms of number of discriminant ASVs), the Endozoicomonadaceae was particularly depleted in side fragments touching *Dictyota* (Supplementary Fig. 5). Comparatively, Rhodobacteraceae, Alteromonadaceae, Rhizobiaceae and Vibrionaceae increased in direct contact, even at the apex of the colonies. These families figured also among the most abundant families, as for example the Endozoicomonadaceae and Rhodobacteraceae comprising 73% and 3.7%, respectively, of all coral microbial sequences (Supplementary Fig.

6a). We, then, plotted mean fold change in abundance in each interaction type relative to control conditions for the 20 taxa with the highest VIP score and/or those with significant difference in abundance between interaction types (Fig. 4.3a & b). Significantly differentially abundant ASVs were only detected in side fragments (ANCOM-BC, FDR-adjusted $p < 0.05$), and colony position did not significantly influence their abundances (ANCOM-BC, FDR-adjusted $p > 0.05$). These ASVs included 3 *Endozoicomonas* decreasing in corals in direct contact while members of the Rhodobacteraceae (i.e., *Cognathisimia*, *Limibaculum*), Alteromonadaceae (i.e., *Aestuariibacter*), Hyphomonadaceae and Phormidesmiaceae families rather increasing in those coral microbiomes (ANOVA, FDR-adjusted $p < 0.05$; Fig. 4.3a). In addition, *Maritinimonas* and *Muricauda* were depleted in corals in both interaction types, the latter became even undetected. Several genera from the Rhodobacteraceae (e.g., *Shimia*., *Yoonia-Loktanella*) were even absent in control conditions and colonized the microbiome of corals touching *Dictyota*, both at the side and apex fragments. In the CSW, the Cryomorpaceae, Rubritaleaceae, SAR86 and Flavobacteriaceae families increased when corals were in direct and close proximity with *Dictyota*, while the Pirellulaceae rather decreased in those samples (Supplementary Fig. 5). They constituted abundant members of the CSW microbiome community comprising ~5% of the bacterial sequences (Supplementary Fig. 6). Several bacterial families increased in CSW of corals in contact with *Dictyota* as Clade 1 (SAR11), Rhodobacteraceae (i.e., *Limibaculum*), Phormidiaceae (i.e., *Lyngbya PCC-7419*), Kiloniellaceae, Hyphomonadaceae, Flavobacteriaceae, Halieaceae and Cellvibrionaceae (Fig. 3b), although not significantly (ANCOM-BC, FDR-adjusted $p > 0.05$; Fig. 4.3b). Only two ASVs, *Synechococcus CC9902* and an unknown Gammaproteobacteria, rather decreased in algal treatments relative to control conditions.

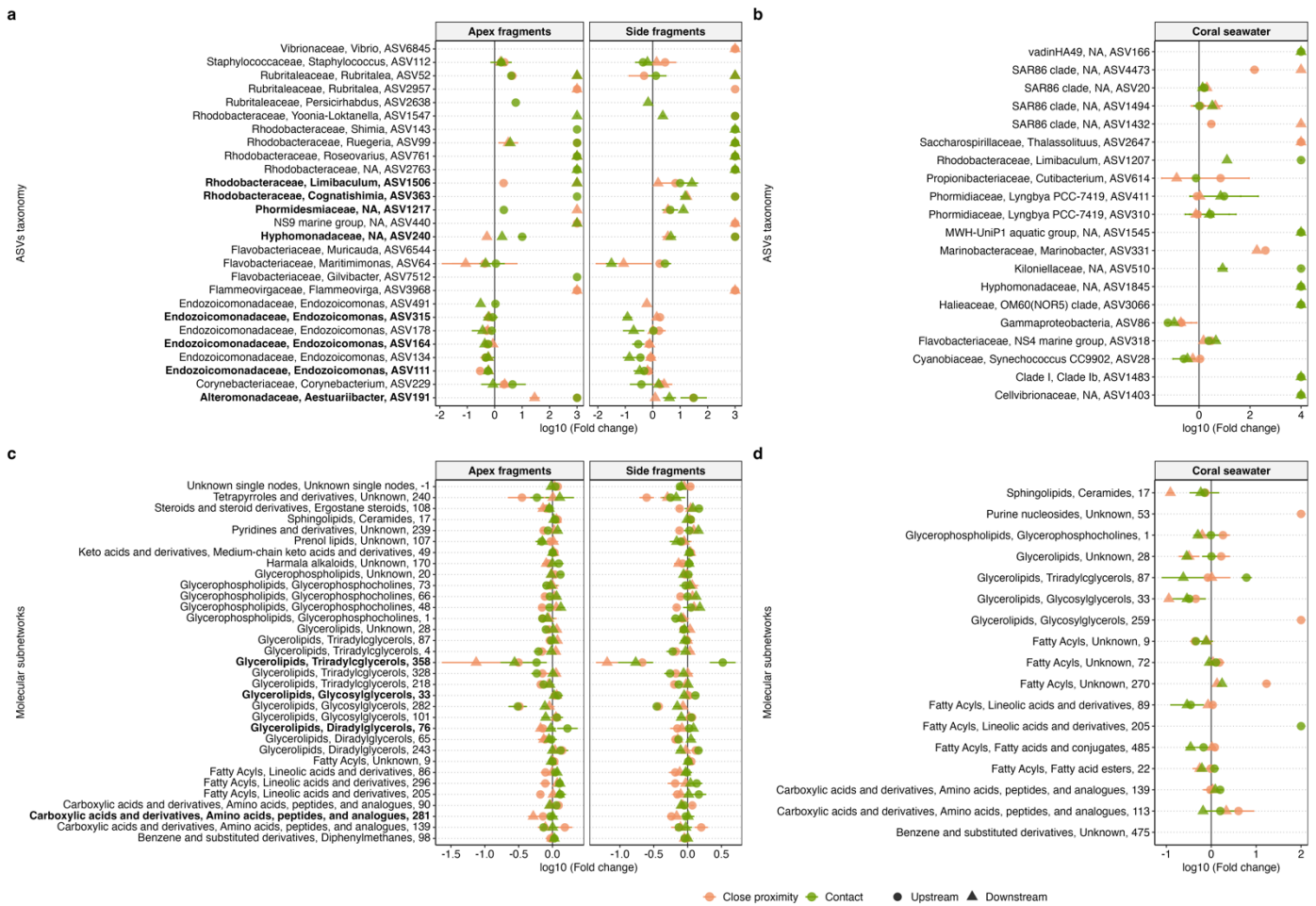


Figure 4.3 | Relative abundance fold changes (mean \pm se) of specific microbial taxa and molecular subnetworks in corals and near-surface coral seawater (CSW). Top 20 most discriminant and significantly differentially abundant ASVs in **a. corals and **b**. CSWs. Selected molecular subnetworks with at least 3 discriminant features and/or one of the top 20 features in **c**. corals and **d**. CSWs. ASVs and networks at the far right were not detected in controls. Fold changes were calculated relative to the mean changes in the control condition and log10 transformed. Significantly differentially abundant ASVs (only in side fragments; see Result section for details) and subnetworks across interaction types are indicated in bold. Fold changes were calculated relative to the mean changes in the control condition and log10 transformed. Relative abundances of discriminant features were summed within each sample across molecular subnetworks. Discriminant ASVs and metabolites were determined by the PLS-DA shown in Supplementary Figure 4.**

2.4. Changes in specific molecular classes relative to control

For the metabolome, we focused on the 1441 MS1 features that had MS2 fragmentation spectra for annotation purposes and identified 623 and 186 discriminant metabolites (VIP score > 1) in corals and CSWs, respectively. We further selected the 42 molecular subnetworks (i.e., clusters of metabolites with alike structure grouped based on their spectral similarity) that had at least 3 discriminant features and/or at least one of the 20 most discriminant features. These subnetworks comprised 353 features and belonged to 13 putative molecular classes (Supplementary Table 5; Supplementary Fig. 6b). Fatty acyls were the most abundant classes

which, summed together, comprised on average 23% and 78% of the total peak area in corals and CSWs, respectively (Supplementary Fig. 6b). Carboxylic acids, glycerolipids and glycerophospholipids were the secondary most abundant molecular classes in coral samples comprising each ~2% of the total peak area on average. Since we detected no significantly differentially abundant subnetworks considering apex and side fragments separately, we assessed significance regardless of sampling location. Colony position had no significant influence on subnetworks relative abundance, so we focused on the effect of interaction type. Out of these 42 subnetworks, only 4 subnetworks within coral metabolomes were significantly differentially abundant, or had at least one feature significantly differentially abundant, between interaction types: subnetworks 358, 76, 281 & 33 (ANOVA on ranks, FDR-adjusted $p < 0.05$; Fig. 4.3c; Supplementary Table 5). Pairwise comparisons showed that the relative abundance of these subnetworks did not significantly differ between direct contact and control treatments (Posthoc FDR-adjusted $p > 0.05$), but they did comparing close proximity to control and direct contact treatments (Posthoc FDR-adjusted $p < 0.05$). Though not always significantly, the coral metabolome exhibited notable changes in the relative abundances of several lipid classes. Glycerolipids such as betain lipids (e.g., subnetwork 358; Fig. 4.4a) and glycosylglycerols (e.g., subnetwork 282; Fig. 4.4b) were depleted in corals in direct contact and close proximity compared to controls (Fig. 4.3c; Supplementary Table 5. Subnetwork 358 was associated with betain lipids and included two fully saturated features, the MGTSA (16:0) and the DGTSA (14:0/16:0), which were the 3rd and 7th strongest discriminant features (Fig. 4.4a; Supplementary Table 6; Supplementary Figs. 7a-b & 8a-b). In subnetwork 282, five out of the six features were discriminant such as the putative DG (16:1/14:0) (Supplementary Table 6a), although their relative abundances did not vary significantly across interaction types (ANOVA, FDR-adjusted $p > 0.05$; Supplementary Fig. 7c). Comparatively, monoradylglycerols (e.g., subnetwork 205), diradylglycerols (e.g., subnetwork 76) and other glycosylglycerols (subnetwork 33) were abundant in direct contact with *Dictyota* and relatively scarce in close proximity (Fig. 4.3c; Fig. 4.4c & d; Supplementary Table 5; Supplementary Fig. 7d-e). One of the monoradylglycerol was putatively identified as MG (18:3) (subnetwork 205; Supplementary Table 6a) and a diradylglycerol, potentially DG (16:0/16:1), was the 5th top VIP (subnetwork 76; Supplementary Table 6a; Supplementary Fig 8c). One glycosylglycerol (e.g., DGDG (14:1/22:6)), from the subnetwork 33, had a higher relative abundance in direct contact (Fig. 4.3c; ANOVA, FDR-adjusted $p < 0.05$; Supplementary Figs. 7f & 8d). In subnetwork 73, we found the PAF-C16 (Supplementary Table 6a; Supplementary Fig. 8e), a metabolite putatively involved in coral immunity (Quinn et al., 2016; Roach et al., 2020). Surprisingly, its

relative abundance was not higher in direct contact with *Dictyota* (Supplementary Fig. 7g). We searched for other potential bioactive lipids, such as the lysoPAF-C16 (subnetwork 73) and the ceramide (18:1/16:0) (subnetwork 17), but none significantly differed in abundance across interaction types (Supplementary Figs. 7h-i & 8f-g). While lipids represented the bulk of discriminant features, subnetwork 281, associated to amino acids and peptides, comprised two features that were the 5th and 11th most discriminant features which decreased in close proximity (Fig. 4.3c; Fig. 4.4e; Supplementary Fig. 7j). However, no annotations or good quality putative formulas could be retrieved (Supplementary Fig. 8h). We also observed an enrichment of ergostane steroids (subnetwork 108) in side fragments touching *Dictyota* (Fig. 4.3c; Supplementary Table 6a). Comparatively, in CSW samples, we observed a global decrease of several molecular classes when corals were in direct contact, although not significantly (ANOVA, FDR-adjusted $p > 0.05$; Fig. 4.3d). Additional discriminant compounds with a good quality putative annotation are listed in Supplementary Table 6b.

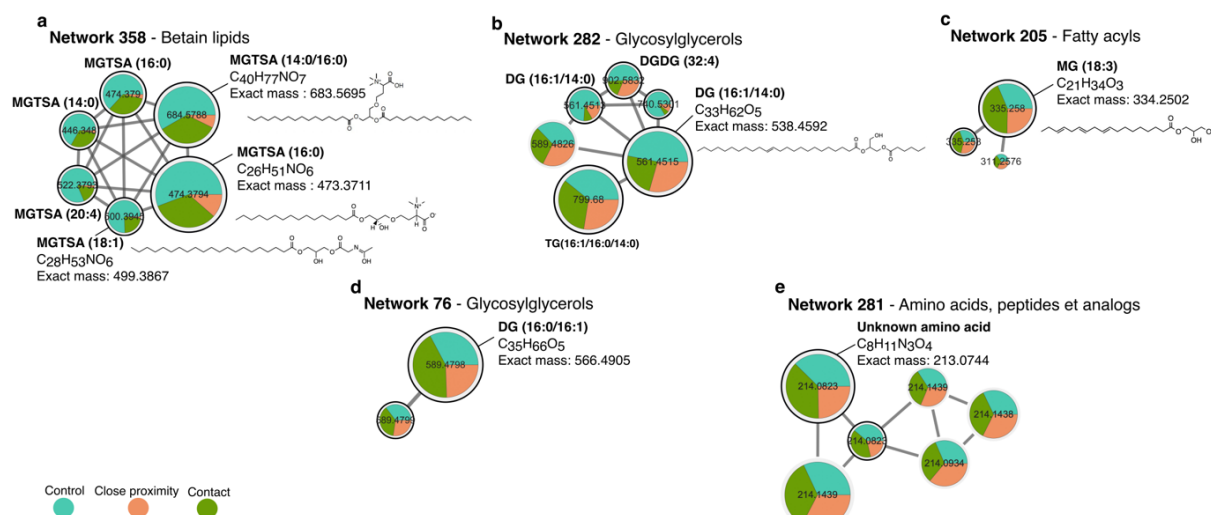


Figure 4.4 | Molecular subnetworks and putative annotations of coral metabolites varying across interaction types. Each node in the networks represents a unique feature with its associated MS/MS spectra labelled by its precursor mass. Nodes are linked by a cosine score > 0.7 (edges). Black circled nodes are discriminant features (i.e., VIP score > 1). Pie charts represent the mean relative abundances (i.e., peak areas) of each node in either control (blue), close proximity (2 cm; orange) or direct (green) interaction. Node are sized relative to the total feature abundance in all coral samples. Putative subnetwork molecular classes were derived from Classyfire ontology via MolNetEnhancer (GNPS) and CANOPUS (SIRIUS). Feature identities and putative formulas were obtained through GNPS and SIRIUS. Exact positions of desaturations are uncertain.

2.5. Identifying correlation between microbes and metabolites within the coral holobiont

We aimed at further investigating the links between microbial taxa and metabolites in the coral samples by integrating the metabarcoding and metabolomic data using the multiblock

PLS-DA model DIABLO (Supplementary Fig. 9; Rohart et al., 2017; Singh et al., 2019). The bipartite network resulted in two clusters composed of 41 metabolites and 27 ASVs with a correlation coefficient > 0.7 or < -0.7 (Fig. 4.5). In the first cluster, diverse ASVs, essentially unique to corals in direct contact, displayed negative correlations with metabolites associated with amino acids/peptides and unknown compounds (Fig. 4.5a; Supplementary Table 6c). Several microbial genera were present in this cluster, among them *Aestuariibacter*, *Endozoicomonas*, *Shimia*, *Vibrio*, *Oleiphilus*, *Ruegeria*, *Leisingera*, and *Thalassotalea*. The second cluster comprised ASVs and metabolites all enriched in coral microbiomes in contact with *Dictyota*. The 4 ASVs, *Cribrihabitans*, *Rhodopirellula*, *Vibrio* and an unclassified Micavibrionales were positively correlated with various metabolites associated to ceramides, purine nucleoside, amino acids, glycerophospholipids and several unknown compounds (Fig. 4.5b).

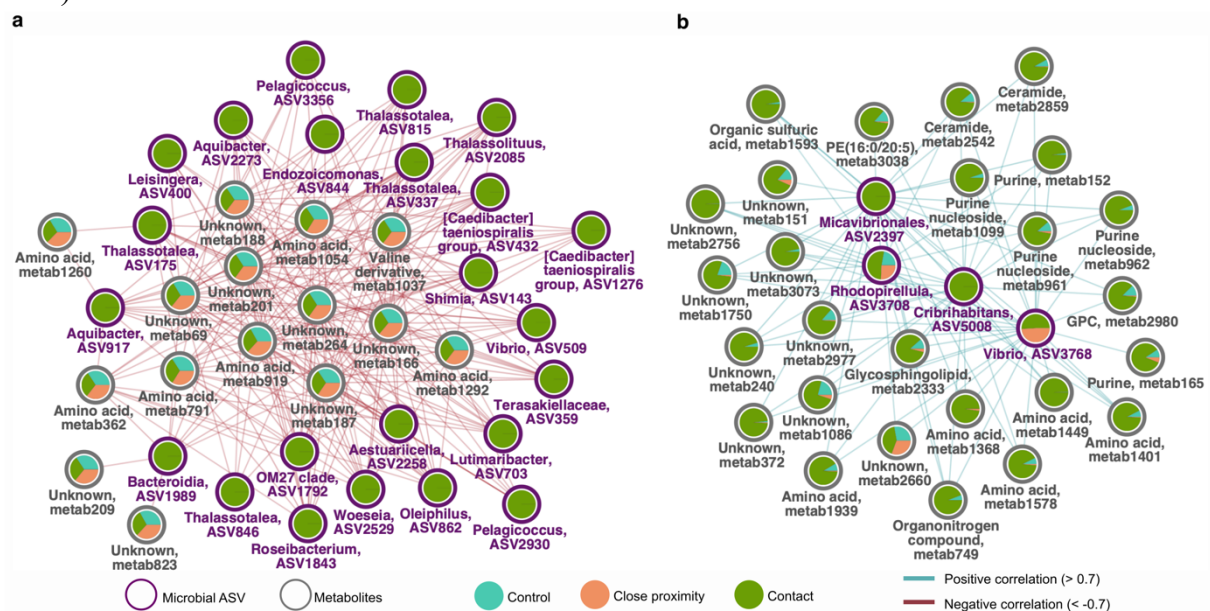


Figure 4.5 | Correlation network of ASVs and metabolites across algal interaction types in coral holobionts. Bipartite network resulted from multiblock DIABLO analysis et generated two clusters **a.** and **b.** A threshold on correlation value was set to 0.7, thereby selecting 25 ASVs and 44 metabolites. Nodes are colored by the ASV/metabolite mean relative abundance in either control (blue), close proximity (2 cm; orange) or direct contact (green) treatment in coral samples. Node contour represents the type of variable: ASV (purple) or metabolite (grey). Metabolite putative formulas and annotations can be found in Supplementary Table 6c.

2.6. Metabolites stoichiometry and energetics

We further explored the coral and CSW metabolome composition by investigating the macronutrient stoichiometry and nominal oxidation states of carbon (NOSC; a proxy for energy gained during catabolism). For each discriminant metabolite, we calculated its elemental composition (i.e., C, H, N, O and P atoms) and its NOSC based on its putative molecular

formula (See Supplementary Methods). Only 337 discriminant features had a good quality formula predicted by SIRIUS. The CSW metabolome had significantly more compounds containing N atoms, as well as CHNO and CHONP stoichiometric patterns, than the coral metabolome (Kruskal-Wallis, $p < 0.05$; Supplementary Fig. 10a and b). Interestingly, N-enriched molecules were more abundant in coral samples than in CSW samples (Kruskal-Wallis, $p < 0.05$; Supplementary Fig. 10c). CSW metabolites had a significantly lower NOSC and higher Gibbs free energy (ΔG^0_{Cox}) values than coral metabolites. NOSC and ΔG^0_{Cox} of coral metabolites were significantly influenced by interaction type, but not by sampling position and colony position (ANOVA on ranks, $p < 0.05$; Supplementary Fig. 10d). However, no difference of NOSC and ΔG^0_{Cox} were detected between interaction types and colony positions for CSW metabolites (ANOVA on ranks, $p > 0.05$).

3. Discussion

Our study demonstrates the negative impacts of direct algal contact on coral holobionts. While both contact and water-mediated interactions altered the microbiome and metabolome composition of *P. acuta*, macro-physiological damages were contact-dependent. When subjected to direct contact with *Dictyota*, *P. acuta* showed macro-physiological damages, including necrosis, bleaching and algal overgrowth. Similar adverse effects have been observed for corals in direct contact with live algae, and previous studies suggest the implication of physical mechanisms, as well as allelopathy and microbial effects (Rasher et al., 2011; Clements et al., 2020; Briggs et al., 2021). In a field study, coral growth and photosynthetic efficiency were suppressed even in contact with inert algal mimic (Clements et al., 2020). However, it is unlikely that, in our study, physical mechanisms alone were responsible for the observed coral damage, as *Dictyota bartayresiana* is known to produce cytotoxic compounds against corals (Rasher & Hay, 2010; Rasher et al., 2011). When corals were located in close proximity to the macroalga, no damage was observed. This result corroborates previous findings under *in-situ* flow conditions (Clements et al., 2018, 2020). For example, Clements et al., 2020 found no water-mediated effects of *Sargassum polycystum* and *Galaxaura rugosa* on *Acropora millepora* on coral physiology. While it has been suggested that waterborne compounds and associated harmful bacteria could result in coral tissue degradation and hypoxia in contact-free interactions (Smith et al., 2006; Barott & Rohwer, 2012; Fong et al., 2020), our results provide further

evidence that, in natural water flow condition, coral tissue damage is spatially constrained to the contact zone with macroalgae, even for allelopathic species such as *Dictyota bartayresiana*.

Upon contact, macro-physiological damages were paired with coral microbiome alterations. The microbiome of live coral tissue touching *Dictyota* increased in diversity and variability relative to the control, although not significantly. Increasing diversity patterns have been often described in coral microbiome in contact with turf and macroalgal competitors, and likely reflect increased bacterial colonization rates and an overwhelmed capacity to regulate microbiome structure (Zaneveld et al., 2016; Pratte et al., 2018; Briggs et al., 2021). A stable microbiome may emerge from selective abiotic conditions at the coral-algal interface allowing for a specific microbial community to thrive (Pratte et al., 2018; Briggs et al., 2021). Despite the lack of significant diversity patterns, we observed contact-driven changes in the coral microbiome that were symptomatic of microbial dysbiosis (i.e., higher abundance of harmful bacteria in the detriment of beneficial ones). Specifically, several taxa affiliated to the Rhodobacteraceae (e.g., *Shimia*), Rubritaleaceae, Cyclobacteriaceae, Hyphomonadaceae and Vibrionaceae (e.g., *Vibrio*), significantly increased when corals were in contact with *Dictyota* (Figs. 4.3 & 4.5). These taxa are often over-represented in stressed holobionts (McDevitt-Irwin et al., 2017; Rosales et al., 2023) and, particularly in corals interacting with turf, macroalgae (Roach et al., 2020; Briggs et al., 2021; Little et al., 2021) or their chemical extracts (Morrow et al., 2017). While significant microbial changes occurred only in coral portions physically touching *Dictyota* (i.e., side fragments), apex fragments (ca. 5 cm apart from side fragments) were also enriched in these taxa, suggesting colony-wide microbial colonization. This result corroborates previous studies showing that coral microbiome can be disturbed far (i.e., > 5 cm) from the zone of contact with the algal competitor (Morrow et al., 2013; Pratte et al., 2018). In addition, some ASVs were closely related to putative coral pathogens, as *Vibrio* and *Thalassotalea*, associated to tissue necrosis (Thompson et al., 2006; Luna et al., 2007). Their enrichment may alter coral holobiont structure by compromising immunity (Vidal-Dupiol et al., 2014), favoring secondary colonization (Rubio-Portillo et al., 2020) and competing with symbionts (Wang et al., 2022). Indeed, several taxa from the Endozoicomadaceae, which are well known coral symbionts (Hochart et al., 2023), decreased at the scale of the whole colony in our study. Through sulfur cycling (Raina et al., 2010), macromolecules transport (Neave et al., 2017b) and provision of essential metabolites (Pogoreutz et al., 2022), these symbionts are likely essential to mitigate stress and to evade pathogenetic invasion (Beatty et al., 2019; Zhang et al., 2021). Interestingly, one *Endozoicomonas* ASV was specific to contact-mediated interactions in the bipartite correlation network (Fig. 4.5a). Genome and metabolic

characteristics suggest that some *Endozoicomonas* strains may have a pathogenetic lifestyle (Pogoreutz & Ziegler, 2023). Corals in direct contact were depleted in other putative beneficial symbionts, including *Muricauda* (Flavobacteriaceae; Dungan et al., 2021). Together, these results suggest that contact with *Dictyota* alters bacterial competitive dynamics leading to microbial changes that could be deleterious for coral holobiont health.

Microbial communities within the CSW were also responsive to direct contact with *Dictyota*. Although we did not detect significantly enriched or depleted ASVs, some microbial families colonized water surrounding corals in contact treatments, such as Rhodobacteraceae, Hyphomonadaceae, Halieaceae and Cellvibrionaceae. These taxa, alongside those specifically colonizing coral holobionts upon algal contact, are abundant members of macroalgal microbiomes and macroalgal-dominated habitats (Bulleri et al., 2018; Paix et al., 2019; Briggs et al., 2021). Therefore, these opportunistic microbes may have been directly transmitted by *Dictyota* to coral surfaces but may also have colonized coral portions further from the contact zone by residing in near-surface water layers. In contrast, we observed a decrease of phototrophic microbes, such as *Synechococcus* CC9902. A mesocosm study by McNally et al., 2017 demonstrated that corals could remove *Synechococcus* cells from the water column. These microbes may have been grazed upon by the coral holobiont, with an increasing rate of grazing following contact-mediated stressors of *Dictyota*, although this would need to be specifically tested. Our stoichiometry and energetics analyses indicated that CSW compounds were enriched in nitrogen compounds, which were likely derived from the coral holobiont metabolism (Ochsenkühn et al., 2018; Wegley Kelly et al., 2022). Coral metabolites in contact-mediated interactions were slightly more reduced and energy-rich than in control conditions, potentially due to the influence of *Dictyota* metabolites (Wegley Kelly et al., 2022). However, this was not observed for CSW metabolites. A fine-scale sampling gradient of near-surface seawater across the coral-algal interaction could have revealed distinct patterns in compound energetics.

Water-mediated interactions led to a distinct microbial community with a loss of beneficial microbes (e.g., *Endozoicomonas*, *Muricauda*) and enrichment of opportunists (e.g., Rhodobacteraceae), but to a lesser extent compared to contact-mediated interactions. While close proximity with *Dictyota* was sufficient to alter coral microbiome structure, it may represent a mild stress as it did not cause any tissue damage. Likewise, a recent laboratory experiment (Fong et al., 2020) showed that the microbiome of *Montipora stellata* colonies in contact and close proximity with the allelopathic alga *Lobophora* sp. differed from control treatments, while negative impacts on coral physiology were contact-dependent. Together these

results indicate that the coral microbiome can respond to close proximity with macroalgae without visible tissue damage or physiological effects. However, even non-dysbiotic changes could represent significant adverse effects for corals. For example, defense potency of coral waters against *Vibrio corallilyticus* was compromised in colonies originating from macroalgal-dominated reefs despite relatively small changes in coral microbiome structure (Beatty et al., 2019). In our study, reduced anti-pathogen defense may have favored the enrichment of opportunists in corals in close proximity with *Dictyota*.

As for microbiome, coral metabolome distinctly responded to contact and close proximity with *Dictyota*. Metabolites constitute essential chemical cues that can provide information on the molecular processes occurring within the coral holobiont (Quinn et al., 2016; Wegley Kelly et al., 2021). For example, to limit the spread of bacterial infection and reduce cellular damages, the coral immune system produce anti-microbial peptides, signaling compounds (e.g., reactive oxygen species - ROS), and a suite of secondary metabolites (Vidal-Dupiol et al., 2011; Toledo-Hernández & Ruiz-Diaz, 2014). Direct contact with *Dictyota bartayresiana* allelochemicals has been suggested to exceed the antioxidant capabilities of the holobiont resulting in necrosis and bleaching if damaged cells are not removed quickly enough (Shearer et al., 2012). Therefore, the unchanged relative abundance of immunity lipids, such as the ceramide (18:1/16:0) (Roach et al., 2020; Little et al., 2021), the PAF-C16 (signaling compound for ROS production) and its precursor the lysoPAF-C16 (Quinn et al., 2016), in the coral metabolome from contact treatments, was surprising. However, we detected other compounds belonging to ceramides, ergostane steroids and amino acids/peptides derivatives that might be relevant for oxidative stress mitigation and coral defense in general (Hillyer et al., 2017; Lu et al., 2020; Tisthammer et al., 2021). In the bipartite network (Fig. 4.5), amino acids/peptides derivatives and ceramides were positively correlated with bacterial taxa enriched in corals in direct contact, potentially illustrating the increased production of these compounds in response to microbial invasion. The depletion of glycerolipids coupled with the increase of fatty acids in direct contact may reflect a switch in energy allocation on stored lipids to compensate the physiological cost of immune response (Hillyer et al., 2017; Smith et al., 2020). In addition, due to their putative roles in immunity pathways (Bergé & Barnathan, 2005; Rocker et al., 2019), fatty acids may have been accumulated by corals through increased heterotrophy (Liu et al., 2022) and/or *de novo* synthesis (Kabeya et al., 2018).

Comparatively, the CSW metabolome composition did not significantly differ across interaction types. However, the decrease of most molecular families may reflect a dampened metabolism of stressed holobionts. In contrast to the microbiome, the coral metabolome

responded to interaction types without distinction between apex and side fragments, supportive of a colony-wide metabolomic response. This result corroborates a study on coral-turf competition which found no correlation between *Orbicella faveolata* metabolome composition and distance to the coral-turf interface (Little et al., 2021). This lack of spatial patterns suggests an exchange of resources within the holobiont, rather than a specific translocation towards to most damaged/exposed portions of the colonies (Smith et al., 2020; Little et al., 2021). However, we found a significant spatial variability in metabolome composition between apex and side fragments, suggesting a differential influence of abiotic factors (i.e., light, chemical gradients) across coral colonies (Roach et al., 2023).

Coral-algal interaction outcomes are difficult to predict being modulated by species identities, but also by environmental factors, such as distance and flow dynamics (Briggs et al., 2021; Brown & Carpenter, 2015; Clements & Hay, 2023). To date, only laboratory studies have brought evidence of detrimental water-mediated effects of algae on corals (Smith et al., 2006; Jorissen et al., 2016; Fong et al., 2020). In the natural environment, effective competition relies on the transport and retention of detrimental microbes and compounds from the alga to the coral surface (Barott & Rohwer, 2012; Brown & Carpenter, 2015; Jorissen et al., 2016). Thus, we expected downstream corals to be more impacted than upstream corals, but our data did not support this hypothesis. Under strong currents, retention times at the downstream sides of coral-macroalgae interaction may not differ from upstream sides (Brown & Carpenter, 2015). In our experiment, high flow regime may have resulted in thin CSW and weak accumulation of algal-derived matter around coral surfaces, thereby limiting water-mediated and colony position effects.

Our study demonstrates that contact and water-mediated interactions distinctly shape the coral microbiome and metabolome composition. By revealing strong associations between specific intracellular coral metabolites and microbes, our data helped to unveil some biological processes within the coral holobiont. To further decipher the consequences of algal interaction on coral holobionts, future work will greatly benefit from more targeted investigations on the roles of specific metabolites and microbes in a multi-omic analysis framework (Garg, 2021; Mohamed et al., 2023). Despite fundamental advancements in metabolite dereplication, our understanding is still dramatically hindered by the “black box” of unknown metabolites. Without a clear mechanistic investigation of the identified molecular biomarkers on holobiont physiology, their putative roles will remain elusive, but such research represents exciting challenges in coral metabolomics (Garg, 2021; Wegley Kelly et al., 2021). Finally, while our data provide key insights in the context-dependencies controlling for coral-algal interaction

outcomes, future research should encompass thorough field investigations under different set of conditions (Clements & Hay, 2023), particularly in the context of climate change which can modify competition dynamics (Del Monaco et al., 2017). All this knowledge will be essential to fully grasp the consequences of algal proliferation on reefs and predict future benthic community trajectories as reefs degrade.

4. Materials and Methods

4.1. Experimental design

This study was conducted in a shallow fringing reef lagoon (2-2.5 m deep) of Moorea, French Polynesia (17°29'14.86"S 149°53'0.76"O) between October and December 2020. We tested the effects of contact- vs water-mediated interaction with *Dictyota bartayresiana* on the coral *Pocillopora acuta* (*P. damicornis* ecomorph β , genetically identified in Schmidt-Roach et al., 2014; Rouzé et al., 2017) by implementing three algal treatments: i) coral colonies in direct contact with a transplanted patch (i.e., 300 cm³) of *Dictyota*, ii) coral colonies in close (i.e., 2 cm) proximity with transplanted patch (i.e., 300 cm³) of *Dictyota*, and iii) coral colonies alone (control). To evaluate the effect of the prevalent current direction on the transport of algal-derived matter towards the corals, one colony was placed upstream and a second colony downstream the algae, relative to the unidirectional west-east current in the lagoon (Hench et al., 2008) (Supplementary Fig. 1). For the control treatment, up- and downstream colonies were ~ 14 cm apart as for the close proximity treatment. Treatments were replicated four times in a randomized block design (total of 24 colonies). A previous study demonstrated the preponderance of chemical over physical competitive mechanisms of *D. bartayresiana* using algal mimics, so algal mimics were not added as procedural controls (Rasher & Hay, 2010; Rasher et al., 2011). The experiment was run over 3 months (October to December 2024). Colony health was visually assessed once a month and the maintenance (e.g., cleaning of fouling organisms, adjustment of algal patch size) was done fortnightly.

4.2. Sampling

In January 2021, coral fragments and associated near-surface water (i.e., CSW ~1 mm from the coral surface, a mix of MBL and DBL; Shashar et al., 1996; Barott & Rohwer, 2012) were sampled for characterization of their microbiome and metabolomic signatures. Water samples were collected first due to the stress induced by fragment pruning. To assess intra-

colony response variability, live coral fragments without *Dictyota* residual tissue (i.e., side fragments in direct contact) were collected at the apex and on the side (i.e., the closest to the interacting zone) of the colonies. One small fragment (1 cm² - 16S rDNA metabarcoding) and one larger fragment (3x3 cm – LC/MSMS metabolomics) were clipped at each location and placed into sterile plastic bags (Whirlpak) underwater. Fragments were flash frozen in carbonic ice after removal of excess water from the bags and three rinses with sterile seawater. Upon return from the field, samples were immediately stored at -80° until processing. Microbiome-intended fragments were stored into 1mL DNASHield at -20°C until DNA extraction. For metabolomics, fragments were freeze-dried for 36h and stored at -20°C until metabolites extraction. Near coral surface seawater samples were collected with 100 mL syringes by withdrawing 10 mL from 10 random healthy spots around the colonies. Each syringe was capped before and after sampling to avoid contamination from surrounding seawater. All samples were kept in a cool box with ice during transport (15-20 min) to the laboratory. For the water microbiome, syringe content was first pre-filtered with GF/D glass filters 2.7 µm (Whatman) and filtered on 47 mm 0.2 µm polyethersulfone filters (Sigma). Filters were cut in small pieces in sterile Petri dish and scalpel to be then stored in 1mL DNA/RNA Shield (Zymo Research, USA). Samples were stored at -20°C until DNA extraction. Water-associated metabolites were extracted *in-situ* by solid-phase extraction (SPE) with Strata cartridges (500 mg/6 mL, Phenomenex, USA) pre-conditioned with 6mL distilled water. Cartridges were capped with a SPE adaptor connected to a teflon tube (Supelco) and their ends were connected to an adaptor followed by the 100 mL syringe. Vacuum was made by pulling the syringe so that the water would flow through the polymeric phase. Back in the laboratory, cartridges were rinsed with 6 mL distilled water and fitted onto a vacuum manifold (Supelco) connected to a vacuum pump (Laboport N820, KNF) for drying. Additionally, four experimental blank CSW samples were prepared using distilled water. Cartridges were freeze-dried and stored at -20°C until compound recovery.

4.3. 16S rDNA gene sequencing and metabarcoding data acquisition

DNA was extracted using the ZymoBIOMICS DNA Miniprep kit (Zymo Research, USA, D4300) according to manufacturer's instructions for samples stored and lysed into DNA/RNA Shield. We processed both the filter pieces and the 1 mL DNASHield for the water samples but only the 1 mL DNASHield for the coral fragments. After extraction, samples were stored at -20°C and dried with a centrifugal evaporator (EZ-2 serie, Genevac) for safe shipment to Genome Quebec for sequencing. Several samples were damaged during shipment, resulting

in the loss of 1 replicate out of the 4 for certain treatment combinations. The hypervariable region V3-V4 of the 16S rDNA gene was amplified using the universal primers 341F (5'-CCTACGGGNGGCWGCAG- 3') and 805R (3'-GACTACHVGGGTATCTAATCC- 5') suggested for marine bacteria and some archaea (Klindworth et al., 2013; Wear et al., 2018). Amplicons were paired-end (2 x 250 bp) sequenced using an Illumina NovaSeq 6000 sequencer by Genome Quebec (Montréal, Canada). Primers were removed with Cutadapt, after having discarded reads with ambiguous N bases (Martin, 2011). DADA2 workflow on R (version 4.2.3) was used for quality filtering, error estimation, denoising, merging and removal of chimeric sequences in order to generate amplicon sequence variants (ASVs; Callahan et al., 2016). We kept only the sequences with a minimum length of 200 bp and a maximum length of 250 bp for the estimation of error rates. NovaSeq provided a very high sequencing depth resulting in 49 459 536 reads across 265 597 ASVs at the end of the processing workflow. We filtered out undesired (i.e., chloroplasts and mitochondrial sequences), rare sequences (i.e., ASVs with at least 2 reads and detected in at least 3 samples), as well as contaminants (N = 150 ASVs) using 8 blank samples (i.e. filter, extraction kits, Genevac, PCR) and the *decontam* R package with the prevalence method (Davis et al., 2018). We assigned taxonomy at the genus level using the Silva reference database (v138.1). The count table, taxonomy table and metadata table were then imported into the *phyloseq* R package (McMurdie & Holmes, 2013). The sequences of discriminant ASVs were BLASTed against the GenBank (16S rRNA sequences for Bacteria and Archaea) to identify closely related matches (Supplementary Table 7).

4.4. Metabolites recovery and mass spectrometry analysis

Coral samples were extracted from 2 g of coral powder after fine grinding with a TissueLyser II (20 s at 20Hz - Qiagen). A solvent mixture of methanol/dichloromethane (10mL, v/v, 1:1) was added into glass tubes with the coral sample matrix. Cartridges (i.e., 500 mg/6 mL) were eluted with 8 mL 100% MeOH (HPLC-MS grade). Two extraction blanks were prepared without coral material. Solvents were removed with a Genevac centrifugal evaporator (EZ-2 serie, SP Industrie, Royaume-Uni) and resolubilized with 100% MeOH (LC-MS grade) at a concentration of 1 mg/mL. Untargeted metabolomic analysis was performed using a UHPLC system (Vanquish Thermo Scientific, MA, USA) coupled to a Q-Exactive Plus Orbitrap mass spectrometer (Thermo Scientific, MA, USA). Aliquots (2µL) of biological samples (N = 66) along with quality control samples (N = 7 coral QCs and N = 7 water QCs) were injected throughout two analytical sequences: 1) CSW samples (full scan in positive ionization mode - MS1) and 2) Coral samples with a QC of coral waters (full scan MS and data

dependent MS2 in positive ionization mode). The CSW QC was added to the second sequence to retrieve fragmentation spectra of features fragmented in the water samples during the MS/MS data extraction on MZmine3 (see next section). Blank samples (N = 10) and QC samples (N = 14) were injected at the beginning and at the end for each analytical sequence to condition the column and assess carry-over effect. A QC of each sample type were injected every 8 samples track analytical repeatability. The mobile phase was H₂O + 1 ‰ formic acid (phase A) and acetonitrile/isopropanol (50/50) + 1 ‰ formic acid (phase B). Please see the Supplementary methods for protocol details and mass spectrometry parameters.

4.5. Metabolomic data acquisition

Files were processed with MZmine 3 (version 3.4.16) for MS extraction and features alignment (Schmid et al., 2023). Please see Supplementary methods for the MZmine workflow and associated parameters. MS1 feature peak areas were exported into a .csv file for statistical analysis on R (version 4.2.3). For network analysis and annotation, we exported a quantitative table comprising peak areas of MS1 features with MS2 data as well as a .mgf file with consensus MS/MS spectra of each feature to be uploaded on the GNPS web platform (Wang et al., 2016) and SIRIUS software (Dührkop et al., 2019). Feature-Based Molecular Networks (FBMN) were built to connect ion features based on their spectral similarity with a precursor ion mass tolerance of 0.02 Da, a cosine score of 0.7 and a minimum of 6 matched peaks (Nothias et al., 2020). We used an extended workflow compiling Dereplicator, Network Annotation Propagation, MS2LDA_MotifDB and MolNetEnhancer (Wang et al., 2016; van der Hooft et al., 2016; da Silva et al., 2018; Ernst et al., 2019) to improve annotation of molecular networks and retrieve their chemical classification (ClassyFire chemical ontology; Feunang et al., 2016). To complete features dereplication, we used the software SIRIUS providing putative molecular formulas and molecular classes using CANOPUS (Dührkop et al., 2019, 2021) and we manually searched compound identities within MarinLit and Lipidmaps databases (Supplementary Methods). The .csv files containing the MS1 peak areas (N = 6458 features of which 3466 had MS2 spectra) were imported in R and cleaned from an in-house script. We removed contaminants using blank samples (i.e., if mean samples/mean blanks < 4), low quality (Dispersion ratio > 0.5, defined in Broadhurst et al., 2018)¹⁰² and rare features (i.e., at least in 3 coral samples and/or 3 CSW samples). The D-ratio was calculated for each sample types (i.e., coral and CSW) and their corresponding QC samples. These filtration steps resulted in 2143 MS1 features of which 1441 had MS2 spectra. To avoid bias attributable to distinct injection

sequences and differential sample matrix, peak areas were normalized by the sum in each sample.

4.6. Statistical analysis

All statistical analyses were performed using the R software (version 4.3.2). Alpha-diversity (Shannon diversity index; *vegan* package 4.6.4; Oksanen et al., 2022) was calculated on rarefied microbiome count data (*phyloseq* package function “rarefy_even_depth”; McMurdie & Holmes, 2013) and all MS1 chemical features. Libraries were rarefied at 16 642 reads, discarding three CSW samples. Multivariate analyses were performed on CLR-transformed microbiome (i.e., counts) and metabolomic (i.e., relative peak areas) data. We examined abundances of microbes and molecules and intra-group variability (beta dispersion; *vegan* package function “betadisper”) using principal component analysis (PCA) and tested group compositional differences with a Permutational Multivariate Analysis of Variance (PERMANOVA; *vegan* package function “adonis2”) and 999 permutations. To discriminate samples by interaction type and to identify discriminant ASVs and metabolites, partial least squares - discriminant analysis (PLS-DA) were run using the *mixOmics* R package (Rohart et al., 2017). Only MS1 features with MS/MS fragmentation spectra were considered for annotation purposes. PLS-DAs were validated by cross-model validation and a permutation test (999 permutations) (Hervé et al., 2018). Discriminant ASVs and metabolites were selected if their VIP score was > 1 (Cocchi et al., 2018). To visualize abundance patterns of the top 20 ASVs and the subnetworks of interest (i.e., at least 3 VIPs and/or one of the 20 top-ranked discriminant metabolites), we calculated log₁₀-transformed mean fold-changes relative to the control treatment. For patterns at the microbial family level, we built a heatmap and a clustering (Euclidian distances and Ward’s minimum variance) of the 20 most discriminant families across the sample groups (i.e., interaction type x colony location) with the mean CLR-transformed abundances. We further kept the discriminant ASVs for subsequent differential abundance analysis using package ANCOM-BC testing the effect of interaction type and colony position within each sampling location (Analysis of Compositions of Microbiomes with Bias Correction; Lin & Peddada, 2020). ASVs differential abundances were considered significant if FDR-adjusted p-values were < 0.05 . Significant differences in metabolite abundance between interaction types and colony positions were assessed with non-parametric ANOVA on ranks (FDR-adjusted $p < 0.05$) as assumptions of normality and homoscedasticity were not met. As colony position and its interactive effect with interaction type were not significantly influencing metabolite abundances, we kept a simple model with interaction type only. To test for entire

subnetworks differential abundances across interaction types, we ran ANOVA (FDR-adjusted $p < 0.05$) on mean summed relative abundances of discriminant feature within each subnetwork. The integration of coral metabarcoding and metabolomic data was performed with multiblock PLS-DA (DIABLO - *mixOmics* R package; Singh et al., 2019). DIABLO provided with correlation coefficients between ASVs and metabolites which were visualized in a bipartite network (cut-off correlation coefficient of 0.7; González et al., 2012). Complementary details can be found in Supplementary Methods.

Data availability. Raw data and R scripts can be downloaded from a Zenodo repository with restricted access: <https://zenodo.org/records/10512352>. Metabarcoding sequence data have been deposited under the NCBI BioProject PRJNA967170. All MS data are publicly accessioned in the Mass Spectrometry Interactive Virtual Environment repository under the MassIVE accession code [MSV000091997](https://massive.ucsd.edu/MSV000091997). FBMN workflows can be accessed in GNPS with the following links :
<https://gnps.ucsd.edu/ProteoSAFe/status.jsp?task=91e6a7e225ed44e895d7edd6c8896a38;>
<https://gnps.ucsd.edu/ProteoSAFe/status.jsp?task=2d02ebfac0e44f9fa3362d4c72f39550> ;
<https://proteomics2.ucsd.edu/ProteoSAFe/status.jsp?task=5b91e8e0868142f687d296d45f084c41> ; <https://gnps.ucsd.edu/ProteoSAFe/status.jsp?task=4599ce0cf9724f9e95e51eb05ecc976f>

Acknowledgements. This work was supported with by the French National Research Agency through the project CORALMATES (ANR-18-CE02-0009-01) lead by M.M.N and by a PhD grant from the Ecole Pratique des Hautes Etudes to C.P.S. The authors are grateful to the French Polynesian government and the Papeto'ai district for collection and research permissions. We thank the CRIOBE station staff for their assistance on the fieldwork. We also thank Génome Québec Innovation Centre for the preparation and sequencing of the 16S rRNA amplicon library and the MSXM/Bio2Mar technical facilities for the mass spectrometry data acquisition.

Author contributions. C.P.S and M.M.N designed the experiment. C.P.S and H.B conducted fieldwork and collected the samples. C.P.S analyzed the data. D.R, I.B and C.L contributed instrumentalization, reagents and analytical tools. C.P.S and M.M.N led the writing of the manuscript. All authors critically contributed to review of the manuscript and gave final approval for its submission.

Competing interests. The authors declare no competing interest.

5. Supplementary Information

5.1. Supplementary Methods

Metabolites recovery and mass spectrometry analysis. Coral seawater (CSW) metabolites were extracted onto Strata-XL solid-phase extraction (SPE) cartridges (500 mg/6 mL, Phenomenex, USA) previously conditioned with 6 mL distilled water. After sample loading, cartridges were rinsed with 6 mL distilled water, dried on the vacuum manifold, freeze-dried and stored at -20 °C until elution. Additionally, experimental blank samples were prepared without samples (i.e., only collecting materials) using distilled water to remove contaminants from the data later on. Cartridges loaded with CSW samples were eluted with 8 mL 100% MeOH (HPLC-MS grade) into pre-weighted glass tubes. MeOH were removed by evaporation with a Genevac centrifugal evaporator EZ-2 serie (SP Industrie, Royaume-Uni) and extracts were stored at -20° C until injection. Coral metabolites were extracted from 2 g of freeze-dried coral powder after fine grinding with a TissueLyser II (20 s at 20Hz - Qiagen). A solvent mixture of methanol/dichloromethane (10 mL, v/v, 1:1) was added into glass tubes with the coral matrix. The resulting mixture was vortexed for 60 s and sonicated (ultrasonic bath, 2min). Extracts were centrifuged 20 min (3500 t/r at 4 °C) and the supernatants were transferred to pre-weighted glass tubes. Methanol and dichloromethane were removed by evaporation with a Genevac centrifugal evaporator (EZ-2 serie, SP Industrie, Royaume-Uni). Two extraction blanks were prepared without coral material. Dry extracts were stored at -20 °C. All extracts were resolubilized with 100% MeOH (LC-MS grade) at a concentration of 1 mg/mL. Pooled quality control samples (QCs, N = 14) were prepared from each sample type (i.e., water and coral) at equimolar concentrations and equally divided into individual HPLC vials. Samples were injected throughout two analytical sequences: 1) coral waters (full scan MS in positive ionization mode - MS1) and 2) coral samples with a CSW QC (full scan MS and data dependent MS2 in positive ionization mode). Two MeOH blanks were injected at the beginning of the sequence for system suitability as well as 8 system-conditioning QC samples. Additionally, QC of each sample type were injected every 8 samples to track analytical drift and mass and retention time accuracy (Broadhurst et al., 2018a). Extraction blanks of each sample type were injected at the beginning and at the end of each analytical sequence to assess carry-over effect and for contaminant detection. All biological samples were injected randomly to avoid systematic bias. Sample metabolomic profiles were acquired from 2µL injection with a UHPLC system (Vanquish Thermo Scientific, MA, USA) coupled to a Q-Exactive Plus Orbitrap mass spectrometer (Thermo Scientific, MA, USA) with a HESI source. Acquisitions were controlled

by the Xcalibur software (Thermo Scientific). The chromatographic separation was carried out on a Luna Omega 1.6 μm Polar C18 column 100x2.1 mm (Phenomenex, Torrance, CA, USA) and consisted of H_2O + 1% formic acid (mobile phase A) and acetonitrile/isopropanol (50/50) + 1% formic acid (mobile phase B). A linear gradient was used with a flow rate of 0.250 mL/min: 0 to 2 min, at 2% B; 2 to 8 min, from 2 to 65% B; 8 to 25 min, from 65 to 100% B; 25 to 27 min, from 100 to 2% B, 27 to 31 min, at 2% B. Mass spectrometer settings were as follows: sheath, auxiliary and sweep gas set at 35, 10 and 0 AU, respectively; capillary voltage, 3500 V in positive mode; capillary temperature, 320 $^\circ\text{C}$; ESI probe heater temperature, 200 $^\circ\text{C}$ and S-lens RF level, 50. For the 1st sequence, full scan mass spectra (MS1) were acquired in positive electrospray ionization mode with a full scan MS window of 100-1500 m/z and a resolution of 35 000. The maximum injection time was set to 100 ms and automatic gain control (AGC) target set at 3×10^6 . For the 2nd sequence, full scan MS resolution was set at 70 000 and MS/MS spectra were acquired in data dependent mode with an isolation window of 1.5 m/z ; MS2 resolution 17 500; AGC target 3×10^5 ; maximum injection time 100 ms. Up to 5 of most intense selected ions per scan were fragmented with a stepped normalized collision energy of 25-35-45 eV. Dynamic exclusion was set to 5 s and isotope peaks were excluded.

Mass spectral data acquisition. Raw MS files were first converted into .mzML files in centroid mode using MSConvert (Chambers et al., 2012) to be then imported into MZmine3 (version 3.4.16; Schmid et al., 2023) for MS extraction and features alignment. Masses were detected in centroid mode at a minimal intensity threshold of 10^5 for MS1 level and 10^3 for MS2 level. Automated data analysis pipeline (ADAP) module (Pluskal et al., 2010; Myers et al., 2017) was used to build chromatograms with a minimum number of 5 scans, a minimum peak height of 5×10^5 and m/z tolerance of 10 ppm. For chromatogram deconvolution using ADAP algorithm, a signal-to-noise ratio of 20 was set, coefficient/area threshold 120, peak duration range 0.01-0.1 min, RT wavelet range 0.01-0.06 min and m/z center calculation in Median mode. MS2 scans were paired with a m/z range of 0.01 Da and RT range of 0.06 min. Isotopes were removed using the isotopic peak grouper with m/z range tolerance 10 ppm, RT tolerance 0.1 min, maximum charge of 2 and selection of the most intense monoisotopic ions. Chromatograms were then aligned (Join Aligner module) with a m/z tolerance of 10 ppm and a RT tolerance of 0.06 min. Weights for m/z and RT were both set to 1. Isotope patterns were compared using the following thresholds: 10 ppm isotope m/z tolerance, 10 minimum intensity and 90% minimum score. The obtained list of features was then gap filled (Peak Finder module) with an intensity of tolerance of 10%, m/z tolerance of 5 ppm and RT tolerance of 0.06 min.

Duplicate peaks were removed with a m/z tolerance of 5 ppm and RT tolerance of 0.03 min. A selection was applied to retain only those isotopes with at least two peaks in an isotopic pattern and present in at least 2 samples. MS1 peak areas were exported into a .csv file for analysis on R. Additionally, for network analysis and annotation purposes, we exported a quantitative table comprising peak areas of MS1 features with MS2 data as well as a .mgf file with consensus MS/MS spectra of each feature to be uploaded on the GNPS web platform (Wang et al., 2016) and SIRIUS software (Dührkop et al., 2019).

Molecular networking, annotation strategy and calculation of Nominal Oxidation State of Carbon (NOSC). Feature-Based Molecular Networks (FBMN) were created with a precursor ion mass tolerance of 0.02 Da, a minimum cosine score of 0.7 and minimum 6 matched peaks. For each pair of nodes (i.e., molecular features), only the top 15 edges were kept. Spectra were annotated through search against the GNPS spectral libraries (e.g., contaminants, MassIVE databases). Additionally, a search for analogs was set with a maximum mass difference of m/z 100 compared to the mass of the precursor ion. To improve the resolution of compounds identities, we run an extended workflow within GNPS using Dereplicator, Network Annotation Propagation and MS2LDA_MotifDB (Wang et al., 2016; van der Hooft et al., 2016; da Silva et al., 2018). Result outputs were combined into the MolNetEnhancer tool (Ernst et al., 2019) assigning a chemical classification (ClassyFire chemical ontology; Feunang et al., 2016) to each subnetwork. All workflows can be accessed with the links in the *Data availability section*. Additionally, we retrieved the putative compound formulas and molecular fingerprints (CSI:FingerID; Dührkop et al., 2015) by calculating molecular formula *de novo* in SIRIUS 5 software (version 5.7.2) using isotope pattern analysis (Böcker et al., 2009) and fragmentation trees (Böcker & Dührkop, 2016). The ZODIAC module using Gibbs sampling was added to increase putative formula confidence (Ludwig et al., 2020). MS2 m/z deviation was set to 5 ppm, keeping maximum 10 potential results. ZODIAC parameters were kept as default. We only considered proposed formulas with a ZODIAC score > 0.95 , explaining at least 4 peaks and at least 85% of the spectral intensity. The CANOPUS module (Dührkop et al., 2021) was used to retrieve the compound classification from its predicted molecular fingerprint to compare with classification results obtained through the GNPS workflow. In the present work, we could generally achieve metabolite annotations at the levels 2 or 3 of the Metabolomics Standards Initiative (Sumner et al., 2007). Discussed metabolites were manually verified and we used the databases MarinLit (<https://marinlit.rsc.org>) and Lipidmaps (<https://www.lipidmaps.org>) to

seek putative annotations. Networks were then all visualized in the Cytoscape software 3.9.1 (Shannon et al., 2003).

From SIRIUS putative molecular formulas, we retrieved the number of the elements C, H, N, O, P and S for each metabolite and calculated the Nominal Oxidation State of Carbon (NOSC) as described in Roach et al., 2020 and Wegley Kelly et al., 2022 using:

$$NOSC = - \left(\frac{-Z + 4a + b + 3c - 2d + 5e - 2f}{a} \right) + 4$$

where Z corresponds to the net charge of the organic compound, which was set to 0 and a , b , c , d , e and f are the number of the elements C, H, N, O, P and S, respectively. The NOSC was used to calculate the Gibbs Free Energy of Carbon Oxidation (ΔG^0_{COX}) following the relationship given by LaRowe & Van Cappellen, 2011 where:

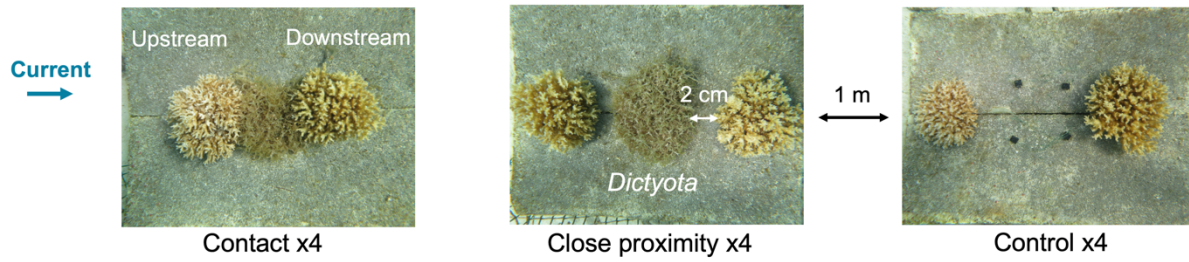
$$\Delta G^0_{\text{COX}} = 60.3 - 28.5 \times \text{NOSC at } 25^\circ \text{ and } 1 \text{ bar}$$

Discriminant analysis and multiomic data integration. Multivariate analyses were performed on CLR-transformed microbiome (i.e., counts) and metabolomic data (i.e., relative peak areas) using the functions “transform” from the package *microbiome* (Lahti & Shetty, 2017) and “logratio.transfo” from the package *mixOmics* (Rohart et al., 2017), respectively, with the addition of a constant equal to half the minimum value. In order to discriminate samples according to the interaction types and to identify discriminant ASVs and metabolites, partial least squares - discriminant analyses (PLS-DAs) were run using the *mixOmics* R package. For this analysis, only MS1 features with MS/MS fragmentation spectra were considered for annotation purposes. PLS-DA had successfully been used on compositional metabolomics and metabarcoding datasets (Kalivodová et al., 2015; Cao et al., 2016). Developed for highly dimensional and colinear data, this analysis enables to reduce the dimensionality of the data and to classify the samples into *a priori* known groups. The optimal number of components were retrieved from the function *perf*. PLS-DAs were validated by cross-model validation (7-fold outer loop CV2 and 6-fold inner loop CV1) to estimate a classification error rate (CER) using the “MVA.test” function in the *RVAideMemoire* R package (Hervé et al., 2018; Hervé, 2023). Pairwise tests were performed with the function “pairwise.MVA.test” by adjusting the p-values with False Discovery Rates. With a permutation test (999 permutations), the null distribution of CER was tested against the observed CER to assess if the clusters were indeed

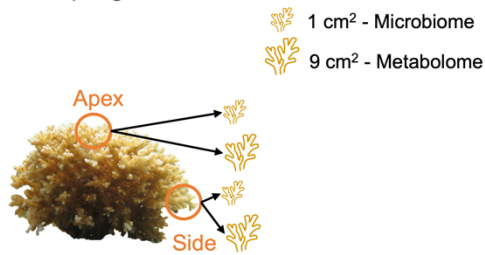
statistically different or if their separations resulted from chance alone. PLS-DA outputs return a VIP score for each variable which define the variable importance in discriminating groups. Conventionally a discriminant variable is considered to have a score > 1 and the higher the score, the higher its relevance in group discrimination (Cocchi et al., 2018). Multi-omics data integration was performed for coral samples with multiblock PLS-DA (DIABLO) analysis available in the *mixOmics* R package using the function “block.splsda” (Singh et al., 2019; Lê Cao & Welham, 2021). As in PLS-DA analysis, DIABLO (Data Integration Analysis for Biomarker discovery) seeks the correlated variables between pair of datasets that also discriminate sample groups. Prior to DIABLO, we run PLS regression analysis which inform on the level of association between the two datasets (i.e. 0.8 for coral), and the obtained correlation coefficient was set in the design matrix of the “block.plsda function”. The optimal number of variables was estimated respectively with the function “tune.block.splsda”. DIABLO outputs were validated by a permutation test based on cross-model validation as described above for the PLS-DA analysis using the function “DIABLO.test” from *RVAideMemoire* package. Bipartite correlation networks comprising variables with a high correlation coefficient (i.e. > 0.7 or < -0.7 ; see González et al., 2012) were further analyzed and visualized on Cytoscape software 3.9.1 (Shannon et al., 2003).

5.2. Supplementary Figures

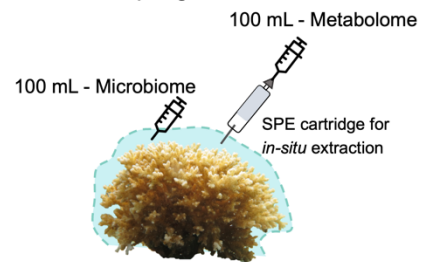
a. Interaction types



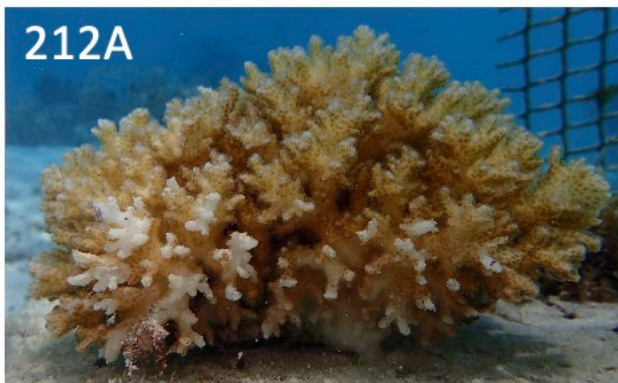
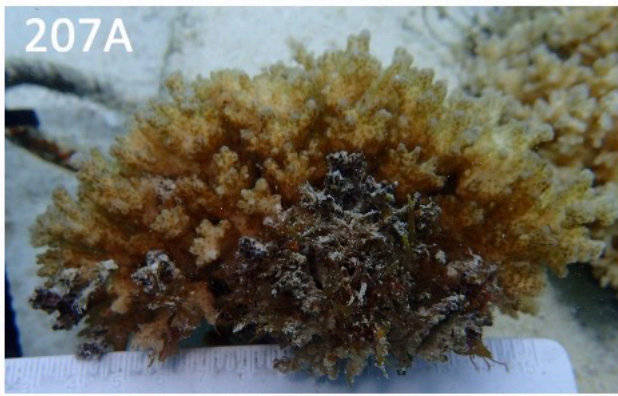
b. Coral sampling location



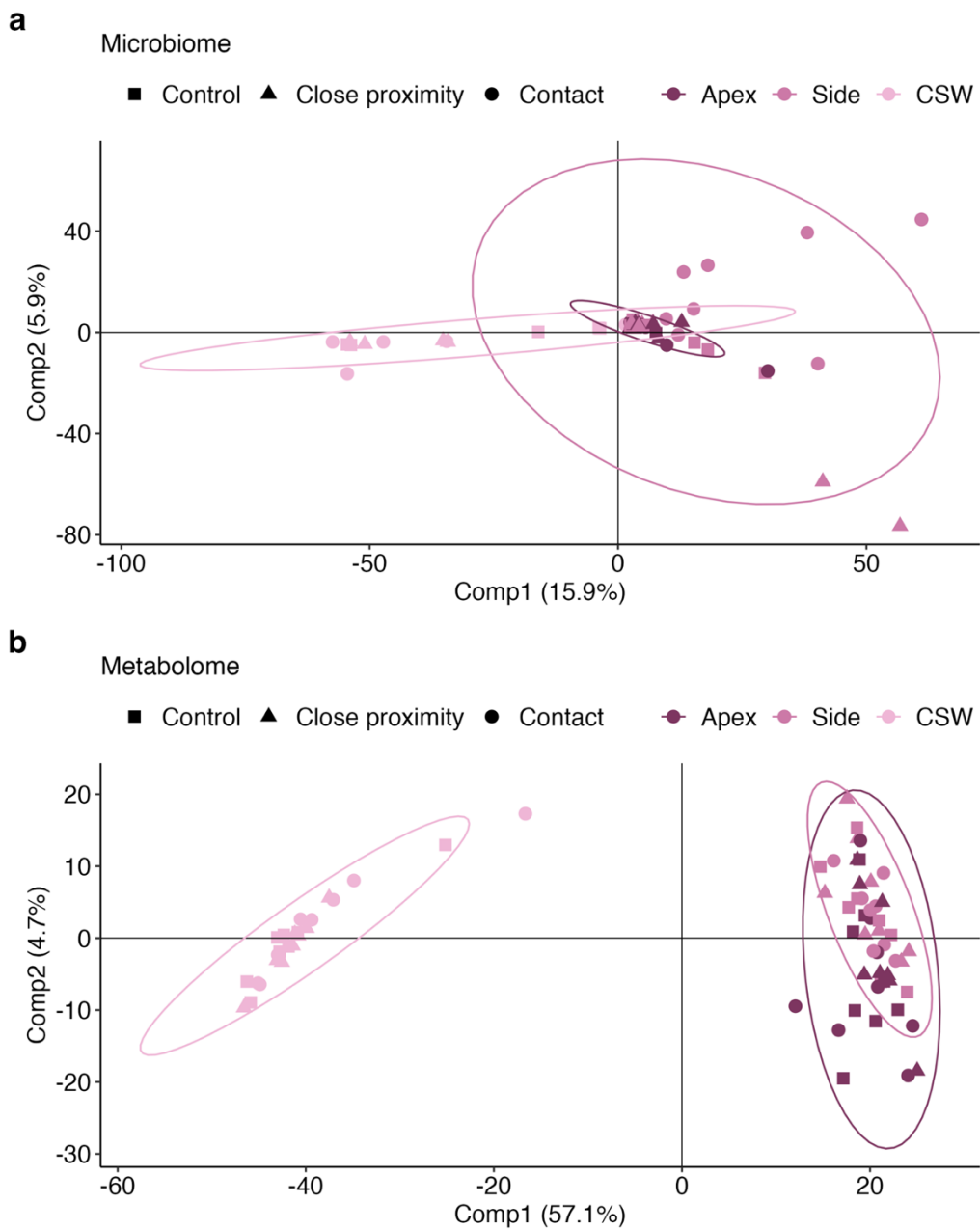
c. Coral seawater sampling



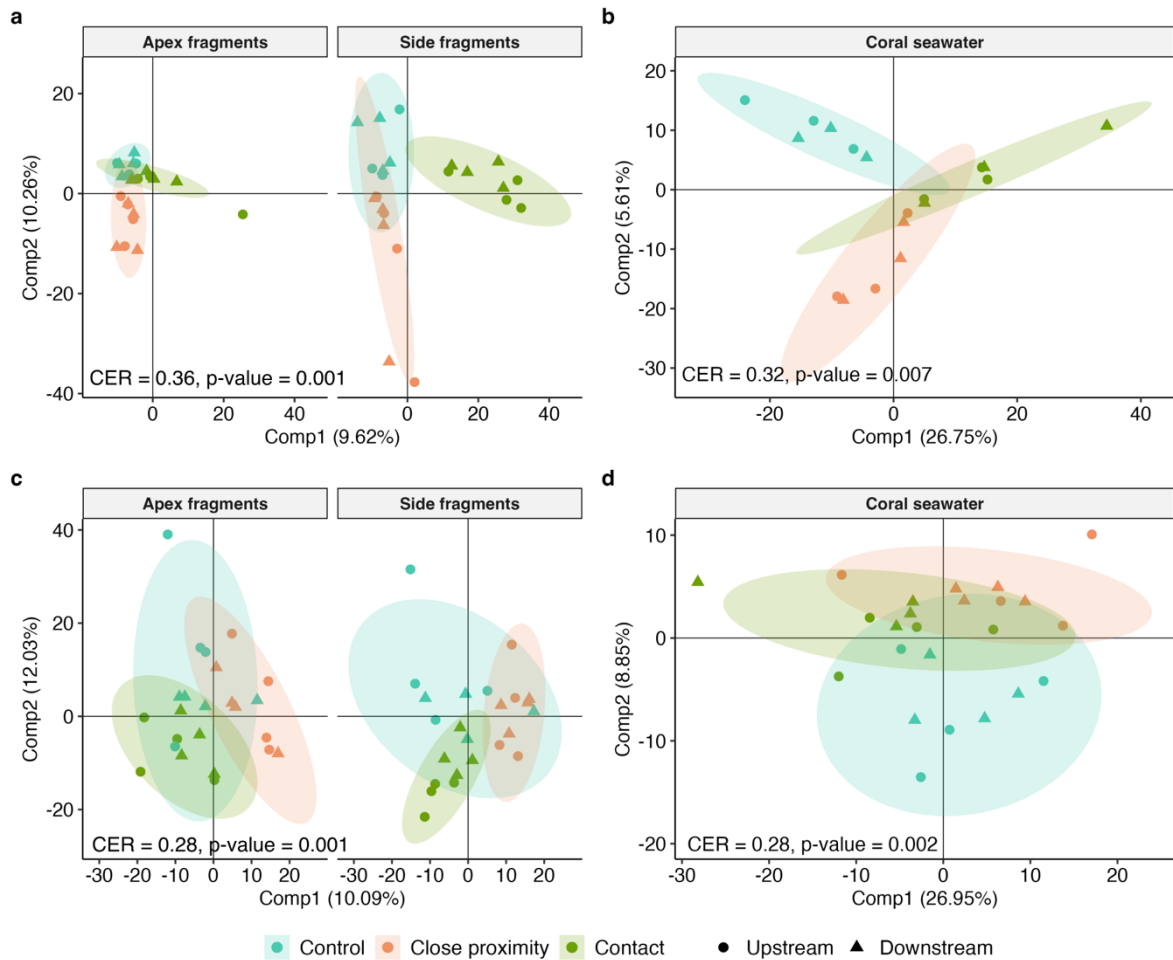
Supplementary Figure 1. Experimental design. Coral colonies of *Pocillopora acuta* were subjected to (a) three interaction types: contact with *Dictyota bartayresiana*, close proximity (2 cm) with *Dictyota* and control (without algae). One colony was placed upstream and a second downstream of the algal treatment. Each treatment combination was randomized in a block design and replicated four times. Two types of samples were collected: (b) coral fragments at the apex and the side of the colony and (c) near-surface coral seawater (CSW < 1 cm from the surface) for the characterization of their microbiome and metabolome.



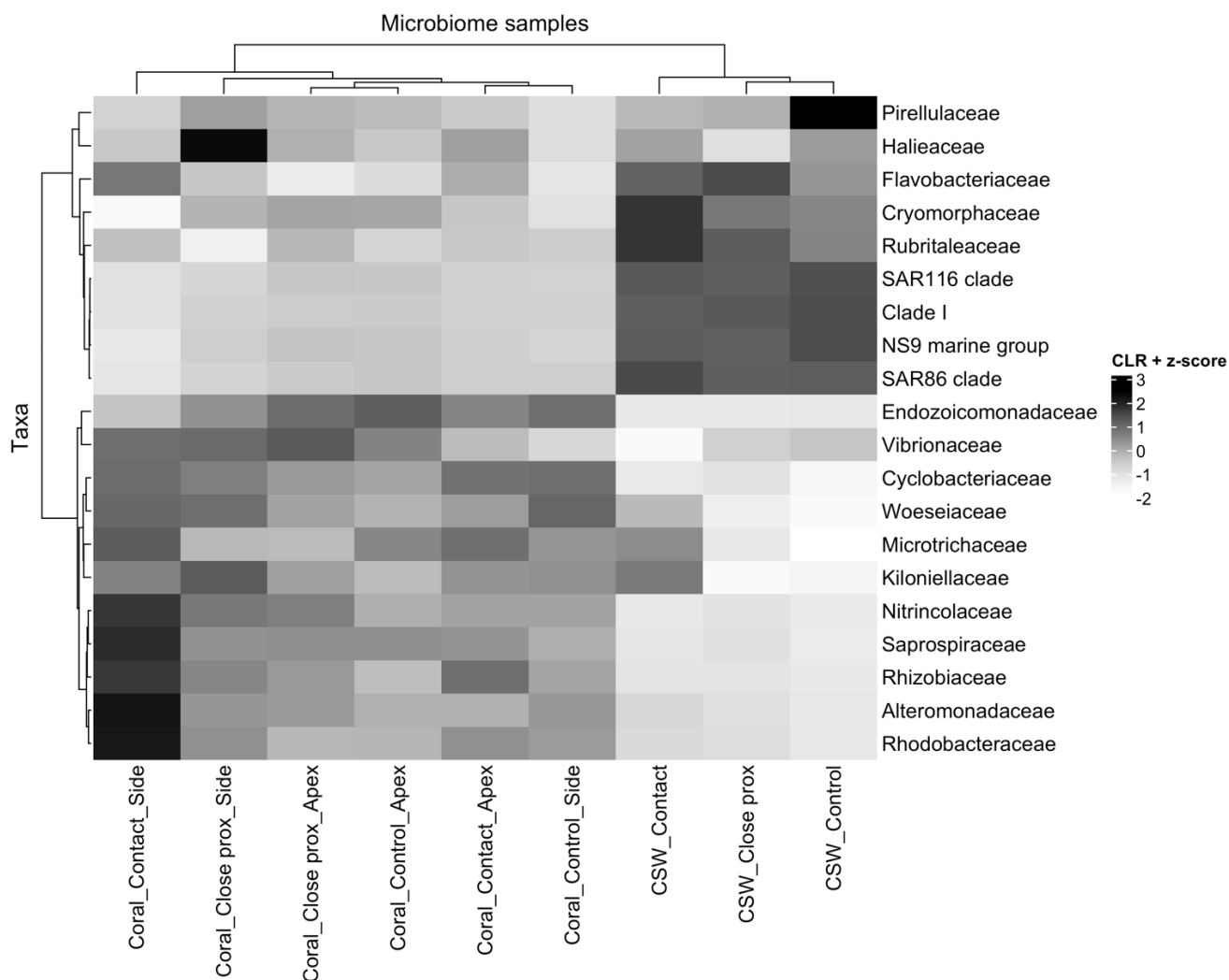
Supplementary Figure 2. Coral damage in direct contact. Examples of *Pocillopora acuta* colonies exposed to direct contact with *Dictyota bartayresiana*. Colonies 207A and 212A were placed upstream the algal patch, while colonies 207B and 212B were placed downstream. At the end of the 3 months, all colonies in contact presented signs of necrosis, algal overgrowth and bleaching at the closest interaction zone.



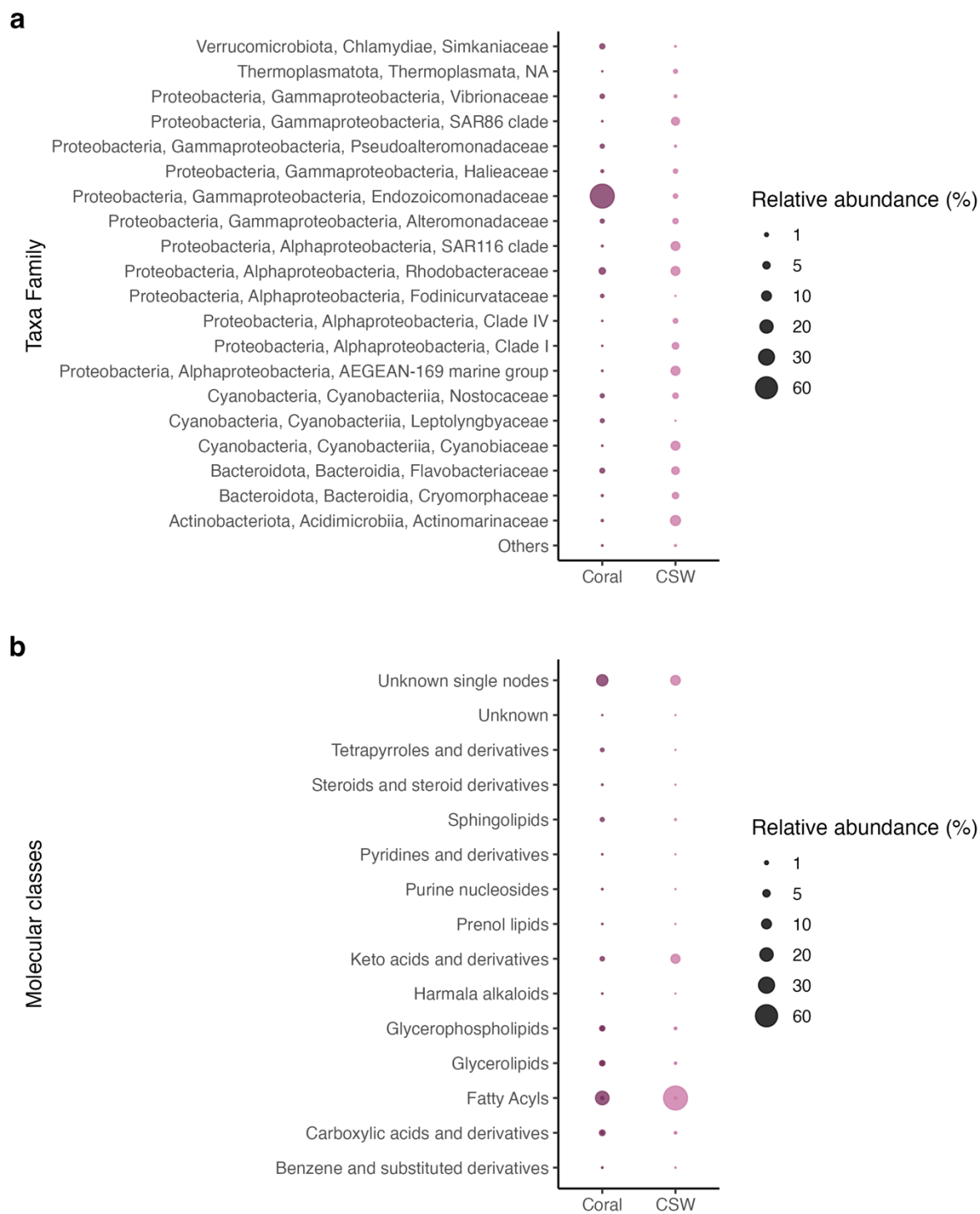
Supplementary Figure 3. PCA score plots of a. microbiome and b. metabolome. Samples are colored according to sampling position and type (i.e., apex and side fragments and coral seawater). Point shapes correspond to the type of interaction: control, close proximity (2 cm away) and contact.



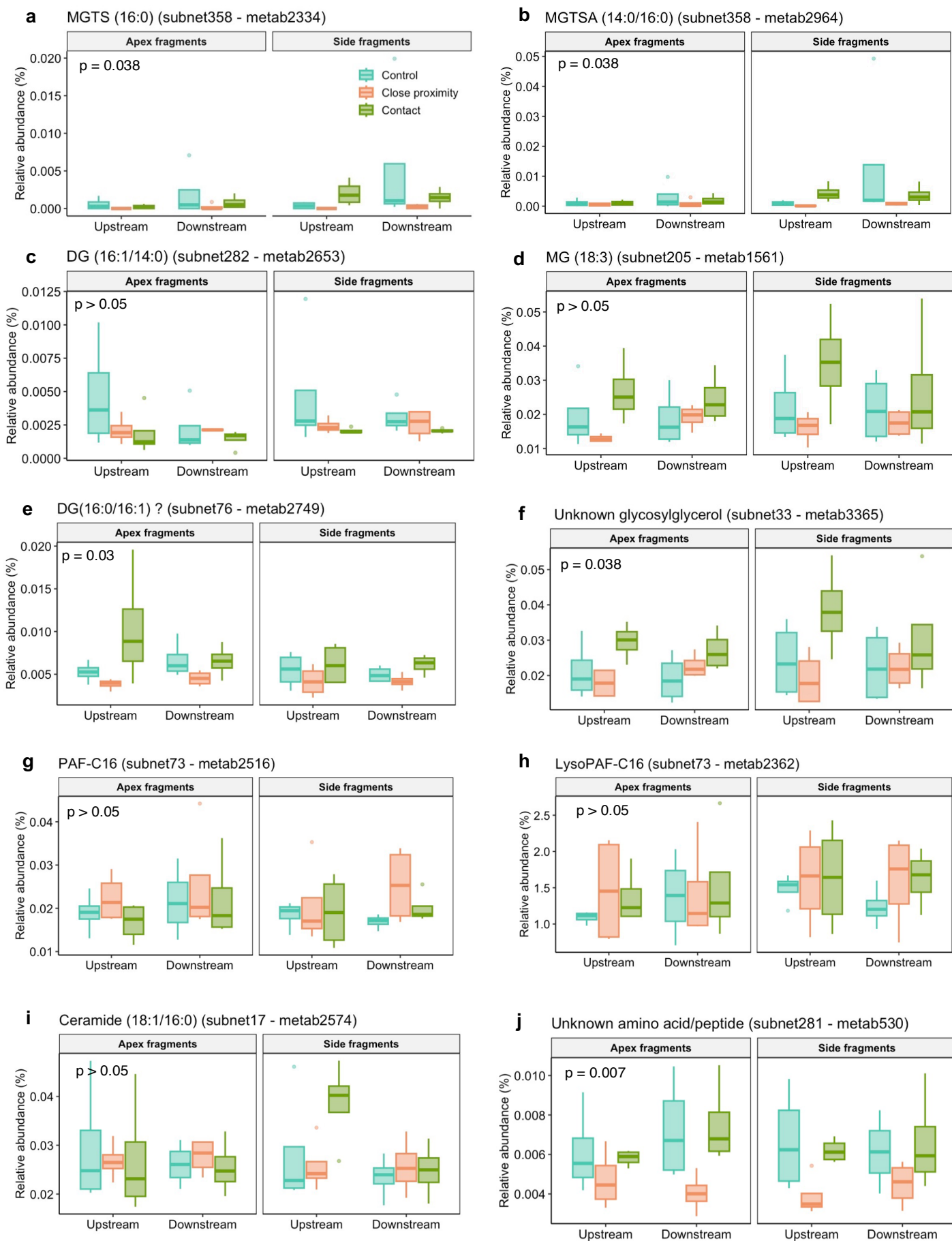
Supplementary Figure 4. Compositional differences of microbiome and metabolome driven by algal interaction type. PLS-DA (supervised ordination) score plots performed on **a.** coral and **b.** CSW metabarcoding data as well as on **c.** coral and **d.** CSW metabolomic data (only MS1 features with MS2 fragmentation data). Analysis were validated by a permutation test based on cross-model validation, the CER represents the proportion of misclassification of samples in their groups and a p-value < 0.05 indicates that the clustering was not obtained by chance alone. Ellipses are 95% data ellipses.



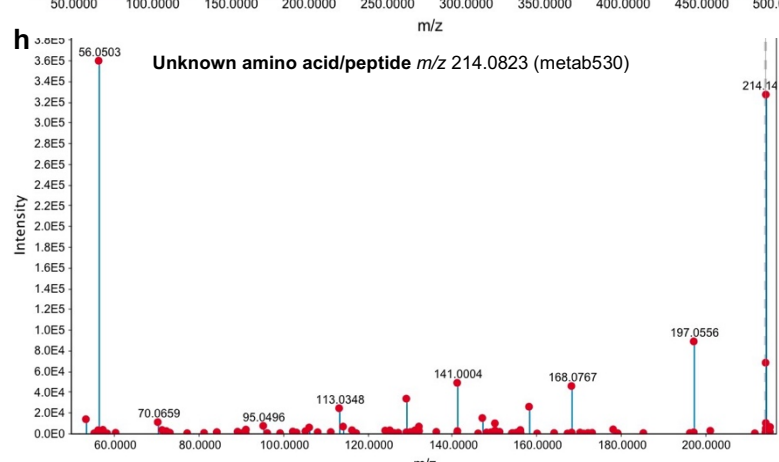
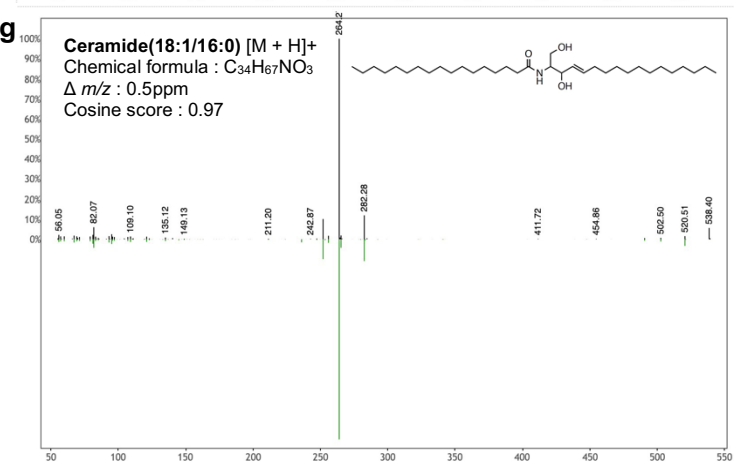
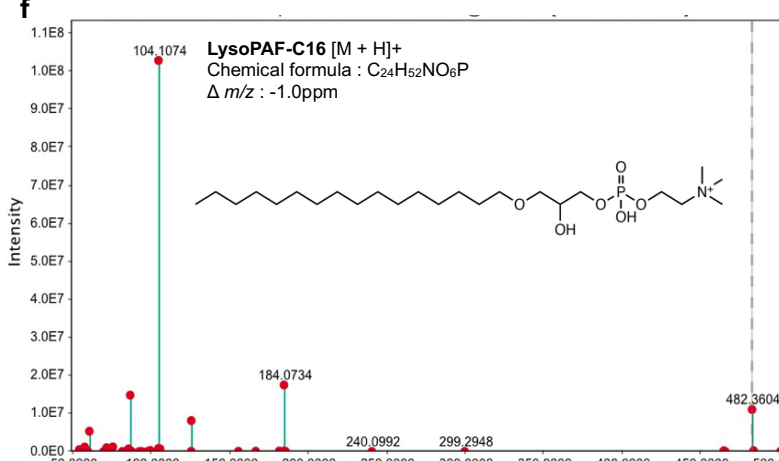
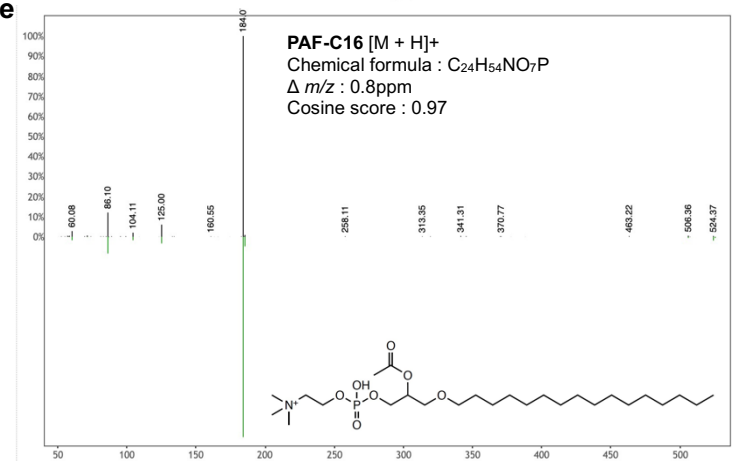
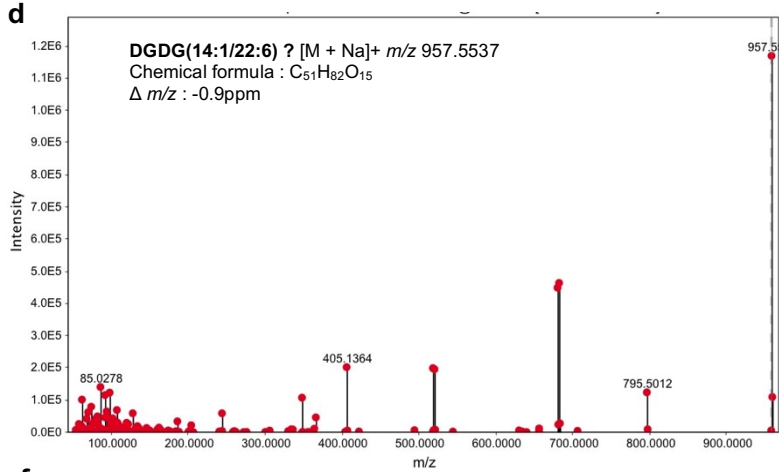
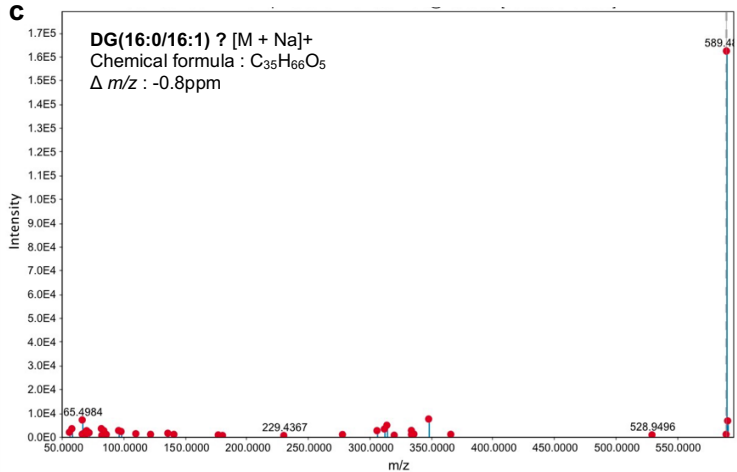
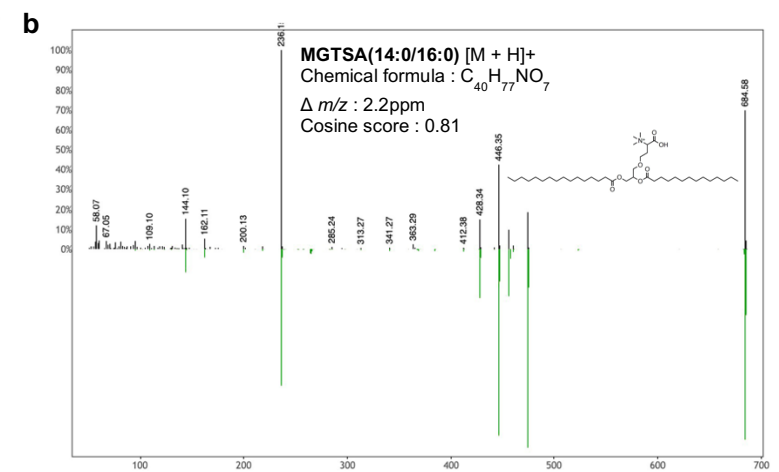
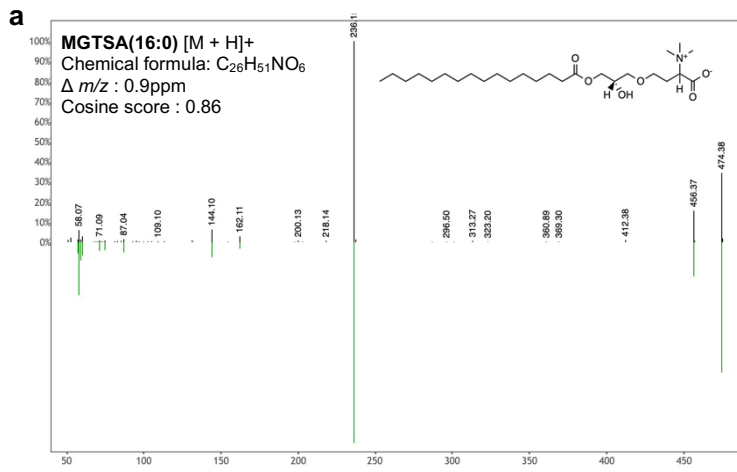
Supplementary Figure 5. Discriminant microbial families. Heatmap representing the mean CLR-transformed abundances of the top 20 microbial families explaining microbiome changes relative to interaction type in coral and near-surface coral seawater (CSW) samples. Due to the weak effect of colony position (up vs. downstream) on microbiome composition (Fig. 4.2), we showed only the abundance of microbial families as a function of the algal interaction type and sampling location. Euclidian distances and Ward's minimum variance method were used for heatmap construction and clustering. Data was scaled by mean-centering and dividing by the standard deviation.



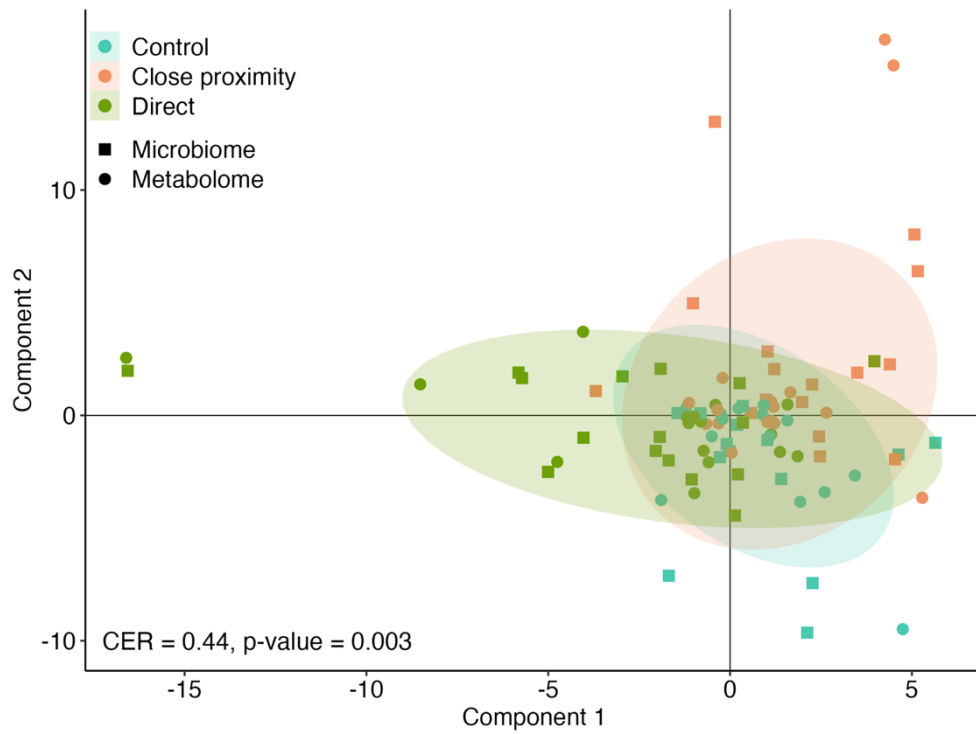
Supplementary Figure 6. a. Microbial community composition of dominant bacterial phyla and families for coral and near-surface coral seawater (CSW) samples. Only the 20 most abundant taxonomic levels are shown. **b.** Summed mean percentage of the total peak area for each molecular classes across the 43 subnetworks of interests.



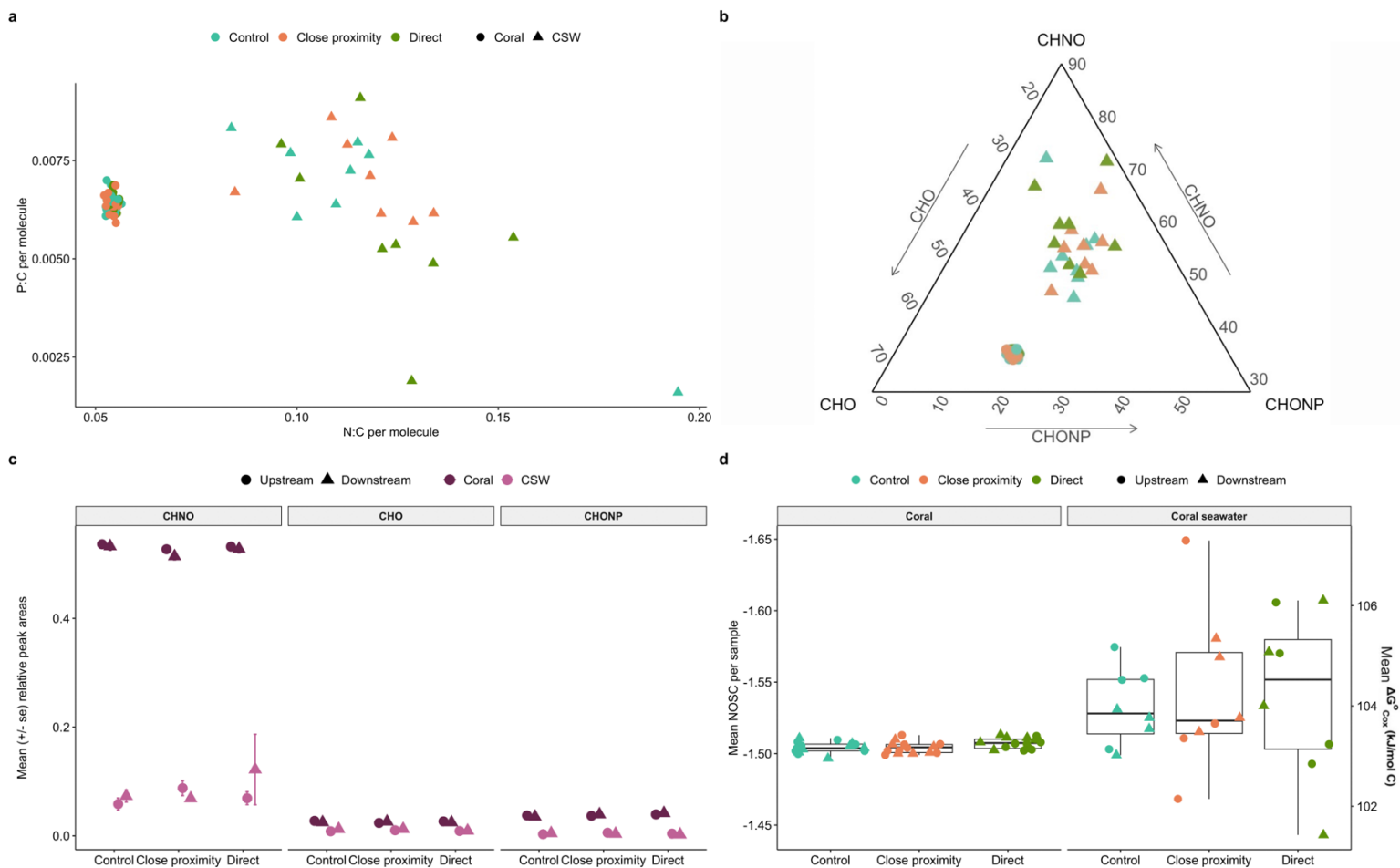
Supplementary Figure 7. Relative abundance (%) of discriminative features shown in Figure 4 and putative annotation of compounds from the coral metabolome. Abundances were compared between interaction types regardless sampling location (i.e., apex and side fragments) by non-parametric ANOVA on ranks as assumptions of normality and homoscedasticity were not met. p-values were FDR-adjusted.



Supplementary Figure 8. MS/MS spectra and mirror MS/MS in case of a GNPS library match of significantly differentially abundant features and immunity compounds. Putative compounds formulas have been generated by SIRIUS, the exact positions of desaturations are uncertain. The cosine score expresses the spectral similarity with the library match.



Supplementary Figure 9. Multiomic composition of coral samples. Score plots of the multi-block PLS-DA (DIABLO) performed on metabarcoding and metabolomic data. Analyses were validated by a permutation test based on cross-model validation, the CER represents the proportion of misclassification and a p-value < 0.05 indicates that the clustering was not obtained by chance alone. Ellipses are 95% data ellipses. Individual PLS-DA are shown in Supplementary Figure 4.



Supplementary Figure 10. Coral and near-surface coral seawater (CSW) metabolites elemental stoichiometry and NOSC. **a.** Mean N:C and P:C per molecule for each sample. **b.** Ternary plot of mean relative abundance of three stoichiometric patterns for each sample. **c.** Mean features relative abundance of three stoichiometric patterns. **d.** Mean NOSC (nominal oxidation state of carbon) and Gibbs free energy of carbon oxidation ($\Delta G^{\circ}_{\text{Cox}}$) in each sample. NOSC and $\Delta G^{\circ}_{\text{Cox}}$ were calculated of each molecule then mean within each sample.

5.3. Supplementary Tables

Supplementary Table 1. Number of ASVs and reads from the 16S rDNA metabarcoding data and MS1 features from untargeted metabolomics (LC-MS/MS) in each sample.

sample	nb_asv	nb_read	nb_msl	treatment	zone	position	replicate	colony
DBL_SP10	1107	292597	591	contact	#N/A	downstream	rep2	207B
DBL_SP11	818	257428	611	control	#N/A	upstream	rep2	208A
DBL_SP12	269	123919	656	control	#N/A	downstream	rep2	208B
DBL_SP13	829	386872	578	contact	#N/A	upstream	rep3	209A
DBL_SP14	480	236265	516	contact	#N/A	downstream	rep3	209B
DBL_SP15	753	281560	558	close prox	#N/A	upstream	rep3	210A
DBL_SP16	696	355619	500	close prox	#N/A	downstream	rep3	210B
DBL_SP17	779	321218	542	control	#N/A	upstream	rep3	211A
DBL_SP18	805	321178	606	control	#N/A	downstream	rep3	211B
DBL_SP19	631	280761	509	contact	#N/A	upstream	rep4	212A
DBL_SP20	34	774	566	contact	#N/A	downstream	rep4	212B
DBL_SP21	127	64844	644	control	#N/A	upstream	rep4	213A
DBL_SP22	104	47027	589	control	#N/A	downstream	rep4	213B
DBL_SP23	36	802	633	close prox	#N/A	upstream	rep4	214A
DBL_SP24	56	18907	615	close prox	#N/A	downstream	rep4	214B
DBL_SP7	490	215088	538	close prox	#N/A	upstream	rep2	206A
DBL_SP8	494	177069	525	close prox	#N/A	downstream	rep2	206B
DBL_SP9	41	1052	682	contact	#N/A	upstream	rep2	207A
P1	162	56710	1636	contact	apex	upstream	rep1	203A
P11	327	93717	1654	control	apex	downstream	rep1	205B
P12	152	88160	1674	control	side	downstream	rep1	205B
P13	273	121663	1600	close prox	apex	upstream	rep2	206A
P14	372	80583	1667	close prox	side	upstream	rep2	206A
P15	247	119959	1656	close prox	apex	downstream	rep2	206B
P16	1097	111562	1685	close prox	side	downstream	rep2	206B
P17	224	94288	1680	contact	apex	upstream	rep2	207A
P18	516	92113	1680	contact	side	upstream	rep2	207A
P19	223	70984	1611	contact	apex	downstream	rep2	207B
P2	1149	123680	1667	contact	side	upstream	rep1	203A
P20	639	143040	1667	contact	side	downstream	rep2	207B
P21	211	81311	1671	control	apex	upstream	rep2	208A
P22	944	126378	1687	control	side	upstream	rep2	208A
P23	162	70442	1634	control	apex	downstream	rep2	208B
P24	181	91293	1695	control	side	downstream	rep2	208B
P25	903	145726	1688	contact	apex	upstream	rep3	209A
P26	711	241048	1678	contact	side	upstream	rep3	209A
P27	220	66755	1675	contact	apex	downstream	rep3	209B
P28	597	174299	1627	contact	side	downstream	rep3	209B
P29	353	96977	1676	close prox	apex	upstream	rep3	210A
P3	429	81678	1637	contact	apex	downstream	rep1	203B
P30	198	88947	1675	close prox	side	upstream	rep3	210A
P31	164	87010	1661	close prox	apex	downstream	rep3	210B
P32	232	83670	1624	close prox	side	downstream	rep3	210B
P33	128	61407	1685	control	apex	upstream	rep3	211A
P34	152	93403	1678	control	side	upstream	rep3	211A
P35	203	108961	1681	control	apex	downstream	rep3	211B
P36	666	121535	1671	control	side	downstream	rep3	211B
P37	173	89474	1691	contact	apex	upstream	rep4	212A
P38	1642	193087	1697	contact	side	upstream	rep4	212A
P39	98	64225	1685	contact	apex	downstream	rep4	212B
P4	390	60308	1662	contact	side	downstream	rep1	203B
P40	1114	174104	1693	contact	side	downstream	rep4	212B
P41	270	79779	1620	control	apex	upstream	rep4	213A
P42	195	109795	1677	control	side	upstream	rep4	213A
P43	114	73086	1672	control	apex	downstream	rep4	213B
P44	615	136097	1695	control	side	downstream	rep4	213B
P45	122	59164	1677	close prox	apex	upstream	rep4	214A
P46	110	69742	1697	close prox	side	upstream	rep4	214A
P47	540	119198	1683	close prox	apex	downstream	rep4	214B
P48	124	88015	1715	close prox	side	downstream	rep4	214B
P5	206	76973	1638	close prox	apex	upstream	rep1	204A
P6	1414	179596	1674	close prox	side	upstream	rep1	204A
P7	437	61547	1643	close prox	apex	downstream	rep1	204B
P8	204	46529	1632	close prox	side	downstream	rep1	204B

Supplementary Table 2. Analysis of Variance comparing the alpha diversity (Shannon's index) of microbiome and metabolome samples that were then assigned to different combinations of algal interaction type (contact, close proximity vs. control), sampling location (apex vs. side) as appropriate, and colony position (up vs. downstream of algae). ANOVA were independently run on coral and associated near-surface coral seawater (CSW) samples. Significant p-values (< 0.05) are in bold.

Source	df	Microbiome			Metabolome		
		MS	F	<i>p-value</i>	MS	F	<i>p-value</i>
1. Coral							
Interaction type (Int)	2	3.71	3.20	0.053	9.6E-4	0.38	0.68
Sampling location (Loc)	1	6.18	5.34	0.027	8.1E-5	4.01	0.077
Colony position (Pos)	1	1.01	0.87	0.357	1.2E-4	0.49	0.431
Int x Loc	2	2.01	1.73	0.191	6.6E-6	0.03	0.888
Int x Pos	2	0.96	0.83	0.448	1.1E-4	0.48	0.423
Loc x Pos	1	0.16	0.14	0.714	3.6E-5	0.15	0.839
Int x Loc x Pos	2	0.31	0.27	0.767	1.7E-4	0.71	0.494
Residuals	34	1.16			2.4E-4		
2. CSW							
Interaction type (Int)	2	0.28	0.69	0.523	0.07	0.74	0.495
Sampling location (Loc)	1	0.39	0.97	0.351	0.05	0.49	0.494
Int x Loc	1	0.18	0.34	0.719	0.17	1.83	0.190
Residuals	9	0.40			0.09		

Supplementary Table 3. Analysis of Variance comparing the beta dispersion of microbiome and metabolome samples that were then assigned to different combinations of algal interaction type, sampling location and colony position. ANOVA were independently run on coral and near-surface coral seawater (CSW) samples. Significant p-values (< 0.05) are indicated in bold.

Source	df	Microbiome			Metabolome		
		MS	F	<i>p-value</i>	MS	F	<i>p-value</i>
1. Coral							
Interaction type (Int)	2	604.3	3.79	0.066	119.6	2.29	0.114
Sampling location (Loc)	1	1350.2	7.03	0.015	1.2	0.02	0.885
Colony position (Pos)	1	1.28	0.01	0.937	69.7	1.34	0.258
Int x Loc	2	196.9	0.59	0.593	21.2	0.40	0.669
Int x Pos	2	46.3	0.14	0.841	87.1	1.67	0.205
Loc x Pos	1	40.8	0.12	0.792	0.9	0.02	0.900
Int x Loc x Pos	2	168.5	0.51	0.759	6.4	0.12	0.889
Residuals	36	332.8			52.1		
2. CSW							
Interaction type (Int)	2	41.15	0.35	0.698	3.02	0.12	0.891
Sampling location (Loc)	1	13.95	0.12	0.732	54.22	2.09	0.165
Int x Loc	2	4.24	0.04	0.963	39.00	1.51	0.249
Residuals	18	113.60			25.91		

Supplementary Table 4. PERMANOVA results testing the effect of algal interaction type, sampling location and colony position on microbial community and metabolome. Run independently on coral and near-surface coral seawater (CSW) samples. Significant p-values (< 0.05) are indicated in bold.

Source	df	Microbiome			Metabolome				
		R2	<i>p</i> -value	Pairwise tests	<i>p</i> -value	R2	<i>p</i> -value	Pairwise tests	<i>p</i> -value
1. Coral									
Interaction type (Int)	2	0.06	0.002	Control vs Contact Control vs Close prox Contact vs Close prox	0.009 0.186 0.013	0.08	0.001	Control vs Contact Control vs Close prox Contact vs Close prox	0.055 0.017 0.002
Sampling location (Loc)	1	0.03	0.006			0.05	0.004		
Colony position (Pos)	1	0.03	0.133			0.04	0.009		
Int x Loc	2	0.05	0.03	Contact: Apex vs Side Close prox: Apex vs Side Control: Apex vs Side Side: Control vs Contact Side: Control vs Close prox Side: Contact vs Close prox Apex: Control vs Contact Apex: Control vs Close prox Apex: Contact vs Close prox	0.003 0.257 0.132 0.004 0.261 0.001 0.642 0.947 0.625	0.02	0.991		
Int x Pos	2	0.04	0.461			0.06	0.017	Contact: Up vs Downstream Close prox: Up vs Downstream Control: Up vs Downstream Up: Control vs Contact Up: Control vs Close prox Up: Contact vs Close prox Down: Control vs Contact Down: Control vs Close prox Down: Contact vs Close prox	0.065 0.036 0.027 0.011 0.008 0.015 0.015 0.246 0.068
Loc x Pos	1	0.02	0.710			0.01	0.917		
Int x Loc x Pos	2	0.04	0.574			0.02	0.990		
Residuals	34								
2. CSW									
Interaction type (Int)	2	0.13	0.022	Control vs Contact Control vs Close prox Contact vs Close prox	0.039 0.15 0.112	0.12	0.086		
Sampling location (Loc)	1	0.06	0.117			0.04	0.592		
Int x Loc	2	0.11	0.179			0.07	0.777		
Residuals	12								

Supplementary Table 5. List of the subnetworks of interest. A total of 42 molecular networks of interests within coral and CSW (near-surface coral seawater) samples across the three interaction types (i.e. control, contact, close proximity) were selected when they had at least 3 discriminant features (VIP score > 1) and/or at least one of the top 20 most discriminant features. Mean summed relative abundance of each subnetwork corresponds to the sum of relative peak areas within each sample and averaged by sample and treatment. Putative molecular classification corresponds to the Classyfire ontology and was retrieved from MolNetEnhancer workflow (GNPS) and CANOPUS (SIRIUS).

Subnet index	Coral control	Coral close prox	Coral contact	CSW control	CSW close prox	CSW contact	Putative superclass	Putative class	Putative subclass	
-1	13,540	14,139	13,335	9,678	9,964	9,084	Unknown single nodes	Unknown single nodes	Unknown single nodes	
1	0,962	0,979	0,997	0,117	0,120	0,083	Lipids and molecules	lipid-like	Glycerophospholipids	Glycerophosphocholines
4	0,780	0,727	0,681	0,000	0,000	0,000	Lipids and molecules	lipid-like	Glycerolipids	Triradylglycerols
9	20,246	21,768	20,363	72,464	70,899	69,979	Lipids and molecules	lipid-like	Fatty Acyls	Unknown
17	1,027	1,079	1,072	0,104	0,089	0,073	Lipids and molecules	lipid-like	Sphingolipids	Ceramides
20	0,232	0,229	0,240	0,025	0,028	0,019	Lipids and molecules	lipid-like	Glycerophospholipids	Unknown
22	0,256	0,243	0,275	0,025	0,020	0,019	Lipids and molecules	lipid-like	Fatty Acyls	Fatty acid esters
28	1,654	1,612	1,564	0,048	0,045	0,025	Lipids and molecules	lipid-like	Glycerolipids	Unknown
33	0,978	0,997	1,026	0,010	0,002	0,004	Lipids and molecules	lipid-like	Glycerolipids	Glycosylglycerols
48	2,005	2,214	2,412	0,231	0,305	0,207	Lipids and molecules	lipid-like	Glycerophospholipids	Glycerophosphocholines
49	1,289	1,258	1,326	8,224	8,629	8,258	Organic acids and derivatives	Keto acids and derivatives	Medium-chain keto acids and derivatives	
53	0,053	0,059	0,060	0,002	0,003	0,001	Nucleosides, nucleotides, and analogues	Purine nucleosides	Unknown	
65	0,020	0,015	0,019	0,000	0,000	0,000	Lipids and molecules	lipid-like	Glycerolipids	Diradylglycerols
66	0,410	0,403	0,435	0,021	0,030	0,018	Lipids and molecules	lipid-like	Glycerophospholipids	Glycerophosphocholines
72	0,021	0,021	0,023	0,009	0,013	0,009	Lipids and molecules	lipid-like	Fatty Acyls	Unknown
73	0,306	0,311	0,307	0,029	0,029	0,021	Lipids and molecules	lipid-like	Glycerophospholipids	Glycerophosphocholines
76	0,009	0,007	0,011	0,000	0,000	0,000	Lipids and molecules	lipid-like	Glycerolipids	Diradylglycerols
86	0,029	0,024	0,030	0,000	0,000	0,001	Lipids and molecules	lipid-like	Fatty Acyls	Lineolic acids and derivatives
87	2,307	2,362	2,294	0,171	0,192	0,135	Lipids and molecules	lipid-like	Glycerolipids	Triradylglycerols
89	0,007	0,006	0,008	0,044	0,022	0,018	Lipids and molecules	lipid-like	Fatty Acyls	Lineolic acids and derivatives
90	2,748	2,695	2,749	0,253	0,279	0,208	Organic acids and derivatives	Carboxylic acids and derivatives	Amino acids, peptides, and analogues	
98	0,036	0,035	0,036	0,000	0,000	0,000	Organoheterocyclic compounds	Benzene and substituted derivatives	Diphenylmethanes	
101	0,021	0,024	0,021	0,000	0,000	0,000	Lipids and molecules	lipid-like	Glycerolipids	Glycosylglycerols
107	0,031	0,031	0,027	0,000	0,000	0,000	Lipids and molecules	lipid-like	Prenol lipids	Unknown
108	0,055	0,051	0,062	0,001	0,002	0,003	Lipids and molecules	lipid-like	Steroids and steroid derivatives	Ergostane steroids
113	0,286	0,375	0,303	0,004	0,015	0,003	Organic acids and derivatives	Carboxylic acids and derivatives	Amino acids, peptides, and analogues	
139	0,031	0,037	0,028	0,003	0,004	0,003	Organic acids and derivatives	Carboxylic acids and derivatives	Amino acids, peptides, and analogues	
170	0,032	0,029	0,034	0,000	0,000	0,000	Alkaloids and derivatives	Harmala alkaloids	Unknown	
205	0,032	0,027	0,042	0,000	0,000	0,000	Lipids and molecules	lipid-like	Fatty Acyls	Lineolic acids and derivatives
212	0,001	0,000	0,006	0,000	0,000	0,000	Organic acids and derivatives	Unknown	Unknown	

218	0,075	0,060	0,063	0,000	0,000	0,000	Lipids and lipid-like molecules	Glycerolipids	Triradylglycerols
239	0,025	0,023	0,028	0,000	0,000	0,000	Organoheterocyclic compounds	Pyridines and derivatives	Unknown
240	0,887	0,659	0,825	0,000	0,000	0,000	Organoheterocyclic compounds	Tetrapyrroles derivatives	and Unknown
243	0,039	0,046	0,044	0,000	0,000	0,000	Lipids and lipid-like molecules	Glycerolipids	Diradylglycerols
259	0,031	0,029	0,027	0,000	0,001	0,000	Organic acids and derivatives	Glycerolipids	Glycosylglycerols
270	0,492	0,971	0,521	0,185	0,208	0,202	Organic compounds oxygen	Fatty Acyls	Unknown
281	0,021	0,019	0,022	0,025	0,024	0,022	Organic acids and derivatives	Carboxylic acids and derivatives	Amino acids, peptides, and analogues
282	0,013	0,007	0,007	0,000	0,000	0,000	Lipids and lipid-like molecules	Glycerolipids	Glycosylglycerols
296	0,060	0,053	0,077	0,001	0,000	0,001	Lipids and lipid-like molecules	Fatty Acyls	Lineolic acids and derivatives
328	0,038	0,033	0,029	0,000	0,000	0,000	Lipids and lipid-like molecules	Glycerolipids	Triradylglycerols
358	0,016	0,002	0,008	0,000	0,000	0,000	Unknown single nodes	Glycerolipids	Triradylglycerols
475	0,000	0,000	0,000	0,000	0,000	0,000	Benzenoids	Benzene and substituted derivatives	Unknown
485	0,003	0,003	0,004	0,005	0,005	0,002	Organoheterocyclic compounds	Fatty Acyls	Fatty acids and conjugates

Supplementary Table 6. Examples of discriminant features (VIP) from **a.** coral, **b.** CSW metabolomes and **c.** microbe-metabolite network; Putative formulas and annotations are the results of the library matches obtained through the GNPS database. search and SIRIUS. Mass errors (ppm) are relative to the theoretical mass based on putative molecular formulas when available or the GNPS match otherwise.

a. Coral

<i>m/z</i>	RT (min)	Adduct	Putative formula (SIRIUS)	Mass error (ppm)	Zodiac score (%)	Nb explained peaks	Explained intensity (%)	Putative annotation	Molecular network
684.5788	21.58	[M+H] ⁺	C ₄₀ H ₇₇ NO ₇	2.2	100	37/58	91	MGTA(14:0/16:0)	358 - Glycerolipids
474.3790	12.84	[M+H] ⁺	C ₂₆ H ₅₁ NO ₆	0.9	33	25/61	88.9	MGTA(16:0)	358 - Glycerolipids
500.3945	13.39	[M+H] ⁺	C ₂₈ H ₅₃ NO ₆	-0.12	100	31/50	91.6	MGTA(18:1)	358 - Glycerolipids
446.3480	11.73	[M+H] ⁺	C ₂₄ H ₄₇ NO ₆	0.9	33	25/34	93.6	MGTA(14:0)	358 - Glycerolipids
522.3793	12.25	[M+H] ⁺	C ₃₀ H ₅₁ NO ₆	0.7	33	32/58	89.4	MGTA(20:4)	358 - Glycerolipids
611.4671	18.55	[M+Na] ⁺	C ₃₇ H ₆₄ O ₅	4.1	100	56/58	98.1	DG(16:0/18:4)	296 - Fatty acyls/Glycerolipids
335.2580	18.11	[M+H] ⁺	C ₂₁ H ₃₄ O ₃	-0.2	100	51/58	97.2	MG(18:3)	205 - Fatty acyls
589.4798	22.13	[M+Na] ⁺	C ₃₃ H ₆₆ O ₅	-0.8	100	52/58	96.7	DG(16:0/16:1)	76 - Glycerolipids
957.5537	17.67	[M+Na] ⁺	C ₅₁ H ₈₂ O ₁₅	-0.9	88.7	45/58	89.1	DGDG(14:1/22:6)	33 - Glycerolipids
799.6800	24.79	[M+Na] ⁺	C ₄₉ H ₉₂ O ₆	1.7	100	53/58	94.1	TG(16:1/16:0/14:0)	282 - Glycerolipids
902.5832	17.83	[M+NH ₄] ⁺	C ₄₇ H ₈₀ O ₁₅	-0.4	99.9	55/58	98.1	DGDG(32:4)	282 - Glycerolipids
561.4515	18.79	[M+Na] ⁺	C ₃₃ H ₆₂ O ₅	4.2	100	55/58	98.1	DG(16:1/14:0)	282 - Glycerolipids
214.0823	1.15	[M+H] ⁺	C ₈ H ₁₁ N ₃ O ₄	0.3	100	19/58	62.9	L-alpha-amino acid	281 - Carboxylic acids and derivatives
524.3714	14.17	[M+H] ⁺	C ₂₆ H ₅₄ NO ₇ P	0.6	100	8/14	97.6	PAF-C16	73 - Glycerophospholipids
468.3088	11.20	[M+H] ⁺	C ₂₂ H ₄₆ NO ₇ P	0.7	100	9/34	96.6	LysoPC(14:0)	73 - Glycerophospholipids
496.3404	12.54	[M+H] ⁺	C ₂₄ H ₅₀ NO ₇ P	1.3	100	9/15	97.5	LysoPC(16:0)	73 - Glycerophospholipids
572.3714	12.80	[M+H] ⁺	C ₃₀ H ₅₄ NO ₇ P	0.6	100	9/28	97.4	LysoPC(22:4)	73 - Glycerophospholipids
520.3403	11.85	[M+H] ⁺	C ₂₆ H ₅₀ NO ₇ P	1.0	100	8/21	97.2	LysoPC(18:2)	73 - Glycerophospholipids
542.3242	11.15	[M+H] ⁺	C ₂₈ H ₄₆ NO ₇ P	0.2	100	6/25	97.2	LysoPC(20:5)	73 - Glycerophospholipids
546.3557	12.29	[M+H] ⁺	C ₂₈ H ₅₂ NO ₇ P	0.5	100	7/48	97.7	LysoPC(20:3)	73 - Glycerophospholipids
482.3604	13.55	[M+H] ⁺	C ₂₄ H ₅₂ NO ₆ P	-1.0	100	13/27	97.4	LysoPAF-C16	48 - Glycerophospholipids
538.5193	21.66	[M+H] ⁺	C ₃₄ H ₆₇ NO ₃	0.5	100	28/58	90.2	Ceramide(18:1/16:0)	17 - Sphingolipids
624.6283	24.42	[M+H] ⁺	C ₄₀ H ₈₁ NO ₃	-2.7	100	39/58	91.8	Ceramide(40:0;O2)	17 - Sphingolipids
377.3198	16.18	[M+H] ⁺	C ₂₈ H ₄₀	-1.3	33.3	50/59	94.6	Ergostapentaene	108 - Steroids
395.3304	16.19	[M+H] ⁺	C ₂₈ H ₄₂ O	-1.1	100	56/58	98.5	Ergostatetraenol	108 - Steroids
996.8004	24.94	[M+NH ₄] ⁺	C ₆₃ H ₁₀₂ O ₆	-1.1	100	57/58	99.1	TG(22:6/22:6/18:0)	28 - Glycerolipids
359.2191	11.24	[M+Na] ⁺	C ₂₀ H ₃₂ O ₄	-1.1	100	46/58	94.6	Long-chain fatty acid	28 - Glycerolipids
840.7069	24.52	[M+NH ₄] ⁺	C ₅₃ H ₉₀ O ₆	-0.8	100	52/59	93.7	TG(22:6/14:0/14:0)	218 - Glycerolipids
633.4515	17.88	[M+Na] ⁺	C ₃₉ H ₆₂ O ₅	4	100	58/58	100	DG(16:2/22:5)	243 - Glycerolipids
687.4981	18.23	[M+Na] ⁺	C ₄₃ H ₆₈ O ₅	3.2	100	56/58	98.4	DG(18:2/22:6)	243 - Glycerolipids
979.7706	24.95	[M+Na] ⁺	C ₆₃ H ₁₀₄ O ₆	-1.9	100	58/58	100	TG(22:6/20:3/18:0)	328 - Glycerolipids
718.5463	19.97	[M+NH ₄] ⁺	C ₃₉ H ₇₂ O ₁₀	-0.1	97.2	38/58	93.2	MGDG(16:1/14:0)	101 - Glycerolipids
298.0969	5.51	[M+H] ⁺	C ₁₁ H ₁₅ N ₅ O ₃ S	0.2	33.3	7/67	97	5'-Methylthioadenosine	53 - Purine nucleosides

Abbreviations: DGTA: putative DGTA or DGTS, DGTA: diacylglycerol-trimethyl-β-alanine DGTS: diacylglycerol trimethyl-homoserine, MGTA: putative MGTA or MGTS, MGTA: monoacylglycerol-trimethyl-β-alanine, MGTS: monoacylglycerol-trimethyl-homoserine, MG : monoacylglycerol, DG: diacylglycerol, MGDG : monogalactosyldiacylglycerol, PAF : platelet-activating factor, PC: phosphocholine, TG : triacylglycerol

Continued Supplementary Table 6

b. CSW

<i>m/z</i>	RT (min)	Adduct	Putative formula (SIRIUS)	Mass error (ppm)	Zodiac score (%)	Nb explained peaks	Explained intensity (%)	Putative annotation	Molecular network
310.2379	10.48	[M+H] ⁺	C ₁₈ H ₃₁ NO ₃	0.7	100	48/58	95.1	Unknown	485 – Fatty acyls
246.0974	1.50	[M+H] ⁺	C ₁₀ H ₁₅ NO ₆	0.8	100	51/58	93.8	Compatible with mycosporine-gly	113 – Carboxylic acids and derivatives
522.3561	13.07	[M+H] ⁺	C ₂₆ H ₅₂ NO ₇ P	1.3	100	15/42	94.5	LysoPC(18:1)	1 - Glycerophospholipids
496.3401	12.81	[M+H] ⁺	C ₂₄ H ₅₀ NO ₇ P	0.7	100	14/44	95.4	LysoPC(16:0)	1 - Glycerophospholipids
520.3398	12.06	[M+H] ⁺	C ₂₆ H ₅₀ NO ₇ P	0.1	100	18/58	96.7	LysoPC(18:2)	1 - Glycerophospholipids
312.2540	7.12	[M+H] ⁺	C ₁₈ H ₃₃ NO ₃	2.2	100	29/34	98.2	Ceramide(10:2/8:0) ?	Single node
609.4517	16.8	[M+Na] ⁺	C ₃₇ H ₆₂ O ₅	4.5	100	56/58	99.0	DG(16:1/18:4)	28 - Glycerolipids
635.4671	17.12	[M+Na] ⁺	C ₃₉ H ₆₄ O ₅	3.9	100	58/58	100	DG(16:1/20:5)	28 - Glycerolipids
738.5872	21.16	[M+H] ⁺	C ₄₃ H ₇₉ NO ₈	-0.9	33.3	46/58	91.3	Long-chain ceramide (analog GalCer(18:2/18:1))	17 - Sphingolipids
981.5546	17.32	[M+Na] ⁺	C ₅₃ H ₈₂ O ₁₅	0.007	98.5	47/58	90.8	DGDG(18:4/20:5)	33 - Glycerolipids

c. Microbe-metabolite network

<i>m/z</i>	RT (min)	Adduct	Putative formula (SIRIUS)	Mass error (ppm)	Zodiac score (%)	Nb explained peaks	Explained intensity (%)	Putative annotation	Molecular network
301.2121	1.16	[M+H] ⁺	C ₁₅ H ₂₈ N ₂ O ₄	-0.3	100	8/25	95.2	Alpha amino acid (metab1260) Lipoamide A ?	90 – Carboxylic acids and derivatives
249.1809	1.09	[M+H] ⁺	C ₁₁ H ₂₄ N ₂ O ₄	0.06	100	5/47	95.3	N-acyl-alpha amino acid (metab791)	90 – Carboxylic acids and derivatives
263.1965	1.11	[M+H] ⁺	C ₁₂ H ₂₆ N ₂ O ₄	-0.1	100	5/14	94.9	Alpha amino acid ester (metab919)	90 – Carboxylic acids and derivatives
277.1756	1.06	[M+H] ⁺	C ₁₂ H ₂₄ N ₂ O ₅	-0.7	100	8/24	95.7	N-acyl-alpha amino acid (metab1054)	90 – Carboxylic acids and derivatives
275.1963	1.13	[M+H] ⁺	C ₁₃ H ₂₆ N ₂ O ₄	-0.8	100	10/21	93.5	Valine and derivatives (metab1037)	90 – Carboxylic acids and derivatives
340.2152	8.69	[M+H] ⁺	C ₁₅ H ₃₃ NO ₅ S	-0.1	99.8	13/31	95.2	Sulfuric acid monoester (metab1593)	Single node
738.5062	20.16	[M+H] ⁺	C ₄₁ H ₇₂ NO ₈ P	-0.8	100	43/60	81.2	PE(16:0/20:5) (metab3038)	436 - Glycerophospholipids
624.6282	24.42	[M+H] ⁺	C ₄₀ H ₈₁ NO ₃	-1.2	100	39/58	91.8	Long-chain ceramide (metab2859) Caulerpicin C22 ?	Single node
284.0986	1.18	[M+Na] ⁺	C ₈ H ₁₅ N ₅ O ₅	7.2	98.9	14/26	86.7	Purine nucleosides (metab1099)	53 – Purine nucleosides
269.0879	1.21	[M+H] ⁺	C ₁₀ H ₁₂ N ₄ O ₅	-0.5	100	11/23	87.6	Purine nucleosides (metab962) N7-2'-deoxypseudoxanthosine ?	53 – Purine nucleosides
315.3006	10.77	[M+H] ⁺	C ₁₈ H ₃₈ N ₂ O ₂	-0.01	100	29/58	94.3	Amino acid (metab1401)	124 – Carboxylic acids and derivatives
312.1474	8.14	[M+H] ⁺	C ₁₂ H ₂₅ NO ₆ S	-0.4	99.8	27/40	91.9	N-acyl amine (metab1368)	212 – Carboxylic acids and derivatives
322.1684	9.13	[M+H] ⁺	C ₁₄ H ₂₇ NO ₅ S	0.4	100	35/55	95.1	N-acyl amine (metab1449)	212 – Carboxylic acids and derivatives
338.1631	8.81	[M+H] ⁺	C ₁₄ H ₂₇ NO ₆ S	-0.3	100	46/58	96.4	N-acyl amine (metab1578)	212 – Carboxylic acids and derivatives
373.3426	10.62	[M+H] ⁺	C ₂₅ H ₄₇ NO ₇	16.7	100	50/59	93.9	Glycosphingolipid (metab2333)	Single node
386.3376	10.67	[M+H] ⁺	C ₂₁ H ₄₃ N ₃ O ₃	-0.3	100	37/58	97.2	Amino acid (metab1939)	114 – Carboxylic acids and derivatives

Supplementary Table 7. Summary of discriminant and differentially abundant ASVs (indicated in bold) and those that were highly correlated (cutoff = 0.7) with metabolites (DIABLO multiblock PLS-DA) in coral samples. 16S rDNA sequences were blasted to find match in the GenBank database. Only putative identities with a sequence similarity > 95% are presented.

ASV	Nb samples	Lowest taxonomic level SILVA	Closest relative (sequence similarity)	Host or environment	Accession number (GenBank)
ASV164	14 control, 13 close prox and 8 contact	<i>Endozoicomonas</i>	<i>Endozoicomonas acroporae</i> strain Acr-14 (94.85%)	Acropora coral	NR_158127
ASV2957	3 close prox apex and 1 no contact side	<i>Rubritalea</i>	<i>Rubritalea tangerina</i> strain YM27-005 (96.49%)	Marine sea hare	NR_041582
ASV6544	4 control	<i>Muricauda</i>	<i>Muricauda marina</i> strain H19-56 (100%)	Surface organic particulate matter	NR_157633
ASV7512	4 control, 1 contact	<i>Gilvibacter</i>	<i>Gilvibacter sediminis</i> strain Mok-1-36 (97.87%)	Marine sediment	NR_041451
ASV112	10 control, 16 close prox and 14 contact	<i>Staphylococcus</i>	<i>Staphylococcus warneri</i> strain AW 25 (100%)	NA	NR_025922
ASV2763	5 contact side, 2 contact apex and 1 close prox	Rhodobacteraceae	<i>Actibacterium pelagium</i> strain JN33 (97.01%)	Seawater	NR_159242
ASV229	5 contact side, 7 contact apex, 8 close prox side, 7 close prox apex, 3 control side & 5 control apex	Corynebacterium	<i>Corynebacterium accolens</i> strain CNCTC Th1/57 (99.27%)	NA	NR_042139
ASV240	8 contact side, 4 contact apex, 4 close prox side, 1 close prox apex, 3 control side & 2 control apex	Hyphomonadaceae	<i>Hyphomonas atlantica</i> strain MCCC 1A09418 (98.51%)	Seawater	NR_178646
ASV229	5 contact side, 7 contact apex, 8 close prox side, 7 close prox apex, 3 control side & 5 control apex	Corynebacterium	<i>Corynebacterium tuberculostearicum</i> strain Medalle X (100%)	Clinical samples	NR_028975
ASV191	8 contact side, 1 contact apex, 2 close prox side, 3 close prox apex, 3 control side & 2 control apex	<i>Aestuariibacter</i>	<i>Aestuariibacter halophilus</i> strain JC2043 (96.26%)	Marine sediment	NR_025721
ASV1236	4 contact side	<i>Ruegeria</i>	<i>Ruegeria conchae</i> strain SR76 (99.5%)	NA	MF594140
ASV844	4 contact side	<i>Endozoicomonas</i>	<i>Endozoicomonas atrinae</i> strain WP70 (95.05%)	Comb pen shell	NR_134024
ASV143	4 contact side and 1 contact apex	<i>Shimia</i>	<i>Shimia isopora</i> strain SCSIO_43724 (100%)	NA	MH283808
ASV2529	4 contact side	<i>Woeseia</i>	<i>Woeseia oceani</i> strain XK5 (94.88%)	Coastal sediment	NR_147719
ASV2258	4 contact side	<i>Aestuariicella</i>	<i>Aestuariicella hydrocarbonica</i> strain SM-6 (95.08%)	Marine sediment	NR_135890
ASV3356	4 contact side	<i>Pelagicoccus</i>	<i>Pelagicoccus litoralis</i> strain H-MN57 (97.42%)	Seawater	NR_041557
ASV3768	3 contact side, 2 contact apex, 1 close prox side, 1 close prox apex	<i>Vibrio</i>	<i>Vibrio alfacensis</i> strain CAIM 1831 (99.77%)	Fish gill	NR_118129
ASV815	3 contact side	<i>Thalassotalea</i>	<i>Thalassotalea euphylliae</i> strain Eup-16 (99.06%)	Coral holobiont	NR_153727
ASV846	2 contact side, 1 contact apex	<i>Thalassotalea</i>	<i>Thalassotalea coralli</i> strain Eup a-8 (99.06%)	Coral holobiont	NR_159306
ASV175	3 contact side	<i>Thalassotalea</i>	<i>Thalassotalea montiporae</i> strain CL-22 (98.37%)	NA	NR_178359
ASV776	3 contact side	<i>Vibrio</i>	<i>Vibrio europaeus</i> strain PP-638 (98.36%)	Marine bivalves larvae	NR_146051
ASV750	3 contact side, 2 contact apex, 2 close prox side, 1 close prox apex and 1 control	<i>Vibrio</i>	<i>Vibrio mediterranei</i> strain 3-16 (99.53%)	NA	MN841923
ASV347	5 contact side, 3 contact apex, 4 close prox side, 2 close prox apex and 4 control	<i>Vibrio</i>	<i>Vibrio alginolyticus</i> strain 2015AW-0011 (100%)	NA	CP051109

Chapter 5

General discussion and research perspectives

1. Summary of main results

The accumulation of human-induced stressors, both globally and locally, have drastically altered the composition of coral reef benthic communities (Smith et al., 2016; Reverter et al., 2022). Macroalgae, benefiting from freed space by mass coral mortality, loss of herbivores and nutrient enrichment, have proliferated on many reefs worldwide, particularly on near-shore reefs (Mumby & Steneck 2008; Adam et al., 2021; Schmitt et al., 2021). The persistence of altered environmental conditions coupled with the efficiency of macroalgal competitive strategies have greatly limited the capacity of reefs to return to a coral-dominated state (Schmitt et al., 2019). Macroalgae can impair not only coral health but also recruitment success, a process essential for the replenishment of coral communities (McCook et al., 2001; Ritson-Williams et al., 2009). Detrimental competition against corals has been made evident upon contact where physical, chemical and microbial stressors act in concert causing coral tissue necrosis, bleaching and mortality (McCook et al., 2001; Rasher et al., 2011; Clements & Hay, 2023). Yet, empirical studies have stressed out the complexity of coral-algal competition by highlighting the role of waterborne allelochemicals but also algal-derived DOM fostering the growth of copiotrophic (i.e., DDAM model) and potentially harmful microbes (Smith et al., 2006; Barott & Rower, 2012; Haas et al., 2016; Evensen et al., 2019b). However, whether these proposed models of water-mediated effects translate into compromised coral health and recruitment success under natural flow conditions is uncertain.

Building on experimental approaches, *in-situ* sampling and multiomic workflow, the overarching goals of my thesis were to advance our understanding of the influence of macroalgae on the chemical and microbial composition of reef waterscapes and the extent to which these waterscapes represent a threat to coral holobionts and recruitment success (Fig. 5.1). In Chapter 2, I revealed an unprecedented small-scale structuration in the multiomic signature of reef waterscapes which varied with macroalgal abundance and across boundary layers within a single reef. Boundary layers (i.e., MBL and BBL) surrounding algal-dominated bommies harbored microbes typically associated with reef degradation and potentially cytotoxic allelochemicals (i.e., diterpenoids). Chapter 3 demonstrated a remarkable tolerance of *P. acuta* microbiome to macroalgal-induced waterscapes. In contrast, coral larvae microbiome from algal-dominated bommies was enriched in putative opportunists and depleted in beneficial microbes. My results revealed that macroalgal-induced parental and environmental effects reduced coral larval and post-settlement survival that could be linked to alterations in the larval microbiome. Finally, Chapter 4 provided evidence of water-mediated effects of

Dictyota bartayresiana under natural flow conditions at a small spatial scale (i.e., 2 cm). Contact and water-mediated interactions distinctly structured the coral microbiome and metabolome, although microbial changes were less pronounced in water-mediated interactions. Coral microbiomes were enriched in opportunistic bacteria concurrently with a loss of beneficial bacteria. Regardless of the interaction type, the relative abundance of coral metabolites suggested an adjustment of energetic reserves, potentially for meeting defense requirements.

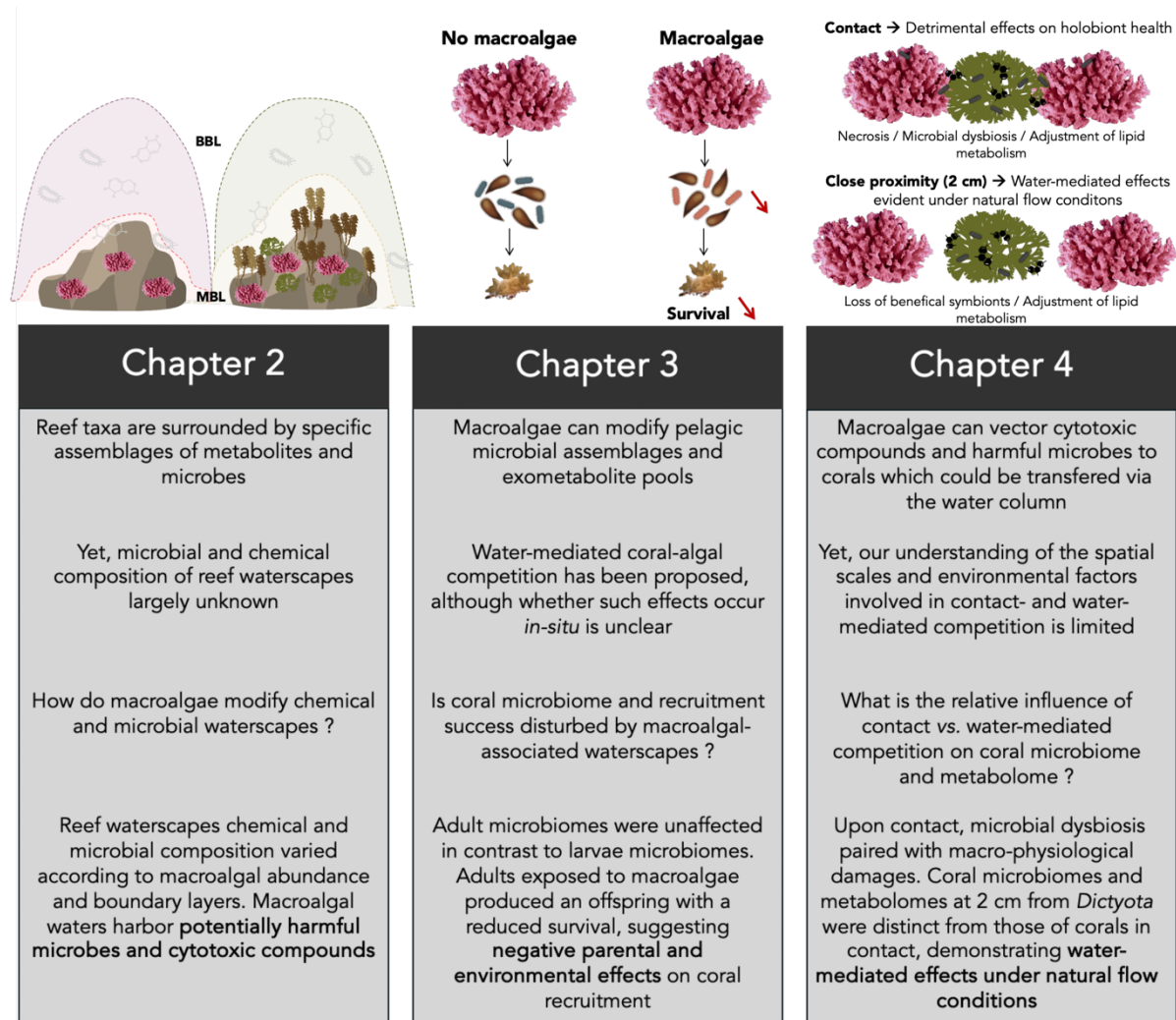


Figure 5.1 | Summary of thesis chapters. This PhD investigated the extent to which algal-associated metabolites and microbes could play a role in water-mediated competition against corals. Chapter 2 focused on the microbial and chemical composition of macroalgae-associated waterscapes. Chapter 3 investigated whether these waterscapes disrupt coral larval and adult microbiomes and recruitment success. Chapter 4 tested the influence of contact-mediated vs. water-mediated effects of *Dictyota bartayresiana* on the coral microbiome and metabolome.

Together my results pinpoint the impact of macroalgae on the microbial and chemical composition of reef waters at the scale of coral bommies (Chapter 2). While the coral adult microbiome appeared insensitive to these macroalgal-induced waterscapes, parental and environmental effects can alter the larval microbiome and reduce the offspring survival

(Chapter 3). I demonstrated that water-mediated effects can occur at very short distance from algae (i.e., 2 cm) by disturbing the coral microbiome and metabolome, although without clear detrimental consequences on coral holobiont health (Chapter 4). This thesis demonstrated that macroalgae can have a significant influence of the chemical and microbial environments on coral reefs which can lead to water-mediated competition under natural flow conditions and inhibition of recruitment success.

In the following sections, I will discuss my results in the light of the hydrodynamic context on lagoonal reefs and the ecologically relevant scales and methods under which water-mediated interactions are tested. I will then elaborate on interesting microbial and chemical patterns highlighted in this work and discuss future research avenues to further our understanding of the specific roles of macroalgal-associated microbes and metabolites. Finally, I will explain how my results can give insights into the future of macroalgal-dominated reefs in terms of reef resilience, as well as in the context of climate change and current restoration incentives.

2. Understanding water-mediated interactions through hydrodynamics

Hydrodynamics has been identified as a key factor influencing water-mediated effects of algae on corals, although the context-dependencies modulating these effects are inadequately understood (Brown & Carpenter 2015; Jorissen et al., 2016; Clements & Hay, 2023). In this thesis, we sought to improve our understanding of the water-mediated mechanisms of coral-algal competition under natural flow conditions by describing the microbial and chemical composition of reef waterscapes (Chapter 2) and of coral tissues and near-surface waters of corals upstream and downstream of algae (Chapter 4). The variability in shape and texture of the reef benthos results in extremely complex and dynamic water movements, challenging our efforts to apprehend these mechanisms (Hench & Rossman et al., 2013; Rogers et al., 2018).

Chapter 2 provided evidence of a remarkable small-scale heterogeneity in the identity and distribution of metabolites and microbes across boundary layers. However, to understand why such spatial patterns occur, we must integrate knowledge of hydrodynamics. For example, the distinction between BBLs may be counterintuitive as one might have expected a mixing due to the influence of surface currents above bommies where flow speed of 0.1-0.3 m/s had previously been measured (Hench et al., 2008; Hench & Rossman, 2013; Rogers et al., 2018). In fact, recirculation zones or eddies have been demonstrated downstream bommies, and even

above them (Hench & Rossman, 2013; Rogers et al., 2018), which may have favored the retention of benthos-derived products and associated microbes. Additionally, the macroalgal canopy can modify hydrodynamics by reducing flow velocity and increasing turbulence above canopies (Hurd, 2000; Kregting et al., 2011; Cornwall et al., 2015). Therefore, despite turbulent conditions, the structure of the reefs likely favored the local retention of organic matter around coral bommies.

In this work, we showed that specific classes of algal compounds would preferentially diffuse away from algal surfaces and that pelagic microbiome community would be structured across boundary layers. For example, we suggested that the chemical structure of lyso-form lipids would make them more polar, hence more likely to be advected in the water column. While our results demonstrated their movement across boundary layers, future research will benefit from modelling approach to advance our understanding of the spatial variability in the movement of waterborne organic matter. In a recent study, physical (e.g., velocity, diffusion coefficient) and biological (e.g., metabolic rates, microbe growth rate) data were combined to build a 3D-model to visualize the movement of dissolved compounds (Candy et al., 2023). Their study revealed *in-situ* variations in DO concentrations with hypoxic conditions in specific localities on the reef, often downstream of bigger structures with reduced flow speed and higher retention times (Candy et al., 2023). In another study, flow speed and dissolution rate of clod cards were reduced on the downstream sides of bommies compared to the upstream sides (Brown & Carpenter, 2015). Consequently, depending on specific locations, sessile organisms can be exposed to highly variable hydrodynamic and biogeochemical conditions, thereby influencing competitive outcomes. Indeed, corals located in zones that can experience hypoxic conditions and accumulation of microbes might suffer from mortality and decreased competitive advantage when faced with algae (Smith et al., 2006; Wangpraseurt et al., 2012; Haas et al., 2014). In Chapter 3, although coral colonies were transplanted on the top half of the bommies, they are likely to have experienced distinct flow conditions (e.g., velocity, turbulence) depending on their respective position on the bommies. Corals placed on the downstream side of bommies or downstream reef formations on the bommies have likely experienced lower flow speed and higher retention of organic matter. Therefore, 1) which physical, biological and chemical properties influence the diffusion of microbes and metabolites and 2) how local topography interacts with algal proximity to influence the exposition of sessile organisms are valuable questions to consider in future research for investigating water-mediated mechanisms of coral-algal competition. Interdisciplinary research combining physics, advanced modelling, biology and chemistry will be essential to tackle these aspects.

Water-mediated effects on corals are highly dependent on interaction context. For example, corals downstream of algae will be more exposed to algal-associated metabolites and microbes, particularly under low flow conditions (Barott & Rowher, 2012; Brown & Carpenter, 2015; Jorissen et al., 2016). Chapter 4 specifically aimed at investigating the context-dependencies under which effective water-mediated competition occurs, particularly the distance from the algae and coral colony position relative to the dominant current direction. By performing this experiment on sand patches, we avoided the confounding effects that reef geometry would play on the advection of algal-associated microbes and metabolites. At 2 cm from *Dictyota bartayresiana*, I found little evidence that downstream corals were more impacted than upstream corals, contradicting aforementioned studies. In addition, the chemical and microbial diversity and composition of near-surface coral waters did not vary with colony position, suggesting weak residency of algal-derived matter around coral surfaces (Chapter 4). However, the lack of effect of hydrodynamics in this study cannot be generalized as reef hydrodynamics vary not only spatially, but also temporally. In the north coast of Mo'orea, flow velocities are higher during the austral summer (November-April) than the austral winter (May-October). The experiment of Chapter 4 took place in January during the austral summer where flow velocities were highest. High flow velocities can result in thin boundary layers and short retention times (Brown & Carpenter, 2015; Jorissen et al., 2016). Beyond seasonal influence, the dominant current may have also varied in direction and velocity throughout the day according to tides and swell conditions (Hench et al., 2008; Davis et al., 2021). In addition, hydrodynamics can interact with algal morphologies. For example, turf can favor the retention of matter at the interaction interface in both high and flow conditions in contrast to *Turbinaria ornata* (Brown & Carpenter, 2015). Turbulent flows favored by high velocity and *Dictyota* thallus may have similarly exposed corals to algal-derived products regardless of their positions. Altogether, my work pinpoints the need for additional data relative to hydrodynamics such as flow velocity, water movement and retention times to better determine the specific contexts under which water-mediated effects can be detrimental to corals. Thorough field studies under various hydrodynamic conditions testing different combinations of factors relative to algal type and spatial scales will be particularly valuable.

3. Ecological relevance of water-mediated competition

Two main models have been proposed in coral-algal water-mediated competition: the DDAM model and the toxicity of hydrophilic allelochemicals (Smith et al., 2006; Barott & Rohwer, 2012; Haas et al., 2016; Morrow et al., 2017; Evensen et al., 2019b). Yet, whether these models constitute reinforcing feedback processes by compromising holobiont health and recruitment success is still unclear. For example, *in-situ* support for the DDAM model has been essentially based on analysis of reef water microbiomes, but not to coral microbiomes (Nelson et al., 2013; Haas et al., 2016; Frade et al., 2020). With chapters 2 and 3, we contributed to fill this knowledge gap by showing alterations in coral larval microbiomes and inhibition of coral recruitment success in response to macroalgal-induced waterscapes. Chapter 2 demonstrated that algal-associated waterscapes were enriched in copiotrophic and potentially detrimental microbes, in alignment with DDAM-supporting studies (Nelson et al., 2013; Wegley Kelly et al., 2014; Haas et al., 2016; Walsh et al., 2017; Frade et al., 2020). While the DDAM model was demonstrated on a global scale, our results showed that some variability may exist within a single reef according to macroalgal abundance (Chapter 2). In addition, putative cytotoxic compounds such as diterpenoids and sesquiterpenoids were detected in algal MBLs and BBL (Chapter 2). On coral bommies, the presence of these microbes and metabolites in reef waters did not affect the microbiome diversity, variability and composition of coral adults (Chapter 3). In contrast, we detected water-mediated effects on the coral adult microbiome composition at 2 cm from the allelopathic alga *Dictyota bartayresiana* (Chapter 4). To my knowledge, only one other field study found a response of the coral microbiome without algal contact and reported a more diverse and variable microbiome as macroalgal abundance increased (Briggs et al., 2021). The lack of consistent results might be due to 1) variable distances between algae and corals and 2) variable identities of the closest algae.

In the DDAM model, it is stipulated that exuded macroalgal DOC supports higher abundance of copiotrophic and virulent microbes and lower oxygen concentrations (Haas et al., 2010; 2016; Frade., et al 2020). Yet, hypoxic zones on reefs have been demonstrated at local scale only, either in specific reef localities (Candy et al., 2023) or at coral-algal interface (Barott et al., 2012; Jorissen et al., 2016). Therefore, it is likely that microbes would concentrate near algal surfaces where DOC emerges rather than somewhere else in the water column. In chapters 2 and 4, bulk measurements of DOC and DO within boundary layers would have helped to clarify the scales at which these effects occur (Wegley Kelly et al., 2022; Candy et al., 2023). Algae such as *Turbinaria ornata* or turf release labile and energy-rich exudates which select for

pathogenic bacterial strains (Nelson et al., 2013; Wegley Kelly et al., 2022). In Chapter 2, the microbiome and metabolome of algal MBLs was species-specific, supporting the selective pressure of algal exudates on microbial communities in alignment with previous studies (Nelson et al., 2013; Walsh et al., 2017; Wegley Kelly et al., 2022). Therefore, the DDAM model may be more relevant to these algae and particularly detrimental to corals at small distance.

Concerning allelochemicals, studies found that lipid-soluble algal extracts applied on coral surfaces were only active at the contact zone, suggesting that water-soluble compounds did not impact other regions of the colonies (Rasher & Hay, 2010; Vieira et al., 2016a). In contrast, hydrophilic fractions disturbed coral physiology, microbiome and recruitment to a greater extent compared to organic fractions, suggesting their diffusion and bioactivity in the water (Vieira et al., 2016a; Morrow et al., 2017; Evensen et al., 2019b; Page et al., 2023). However, such effects may have been overestimated. For example, water-soluble extracts were applied directly to coral surfaces (Vieira et al., 2016a; Morrow et al., 2017). In addition, extraction protocols may have recovered compounds that would not be normally available under natural conditions (Paige et al., 2023). The alga *Dictyota bartayresiana* is known for its production of cytotoxic allelochemicals (Rasher et al., 2011; Shearer et al., 2012; Longo & Hay, 2017). In Chapter 2, the detection of diterpenoids in the MBL of this species suggests that this alga might be more prone to compete via waterborne chemical effects. Yet, at the scale of coral bommies, we detected no significant changes in the microbiome of coral adults (Chapter 3). On bommies, coral distances from the closest algae were not recorded and these might have been greater than 2 cm, distance at which water-mediated effects were demonstrated on coral microbiomes and metabolomes (Chapter 4). Varying effects across distances could be due to a concentration-dependent effect where concentration threshold will determine compound potency and/or to a cocktail effect where compound bioactivity increases in the presence of others (Slattery & Lesser, 2014). While this work could not distinguish between the effects of hydrophilic allelochemicals, from bacterial invasion and local hypoxia, my results showed that these effects impact coral adult microbiomes at a small (i.e., 2 cm) spatial scale (i.e., comparing results from chapters 3 and 4). However, there is still major knowledge gaps to be addressed regarding the species-specific strategies and associated spatial scales at which macroalgae may effectively compete with corals.

The life cycle of corals has the particularity to comprise both a pelagic phase and a benthic phase. Each of these steps can be impacted by water-mediated effects at different scales from the large scale when larvae are pelagic (i.e., within the upper water column (i.e., BBL) and wider) to the near-benthos scale when larvae probe the substratum to settle on and as a coral

recruit. Coral larvae can remain planktonic for more than a month (Harii et al., 2002; Graham et al., 2008). In Chapter 2, we support the idea that larvae could be exposed to negative chemical and microbial conditions as they swim across boundary layers dominated by algal assemblages. Our findings in Chapter 3 indicated that water from algal-dominated BBL reduced larval survival by 6% relative to that of algal-removed BBL. Similarly, waters collected on macroalgal-dominated reefs strongly decreased larval survival of *Pocillopora damicornis* compared to water from algal-dominated bommies in Fiji, yet the sampled boundary layer and the identity of nearest sessile organisms were not specified (Beatty et al., 2018). Macroalgal waters can have more nuanced effects on coral larvae than lethal vs. non-lethal effects by altering their capacity to find a suitable substrate (Antonio-Martínez et al., 2020). Larvae have limited movement capacities, ranging essentially from upward and downward active swims with direction switching, which can be triggered in response to positive and negative waterborne cues (Koehl et al., 2007; Takeda-Sakazume et al., 2022). For example, larvae may be able to avoid algal-dominated patches within shifted reefs (Johns et al., 2018). In our settlement experiment on the effect of macroalgal-induced environment (Chapter 3), using MBL as tested water could have been a useful addition as we would have remained at the same spatial scale as the tiles. Algal MBLs could have decreased larval settlement on tiles from algal-dominated bommies due to a higher concentration of negative cues. In this context, promising avenues for future research are to investigate the sensory capabilities and behavioral responses of coral larvae to identify the chemical and microbial cues which they respond to (Fig. 5.2). Choice flumes might be particularly adequate to test underlying hypotheses of avoidance vs. preference of waters collected at different distances from macroalgae, as well as waters primed with specific cues (e.g., diterpenoids). However, devices and protocols for such experiments need to follow good practices to ensure data quality (Jutfelt et al., 2017).

To conclude, our experimental approach under natural flow conditions and using water collected from the field allowed to demonstrate water-mediated effects of macroalgae on coral adults and early life stages. Yet, the relative roles of macroalgal-associated microbes and metabolites remain to be investigated. It appears now essential to estimate natural concentrations of polar and apolar exometabolites and pelagic microbes across boundary layers associated to distinct algal species (Fig. 5.2). Laboratory-based studies are needed to specifically test the effects of natural concentrations on corals. Such studies could help to establish dose-responses and determine whether these responses are ecologically relevant under *in-situ* concentrations. Proposed mechanisms will have to be validated in the field taking into

account additional environmental factors (e.g., hydrodynamic context) and the transport properties of microbes and metabolites under which water-mediated effects are investigated.

4. From “who is there?” to “what are they doing?”

4.1. Notable microbes and metabolites patterns

This thesis research relied on experimental approaches where I specifically manipulated the presence *vs.* absence of macroalgal assemblages (chapters 2 and 3) and the type of coral-algal interaction (Chapter 4). Doing so, I could directly link my observations to the specific conditions that were tested. While microbial and chemical compositional changes were the result of these experimental manipulations, we still have little knowledge about the mechanisms behind the observed patterns. In this work, I described compositional changes and co-occurrences of microbes and metabolites revealing “who is there” participating in baseline knowledge of key biological components involved in reef ecosystem health.

Reef water microbiomes have disproportionately been more investigated than their chemical counterparts. As such, Chapter 2 provides critical knowledge about not only the identity of microbes and metabolites within reef waters but also their spatial variability. Through data integration, I revealed microbe-metabolite correlations that could represent key targets for future research. For example, in algal MBLs, several metabolites with antibacterial and antifouling properties were negatively correlated with microbial genera: e.g., Diterpenoid – *XY-R5* and SQDG – *Citreicella* (Chapter 2). Interestingly, the genus *Citreicella* was depleted in the microbiome of larvae brooded by parents from algal-dominated bommies (Chapter 3). In addition, organooxygen and organonitrogen compounds were positively correlated with various bacterial genera. These compounds could constitute growth substrates for these bacteria (Lory, 2014; Pujalte et al., 2014). Microbialization has been identified as a key process driving the loss of ecosystem processes (Nelson et al., 2023). Investigating which and how specific metabolites influence microbial metabolism might be key to understand the stability of macroalgal-dominated states. As most research, Chapter 2 focused on the links between algal-derived exometabolites and pelagic microbes. Yet, marine microbes can also be an important source of secondary metabolites (Modolon et al., 2020; Petersen et al., 2020). Therefore, a critical question that needs further investigation is to what extent metabolites produced by microbes shape their chemical environment; that is to tear apart the influence of benthic

exometabolomes from the microbial exometabolomes in the multiomic signatures of reef waters and reef metabolism (Fig. 5.2).

Two of my chapters focused on holobiont responses to macroalgal competition by investigating coral adult microbiome and metabolome and coral larval microbiome (chapters 3 and 4). Changes in microbiome diversity, variability and composition have often been described as symptoms of a sensitive microbiome, but we still have little knowledge on how it translates to host biology (McDevitt-Irwin et al., 2017; Clements & Hay, 2023). For example, my results highlighted microbial families enriched in the microbiome of corals in contact and water-mediated interactions with *Dictyota*, such as Rhodobacteraceae, Rubritaleaceae and Vibrionaceae (Chapter 4). These taxa have been flagged as opportunists due to their prevalence in the microbiome of corals impacted by algal competition or other stresses (Vega Thurber et al., 2012; Zaneveld et al., 2016; McDevitt-Irwin et al., 2017; Morrow et al., 2017). In contact-mediated interaction with *Dictyota*, their enrichment paired with a loss of putative bacterial symbionts (e.g., *Endozoicomonas*) and macro-physiological damages suggestive of microbial dysbiosis (Chapter 4). In addition, Chapter 3 brings important new knowledge on the factors structuring coral larval microbiome and the nature of larvae-bacteria associations. Macroalgal-induced environment led to alterations in the larval microbiome, with a loss of putative symbionts (e.g., *Sulfitobacter*, *Vibrio*), which were correlated with a lower larval survival (Chapter 3). However, it is important to consider that it is not because microbial changes are concurrent with coral demise that they are the cause. Microbial responses to stress could also constitute a symptom. In addition, we do not know what is the relative influence of algal-derived allelochemicals and associated microbes in these observations. Indeed, both algal chemical extracts and isolated bacteria can alter coral microbiome composition and physiology (Morrow et al., 2012, 2017; Vieira et al., 2016a, 2016b). Thus, establishing causal links between the source of stress, stress-related phenotypic variations and microbial dynamics constitutes research priorities (Fig. 5.2). Sampling coral microbiomes over a time gradient could help to understand microbiome changes by describing their successional stages (Vega Thurber et al., 2020). Specifically, were opportunists the first taxa to colonize coral microbiome? Did they compete with beneficial bacteria? Is it the loss of symbionts that opened up niche space? Did opportunists cause a decline in host health and increase the virulence of co-occurring bacteria? Coral mucus is a very responsive and dynamic habitat which harbors bacteria that can produce antibacterial metabolites (Ritchie, 2006; Pollock et al., 2018). Its sampling would, therefore, constitute a promising non-invasive way to better understand the dynamics of microbial dysbiosis and the putative roles of involved microbes.

In addition, the nature of coral-bacteria associations could change under certain conditions. For example, under high nutrient availability, the commensal coral bacterium *Candidatus Aquarickettsia* (order Rickettsiales) can turn parasitic consuming host nutrients (Klinges et al., 2019). In chapters 3 and 4, I detected the known coral pathogen *Vibrio coralliilyticus* in coral adult and larval samples. This microbe could compete with symbiotic bacteria (Wang et al., 2022) and facilitate the virulence of others in a temperature-dependent manner (Rubio-Portillo et al., 2020). Future research is needed to investigate how competitive dynamics of microbial symbionts change in stressed holobionts, and how this translates to coral demise (Fig. 5.2). A surprising result was the colonization of an *Endozoicomonas* in the microbiome of corals in direct contact with *Dictyota* (Chapter 4). Although *Endozoicomonas* are well described coral symbionts associated with diverse beneficial functions for their host (Neave et al., 2017b; Pogoreutz et al., 2022), this result suggests that strains of closely related taxa could exhibit a range of roles (Pogoreutz & Ziegler, 2023). Another interesting result was the decrease in phototrophic bacteria *Synechococcus* in near-surface waters of corals in contact and water-mediated interactions (Chapter 4). Corals can graze upon bacterial cells such as *Synechococcus* (McNally et al., 2017) and increase their heterotrophic rates to compensate energy depletion after bleaching (Hughes & Grottoli, 2013). Therefore, corals may rely more extensively on heterotrophy to modulate their energy demands as they compete with algae.

4.2. Linking patterns to mechanisms through experimental and multiomic research

To further advance the aforementioned perspectives, future experimental research could benefit from incubation and microbial co-culture experiments. For example, the intrinsic link between microbes and metabolites has been demonstrated by incubating natural microbial communities with benthic-derived exudates (Nelson et al., 2013; Weber et al., 2022). In future research, the nature (e.g., trophic or defensive) of microbe-metabolite interactions could be investigated by spiking specific algal compounds into microbial cultures from either coral or planktonic microbiomes, with subsequent measures of microbial responses to these additions. Metabolic activity of microbes can be revealed by “omic” sciences, such as metatranscriptomics and metabolomics, and label-based approaches (Engelberts et al., 2021). For example, coral tissue extracts stimulated the expression of genes of *Endozoicomonas* cultures related to symbiosis establishment (Pogoreutz et al., 2022). Label-based approaches paired with cell-level chemical imaging techniques, such as NanoSIMS (nanoscale secondary ion mass spectrometry), make possible to track the assimilation and translocation of labelled isotopes by

microbes and to visualize them in coral cells (Ceh et al., 2013b; Gibbin et al., 2018). In adult corals, ^{15}N -labelled *Vibrio coralliilyticus* were tracked over time revealing movement of this pathogen in coral tissues throughout the infection process (Gibbin et al., 2018). These methods are also greatly valuable as they allow to map the directionality of microbe-metabolites interactions. In the context of my research, these methods could be used to investigate which and how specific algal exometabolites influence microbial activity. Another promising area of research would be to investigate the translocation of maternal metabolites to the offspring and how this translocation is affected by algal stress (Fig. 5.2). In addition, future research will benefit from co-culture experiments by manipulating the identity of interacting microbes to gain insight into the consequences of opportunist taxa invasion on microbial symbionts and host biology. Such experiments have proven extremely insightful to understand the chemical cross-talk between holobiont members and the dynamics of microbe-microbe interactions (Rubio-Portillo et al., 2020; Wang et al., 2022; Matthews et al., 2023). For example, the analysis of transcriptomic data of two coral pathogens (Vibrios) revealed an overexpression of virulence factor genes when cultivated in co-cultures with consequences on their virulence against coral holobionts (Rubio-Portillo et al., 2020). Combined, these advanced methods could help to decipher the roles of microbes and metabolites on reef metabolism and holobiont functioning and how these processes are disrupted by macroalgal proliferation. Yet, such efforts would require extensive interdisciplinary and collaborative research to be successful.

One of the biggest challenges I faced throughout this PhD research was the annotation of highlighted metabolites and subsequent proposition of their putative roles. Similarly, metabarcoding is highly limited by low taxonomic resolution as the sequencing of sub-regions does not allow to discriminate among closely related taxa (Johnson et al., 2019). Overcoming these steps should be a priority to advance the potential of multiomics to apprehend reef and holobiont functioning as ecosystem state changes. To alleviate these limitations, some key steps in metabolomics would be to: improve *in-situ* sampling, build marine- and even coral-specific spectral libraries, and elaborate standards for quantification of targeted metabolites. Exometabolites are particularly challenging to sample as they are diluted in trace quantities and might biodegrade quickly after sampling. In Chapter 4, we sampled coral exometabolomes in surface water near corals *in-situ* using SPE cartridges to directly capture exometabolites. Recently, a device called I-SMEL (In-Situ Marine Molecule Logger) was developed to capture metabolites in the field with SPE disks allowing to sample large body masses (Mauduit et al., 2023), which would have been particularly suitable for sampling MBLs or BBLs in Chapter 2. Immediately capturing exometabolites above emitting organisms and before any

transformations would greatly help to investigate their origins and identities. To propose putative annotations, researchers extensively rely on *in-silico* tools, such as those proposed in the GNPS platform and the SIRIUS software (Wang et al., 2016; Ernst et al., 2019; Dührkop et al., 2019). While they tremendously advanced the possibilities to annotate unknown metabolites, a majority often remain unclassified (da Silva et al., 2015; Lawson et al., 2021; chapters 2 and 4) and the expertise of analytic chemists is fundamental for verification. Therefore, shared spectral libraries specific to reef metabolomics would increase our annotation efforts. In addition, some protocols could allow to improve the recovery and quantification of specific compounds, such as nitrogen-containing compounds, to constitute standard libraries (Widner et al., 2021). Concerning metabarcoding, taxonomic resolution could be improved by sequencing full 16S gene (Johnson et al., 2019). While culture-based approaches are still hampered by the small fraction of coral bacteria that can be successfully cultured, studies could participate in the elaboration of a catalog displaying genomic, metabolic and physiologic traits of coral-associated microbes helping researchers to interpret microbial patterns (Sweet et al., 2021).

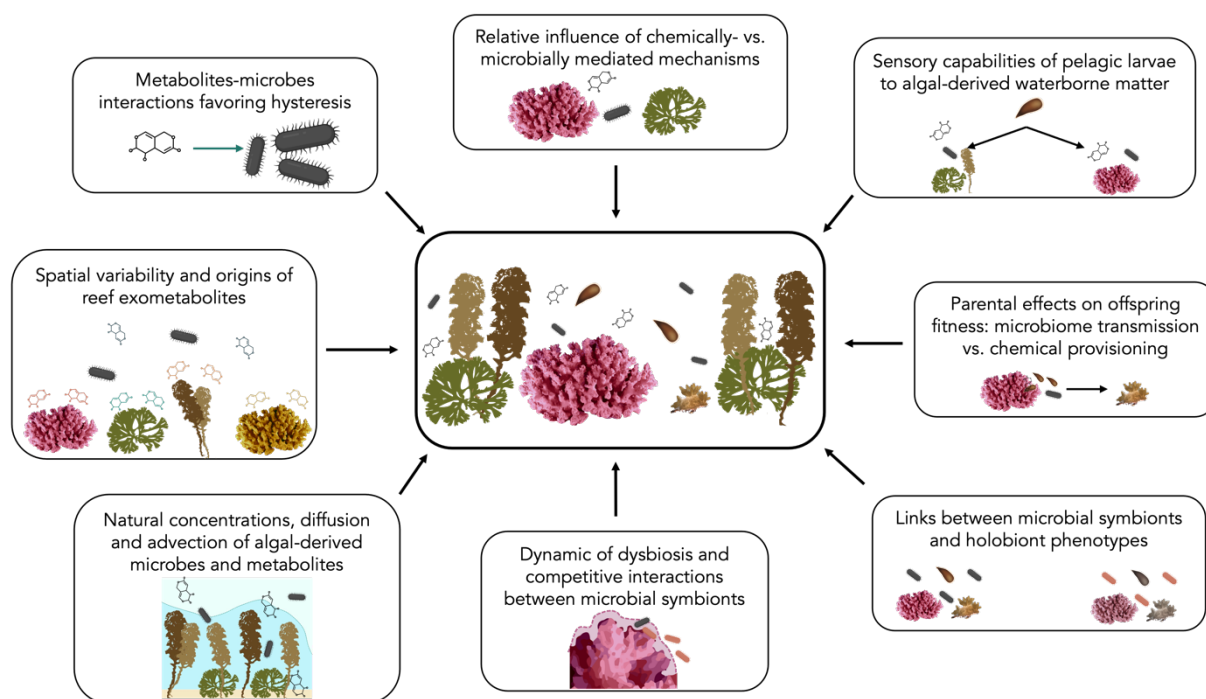


Figure 5.2 | Key research perspectives highlighted in this PhD research to further understand the roles of algal-associated microbes and metabolites on reef metabolism and resilience. These include: 1. Better understanding the movement of algal-derived metabolites and microbes across boundary layers with ambient hydrodynamics, and how these interact together. It is also important 2. To assess how these waterborne substances affect coral holobionts across life stages and 3. To establish the causal links between microbial dynamics and holobiont health.

5. Perspectives on future macroalgal-dominated reefs

In this research, I found that the microbiome of *P. acuta* is remarkably stable to macroalgal proximity despite notable changes in the metabolome and microbiome composition of reef waters surrounding corals (chapters 2 and 3). This pattern supports previous findings on Pocilloporids microbiome exposed to nutrient enrichment (Pogoreutz et al., 2018; Ziegler et al., 2019), heat stress (Epstein et al., 2019b; Botté et al., 2022; Price et al., 2023) and macroalgal dominance (Beatty et al., 2018). Yet, it is still unclear whether microbiome stability confers benefits or disadvantages to coral resistance (Rasher et al., 2011; Guest et al., 2012; Beatty et al., 2019; Price et al., 2023). In fact, their competitive life-history traits, with high growth rate and reproductive outputs, have likely allowed these “winners” to become some of most dominant corals on the degraded reefs of French Polynesia (Traçon et al., 2011; Darling et al., 2012; Holbrook et al., 2018). In Chapter 3, corals transplanted to algal-dominated bommies produced an offspring that was less robust than those of algal-removed bommies. Interestingly, parental and environmental effects interacted on algal-dominated bommies where recruits brooded by parents from algal-dominated bommies survived ~ 50% less than those brooded by parents from algal-removed bommies. In contrast, settlement rates were unaffected by these effects, corroborating the lack of selectivity of Pocilloporid recruits (Gouezo et al., 2020). As macroalgae proliferate, adults in close proximity with macroalgae may produce a less robust offspring who, upon settlement in macroalgal-dominated habitats, will suffer from enhanced mortality. In turn, this could dramatically reduce coral replenishment. These patterns could induce a selection of the fittest offspring which over time may result in acclimatization and/or enhanced tolerance to macroalgae, but this remains to be evaluated. While parental effects have essentially been investigated relative to climate-related stressors (Putnam & Gates, 2015; Zhou et al. 2021., Rodrigues & Padilla-Gamiño, 2022), there is an urgent need to conceptualize these effects under interspecific competition.

The cumulative impact of anthropogenic activities leading to the rise of ocean temperatures and acidification are expected to increase in the next years constituting a growing threat for coral communities (Spalding & Brown, 2015; Hughes et al., 2017). These climate-related stressors could positively interact with macroalgal competition to further compromise coral persistence. For example, coral mortality in herbivore exclusion and nutrient enrichment plots increased by 80% during the warmest months compared to control plots (Zaneveld et al., 2016). In another study, coral survival after El Niño event decreased from 40% on reefs with low levels of local disturbances to 15% on reefs with high levels of local disturbances

(McDevitt-Irwin et al., 2019). Elevated $p\text{CO}_2$ can increase the damage that macroalgal contact causes to corals (Diaz-Pulido et al., 2011; Del Monaco et al., 2017). Some species could even become allelopathic under predicted climate scenarios. This has already been demonstrated for *Dictyota cervicornis* whose lipid-soluble extracts became more potent under elevated $p\text{CO}_2$ compared to ambient conditions (Del Monaco et al., 2017). In addition, global stressors could influence the nature of coral-microbe interactions. For example, increasing temperature could increase the pathogenicity of the bacteria *Vibrio coralliilyticus* (Ben-Haim et al., 2003; Vidal-Dupiol et al., 2014; Beatty et al., 2019), a genus detected in my coral samples (chapters 3 and 4). Cumulative stressors may have antagonist rather than additive effects on the structure of the coral microbiome (Maher et al., 2019; McDevitt-Irwin et al., 2019). Therefore, there is an urgent need to understand the extent to which macroalgal competition and global stressors interact to drive microbiome changes and how this affects coral resilience. In this context, protecting corals from local disturbances favoring macroalgal proliferation may help coral reefs to persist in the face of climate-related stressors.

To restore coral reefs, initiatives are essentially focused on increasing coral abundance through methods like transplantation or larval seeding, rather than employing stress-alleviating measures, such as restocking herbivores or manually removing macroalgae (Ceccarelli et al., 2018; Hughes et al., 2023). In this thesis, I demonstrated that within a single reef macroalgae could have microbial and chemical effects of macroalgae at the scale of coral bommies (Chapter 2). In addition, larvae and post-settlement survival was reduced in these macroalgal-dominated environments (Chapter 3). Recent studies have demonstrated that the local removal of macroalgae over three years results in a 47% increase in coral cover and threefold increase in coral recruitment (Smith et al., 2022, 2023). In addition, adult corals seem resilient to macroalgal contact or their chemical extracts (Fong et al., 2023; van Duyl et al., 2023). Altogether, these studies provide further incentives for macroalgal removal. Removing macroalgae can be done manually or by shading but it remains labor intensive (Dajka et al., 2021; Ceccarelli et al., 2018). Citizen-based projects could expand the spatial scale of restored areas and lead to positive project outcomes (Smith et al., 2022, 2023). Such initiatives started on the island of Tahiti in collaboration with local associations, start-ups and academic research institutes (i.e., the To'a Nu'uroa project). Beyond restoration incentives, these projects aim at finding new ways to exploit algal waste and increase community involvement and awareness. However, odds of algal regrowth can be high if not associated with complementary measures, such as herbivore restocking (e.g., fish, urchins; Bulleri et al 2022; Spiers & Frazer, 2023) and watershed management for reducing nutrient inputs (Adam et al., 2021). In coral

transplantation, dense and co-beneficial multi-specific assemblages could be used to favor priority effects in the benefit of coral communities (Adam et al., 2022; Engelhardt et al 2023). In addition, unexpected effects can occur. For example, the removal of canopy-forming algae such as *Sargassum* can lead to the increase of turf and *Lobophora* (Ceccarelli et al., 2018; Smith et al., 2023). Yet, “prevention is better than cure”. It is now absolutely critical to avoid further algal proliferation, such as that currently occurring in the fore reefs of Mo’orea (pers. obs). Thorough surveys should be conducted to describe the dynamics of algal community composition over time and space. Key future challenge would be to estimate whether these cumulative restoration measures could help reaching the tipping point at which benthic communities reverse towards a coral-dominated state.

6. Conclusion

Facing the extensive macroalgal proliferation on coral reefs, this thesis responded to the pressing need to better understand the extent and mechanisms by which macroalgae can effectively limit coral recovery. This work provided detailed inventories of microorganisms and metabolites associated with coral-macroalgal competition and revealed key microbe-metabolite interactions. Collectively, it marked an important step in the understanding of the contact and water-mediated mechanisms by which macroalgal-associated microbes and metabolites alter coral health and recruitment success. To further elucidate their specific impacts on coral holobiont biology and their contributions in maintaining phase shifts, a key step would be to manipulate interacting microbes and metabolites under controlled conditions. Such experimental approaches would benefit from multiomic and quantitative frameworks to describe microbial and host responses. Field-based studies under realistic ecological conditions, taking into account reef morphology, hydrodynamics and the natural concentrations of microbes and metabolites will be essential to validate the proposed mechanisms. Although evidence for reversing macroalgal-dominated states is limited, local eradication efforts of macroalgae offer potential for coral recovery. Microbes and metabolites are essential components of coral reef ecosystems and understanding their distributions and functions will be paramount for apprehending and enhancing the resilience of these highly threatened ecosystems.

References

- Adam, T. C., Burkepile, D. E., Holbrook, S. J., Carpenter, R. C., Claudet, J., Loiseau, C., Thiault, L., Brooks, A. J., Washburn, L., & Schmitt, R. J. (2021). Landscape-scale patterns of nutrient enrichment in a coral reef ecosystem: implications for coral to algae phase shifts. *Ecological Applications*, *31*(1), 1–16. <https://doi.org/10.1002/eap.2227>
- Adam, T. C., Holbrook, S. J., Burkepile, D. E., Speare, K. E., Brooks, A. J., Ladd, M. C., Shantz, A. A., Vega Thurber, R., & Schmitt, R. J. (2022). Priority effects in coral–macroalgae interactions can drive alternate community paths in the absence of top-down control. *Ecology*, *103*(12), 1–17. <https://doi.org/10.1002/ecy.3831>
- Adam, T. C., Schmitt, R. J., Holbrook, S. J., Brooks, A. J., Edmunds, P. J., Carpenter, R. C., & Bernardi, G. (2011). Herbivory, connectivity, and ecosystem resilience: Response of a coral reef to a large-scale perturbation. *PLoS ONE*, *6*(8). <https://doi.org/10.1371/journal.pone.0023717>
- Adjeroud, M., Kayal, M., Iborra-Cantonnet, C., Vercelloni, J., Bosserelle, P., Liao, V., Chancerelle, Y., Claudet, J., & Penin, L. (2018). Recovery of coral assemblages despite acute and recurrent disturbances on a South Central Pacific reef. *Scientific Reports*, *8*(1), 1–8. <https://doi.org/10.1038/s41598-018-27891-3>
- Adjeroud, M., Michonneau, F., Edmunds, P. J., Chancerelle, Y., de Loma, T. L., Penin, L., Thibaut, L., Vidal-Dupiol, J., Salvat, B., & Galzin, R. (2009). Recurrent disturbances, recovery trajectories, and resilience of coral assemblages on a South Central Pacific reef. *Coral Reefs*, *28*(3), 775–780. <https://doi.org/10.1007/s00338-009-0515-7>
- Ainsworth, T. D., Krause, L., Bridge, T., Torda, G., Raina, J. B., Zakrzewski, M., Gates, R. D., Padilla-Gamiño, J. L., Spalding, H. L., Smith, C., Woolsey, E. S., Bourne, D. G., Bongaerts, P., Hoegh-Guldberg, O., & Leggat, W. (2015). The coral core microbiome identifies rare bacterial taxa as ubiquitous endosymbionts. *ISME Journal*, *9*(10), 2261–2274. <https://doi.org/10.1038/ismej.2015.39>
- Ali, M. S., & Pervez, M. K. (2003). Ring-a hydroxylated dolastanes from the marine Brown alga *Dictyota Dichotoma* (Huds.) Lamour. *Natural Product Research*, *17*(4), 281–286. <https://doi.org/10.1080/1057563031000072514>
- Ali, M. S., Pervez, M. K., Saleem, M., & Ahmed, F. (2003). Dichotenone-A and -B: Two new enones from the marine brown alga *Dictyota dichotoma* (Hudson) lamaour. *Natural Product Research*, *17*(5), 301–306. <https://doi.org/10.1080/1057563031000072523>
- Amsler, C. D., & Fairhead, V. A. (2005). Defensive and sensory chemical ecology of brown algae. *Advances in Botanical Research*, *43*(C), 1–91. [https://doi.org/10.1016/S0065-2296\(05\)43001-3](https://doi.org/10.1016/S0065-2296(05)43001-3)
- Andras, T. D., Alexander, T. S., Gahlana, A., Parry, R. M., Fernandez, F. M., Kubanek, J., Wang, M. D., & Hay, M. E. (2012). Seaweed allelopathy against coral: surface distribution of a seaweed secondary metabolite by imaging mass spectrometry. *Journal of Chemical Ecology*, *38*(10), 1203–1214. <https://doi.org/10.1007/s10886-012-0204-9>

- Andrew, S. (2010). FastQC: a quality control tool for high throughput sequence data.
- Antonio-Martínez, F., Henaut, Y., Vega-Zepeda, A., Cerón-Flores, A. I., Raigoza-Figueras, R., Cetz-Navarro, N. P., & Espinoza-Avalos, J. (2020). Leachate effects of pelagic *Sargassum* spp. on larval swimming behavior of the coral *Acropora palmata*. *Scientific Reports*, *10*(1), 0–13. <https://doi.org/10.1038/s41598-020-60864-z>
- Apprill, A., Holm, H., Santoro, A. E., Becker, C., Neave, M., Hughen, K., Donà, A. R., Aeby, G., Work, T., Weber, L., & McNally, S. (2021). Microbial ecology of coral-dominated reefs in the Federated States of Micronesia. *Aquatic Microbial Ecology*, *86*, 115–136. <https://doi.org/10.3354/AME01961>
- Apprill, A., Marlow, H. Q., Martindale, M. Q., & Rappé, M. S. (2009). The onset of microbial associations in the coral *Pocillopora meandrina*. *ISME Journal*, *3*(6), 685–699. <https://doi.org/10.1038/ismej.2009.3>
- Arnold, S. N., & Steneck, R. S. (2011). Settling into an increasingly hostile world: The rapidly closing “recruitment window” for corals. *PLoS ONE*, *6*(12). <https://doi.org/10.1371/journal.pone.0028681>
- Arnold, S. N., Steneck, R. S., & Mumby, P. J. (2010). Running the gauntlet: Inhibitory effects of algal turfs on the processes of coral recruitment. *Marine Ecology Progress Series*, *414*, 91–105. <https://doi.org/10.3354/meps08724>
- Aronson, R. B., & Precht, W. F. (2006). Conservation, precaution, and Caribbean reefs. *Coral Reefs*, *25*(3), 441–450. <https://doi.org/10.1007/s00338-006-0122-9>
- Azizan, A., Maulidiani, M., Rudiyanto, R., Shaari, K., Ismail, I. S., Nagao, N., & Abas, F. (2020). Mass spectrometry-based metabolomics combined with quantitative analysis of the microalgal diatom (*Chaetoceros calcitrans*). *Marine Drugs*, *18*(8), 3–5. <https://doi.org/10.3390/MD18080403>
- Baird, A. H., & Morse, A. N. C. (2004). Induction of metamorphosis in larvae of the brooding corals *Acropora palifera* and *Stylophora pistillata*. *Marine and Freshwater Research*, *55*(5), 469–472. <https://doi.org/10.1071/MF03121>
- Barbosa, J. P., Teixeira, V. L., & Pereira, R. C. (2004). A dolabellane diterpene from the brown alga *Dictyota paffii* as chemical defense against herbivores. *Botanica Marina*, *47*(2), 147–151. <https://doi.org/10.1515/BOT.2004.015>
- Barott, K. L., Rodriguez-Brito, B., Janouškovec, J., Marhaver, K. L., Smith, J. E., Keeling, P., & Rohwer, F. L. (2011). Microbial diversity associated with four functional groups of benthic reef algae and the reef-building coral *Montastraea annularis*. *Environmental Microbiology*, *13*(5), 1192–1204. <https://doi.org/10.1111/j.1462-2920.2010.02419.x>
- Barott, K. L., Rodriguez-Mueller, B., Youle, M., Marhaver, K. L., Vermeij, M. J. A., Smith, J. E., & Rohwer, F. L. (2012). Microbial to reef scale interactions between the reef-building coral *Montastraea annularis* and benthic algae. *Proceedings of the Royal Society B: Biological Sciences*, *279*(1733), 1655–1664. <https://doi.org/10.1098/rspb.2011.2155>

- Barott, K. L., & Rohwer, F. L. (2012). Unseen players shape benthic competition on coral reefs. *Trends in Microbiology*, 20(12), 621–628. <https://doi.org/10.1016/j.tim.2012.08.004>
- Barott, K., Smith, J., Dinsdale, E., Hatay, M., Sandin, S., & Rohwer, F. (2009). Hyperspectral and physiological analyses of coral-algal interactions. *PLoS ONE*, 4(11). <https://doi.org/10.1371/journal.pone.0008043>
- Bates, D., Mächler, M., Bolker, B. M., & Walker, S. C. (2015). Fitting linear mixed-effects models using lme4. *Journal of Statistical Software*, 67(1). <https://doi.org/10.18637/jss.v067.i01>
- Bayer, T., Neave, M. J., Alsheikh-Hussain, A., Aranda, M., Yum, L. K., Mincer, T., Hughen, K., Apprill, A., & Voolstra, C. R. (2013). The microbiome of the red sea coral *Stylophora pistillata* is dominated by tissue-associated endozoicomonas bacteria. *Applied and Environmental Microbiology*, 79(15), 4759–4762. <https://doi.org/10.1128/AEM.00695-13>
- Beatty, D. S., Clements, C. S., Stewart, F. J., & Hay, M. E. (2018). Intergenerational effects of macroalgae on a reef coral: major declines in larval survival but subtle changes in microbiomes. *Marine Ecology Progress Series*, 589, 97–114. <https://doi.org/10.3354/meps12465>
- Beatty, D. S., Valayil, J. M., Clements, C. S., Ritchie, K. B., Stewart, F. J., & Hay, M. E. (2019). Variable effects of local management on coral defenses against a thermally regulated bleaching pathogen. *Science Advances*, 5(10), 1–10. <https://doi.org/10.1126/sciadv.aay1048>
- Becker, C. C., Weber, L., Zgliczynski, B., Sullivan, C., Sandin, S., Muller, E., Clark, A. S., Kido Soule, M. C., Longnecker, K., Kujawinski, E. B., & Apprill, A. (2023). Microorganisms and dissolved metabolites distinguish Florida's Coral Reef habitats. *PNAS Nexus*, 2(9), 1–14. <https://doi.org/10.1093/pnasnexus/pgad287>
- Beisner, B. E., Haydon, D. T., & Cuddington, K. (2003). Alternative stable states in ecology. *Frontiers in Ecology and the Environment*, 1(7), 376. <https://doi.org/10.2307/3868190>
- Bellwood, D. R., Hughes, T. P., Folke, C., & Nyström, M. (2004). Confronting the coral reef crisis. In *Nature* (Vol. 429, Issue 6994, pp. 827–833). <https://doi.org/10.1038/nature02691>
- Ben-haim, Y., Zicherman-keren, M., & Rosenberg, E. (2003). Temperature-regulated bleaching and lysis of the coral. *Applied and Environmental Microbiology*, 69(7), 4236–4242. <https://doi.org/10.1128/AEM.69.7.4236>
- Bergé, J. P., & Barnathan, G. (2005). Fatty acids from lipids of marine organisms: Molecular biodiversity, roles as biomarkers, biologically active compounds, and economical aspects. *Advances in Biochemical Engineering/Biotechnology*, 96(August), 49–125. <https://doi.org/10.1007/b135782>
- Bernasconi, R., Stat, M., Koenders, A., Papparini, A., Bunce, M., & Huggett, M. J. (2019). Establishment of coral-bacteria symbioses reveal changes in the core bacterial community with host ontogeny. *Frontiers in Microbiology*, 10(JULY), 1–16. <https://doi.org/10.3389/fmicb.2019.01529>

- Birrell, C. L., McCook, L. J., Willis, B. L., & Harrington, L. (2008b). Chemical effects of macroalgae on larval settlement of the broadcast spawning coral *Acropora millepora*. *Marine Ecology Progress Series*, 362, 129–137. <https://doi.org/10.3354/meps07524>
- Birrell, C., Willis, B. L., & Diaz-Pulido, G. (2008a). Effects of benthic algae on the replenishment of corals and the implications for the resilience of coral reefs. *Oceanography and Marine Biology*, 46, 25–63. <https://doi.org/10.1201/9781420065756.ch2>
- Bittick, S. J., Bilotti, N. D., Peterson, H. A., & Stewart, H. L. (2010). *Turbinaria ornata* as an herbivory refuge for associate algae. *Marine Biology*, 157(2), 317–323. <https://doi.org/10.1007/s00227-009-1319-6>
- Bittick, S. J., Clausing, R. J., Fong, C. R., Scoma, S. R., & Fong, P. (2019). A rapidly expanding macroalga acts as a foundational species providing trophic support and habitat in the South Pacific. *Ecosystems*, 22(1), 165–173. <https://doi.org/10.1007/s10021-018-0261-1>
- Blackall, L. L., Wilson, B., & Van Oppen, M. J. H. (2015). Coral-the world's most diverse symbiotic ecosystem. *Molecular Ecology*, 24(21), 5330–5347. <https://doi.org/10.1111/mec.13400>
- Böcker, S., & Dührkop, K. (2016). Fragmentation trees reloaded. *Journal of Cheminformatics*, 8(1), 1–26. <https://doi.org/10.1186/s13321-016-0116-8>
- Böcker, S., Letzel, M. C., Lipták, Z., & Pervukhin, A. (2009). SIRIUS: Decomposing isotope patterns for metabolite identification. *Bioinformatics*, 25(2), 218–224. <https://doi.org/10.1093/bioinformatics/btn603>
- Bogaert, K. A., Delva, S., & De Clerck, O. (2020). Concise review of the genus *Dictyota* J.V. Lamouroux. *Journal of Applied Phycology*, 32(3), 1521–1543. <https://doi.org/10.1007/s10811-020-02121-4>
- Bonaldo, R. M., & Hay, M. E. (2014). Seaweed-coral interactions: Variance in seaweed allelopathy, coral susceptibility, and potential effects on coral resilience. *PLoS ONE*, 9(1), 30–34. <https://doi.org/10.1371/journal.pone.0085786>
- Botté, E. S., Cantin, N. E., Mocellin, V. J. L., O'Brien, P. A., Rocker, M. M., Frade, P. R., & Webster, N. S. (2022). Reef location has a greater impact than coral bleaching severity on the microbiome of *Pocillopora acuta*. *Coral Reefs*, 41(1), 63–79. <https://doi.org/10.1007/s00338-021-02201-y>
- Bourne, D. G., Morrow, K. M., & Webster, N. S. (2016). Insights into the coral microbiome: underpinning the health and resilience of reef ecosystems. *Annual Review of Microbiology*, 70(1), 317–340. <https://doi.org/10.1146/annurev-micro-102215-095440>
- Box, Steve, J., & Mumby, Peter, J. (2007). Effect of macroalgal competition on growth and survival of juvenile Caribbean corals. *Marine Ecology Progress Series*, 342, 139–149.

- Brandl, S. J., Hoey, A. S., & Bellwood, D. R. (2014). Micro-topography mediates interactions between corals, algae, and herbivorous fishes on coral reefs. *Coral Reefs*, 33(2), 421–430. <https://doi.org/10.1007/s00338-013-1110-5>
- Briggs, A. A., Brown, A. L., Osenberg, C. W., & Briggs, A. A. (2021). Local versus site-level effects of algae on coral microbial communities. *Royal Society Open Science*, 8(210035).
- Briggs, C. J., Adam, T. C., Holbrook, S. J., & Schmitt, R. J. (2018). Macroalgae size refuge from herbivory promotes alternative stable states on coral reefs. *PLoS ONE*, 13(9), 1–14. <https://doi.org/10.1371/journal.pone.0202273>
- Broadbent, A. D., Jones, G. B., & Jones, R. J. (2002). DMSP in corals and benthic algae from the Great Barrier Reef. *Estuarine, Coastal and Shelf Science*, 55(4), 547–555. <https://doi.org/10.1006/ecss.2002.1021>
- Broadhurst, D., Goodacre, R., Reinke, S. N., Kuligowski, J., Wilson, I. D., Lewis, M. R., & Dunn, W. B. (2018). Guidelines and considerations for the use of system suitability and quality control samples in mass spectrometry assays applied in untargeted clinical metabolomic studies. *Metabolomics*, 14(6), 1–17. <https://doi.org/10.1007/s11306-018-1367-3>
- Brown, A. L., & Carpenter, R. C. (2015). Water flow influences the mechanisms and outcomes of interactions between massive *Porites* and coral reef algae. *Marine Biology*, 162(2), 459–468. <https://doi.org/10.1007/s00227-014-2593-5>
- Brown, K. T., Bender-Champ, D., Kubicek, A., van der Zande, R., Achlatis, M., Hoegh-Guldberg, O., & Dove, S. G. (2018). The dynamics of coral-algal interactions in space and time on the southern Great Barrier Reef. *Frontiers in Marine Science*, 5(MAY), 1–13. <https://doi.org/10.3389/fmars.2018.00181>
- Brown, M. V., Ostrowski, M., Grzymiski, J. J., & Lauro, F. M. (2014). A trait-based perspective on the biogeography of common and abundant marine bacterioplankton clades. *Marine Genomics*, 15, 17–28. <https://doi.org/10.1016/j.margen.2014.03.002>
- Bruckner, A., Chiriboga, A., Cortés, J., Delbeek, J. C., & Devantier, L. (2008). Climate change and local impacts. *Science*, 321(5888), 560–563. <http://www.sciencemag.org/content/321/5888/560.abstract>
- Bruno, J. F., Precht, W. F., Vroom, P. S., & Aronson, R. B. (2014). Coral reef baselines: How much macroalgae is natural? *Marine Pollution Bulletin*, 80(1–2), 24–29. <https://doi.org/10.1016/j.marpolbul.2014.01.010>
- Bruno, J. F., & Selig, E. R. (2007). Regional decline of coral cover in the Indo-Pacific: Timing, extent, and subregional comparisons. *PLoS ONE*, 2(8). <https://doi.org/10.1371/journal.pone.0000711>
- Bruno, J. F., Sweatman, H., Precht, W. F., Selig, E. R., & Schutte, V. G. W. (2009). Assessing evidence of phase shifts from coral to macroalgal dominance on coral reefs. *Ecology*, 90(6), 1478–1484. <https://doi.org/10.1890/08-1781.1>

- Bulleri, F., Pozas-Schacre, C., Bischoff, H., Bramanti, L., D'agata, S., Gasc, J., & Nugues, M. M. (2022). Compounded effects of sea urchin grazing and physical disturbance on macroalgal canopies in the lagoon of Moorea, French Polynesia. *Marine Ecology Progress Series*, 697, 45–56. <https://doi.org/10.3354/meps14137>
- Bulleri, F., Thiault, L., Mills, S. C., Nugues, M. M., Eckert, E. M., Corno, G., & Claudet, J. (2018). Erect macroalgae influence epilithic bacterial assemblages and reduce coral recruitment. *Marine Ecology Progress Series*, 597, 65–77. <https://doi.org/10.3354/meps12583>
- Burke, L., Reytar, K., Spalding, M., & Perry, A. (2011). Reefs at Risk Revisited. In *Defenders* (Vol. 74, Issue 3). <http://www.pubmedcentral.nih.gov/articlerender.fcgi?artid=3150666&tool=pmcentrez&endertype=abstract>
- Bustamam, M. S. A., Pantami, H. A., Azizan, A., Shaari, K., Min, C. C., Abas, F., Nagao, N., Maulidiani, M., Banerjee, S., Sulaiman, F., & Ismail, I. S. (2021). Complementary Analytical Platforms of NMR Spectroscopy and LCMS Analysis in the Metabolite Profiling of *Isochrysis galbana*. *Marine Drugs*, 19(3). <https://doi.org/10.3390/MD19030139>
- Cai, L., Tian, R. M., Zhou, G., Tong, H., Wong, Y. H., Zhang, W., Chui, A. P. Y., Xie, J. Y., Qiu, J. W., Ang, P. O., Liu, S., Huang, H., & Qian, P. Y. (2018). Exploring coral microbiome assemblages in the South China Sea. *Scientific Reports*, 8(1), 1–13. <https://doi.org/10.1038/s41598-018-20515-w>
- Callahan, B. J., McMurdie, P. J., Rosen, M. J., Han, A. W., Johnson, A. J. A., & Holmes, S. P. (2016). DADA2: High-resolution sample inference from Illumina amplicon data. *Nature Methods*, 13(7), 581–583. <https://doi.org/10.1038/nmeth.3869>
- Candy, A. S., Taylor Parkins, S. K., Van Duyl, F. C., Mueller, B., Arts, M. G. I., Barnes, W., Carstensen, M., Scholten, Y. J. H., El-Khaled, Y. C., Wild, C., Wegley Kelly, L., Nelson, C. E., Sandin, S. A., Vermeij, M. J. A., Rohwer, F. L., Picioreanu, C., Stocchi, P., & Haas, A. F. (2023). Small-scale oxygen distribution patterns in a coral reef. *Frontiers in Marine Science*, 10(April), 1–13. <https://doi.org/10.3389/fmars.2023.1135686>
- Cannon, S. E., Donner, S. D., Liu, A., González Espinosa, P. C., Baird, A. H., Baum, J. K., Bauman, A. G., Beger, M., Benkwitt, C. E., Birt, M. J., Chancerelle, Y., Cinner, J. E., Crane, N. L., Denis, V., Depczynski, M., Fadli, N., Fenner, D., Fulton, C. J., Golbuu, Y., ... Wilson, S. K. (2023). Macroalgae exhibit diverse responses to human disturbances on coral reefs. *Global Change Biology*, 29(12), 3318–3330. <https://doi.org/10.1111/gcb.16694>
- Cao, K. A. L., Costello, M. E., Lakis, V. A., Bartolo, F., Chua, X. Y., Brazeilles, R., & Rondeau, P. (2016). MixMC: A multivariate statistical framework to gain insight into microbial communities. *PLoS ONE*, 11(8), e0160169. <https://doi.org/10.1371/journal.pone.0160169>
- Carriot, N., Paix, B., Greff, S., Viguier, B., Briand, J. F., & Culioli, G. (2021). Integration of LC/MS-based molecular networking and classical phytochemical approach allows in-depth annotation of the metabolome of non-model organisms - The case study of the brown

- Ceccarelli, D. M., Loffler, Z., Bourne, D. G., Al Moajil-Cole, G. S., Boström-Einarsson, L., Evans-Illidge, E., Fabricius, K., Glasl, B., Marshall, P., McLeod, I., Read, M., Schaffelke, B., Smith, A. K., Jorda, G. T., Williamson, D. H., & Bay, L. (2018). Rehabilitation of coral reefs through removal of macroalgae: state of knowledge and considerations for management and implementation. *Restoration Ecology*, 26(5), 827–838. <https://doi.org/10.1111/rec.12852>
- Ceh, J., Kilburn, M. R., Cliff, J. B., Raina, J. B., Van Keulen, M., & Bourne, D. G. (2013b). Nutrient cycling in early coral life stages: *Pocillopora damicornis* larvae provide their algal symbiont (Symbiodinium) with nitrogen acquired from bacterial associates. *Ecology and Evolution*, 3(8), 2393–2400. <https://doi.org/10.1002/ece3.642>
- Ceh, J., van Keulen, M., & Bourne, D. G. (2013a). Intergenerational transfer of specific bacteria in corals and possible implications for offspring fitness. *Microbial Ecology*, 65(1), 227–231. <https://doi.org/10.1007/s00248-012-0105-z>
- Chambers, M. C., MacLean, B., Burke, R., Amodei, D., Ruderman, D. L., Neumann, S., Gatto, L., Fischer, B., Pratt, B., Egertson, J., Hoff, K., Kessner, D., Tasman, N., Shulman, N., Frewen, B., Baker, T. A., Brusniak, M. Y., Paulse, C., Creasy, D., ... Mallick, P. (2012). A cross-platform toolkit for mass spectrometry and proteomics. *Nature Biotechnology*, 30(10), 918–920. <https://doi.org/10.1038/nbt.2377>
- Chen, J., Li, H., Zhao, Z., Xia, X., Li, B., Zhang, J., & Yan, X. (2018a). Diterpenes from the marine algae of the genus dictyota. *Marine Drugs*, 16(5), 1–25. <https://doi.org/10.3390/md16050159>
- Chiou, S. F., Kuo, J., Wong, T. Y., Fan, T. Y., Tew, K. S., & Liu, J. K. (2010). Analysis of the coral associated bacterial community structures in healthy and diseased corals from off-shore of southern Taiwan. *Journal of Environmental Science and Health - Part B Pesticides, Food Contaminants, and Agricultural Wastes*, 45(5), 408–415. <https://doi.org/10.1080/03601231003800032>
- Choat, J. H., Clements, K. D., & Robbins, W. D. (2002). The trophic status of herbivorous fishes on coral reefs 1: Dietary analyses. *Marine Biology*, 140(3), 613–623. <https://doi.org/10.1007/s00227-001-0715-3>
- Chong-Seng, K. M., Graham, N. A. J., & Pratchett, M. S. (2014). Bottlenecks to coral recovery in the Seychelles. *Coral Reefs*, 33(2), 449–461. <https://doi.org/10.1007/s00338-014-1137-2>
- Chong-Seng, K. M., Mannering, T. D., Pratchett, M. S., Bellwood, D. R., & Graham, N. A. J. (2012). The influence of coral reef benthic condition on associated fish assemblages. *PLoS ONE*, 7(8), 1–10. <https://doi.org/10.1371/journal.pone.0042167>
- Clements, C. S., Burns, A. S., Stewart, F. J., & Hay, M. E. (2020). Seaweed-coral competition in the field: effects on coral growth, photosynthesis and microbiomes require direct

- contact. *Proceedings. Biological Sciences*, 287(1927), 20200366. <https://doi.org/10.1098/rspb.2020.0366>
- Clements, C. S., & Hay, M. E. (2023). Disentangling the impacts of macroalgae on corals via effects on their microbiomes. *Frontiers in Ecology and Evolution*, June, 1–9. <https://doi.org/10.3389/fevo.2023.1083341>
- Clements, C. S., Rasher, D. B., Hoey, A. S., Bonito, V. E., & Hay, M. E. (2018). Spatial and temporal limits of coral-macroalgal competition: The negative impacts of macroalgal density, proximity, and history of contact. *Marine Ecology Progress Series*, 586(January), 11–20. <https://doi.org/10.3354/meps12410>
- Cocchi, M., Biancolillo, A., & Marini, F. (2018). Chemometric methods for classification and feature selection. In *Comprehensive Analytical Chemistry* (Vol. 82, pp. 265–299). Elsevier B.V. <https://doi.org/10.1016/bs.coac.2018.08.006>
- Coker, D. J., Wilson, S. K., & Pratchett, M. S. (2014). Importance of live coral habitat for reef fishes. *Reviews in Fish Biology and Fisheries*, 24(1), 89–126. <https://doi.org/10.1007/s11160-013-9319-5>
- Cornwall, C. E., Pilditch, C. A., Hepburn, C. D., & Hurd, C. L. (2015). Canopy macroalgae influence understory corallines' metabolic control of near-surface pH and oxygen concentration. *Marine Ecology Progress Series*, 525, 81–95. <https://doi.org/10.3354/meps11190>
- Côté, I. M., Gill, J. A., Gardner, T. A., & Watkinson, A. R. (2005). Measuring coral reef decline through meta-analyses. *Philosophical Transactions of the Royal Society B: Biological Sciences*, 360(1454), 385–395. <https://doi.org/10.1098/rstb.2004.1591>
- Crisp, S. K., Tebbett, S. B., & Bellwood, D. R. (2022). A critical evaluation of benthic phase shift studies on coral reefs. *Marine Environmental Research*, 178(May), 105667. <https://doi.org/10.1016/j.marenvres.2022.105667>
- Cronin, G., & Hay, M. E. (1996). Induction of seaweed chemical defenses by amphipod grazing. *Ecological Society of America*, 77(8), 2287–2301.
- Cuevas, B., Arroba, A. I., de los Reyes, C., Gómez-Jaramillo, L., González-Montelongo, M. C., & Zubía, E. (2021). Diterpenoids from the brown alga *Rugulopteryx okamurae* and their anti-inflammatory activity. *Marine Drugs*, 19(12). <https://doi.org/10.3390/md19120677>
- Cuevas, B., Arroba, A. I., de los Reyes, C., & Zubía, E. (2023). Rugulopteryx-derived spatane, secospatane, prenylcubebane and prenylkelsoane diterpenoids as inhibitors of nitric oxide production. *Marine Drugs*, 21(252), 50–59.
- Cunha, T. J., Güth, A. Z., Bromberg, S., & Sumida, P. Y. G. (2013). Macrofauna associated with the brown algae *Dictyota spp.* (Phaeophyceae, Dictyotaceae) in the Sebastião Gomes Reef and Abrolhos Archipelago, Bahia, Brazil. *Continental Shelf Research*, 70(August 1995), 140–149. <https://doi.org/10.1016/j.csr.2013.09.001>

- Cutignano, A., Luongo, E., Nuzzo, G., Pagano, D., Manzo, E., Sardo, A., & Fontana, A. (2016). Profiling of complex lipids in marine microalgae by UHPLC/tandem mass spectrometry. *Algal Research*, *17*, 348–358. <https://doi.org/10.1016/j.algal.2016.05.016>
- da Silva, R. R., Dorrestein, P. C., & Quinn, R. A. (2015). Illuminating the dark matter in metabolomics. *Proceedings of the National Academy of Sciences of the United States of America*, *112*(41), 12549–12550. <https://doi.org/10.1073/pnas.1516878112>
- da Silva, R. R., Wang, M., Nothias, L. F., van der Hooft, J. J. J., Caraballo-Rodríguez, A. M., Fox, E., Balunas, M. J., Klassen, J. L., Lopes, N. P., & Dorrestein, P. C. (2018). Propagating annotations of molecular networks using in silico fragmentation. *PLoS Computational Biology*, *14*(4), 1–26. <https://doi.org/10.1371/journal.pcbi.1006089>
- Dajka, J. C., Beasley, V., Gendron, G., Barlow, J., & Graham, N. A. J. (2021). Weakening macroalgal feedbacks through shading on degraded coral reefs. *Aquatic Conservation: Marine and Freshwater Ecosystems*, *31*(7), 1660–1669. <https://doi.org/10.1002/aqc.3546>
- Damjanovic, K., Menéndez, P., Blackall, L. L., & van Oppen, M. J. H. (2020). Mixed-mode bacterial transmission in the common brooding coral *Pocillopora acuta*. *Environmental Microbiology*, *22*(1), 397–412. <https://doi.org/10.1111/1462-2920.14856>
- Darling, E. S., Alvarez-Filip, L., Oliver, T. A., Mcclanahan, T. R., & Côté, I. M. (2012). Evaluating life-history strategies of reef corals from species traits. *Ecology Letters*, *15*(12), 1378–1386. <https://doi.org/10.1111/j.1461-0248.2012.01861.x>
- Davis, K. A., Pawlak, G., & Monismith, S. G. (2021). Turbulence and coral reefs. *Annual Review of Marine Science*, *13*, 343–373. <https://doi.org/10.1146/annurev-marine-042120-071823>
- Davis, N. M., Proctor, D. M., Holmes, S. P., Relman, D. A., & Callahan, B. J. (2018). Simple statistical identification and removal of contaminant sequences in marker-gene and metagenomics data. *Microbiome*, *6*(1), 1–14. <https://doi.org/10.1186/s40168-018-0605-2>
- Davis, S. L. (2018). Associational refuge facilitates phase shifts to macroalgae in a coral reef ecosystem. *Ecosphere*, *9*(5). <https://doi.org/10.1002/ecs2.2272>
- Davy, S. K., Allemand, D., & Weis, V. M. (2012). Cell biology of cnidarian-dinoflagellate symbiosis. *Microbiology and Molecular Biology Reviews*, *76*(2), 229–261. <https://doi.org/10.1128/mubr.05014-11>
- Del Monaco, C., Hay, M. E., Gartrell, P., Mumby, P. J., & Diaz-Pulido, G. (2017). Effects of ocean acidification on the potency of macroalgal allelopathy to a common coral. *Scientific Reports*, *7*, 1–10. <https://doi.org/10.1038/srep41053>
- Dell, C. L. A., Longo, G. O., & Hay, M. E. (2016). Positive feedbacks enhance macroalgal resilience on degraded coral reefs. *PLoS ONE*, *11*(5), 1–17. <https://doi.org/10.1371/journal.pone.0155049>
- Denis, V., Loubeyres, M., Doo, S. S., de Palmas, S., Keshavmurthy, S., Hsieh, H. J., & Chen, C. A. (2014). Can benthic algae mediate larval behavior and settlement of the coral

Acropora muricata? *Coral Reefs*, 33(2), 431–440. <https://doi.org/10.1007/s00338-014-1127-4>

- Dennison, W. C., & Barnes, D. J. (1988). Effect of water motion on coral photosynthesis and calcification. *Journal of Experimental Marine Biology and Ecology*, 115(1), 67–77. [https://doi.org/10.1016/0022-0981\(88\)90190-6](https://doi.org/10.1016/0022-0981(88)90190-6)
- Diaz-Pulido, G. (2019). Macroalgae. In P. Hutchings, M. Kingsford, & O. Hoegh-Guldberg (Eds.), *The Great Barrier Reef: Biology, Environment and Management* (Second Ed., pp. 146–156). CSIRO Publishing. <https://doi.org/10.1071/9781486308200>
- Diaz-Pulido, G., Gouezo, M., Tilbrook, B., Dove, S., & Anthony, K. R. N. (2011). High CO₂ enhances the competitive strength of seaweeds over corals. *Ecology Letters*, 14(2), 156–162. <https://doi.org/10.1111/j.1461-0248.2010.01565.x>
- Diaz-Pulido, G., Harii, S., McCook, L. J., & Hoegh-Guldberg, O. (2010). The impact of benthic algae on the settlement of a reef-building coral. *Coral Reefs*, 29(1), 203–208. <https://doi.org/10.1007/s00338-009-0573-x>
- Dinsdale, E. A., Pantos, O., Smriga, S., Edwards, R. A., Angly, F., Wegley, L., Hatay, M., Hall, D., Brown, E., Haynes, M., Krause, L., Sala, E., Sandin, S. A., Thurber, R. V., Willis, B. L., Azam, F., Knowlton, N., & Rohwer, F. (2008). Microbial ecology of four coral atolls in the Northern Line Islands. *PLoS ONE*, 3(2), e1584. <https://doi.org/10.1371/journal.pone.0001584>
- Dittmar, T., Koch, B., Hertkorn, N., & Kattner, G. (2008). A simple and efficient method for the solid-phase extraction of dissolved organic matter (SPE-DOM) from seawater. *Limnology and Oceanography: Methods*, 6(6), 230–235. <https://doi.org/10.4319/lom.2008.6.230>
- Done, T. J., Dayton, P. K., Dayton, A. E., & Steger, R. (1991). Regional and local variability in recovery of shallow coral communities: Moorea, French Polynesia and central Great Barrier Reef. *Coral Reefs*, 9(4), 183–192. <https://doi.org/10.1007/BF00290420>
- Doropoulos, C., Roff, G., Bozec, Y.-M., Zupan, M., Werminghausen, J., & Mumby, P. J. (2016). Characterizing the ecological trade-offs throughout the early ontogeny of coral recruitment. *Ecological Monographs*, 86(1), 20–44.
- Duffy, J. E., & Hay, M. E. (1990). Seaweed adaptations to herbivory. *BioScience*, 40(5), 368–375.
- Dührkop, K., Fleischauer, M., Ludwig, M., Aksenov, A. A., Melnik, A. V., Meusel, M., Dorrestein, P. C., Rousu, J., & Böcker, S. (2019). SIRIUS 4: a rapid tool for turning tandem mass spectra into metabolite structure information. *Nature Methods*, 16(4), 299–302. <https://doi.org/10.1038/s41592-019-0344-8>
- Dührkop, K., Nothias, L. F., Fleischauer, M., Reher, R., Ludwig, M., Hoffmann, M. A., Petras, D., Gerwick, W. H., Rousu, J., Dorrestein, P. C., & Böcker, S. (2021). Systematic classification of unknown metabolites using high-resolution fragmentation mass spectra. *Nature Biotechnology*, 39(4), 462–471. <https://doi.org/10.1038/s41587-020-0740-8>

- Dührkop, K., Shen, H., Meusel, M., Rousu, J., & Böcker, S. (2015). Searching molecular structure databases with tandem mass spectra using CSI:FingerID. *Proceedings of the National Academy of Sciences of the United States of America*, *112*(41), 12580–12585. <https://doi.org/10.1073/pnas.1509788112>
- Dungan, A. M., Bulach, D., Lin, H., van Oppen, M. J. H., & Blackall, L. L. (2021). Development of a free radical scavenging bacterial consortium to mitigate oxidative stress in cnidarians. *Microbial Biotechnology*, *14*(5), 2025–2040. <https://doi.org/10.1111/1751-7915.13877>
- Dunne, A. F., Tietbohl, M. D., Nuber, C., Berumen, M., & Jones, B. H. (2023). Fish-mediated nutrient flows from macroalgae habitats to coral reefs in the Red Sea. *Marine Environmental Research*, *185*(January), 105884. <https://doi.org/10.1016/j.marenvres.2023.105884>
- Dworjanyn, S. A., De Nys, R., & Steinberg, P. D. (1999). Localisation and surface quantification of secondary metabolites in the red alga *Delisea pulchra*. *Marine Biology*, *133*(4), 727–736. <https://doi.org/10.1007/s002270050514>
- Eddy, T. D., Lam, V. W. Y., Reygondeau, G., Cisneros-Montemayor, A. M., Greer, K., Palomares, M. L. D., Bruno, J. F., Ota, Y., & Cheung, W. W. L. (2021). Global decline in capacity of coral reefs to provide ecosystem services. *One Earth*, *4*(9), 1278–1285. <https://doi.org/10.1016/j.oneear.2021.08.016>
- Eggertsen, L., Ferreira, C. E. L., Fontoura, L., Kautsky, N., Gullström, M., & Berkström, C. (2017). Seaweed beds support more juvenile reef fish than seagrass beds in a south-western Atlantic tropical seascape. *Estuarine, Coastal and Shelf Science*, *196*, 97–108. <https://doi.org/10.1016/j.ecss.2017.06.041>
- Engelberts, J. P., Robbins, S. J., Damjanovic, K., & Webster, N. S. (2021). Integrating novel tools to elucidate the metabolic basis of microbial symbiosis in reef holobionts. *Marine Biology*, *168*(12). <https://doi.org/10.1007/s00227-021-03952-6>
- Engelhardt, K. E., Vetter, J., Wöhrmann-Zipf, F., Dietzmann, A., Proll, F. M., Reifert, H., Schüll, I., Stahlmann, M., & Ziegler, M. (2023). Contact-free impacts of sessile reef organisms on stony coral productivity. *Communications Earth and Environment*, *4*(396), 1–11. <https://doi.org/10.1038/s43247-023-01052-5>
- Enoki, N., Ishida, R., & Matsumoto, T. (1982). Structures and conformations of new nine-membered ring diterpenoids from the marine alga *Dictyota dichotoma*. *Chemistry Letters*, *11*(11), 1749–1752. <https://doi.org/10.1246/cl.1982.1749>
- Epstein, H. E., Torda, G., Munday, P. L., & van Oppen, M. J. H. (2019a). Parental and early life stage environments drive establishment of bacterial and dinoflagellate communities in a common coral. *ISME Journal*, *13*(6), 1635–1638. <https://doi.org/10.1038/s41396-019-0358-3>
- Epstein, H. E., Torda, G., & van Oppen, M. J. H. (2019b). Relative stability of the *Pocillopora acuta* microbiome throughout a thermal stress event. *Coral Reefs*, *38*(2), 373–386. <https://doi.org/10.1007/s00338-019-01783-y>

- Ernst, M., Kang, K. Bin, Caraballo-Rodríguez, A. M., Nothias, L. F., Wandy, J., Chen, C., Wang, M., Rogers, S., Medema, M. H., Dorrestein, P. C., & van der Hooft, J. J. J. (2019). Molnetenhancer: Enhanced molecular networks by integrating metabolome mining and annotation tools. *Metabolites*, *9*(7), 1–25. <https://doi.org/10.3390/metabo9070144>
- Erwin, P. M., Song, B., & Szmant, A. M. (2008). Settlement behavior of *Acropora palmata* planulae: Effects of biofilm age and crustose coralline algal cover. *Proceedings of the 11th International Coral Reef Symposium, Florida*, *24*, 1219–1223.
- Evans, R. D., Wilson, S. K., Field, S. N., & Moore, J. A. Y. (2014). Importance of macroalgal fields as coral reef fish nursery habitat in north-west Australia. *Marine Biology*, *161*(3), 599–607. <https://doi.org/10.1007/s00227-013-2362-x>
- Evensen, N., Morrow, K., Mumby, P., Motti, C., & Doropoulos, C. (2019b). Inhibition of coral settlement at multiple spatial scales by a pervasive algal competitor. *Marine Ecology Progress Series*, *612*, 29–42. <https://doi.org/10.3354/meps12879>
- Evensen, N. R., Doropoulos, C., Wong, K. J., & Mumby, P. J. (2019a). Stage-specific effects of *Lobophora* on the recruitment success of a reef-building coral. *Coral Reefs*, *38*(3), 489–498. <https://doi.org/10.1007/s00338-019-01804-w>
- Evensen, N. R., Vanwonderghem, I., Doropoulos, C., Gouezo, M., Botté, E. S., Webster, N. S., & Mumby, P. J. (2021). Benthic micro- and macro-community succession and coral recruitment under overfishing and nutrient enrichment. *Ecology*, *102*(12), 1–16. <https://doi.org/10.1002/ecy.3536>
- Fabricius, K. E., Crossman, K., Jonker, M., Mongin, M., & Thompson, A. (2023). Macroalgal cover on coral reefs: Spatial and environmental predictors, and decadal trends in the Great Barrier Reef. *PLoS ONE*, *18*(1), 1–21. <https://doi.org/10.1371/journal.pone.0279699>
- Falkowski, P. G., Dubinsky, Z., Muscatine, L., & Porter, J. W. (1984). Light and the bioenergetics of a symbiotic coral. *BioScience*, *34*(11), 705–709.
- Fernandes, N., Case, R. J., Longford, S. R., Seyedsayamdost, M. R., Steinberg, P. D., Kjelleberg, S., & Thomas, T. (2011). Genomes and virulence factors of novel bacterial pathogens causing bleaching disease in the marine red alga *Delisea pulchra*. *PLoS ONE*, *6*(12), e27387. <https://doi.org/10.1371/journal.pone.0027387>
- Fernandez, E., Ostrowski, M., Siboni, N., Seymour, J. R., & Petrou, K. (2021). Uptake of dimethylsulfoniopropionate (DMSP) by natural microbial communities of the Great Barrier Reef (GBR), Australia. *Microorganisms*, *9*(9), 1–23. <https://doi.org/10.3390/microorganisms9091891>
- Feunang, Y. D., Eisner, R., Knox, C., Chepelev, L., Hastings, J., Owen, G., Fahy, E., Steinbeck, C., Subramanian, S., Bolton, E., Greiner, R., & Wishart, D. S. (2016). ClassyFire: automated chemical classification with a comprehensive, computable taxonomy. *Journal of Cheminformatics*, *8*(1), 1–20. <https://doi.org/10.1186/s13321-016-0174-y>

- Fiore, C. L., Freeman, C. J., & Kujawinski, E. B. (2017). Sponge exhalent seawater contains a unique chemical profile of dissolved organic matter. *PeerJ*, *5*:e2870(1), 1–22. <https://doi.org/10.7717/peerj.2870>
- Fong, C. R., Chancellor, K. S., Renzi, J. J., Robinson, D. R., Barber, P. H., Habtes, S. Y., & Fong, P. (2018). Epibionts on *Turbinaria ornata*, a secondary foundational macroalga on coral reefs, provide diverse trophic support to fishes. *Marine Environmental Research*, *141*(August), 39–43. <https://doi.org/10.1016/j.marenvres.2018.08.001>
- Fong, J., Deignan, L. K., Bauman, A. G., Steinberg, P. D., Mcdougald, D., Todd, P. A., & Kelly, L. W. (2020). Contact- and water-mediated effects of macroalgae on the physiology and microbiome of three Indo-Pacific coral species. *Frontiers in Marine Science*, *6*(January), 1–11. <https://doi.org/10.3389/fmars.2019.00831>
- Fong, J., Lim, Z. W., Bauman, A. G., Valiyaveetil, S., Liao, L. M., Yip, Z. T., & Todd, P. A. (2019). Allelopathic effects of macroalgae on *Pocillopora acuta* coral larvae. *Marine Environmental Research*, *March*. <https://doi.org/10.1016/j.marenvres.2019.06.007>
- Fong, J., Tang, P. P. Y., Deignan, L. K., Seah, J. C. L., Mcdougald, D., Rice, S. A., & Todd, P. A. (2023). Chemically mediated interactions with macroalgae negatively affect coral health but induce limited changes in coral microbiomes. *Microorganisms*, *11*(2261), 1–13.
- Fong, P., Frazier, N. M., Tompkins-Cook, C., Muthukrishnan, R., & Fong, C. R. (2016). Size matters: experimental partitioning of the strength of fish herbivory on a fringing coral reef in Moorea, French Polynesia. *Marine Ecology*, *37*(5), 933–942. <https://doi.org/10.1111/maec.12298>
- Fong, P., & Paul, V. J. (2011). Coral reef algae. In Z. Dubinsky & N. Stambler (Eds.), *Coral Reefs: An Ecosystem in Transition* (Issue August 2015, pp. 241–271). Springer Dordrecht. <https://doi.org/https://doi.org/10.1007/978-94-007-0114-4>
- Foster, N. L., Box, S. J., & Mumby, P. J. (2008). Competitive effects of macroalgae on the fecundity of the reef-building coral *Montastraea annularis*. *Marine Ecology Progress Series*, *367*(Lirman 2001), 143–152. <https://doi.org/10.3354/meps07594>
- Frade, P. R., Glasl, B., Matthews, S. A., Mellin, C., Serrão, E. A., Wolfe, K., Mumby, P. J., Webster, N. S., & Bourne, D. G. (2020). Spatial patterns of microbial communities across. *Communications Biology*, *3*(442), 1–14. <https://doi.org/10.1038/s42003-020-01166-y>
- Frade, P. R., Schwaninger, V., Glasl, B., Sintes, E., Hill, R. W., Simo, R., & Herndl, G. J. (2016). Dimethylsulfoniopropionate in corals and its interrelations with bacterial assemblages in coral surface mucus. *Environmental Chemistry*, *13*(2), 252–265.
- Freire, I., Gutner-Hoch, E., Muras, A., Benayahu, Y., & Otero, A. (2019). The effect of bacteria on planula-larvae settlement and metamorphosis in the octocoral *Rhytisma fulvum fulvum*. *PLoS ONE*, *14*(9), 1–18. <https://doi.org/10.1371/journal.pone.0223214>
- Frölicher, T. L., Fischer, E. M., & Gruber, N. (2018). Marine heatwaves under global warming. *Nature*, *560*(7718), 360–364. <https://doi.org/10.1038/s41586-018-0383-9>

- Furukawa, T., Nishida, M., Hada, T., Kuramochi, K., Sugawara, F., Kobayashi, S., Lijima, H., Shimada, H., Yoshida, H., & Mizushima, Y. (2007). Inhibitory effect of sulfoquinovosyl diacylglycerol on prokaryotic DNA polymerase I activity and cell growth of *Escherichia coli*. *Journal of Oleo Science*, 56(1), 43–47. <https://doi.org/10.5650/jos.56.43>
- Garg, N. (2021). Metabolomics in functional interrogation of individual holobiont members. *MSystems*, 6(4). <https://doi.org/10.1128/msystems.00841-21>
- Garren, M., Son, K., Raina, J. B., Rusconi, R., Menolascina, F., Shapiro, O. H., Tout, J., Bourne, D. G., Seymour, J. R., & Stocker, R. (2014). A bacterial pathogen uses dimethylsulfoniopropionate as a cue to target heat-stressed corals. *ISME Journal*, 8(5), 999–1007. <https://doi.org/10.1038/ismej.2013.210>
- Gast, G. J., Wiegman, S., Wieringa, E., Van Duyl, F. C., & Bak, R. P. M. (1998). Bacteria in coral reef water types: Removal of cells, stimulation of growth and mineralization. *Marine Ecology Progress Series*, 167, 37–45. <https://doi.org/10.3354/meps167037>
- Gerwick, W. H., & Fenical, W. (1981). Spatane diterpenoids from the tropical marine alga *Stoechospermum marginatum* (Dictyotaceae). *The Journal of Organic Chemistry*, 46(11), 2233–2241.
- Ghisalberti, M., & Nepf, H. (2006). The structure of the shear layer in flows over rigid and flexible canopies. *Environmental Fluid Mechanics*, 6(3), 277–301. <https://doi.org/10.1007/s10652-006-0002-4>
- Gibbin, E., Gavish, A., Domart-Coulon, I., Kramarsky-Winter, E., Shapiro, O., Meibom, A., & Vardi, A. (2018). Using NanoSIMS coupled with microfluidics to visualize the early stages of coral infection by *Vibrio coralliilyticus*. *BMC Microbiology*, 18(1), 1–10. <https://doi.org/10.1186/s12866-018-1173-0>
- Gignoux-Wolfsohn, S. A., Aronson, F. M., & Vollmer, S. V. (2017). Complex interactions between potentially pathogenic, opportunistic, and resident bacteria emerge during infection on a reef-building coral. *FEMS Microbiology Ecology*, 93(7), 1–10. <https://doi.org/10.1093/FEMSEC/FIX080>
- Gil-Turnes, M. S., Hay, M. E., & Fenical, W. (1989). Symbiotic marine bacteria chemically defend crustacean embryos from a pathogenic fungus. *Science*, 246(4926), 116–118. <https://doi.org/10.1126/science.2781297>
- Glasl, B., Herndl, G. J., & Frade, P. R. (2016). The microbiome of coral surface mucus has a key role in mediating holobiont health and survival upon disturbance. *ISME Journal*, 10(9), 2280–2292. <https://doi.org/10.1038/ismej.2016.9>
- Glasl, B., Robbins, S., Frade, P. R., Marangon, E., Laffy, P. W., Bourne, D. G., & Webster, N. S. (2020). Comparative genome-centric analysis reveals seasonal variation in the function of coral reef microbiomes. *ISME Journal*, 14(6), 1435–1450. <https://doi.org/10.1038/s41396-020-0622-6>

- Gleason, D. F., Danilowicz, B. S., & Nolan, C. J. (2009). Reef waters stimulate substratum exploration in planulae from brooding Caribbean corals. *Coral Reefs*, 28(2), 549–554. <https://doi.org/10.1007/s00338-009-0480-1>
- Gleason, D. F., & Hofmann, D. K. (2011). Coral larvae: From gametes to recruits. *Journal of Experimental Marine Biology and Ecology*, 408(1–2), 42–57. <https://doi.org/10.1016/j.jembe.2011.07.025>
- Gloor, G. B., Macklaim, J. M., Pawlowsky-Glahn, V., & Egozcue, J. J. (2017). Microbiome datasets are compositional: And this is not optional. *Frontiers in Microbiology*, 8(NOV), 1–6. <https://doi.org/10.3389/fmicb.2017.02224>
- Godwin, S., Bent, E., Borneman, J., & Pereg, L. (2012). The role of coral-associated bacterial communities in Australian Subtropical White Syndrome of *Turbinaria mesenterina*. *PLoS ONE*, 7(9), e44243. <https://doi.org/10.1371/journal.pone.0044243>
- González, I., Cao, K. A. L., Davis, M. J., & Déjean, S. (2012). Visualising associations between paired “omics” data sets. *BioData Mining*, 5(1), 1–23. <https://doi.org/10.1186/1756-0381-5-19>
- Gouezo, M., Olsudong, D., Fabricius, K., Harrison, P., Golbuu, Y., & Doropoulos, C. (2020). Relative roles of biological and physical processes influencing coral recruitment during the lag phase of reef community recovery. *Scientific Reports*, 10(1), 1–12. <https://doi.org/10.1038/s41598-020-59111-2>
- Graham, E. M., Baird, A. H., & Connolly, S. R. (2008). Survival dynamics of scleractinian coral larvae and implications for dispersal. *Coral Reefs*, 27(3), 529–539. <https://doi.org/10.1007/s00338-008-0361-z>
- Graham, N. A. J., Jennings, S., MacNeil, M. A., Mouillot, D., & Wilson, S. K. (2015). Predicting climate-driven regime shifts versus rebound potential in coral reefs. *Nature*, 518(7537), 94–97. <https://doi.org/10.1038/nature14140>
- Graham, N. A. J., & Nash, K. L. (2013). The importance of structural complexity in coral reef ecosystems. *Coral Reefs*, 32(2), 315–326. <https://doi.org/10.1007/s00338-012-0984-y>
- Guella, G., Chiasera, G., N'Diaye, I., & Pietra, F. (1994). Xenicane diterpenes revisited: Thermal (E)→(Z) isomerization and conformational motions. A unifying picture. *Helvetica Chimica Acta*, 77(5), 1203–1221. <https://doi.org/10.1002/hlca.19940770503>
- Guest, J. R., Baird, A. H., Maynard, J. A., Muttaqin, E., Edwards, A. J., Campbell, S. J., Yewdall, K., Affendi, Y. A., & Chou, L. M. (2012). Contrasting patterns of coral bleaching susceptibility in 2010 suggest an adaptive response to thermal stress. *PLoS ONE*, 7(3), 1–8. <https://doi.org/10.1371/journal.pone.0033353>
- Guibert, I., Bonnard, I., Pochon, X., Zubia, M., Sidobre, C., Lecellier, G., & Berteaux-Lecellier, V. (2019). Differential effects of coral-giant clam assemblages on biofouling formation. *Scientific Reports*, 9(1). <https://doi.org/10.1038/s41598-019-39268-1>

- Guillonau, R., Baraquet, C., Bazire, A., & Molmeret, M. (2018). Multispecies biofilm development of marine bacteria implies complex relationships through competition and synergy and modification of matrix components. *Frontiers in Microbiology*, 9(AUG), 1–15. <https://doi.org/10.3389/fmicb.2018.01960>
- Guschina, I. A., & Harwood, J. L. (2006). Lipids and lipid metabolism in eukaryotic algae. *Progress in Lipid Research*, 45(2), 160–186. <https://doi.org/10.1016/j.plipres.2006.01.001>
- Haas, A., el-Zibdah, M., & Wild, C. (2010). Seasonal monitoring of coral-algae interactions in fringing reefs of the Gulf of Aqaba, Northern Red Sea. *Coral Reefs*, 29(1), 93–103. <https://doi.org/10.1007/s00338-009-0556-y>
- Haas, A. F., Fairoz, M. F. M., Kelly, L. W., Nelson, C. E., Dinsdale, E. A., Edwards, R. A., Giles, S., Hatay, M., Hisakawa, N., Knowles, B., Lim, Y. W., Maughan, H., Pantos, O., Roach, T. N. F., Sanchez, S. E., Silveira, C. B., Sandin, S., Smith, J. E., & Rohwer, F. (2016). Global microbialization of coral reefs. *Nature Microbiology*, 1(6), 1–7. <https://doi.org/10.1038/nmicrobiol.2016.42>
- Haas, A. F., Gregg, A. K., Smith, J. E., Abieri, M. L., Hatay, M., & Rohwer, F. (2013b). Visualization of oxygen distribution patterns caused by coral and algae. *PeerJ*, 1, e106. <https://doi.org/10.7717/peerj.106>
- Haas, A. F., Jantzen, C., Naumann, M. S., Iglesias-Prieto, R., & Wild, C. (2010). Organic matter release by the dominant primary producers in a Caribbean reef lagoon: Implication for in situ O₂ availability. *Marine Ecology Progress Series*, 409(Lesser 2004), 27–39. <https://doi.org/10.3354/meps08631>
- Haas, A. F., Nelson, C. E., Kelly, L. W., Carlson, C. A., Rohwer, F., Leichter, J. J., Wyatt, A., & Smith, J. E. (2011). Effects of coral reef benthic primary producers on dissolved organic carbon and microbial activity. *PLoS ONE*, 6(11), e27973. <https://doi.org/10.1371/journal.pone.0027973>
- Haas, A. F., Nelson, C. E., Rohwer, F., Wegley-Kelly, L., Quistad, S. D., Carlson, C. A., Leichter, J. J., Hatay, M., & Smith, J. E. (2013a). Influence of coral and algal exudates on microbially mediated reef metabolism. *PeerJ*, 1, e108. <https://doi.org/10.7717/peerj.108>
- Haas, A. F., Smith, J. E., Thompson, M., & Deheyn, D. D. (2014). Effects of reduced dissolved oxygen concentrations on physiology and fluorescence of hermatypic corals and benthic algae. *PeerJ*, 2014(1), 1–19. <https://doi.org/10.7717/peerj.235>
- Harii, S., Kayanne, H., Takigawa, H., Hayashibara, T., & Yamamoto, M. (2002). Larval survivorship, competency periods and settlement of two brooding corals, *Heliopora coerulea* and *Pocillopora damicornis*. *Marine Biology*, 141(1), 39–46. <https://doi.org/10.1007/s00227-002-0812-y>
- Hartig, F. (2017). DHARMA: Residual diagnostics for hierarchical (multi-level/mixed) regression models. *R package version 0.4.6*.

- Hatcher, B. G. (1984). A maritime accident provides evidence for alternate stable states in benthic communities on coral reefs. *Coral Reefs*, 3(4), 199–204. <https://doi.org/10.1007/BF00288255>
- Hatcher, B. G. (1988). Reef primary productivity: a beggar's banquet. *Tree*, 3(5), 106–111. [https://doi.org/10.1016/0169-5347\(88\)90117-6](https://doi.org/10.1016/0169-5347(88)90117-6)
- Hatcher, B. G. (1997). Coral reef ecosystems - how much greater is the whole than the sum of the parts. *Coral Reefs*, 16, 77–91.
- Haydon, T. D., Matthews, J. L., Seymour, J. R., Raina, J., Seymour, J. E., Chartrand, K., Camp, E. F., Suggett, D. J., Jr, S., J-b, R., Je, S., Ef, C., Metabolomic, S. D. J., & Haydon, T. D. (2023). Metabolomic signatures of corals thriving across extreme reef habitats reveal strategies of heat stress tolerance. *Proceedings of the Royal Society B*, 290.
- Heavisides, E., Rouger, C., Reichel, A. F., Ulrich, C., Wenzel-Storjohann, A., Sebens, S., & Tasdemir, D. (2018). Seasonal variations in the metabolome and bioactivity profile of *Fucus vesiculosus* extracted by an optimised, pressurised liquid extraction protocol. *Marine Drugs*, 16(12), 1–28. <https://doi.org/10.3390/md16120503>
- Hench, J. L., Leichter, J. J., & Monismith, S. G. (2008). Episodic circulation and exchange in a wave-driven coral reef and lagoon system. *Limnology and Oceanography*, 53(6), 2681–2694. <https://doi.org/10.4319/lo.2008.53.6.2681>
- Hench, J. L., & Rosman, J. H. (2013). Observations of spatial flow patterns at the coral colony scale on a shallow reef flat. *Journal of Geophysical Research: Oceans*, 118(3), 1142–1156. <https://doi.org/10.1002/jgrc.20105>
- Heringdorf, Dagmar. M. z. (2008). Lysophospholipids. In S. Offermanns & W. Rosenthal (Eds.), *Encyclopedia of Molecular Pharmacology* (pp. 710–716). Springer, Berlin, Heidelberg. https://doi.org/https://doi.org/10.1007/978-3-540-38918-7_90
- Herren, L. W., Walters, L. J., & Beach, K. S. (2006). Fragment generation, survival, and attachment of *Dictyota spp.* at Conch Reef in the Florida Keys, USA. *Coral Reefs*, 25(2), 287–295. <https://doi.org/10.1007/s00338-006-0096-7>
- Hervé, M. R. (2023). Package ‘RVAideMemoire’: Testing and plotting procedures for biostatistics. *R package 0.9-81-2*
- Hervé, M. R., Nicolè, F., & Lê Cao, K. A. (2018). Multivariate analysis of multiple datasets: a practical guide for chemical ecology. *Journal of Chemical Ecology*, 44(3), 215–234. <https://doi.org/10.1007/s10886-018-0932-6>
- Hicks, C. C., & Cinner, J. E. (2014). Social, institutional, and knowledge mechanisms mediate diverse Ecosystem service benefits from coral reefs. *Proceedings of the National Academy of Sciences of the United States of America*, 111(50), 17791–17796. <https://doi.org/10.1073/pnas.1413473111>
- Hillyer, K. E., Dias, D. A., Lutz, A., Wilkinson, S. P., Roessner, U., & Davy, S. K. (2017). Metabolite profiling of symbiont and host during thermal stress and bleaching in the coral

- Acropora aspera*. *Coral Reefs*, 36(1), 105–118. <https://doi.org/10.1007/s00338-016-1508-y>
- Hochart, C., Paoli, L., Ruscheweyh, H., Salazar, G., Boissin, E., Romac, S., Poulain, J., Bourdin, G., Iwankow, G., Moulin, C., Ziegler, M., Porro, B., Armstrong, E. J., Hume, B. C. C., Aury, J., Pogoreutz, C., Paz-garcía, D. A., Planes, S., Thurber, R. V., ... Galand, P. E. (2023). Ecology of Endozoicomonadaceae in three coral genera across the Pacific Ocean. *Nature Communications*, 14(October 2022). <https://doi.org/10.1038/s41467-023-38502-9>
- Hoegh-Guldberg, O., Mumby, P. J., Hooten, A. J., Steneck, R. S., Greenfield, P., Gomez, E., Harvell, C. D., Sale, P. F., Edwards, A. J., Caldeira, K., Knowlton, N., Eakin, C. M., Iglesias-Prieto, R., Muthiga, N., Bradbury, R. H., Dubi, A., & Hatziolos, M. E. (2007). Coral reefs under rapid climate change and ocean acidification. *Science (New York, N.Y.)*, 318(5857), 1737–1742. <https://doi.org/10.1126/science.1152509>
- Hoey, A. S., & Bellwood, D. R. (2011). Suppression of herbivory by macroalgal density: A critical feedback on coral reefs? *Ecology Letters*, 14(3), 267–273. <https://doi.org/10.1111/j.1461-0248.2010.01581.x>
- Holbrook, S. J., Adam, T. C., Edmunds, P. J., Schmitt, R. J., Carpenter, R. C., Brooks, A. J., Lenihan, H. S., & Briggs, C. J. (2018). Recruitment drives spatial variation in recovery rates of resilient coral reefs. *Scientific Reports*, 8(1), 1–11. <https://doi.org/10.1038/s41598-018-25414-8>
- Holbrook, S. J., Schmitt, R. J., Adam, T. C., & Brooks, A. J. (2016). Coral reef resilience, tipping points and the strength of herbivory. *Scientific Reports*, 6(November), 1–11. <https://doi.org/10.1038/srep35817>
- Huggett, M. J., & Apprill, A. (2019). Coral microbiome database: Integration of sequences reveals high diversity and relatedness of coral-associated microbes. *Environmental Microbiology Reports*, 11(3), 372–385. <https://doi.org/10.1111/1758-2229.12686>
- Hughes, A. D., & Grottoli, A. G. (2013). Heterotrophic compensation: A possible mechanism for resilience of coral reefs to global warming or a sign of prolonged stress? *PLoS ONE*, 8(11), 1–10. <https://doi.org/10.1371/journal.pone.0081172>
- Hughes, T. P. (1994). Catastrophes, phase shifts, and large-scale reef degradation in the Caribbean. *Science*, 265(September), 1547–1551.
- Hughes, T. P., Anderson, K. D., Connolly, S. R., Heron, S. F., Kerry, J. T., Lough, J. M., Baird, A. H., Baum, J. K., Berumen, M. L., Bridge, T. C., Claar, D. C., Eakin, C. M., Gilmour, J. P., Graham, N. A. J., Harrison, H., Hobbs, J.-P. A., Hoey, A. S., Hoogenboom, M., Lowe, R. J., ... Wilson, S. K. (2018). Spatial and temporal patterns of mass bleaching of corals in the Anthropocene. *Published Science*, 5(80), 80–83. <https://doi.org/10.1126/science.aan8048>
- Hughes, T. P., Baird, A. H., Morrison, T. H., & Torda, G. (2023). Principles for coral reef restoration in the Anthropocene. *One Earth*, 6(6), 656–665. <https://doi.org/10.1016/j.oneear.2023.04.008>

- Hughes, T. P., Barnes, M. L., Bellwood, D. R., Cinner, J. E., Cumming, G. S., Jackson, J. B. C., Kleypas, J., Leemput, I. A. Van De, Lough, J. M., Morrison, T. H., Palumbi, S. R., Nes, E. H. Van, & Scheffer, M. (2017). *Coral reefs in the Anthropocene*. <https://doi.org/10.1038/nature22901>
- Hughes, T. P., Graham, N. A. J., Jackson, J. B. C., Mumby, P. J., & Steneck, R. S. (2010). Rising to the challenge of sustaining coral reef resilience. *Trends in Ecology and Evolution*, 25(11), 633–642. <https://doi.org/10.1016/j.tree.2010.07.011>
- Hughes, T. P., Reed, D. C., & Boyle, M. J. (1987). Herbivory on coral reefs: community structure following mass mortalities of sea urchins. *Journal of Experimental Marine Biology and Ecology*, 113(1), 39–59. [https://doi.org/10.1016/0022-0981\(87\)90081-5](https://doi.org/10.1016/0022-0981(87)90081-5)
- Hughes, T. P., Rodrigues, M. J., Bellwood, D. R., Ceccarelli, D., Hoegh-Guldberg, O., McCook, L., Moltschaniwskyj, N., Pratchett, M. S., Steneck, R. S., & Willis, B. (2007). Phase shifts, herbivory, and the resilience of coral reefs to climate change. *Current Biology*, 17(4), 360–365. <https://doi.org/10.1016/j.cub.2006.12.049>
- Huntley, N., Brandt, M. E., Becker, C. C., Miller, C. A., Meiling, S. S., Correa, A. M. S., Holstein, D. M., Muller, E. M., Mydlarz, L. D., Smith, T. B., & Apprill, A. (2022). Experimental transmission of Stony Coral Tissue Loss Disease results in differential microbial responses within coral mucus and tissue. *ISME Communications*, 2(1), 1–11. <https://doi.org/10.1038/s43705-022-00126-3>
- Hurd, C. L. (2000). Water motion, marine macroalgal physiology, and production. *Journal of Phycology*, 36(3), 453–472. <https://doi.org/10.1046/j.1529-8817.2000.99139.x>
- Idjadi, J. A., Haring, R. N., & Precht, W. F. (2010). Recovery of the sea urchin *Diadema antillarum* promotes scleractinian coral growth and survivorship on shallow Jamaican reefs. *Marine Ecology Progress Series*, 403(Woodley 1989), 91–100. <https://doi.org/10.3354/meps08463>
- Ioannou, E., Zervou, M., Ismail, A., Ktari, L., Vagias, C., & Roussis, V. (2009). 2,6-Cyclo-xenicanes from the brown algae *Dilophus fasciola* and *Dilophus spiralis*. *Tetrahedron*, 65(51), 10565–10572. <https://doi.org/10.1016/j.tet.2009.10.081>
- Isomura, N., & Nishihira, M. (2001). Size variation of planulae and its effect on the lifetime of planulae in three pocilloporid corals. *Coral Reefs*, 20(3), 309–315. <https://doi.org/10.1007/s003380100180>
- Jessen, C., Villa Lizcano, J. F., Bayer, T., Roder, C., Aranda, M., Wild, C., & Voolstra, C. R. (2013). In-situ effects of eutrophication and overfishing on physiology and bacterial diversity of the Red Sea coral *Acropora hemprichii*. *PLoS ONE*, 8(4). <https://doi.org/10.1371/journal.pone.0062091>
- Johns, K. A., Emslie, M. J., Hoey, A. S., Osborne, K., Jonker, M. J., & Cheal, A. J. (2018). Macroalgal feedbacks and substrate properties maintain a coral reef regime shift. *Ecosphere*, 9(7). <https://doi.org/10.1002/ecs2.2349>

- Johnson, G. C., Pezner, A. K., Sura, S. A., & Fong, P. (2018). Nutrients and herbivory, but not sediments, have opposite and independent effects on the tropical macroalga, *Padina boryana*. *Journal of Experimental Marine Biology and Ecology*, 507(February), 17–22. <https://doi.org/10.1016/j.jembe.2018.07.004>
- Johnson, J. S., Spakowicz, D. J., Hong, B. Y., Petersen, L. M., Demkowicz, P., Chen, L., Leopold, S. R., Hanson, B. M., Agresta, H. O., Gerstein, M., Sodergren, E., & Weinstock, G. M. (2019). Evaluation of 16S rRNA gene sequencing for species and strain-level microbiome analysis. *Nature Communications*, 10(1), 1–11. <https://doi.org/10.1038/s41467-019-13036-1>
- Jongaramruong, J., & Kongkam, N. (2007). Novel diterpenes with cytotoxic, anti-malarial and anti-tuberculosis activities from a brown alga *Dictyota sp.* *Journal of Asian Natural Products Research*, 9(8), 743–751. <https://doi.org/10.1080/10286020701189203>
- Jorissen, H., Galand, P. E., Bonnard, I., Meiling, S., Raviglione, D., Meistertzheim, A. L., Hédouin, L., Banaigs, B., Payri, C. E., & Nugues, M. M. (2021). Coral larval settlement preferences linked to crustose coralline algae with distinct chemical and microbial signatures. *Scientific Reports*, 11(1), 1–11. <https://doi.org/10.1038/s41598-021-94096-6>
- Jorissen, H., Skinner, C., Osinga, R., Beer, D. De, & Nugues, M. M. (2016). Evidence for water-mediated mechanisms in coral – algal interactions. *Proceedings of the Royal Society B-Biological Sciences*, 283(1836), 20161137.
- Jung, M. Y., Shin, K. S., Kim, S., Kim, S. J., Park, S. J., Kim, J. G., Cha, I. T., Kim, M. N., & Rhee, S. K. (2013). *Hoeflea halophila sp. nov.*, a novel bacterium isolated from marine sediment of the East Sea, Korea. *Antonie van Leeuwenhoek, International Journal of General and Molecular Microbiology*, 103(5), 971–978. <https://doi.org/10.1007/s10482-013-9876-6>
- Jutfelt, F., Sundin, J., Raby, G. D., Krång, A. S., & Clark, T. D. (2017). Two-current choice flumes for testing avoidance and preference in aquatic animals. *Methods in Ecology and Evolution*, 8(3), 379–390. <https://doi.org/10.1111/2041-210X.12668>
- Kabeya, N., Fonseca, M. M., Ferrier, D. E. K., Navarro, J. C., Bay, L. K., Francis, D. S., Tocher, D. R., Castro, L. F. C., & Monroig, Ó. (2018). Genes for de novo biosynthesis of omega-3 polyunsaturated fatty acids are widespread in animals. *Science Advances*, 4(5), 1–9. <https://doi.org/10.1126/sciadv.aar6849>
- Kalivodová, A., Hron, K., Filzmoser, P., Najdekr, L., Janečková, H., & Adam, T. (2015). PLS-DA for compositional data with application to metabolomics. *Journal of Chemometrics*, 29(1), 21–28. <https://doi.org/10.1002/cem.2657>
- Kayal, M., Lenihan, H. S., Brooks, A. J., Holbrook, S. J., Schmitt, R. J., & Kendall, B. E. (2018). Predicting coral community recovery using multi-species population dynamics models. *Ecology Letters*, 21(12), 1790–1799. <https://doi.org/10.1111/ele.13153>
- Kayal, M., Vercelloni, J., Lison de Loma, T., Bosserelle, P., Chancerelle, Y., Geoffroy, S., Stievenart, C., Michonneau, F., Penin, L., Planes, S., & Adjeroud, M. (2012). Predator crown-of-thorns starfish (*Acanthaster planci*) outbreak, mass mortality of corals, and

- cascading effects on reef fish and benthic communities. *PLoS ONE*, 7(10). <https://doi.org/10.1371/journal.pone.0047363>
- Kegler, P., Kegler, H. F., Gärdes, A., Ferse, S. C. A., Lukman, M., Alfiansah, Y. R., Hassenrück, C., & Kunzmann, A. (2017). Bacterial biofilm communities and coral larvae settlement at different levels of anthropogenic impact in the Spermonde Archipelago, Indonesia. *Frontiers in Marine Science*, 4(AUG), 1–15. <https://doi.org/10.3389/fmars.2017.00270>
- Kellogg, C. A. (2004). Tropical Archaea: Diversity associated with the surface microlayer of corals. *Marine Ecology Progress Series*, 273, 81–88. <https://doi.org/10.3354/meps273081>
- Kenkel, C. D., Setta, S. P., & Matz, M. V. (2015). Heritable differences in fitness-related traits among populations of the mustard hill coral, *Porites astreoides*. *Heredity*, 115(6), 509–516. <https://doi.org/10.1038/hdy.2015.52>
- Kido Soule, M. C., Longnecker, K., Johnson, W. M., & Kujawinski, E. B. (2015). Environmental metabolomics: Analytical strategies. *Marine Chemistry*, 177, 374–387. <https://doi.org/10.1016/j.marchem.2015.06.029>
- Klindworth, A., Pruesse, E., Schweer, T., Peplies, J., Quast, C., Horn, M., & Glöckner, F. O. (2013). Evaluation of general 16S ribosomal RNA gene PCR primers for classical and next-generation sequencing-based diversity studies. *Nucleic Acids Research*, 41(1), 1–11. <https://doi.org/10.1093/nar/gks808>
- Kline, D. I., Kuntz, N. M., Breitbart, M., Knowlton, N., & Rohwer, F. (2006). Role of elevated organic carbon levels and microbial activity in coral mortality. *Marine Ecology Progress Series*, 314, 119–125. <https://doi.org/10.3354/meps314119>
- Klinges, J. G., Rosales, S. M., McMinds, R., Shaver, E. C., Shantz, A. A., Peters, E. C., Eitel, M., Wörheide, G., Sharp, K. H., Burkepile, D. E., Silliman, B. R., & Vega Thurber, R. L. (2019). Phylogenetic, genomic, and biogeographic characterization of a novel and ubiquitous marine invertebrate-associated Rickettsiales parasite, *Candidatus Aquarickettsia rohweri*, gen. nov., sp. nov. *ISME Journal*, 13(12), 2938–2953. <https://doi.org/10.1038/s41396-019-0482-0>
- Knowlton, N. (2001). The future of coral reefs. *Proceedings of the National Academy of Sciences of the United States of America*, 98(10), 5419–5425. <https://doi.org/10.1073/pnas.091092998>
- Knowlton, N., Brainard, R. E., Fisher, R., Moews, M., Plaisance, L., & Caley, M. J. (2010). Chapter 4: Coral Reef Biodiversity. *Life in the World's Oceans: Diversity, Distribution and Abundance*, 65–78.
- Knowlton, N., & Jackson, J. B. C. (2001). The ecology of coral reefs. Chapter 15. In *Marine community ecology* (Issue Paulay 1997, pp. 395–422).
- Koehl, M. A. R., Strother, J. A., Reidenbach, M. A., Koseff, J. R., & Hadfield, M. G. (2007). Individual-based model of larval transport to coral reefs in turbulent, wave-driven flow: Behavioral responses to dissolved settlement inducer. *Marine Ecology Progress Series*, 335(June 2014), 1–18. <https://doi.org/10.3354/meps335001>

- König, G. M., Wright, A. D., Sticher, O., & Ruegger, H. (1993). Four new hydroazulenoid diterpenes from the tropical marine brown alga *Dictyota volubilis*. *Planta Medica*, 59(2), 174–178. [https://doi.org/10.1016/S0040-4020\(01\)86260-8](https://doi.org/10.1016/S0040-4020(01)86260-8)
- Krediet, C. J., Ritchie, K. B., Paul, V. J., & Teplitski, M. (2013). Coral-associated microorganisms and their roles in promoting coral health and thwarting diseases. *Proceedings of the Royal Society B*, 280.
- Kregting, L. T., Stevens, C. L., Cornelisen, C. D., Pilditch, C. A., & Hurd, C. L. (2011). Effects of a small-bladed macroalgal canopy on benthic boundary layer dynamics: Implications for nutrient transport. *Aquatic Biology*, 14(1), 41–56. <https://doi.org/10.3354/ab00369>
- Kubaneck, J., Whalen, K. E., Engel, S., Kelly, S. R., Henkel, T. P., Fenical, W., & Pawlik, J. R. (2002). Multiple defensive roles for triterpene glycosides from two Caribbean sponges. *Oecologia*, 131(1), 125–136. <https://doi.org/10.1007/s00442-001-0853-9>
- Kuffner, I. B., Walters, L. J., Becerro, M. A., Paul, V. J., Ritson-Williams, R., & Beach, K. S. (2006). Inhibition of coral recruitment by macroalgae and cyanobacteria. *Marine Ecology Progress Series*, 323, 107–117. <https://doi.org/10.3354/meps323107>
- Kuhn, M. (2008). Building predictive models in R using the caret package. *Journal of Statistical Software*, 28(5), 1–26. <https://doi.org/10.18637/jss.v028.i05>
- Kuntz, N. M., Kline, D. I., Sandin, S. A., & Rohwer, F. (2005). Pathologies and mortality rates caused by organic carbon and nutrient stressors in three Caribbean coral species. *Marine Ecology Progress Series*, 294, 173–180. <https://doi.org/10.3354/meps294173>
- Lachnit, T., Fischer, M., Künzel, S., Baines, J. F., & Harder, T. (2013). Compounds associated with algal surfaces mediate epiphytic colonization of the marine macroalga *Fucus vesiculosus*. *FEMS Microbiology Ecology*, 84(2), 411–420. <https://doi.org/10.1111/1574-6941.12071>
- Lahti, L., & Shetty, S. (2017). Tools for microbiome analysis in R.
- LaRowe, D. E., & Van Cappellen, P. (2011). Degradation of natural organic matter: A thermodynamic analysis. *Geochimica et Cosmochimica Acta*, 75(8), 2030–2042. <https://doi.org/10.1016/j.gca.2011.01.020>
- Lawson, C. A., Raina, J. B., Deschaseaux, E., Hrebien, V., Possell, M., Seymour, J. R., & Suggett, D. J. (2021). Heat stress decreases the diversity, abundance and functional potential of coral gas emissions. *Global Change Biology*, 27(4), 879–891. <https://doi.org/10.1111/gcb.15446>
- Lê Cao, K.-A., & Welham, Z. M. (2021). Multivariate Data Integration Using R. In *Multivariate Data Integration Using R*. <https://doi.org/10.1201/9781003026860>
- Leite, D. C. A., Leão, P., Garrido, A. G., Lins, U., Santos, H. F., Pires, D. O., Castro, C. B., van Elsas, J. D., Zilberberg, C., Rosado, A. S., & Peixoto, R. S. (2017). Broadcast spawning

- coral *Mussismilia hispida* can vertically transfer its associated bacterial core. *Frontiers in Microbiology*, 8(FEB), 1–12. <https://doi.org/10.3389/fmicb.2017.00176>
- Lema, K. A., Bourne, D. G., & Willis, B. L. (2014). Onset and establishment of diazotrophs and other bacterial associates in the early life history stages of the coral *Acropora millepora*. *Molecular Ecology*, 23(19), 4682–4695. <https://doi.org/10.1111/mec.12899>
- Lesser, M. P., Mazel, C. H., Gorbunov, M. Y., & Falkowski, P. G. (2004). Discovery of symbiotic nitrogen-fixing cyanobacteria in corals. *Science*, 305(5686), 997–1000. <https://doi.org/10.1126/science.1099128>
- Lewis, J. B. (1977). Processes of organic production on coral reefs. *Biological Reviews*, 52, 305–347.
- Lin, H., & Peddada, S. Das. (2020). Analysis of compositions of microbiomes with bias correction. *Nature Communications*, 11(1), 1–11. <https://doi.org/10.1038/s41467-020-17041-7>
- Lirman, D. (2001). Competition between macroalgae and corals: Effects of herbivore exclusion and increased algal biomass on coral survivorship and growth. *Coral Reefs*, 19(4), 392–399. <https://doi.org/10.1007/s003380000125>
- Little, M., George, E. E., Arts, M. G. I., Shivak, J., Benler, S., Huckeba, J., Quinlan, Z. A., Boscaro, V., Mueller, B., Güemes, A. G. C., Rojas, M. I., White, B., Petras, D., Silveira, C. B., Haas, A. F., Kelly, L. W., Vermeij, M. J. A., Quinn, R. A., Keeling, P. J., ... Roach, T. N. F. (2021). Three-Dimensional molecular cartography of the Caribbean reef-building coral *Orbicella faveolata*. *Frontiers in Marine Science*, 8(April), 1–22. <https://doi.org/10.3389/fmars.2021.627724>
- Liu, C., Zhang, Y., Huang, L., Yu, X., Luo, Y., Jiang, L., Sun, Y., Liu, S., & Huang, H. (2022). Differences in fatty acids and lipids of massive and branching reef-building corals and response to environmental changes. *Frontiers in Marine Science*, 9(May), 1–10. <https://doi.org/10.3389/fmars.2022.882663>
- Liu, J., Zhang, Y., Liu, J., Zhong, H., Williams, B. T., Zheng, Y., Curson, A. R. J., Sun, C., Sun, H., Song, D., Mackenzie, B. W., Martínez, A. B., Todd, J. D., & Zhang, X. H. (2021). Bacterial dimethylsulfoniopropionate biosynthesis in the east china sea. *Microorganisms*, 9(3), 1–22. <https://doi.org/10.3390/microorganisms9030657>
- Longo, G. O., & Hay, M. E. (2017). Seaweed allelopathy to corals: are active compounds on, or in, seaweeds? *Coral Reefs*, 36(1), 247–253. <https://doi.org/10.1007/s00338-016-1526-9>
- Lory, S. (2014). The family Mycobacteriaceae. In E. Rosenberg, E. F. Delong, F. Thompson, S. Lory, & E. Stackebrandt (Eds.), *The Prokaryotes: Actinobacteria* (pp. 571–575). https://doi.org/10.1007/978-3-642-30138-4_339
- Lu, C., Zhang, Q., Huang, Q., Wang, S., Qin, X., Ren, T., & Xie, R. (2022). Significant shifts in microbial communities associated with scleractinian corals in response to algae overgrowth. *Microorganisms*, 10(2196), 1–15.

- Lu, Y., Jiang, J., Zhao, H., Han, X., Xiang, Y., & Zhou, W. (2020). Clade-specific sterol metabolites in dinoflagellate endosymbionts are associated with coral bleaching in response to environmental cues. *MSystems*, 5(5), e00765-20. <https://doi.org/10.1128/msystems.00765-20>
- Ludwig, M., Nothias, L. F., Dührkop, K., Koester, I., Fleischauer, M., Hoffmann, M. A., Petras, D., Vargas, F., Morsy, M., Aluwihare, L., Dorrestein, P. C., & Böcker, S. (2020). Database-independent molecular formula annotation using Gibbs sampling through ZODIAC. *Nature Machine Intelligence*, 2(10), 629–641. <https://doi.org/10.1038/s42256-020-00234-6>
- Luna, G. M., Biavasco, F., & Danovaro, R. (2007). Bacteria associated with the rapid tissue necrosis of stony corals. *Environmental Microbiology*, 9(7), 1851–1857. <https://doi.org/10.1111/j.1462-2920.2007.01287.x>
- Ma, L., Becker, C., Weber, L., Sullivan, C., Zgliczynski, B., Sandin, S., Brandt, M., Smith, T. B., & Apprill, A. (2022). Biogeography of reef water microbes from within-reef to global scales. *Aquatic Microbial Ecology*, 88, 81–94. <https://doi.org/10.3354/ame01985>
- MacKnight, N. J., Cobleigh, K., Lasseigne, D., Chaves-Fonnegra, A., Gutting, A., Dimos, B., Antoine, J., Fuess, L., Ricci, C., Butler, C., Muller, E. M., Mydlarz, L. D., & Brandt, M. (2021). Microbial dysbiosis reflects disease resistance in diverse coral species. *Communications Biology*, 4(1), 1–11. <https://doi.org/10.1038/s42003-021-02163-5>
- Maher, R. L., Rice, M. M., McMinds, R., Burkepile, D. E., & Vega Thurber, R. (2019). Multiple stressors interact primarily through antagonism to drive changes in the coral microbiome. *Scientific Reports*, 9(1), 1–12. <https://doi.org/10.1038/s41598-019-43274-8>
- Maire, J., Girvan, S. K., Barkla, S. E., Perez-Gonzalez, A., Suggett, D. J., Blackall, L. L., & van Oppen, M. J. H. (2021). Intracellular bacteria are common and taxonomically diverse in cultured and in hospite algal endosymbionts of coral reefs. *The ISME Journal*, 15(7), 2028–2042. <https://doi.org/10.1038/s41396-021-00902-4>
- Maire, J., Tandon, K., Collingro, A., van de Meene, A., Damjanovic, K., Gotze, C. R., Stephenson, S., Philip, G. K., Horn, M., Cantin, N. E., Blackall, L. L., & van Oppen, M. J. H. (2023). Colocalization and potential interactions of Endozoicomonas and chlamydiae in microbial aggregates of the coral *Pocillopora acuta*. *Science Advances*, 9(20), 1–16. <https://doi.org/10.1126/sciadv.adg0773>
- Mannocho-russo, H., Swift, S. O. I., Nakayama, K. K., Wall, C. B., Gentry, E. C., Panitchpakdi, M., Caraballo-rodriguez, A. M., Aron, A. T., Petras, D., Dorrestein, K., Dorrestein, T. K., Williams, T. M., Nalley, E. M., Altman-kurosaki, N. T., Martinelli, M., Kuwabara, J. Y., Darcy, J. L., Bolzani, V. S., Kelly, L. W., ... Nelson, C. E. (2023). Microbiomes and metabolomes of dominant coral reef primary producers illustrate a potential role for immunolipids in marine symbioses. *Communications Biology*, 6(896), 1–19. <https://doi.org/10.1038/s42003-023-05230-1>
- Marangon, E., Uthicke, S., Patel, F., Marzinelli, E. M., Bourne, D. G., Webster, N. S., & Laffy, P. W. (2023). Life-stage specificity and cross-generational climate effects on the

- microbiome of a tropical sea urchin (Echinodermata: Echinoidea). *Molecular Ecology*, October 2022, 1–16. <https://doi.org/10.1111/mec.1712>
- Marcellin-Gros, R., Piganeau, G., & Stien, D. (2020). Metabolomic insights into marine phytoplankton diversity. *Marine Drugs*, 18(2), 1–14. <https://doi.org/10.3390/md18020078>
- Martin, M. (2011). Cutadapt removes adapter sequences from high throughput sequencing reads. *EMBnet.Journal*, 17(1).
- Martinez, E., Maamaatuaiahutapu, K., Payri, C., & Ganachaud, A. (2007). *Turbinaria ornata* invasion in the Tuamotu Archipelago, French Polynesia: Ocean drift connectivity. *Coral Reefs*, 26(1), 79–86. <https://doi.org/10.1007/s00338-006-0160-3>
- Mass, T., Genin, A., Shavit, U., Grinstein, M., & Tchernov, D. (2010). Flow enhances photosynthesis in marine benthic autotrophs by increasing the efflux of oxygen from the organism to the water. *Proceedings of the National Academy of Sciences of the United States of America*, 107(6), 2527–2531. <https://doi.org/10.1073/pnas.0912348107>
- Matthews, J. L., Khalil, A., Siboni, N., Bougoure, J., Guagliardo, P., Kuzhiumparambil, U., DeMaere, M., Le Reun, N. M., Seymour, J. R., Suggett, D. J., & Raina, J. B. (2023). Coral endosymbiont growth is enhanced by metabolic interactions with bacteria. *Nature Communications*, 14(1). <https://doi.org/10.1038/s41467-023-42663-y>
- Mauduit, M., Derrien, M., Grenier, M., Greff, S., Molinari, S., Chevalloné, P., Simmler, C., & Pérez, T. (2023). In-situ capture and real-time enrichment of marine chemical diversity. *ACS Central Science*, 2. <https://doi.org/10.1021/acscentsci.3c00661>
- Maypa, A. P., & Raymundo, L. J. (2004). Algae-coral interactions: mediation of coral settlement, early survival, and growth by macroalgae. *Silliman Journal*, 45(2).
- McCauley, M., Goulet, T., & Jackson, C. (2022). Meta-analysis of cnidarian microbiomes reveals insights into the structure, specificity, and fidelity of marine associations. *Nature Communications*, 14(4899). <https://doi.org/10.1038/s41467-023-39876-6>
- McCook, L. J., Jompa, J., & Diaz-Pulido, G. (2001). Competition between corals and algae on coral reefs: A review of evidence and mechanisms. *Coral Reefs*, 19(4), 400–417. <https://doi.org/10.1007/s003380000129>
- McDevitt-Irwin, J. M., Baum, J. K., Garren, M., & Vega Thurber, R. L. (2017). Responses of coral-associated bacterial communities to local and global stressors. *Frontiers in Marine Science*, 4(AUG), 1–16. <https://doi.org/10.3389/fmars.2017.00262>
- McDevitt-Irwin, J. M., Garren, M., McMinds, R., Vega Thurber, R., & Baum, J. K. (2019). Variable interaction outcomes of local disturbance and El Niño-induced heat stress on coral microbiome alpha and beta diversity. *Coral Reefs*, 38(2), 331–345. <https://doi.org/10.1007/s00338-019-01779-8>
- McMurdie, P. J., & Holmes, S. (2013). Phyloseq: An R package for reproducible interactive analysis and graphics of microbiome census data. *PLoS ONE*, 8(4). <https://doi.org/10.1371/journal.pone.0061217>

- McNally, S. P., Parsons, R. J., Santoro, A. E., & Apprill, A. (2017). Multifaceted impacts of the stony coral *Porites astreoides* on picoplankton abundance and community composition. *Limnology and Oceanography*, *62*(1), 217–234. <https://doi.org/10.1002/lno.10389>
- Meyer, J. L., Castellanos-Gell, J., Aeby, G. S., Häse, C. C., Ushijima, B., & Paul, V. J. (2019). Microbial community shifts associated with the ongoing stony coral tissue loss disease outbreak on the Florida Reef Tract. *Frontiers in Microbiology*, *10*(September), 1–12. <https://doi.org/10.3389/fmicb.2019.02244>
- Michalek-Wagner, K., & Willis, B. L. (2001). Impacts of bleaching on the soft coral *Lobophytum compactum*. II. Biochemical changes in adults and their eggs. *Coral Reefs*, *19*(3), 240–246. <https://doi.org/10.1007/PL00006959>
- Mitchell, R., & Ducklow, H. W. (1979). Composition of mucus release by coral reef coelenterates. *Lim*, *24*(4), 706–714.
- Moberg, F., & Folke, C. (1999). Ecological goods and services of coral reef ecosystems. *Ecological Economics*, *29*(2), 215–233. [https://doi.org/10.1016/S0921-8009\(99\)00009-9](https://doi.org/10.1016/S0921-8009(99)00009-9)
- Modolon, F., Barno, A. R., Villela, H. D. M., & Peixoto, R. S. (2020). Ecological and biotechnological importance of secondary metabolites produced by coral-associated bacteria. *Journal of Applied Microbiology*, *129*(6), 1441–1457. <https://doi.org/10.1111/jam.14766>
- Mohamed, A. R., Ochsenkühn, M. A., Kazlak, A., Moustafa, A., & Amin, S. A. (2023). The coral microbiome: Towards an understanding of the molecular mechanisms of coral-microbiota interactions. *FEMS Microbiology Reviews*, *March*, 1–26. <https://doi.org/10.1093/femsre/fuad005>
- Mohimani, H., Gurevich, A., Shlemov, A., Mikheenko, A., Korobeynikov, A., Cao, L., Shcherbin, E., Nothias, L. F., Dorrestein, P. C., & Pevzner, P. A. (2018). Dereplication of microbial metabolites through database search of mass spectra. *Nature Communications*, *9*(1), 1–12. <https://doi.org/10.1038/s41467-018-06082-8>
- Monteil, Y., Teo, A., Fong, J., Bauman, A. G., & Todd, P. A. (2020). Effects of macroalgae on coral fecundity in a degraded coral reef system. *Marine Pollution Bulletin*, *151*(January), 110890. <https://doi.org/10.1016/j.marpolbul.2020.110890>
- Morrow, K. M., Bromhall, K., Motti, C. A., Munn, C. B., & Bourne, D. G. (2017). Allelochemicals produced by brown macroalgae of the *Lobophora* genus are active against coral larvae and associated bacteria, supporting pathogenic shifts to *Vibrio* dominance. *Applied and Environmental Microbiology*, *83*(1), 1–19. <https://doi.org/10.1128/AEM.02391-16>
- Morrow, K. M., Liles, M. R., Paul, V. J., Moss, A. G., & Chadwick, N. E. (2013). Bacterial shifts associated with coral-macroalgal competition in the Caribbean Sea. *Marine Ecology Progress Series*, *488*, 103–117. <https://doi.org/10.3354/meps10394>
- Morrow, K. M., Paul, V. J., Liles, M. R., & Chadwick, N. E. (2011). Allelochemicals produced by Caribbean macroalgae and cyanobacteria have species-specific effects on reef coral

- microorganisms. *Coral Reefs*, 30(2), 309–320. <https://doi.org/10.1007/s00338-011-0747-1>
- Morrow, K. M., Ritson-Williams, R., Ross, C., Liles, M. R., & Paul, V. J. (2012). Macroalgal extracts induce bacterial assemblage shifts and sublethal tissue stress in Caribbean corals. *PLoS ONE*, 7(9), 1–12. <https://doi.org/10.1371/journal.pone.0044859>
- Mumby, P. J., Hastings, A., & Edwards, H. J. (2007). Thresholds and the resilience of Caribbean coral reefs. *Nature*, 450(7166), 98–101. <https://doi.org/10.1038/nature06252>
- Mumby, P. J., & Steneck, R. S. (2008). Coral reef management and conservation in light of rapidly evolving ecological paradigms. In *Trends in Ecology and Evolution* (Vol. 23, Issue 10, pp. 555–563). <https://doi.org/10.1016/j.tree.2008.06.011>
- Mumby, P. J., Steneck, R. S., Adjeroud, M., & Arnold, S. N. (2016). High resilience masks underlying sensitivity to algal phase shifts of Pacific coral reefs. *Oikos*, 125(5), 644–655. <https://doi.org/10.1111/oik.02673>
- Munn, C. B. (2015). The role of vibrios in diseases of corals. *Microbiology Spectrum*, 3(4). <https://doi.org/10.1128/microbiolspec.ve-0006-2014>
- Muscatine, L., & Porter, J. W. (1977). Reef Corals: Mutualistic Symbioses Adapted to Nutrient-Poor Environments. *BioScience*, 27(7), 454–460. <https://doi.org/10.2307/1297526>
- Myers, O. D., Sumner, S. J., Li, S., Barnes, S., & Du, X. (2017). One step forward for reducing false positive and false negative compound identifications from mass spectrometry metabolomics data: new algorithms for constructing extracted ion chromatograms and detecting chromatographic peaks. *Analytical Chemistry*, 89(17), 8696–8703. <https://doi.org/10.1021/acs.analchem.7b00947>
- Neave, M. J., Michell, C. T., Apprill, A., & Voolstra, C. R. (2017b). Endozoicomonas genomes reveal functional adaptation and plasticity in bacterial strains symbiotically associated with diverse marine hosts. *Scientific Reports*, 7(January), 1–12. <https://doi.org/10.1038/srep40579>
- Neave, M. J., Rachmawati, R., Xun, L., Michell, C. T., Bourne, D. G., Apprill, A., & Voolstra, C. R. (2017a). Differential specificity between closely related corals and abundant Endozoicomonas endosymbionts across global scales. *ISME Journal*, 11(1), 186–200. <https://doi.org/10.1038/ismej.2016.95>
- Negri, A. P., Webster, N. S., Hill, R. T., & Heyward, A. J. (2001). Metamorphosis of broadcast spawning corals in response to bacteria isolated from crustose algae. *Marine Ecology Progress Series*, 223, 121–131. <https://doi.org/10.3354/meps223121>
- Nelson, C. E., Goldberg, S. J., Wegley Kelly, L., Haas, A. F., Smith, J. E., Rohwer, F., & Carlson, C. A. (2013). Coral and macroalgal exudates vary in neutral sugar composition and differentially enrich reef bacterioplankton lineages. *ISME Journal*, 7(5), 962–979. <https://doi.org/10.1038/ismej.2012.161>

- Nelson, C. E., Wegley Kelly, L., & Haas, A. F. (2023). Microbial interactions with dissolved organic matter are central to coral reef ecosystem function and resilience. *Annual Review of Marine Science*, 15, 431–460. <https://doi.org/10.1146/annurev-marine-042121-080917>
- Norström, A. V., Nyström, M., Lokrantz, J., & Folke, C. (2009). Alternative states on coral reefs: Beyond coral-macroalgal phase shifts. *Marine Ecology Progress Series*, 376(Hatcher 1984), 293–306. <https://doi.org/10.3354/meps07815>
- Nothias, L. F., Petras, D., Schmid, R., Dührkop, K., Rainer, J., Sarvepalli, A., Protsyuk, I., Ernst, M., Tsugawa, H., Fleischauer, M., Aicheler, F., Aksenov, A. A., Alka, O., Allard, P. M., Barsch, A., Cachet, X., Caraballo-Rodriguez, A. M., Da Silva, R. R., Dang, T., ... Dorrestein, P. C. (2020). Feature-based molecular networking in the GNPS analysis environment. *Nature Methods*, 17(9), 905–908. <https://doi.org/10.1038/s41592-020-0933-6>
- Nugues, M. M., Smith, G. W., Van Hooidek, R. J., Seabra, M. I., & Bak, R. P. M. (2004). Algal contact as a trigger for coral disease. *Ecology Letters*, 7(10), 919–923. <https://doi.org/10.1111/j.1461-0248.2004.00651.x>
- Nyholm, S. V., & McFall-Ngai, M. J. (2004). The winnowing: Establishing the squid - *Vibrios* symbiosis. *Nature Reviews Microbiology*, 2(8), 632–642. <https://doi.org/10.1038/nrmicro957>
- Nyström, M., Norström, A. V., Blenckner, T., de la Torre-Castro, M., Eklöf, J. S., Folke, C., Österblom, H., Steneck, R. S., Thyresson, M., & Troell, M. (2012). Confronting feedbacks of degraded marine ecosystems. *Ecosystems*, 15(5), 695–710. <https://doi.org/10.1007/s10021-012-9530-6>
- Ochsenkühn, M. A., Schmitt-Kopplin, P., Harir, M., & Amin, S. A. (2018). Coral metabolite gradients affect microbial community structures and act as a disease cue. *Communications Biology*, 1(1), 1–10. <https://doi.org/10.1038/s42003-018-0189-1>
- Oksanen, A. J., Blanchet, F. G., Friendly, M., Kindt, R., Legendre, P., Mcglinn, D., Minchin, P. R., Hara, R. B. O., Simpson, G. L., Solymos, P., Stevens, M. H. H., & Szoecs, E. (2022). vegan: Community Ecology package. *R package version 2.6.4*.
- O’Neil, J. M., & Capone, D. G. (2008). Nitrogen cycling in coral reef environments. In *Nitrogen in the Marine Environment* (pp. 949–989). <https://doi.org/10.1016/B978-0-12-372522-6.00021-9>
- Othmani, A., Briand, J. F., Ayé, M., Molmeret, M., & Culioli, G. (2016). Surface metabolites of the brown alga *Taonia atomaria* have the ability to regulate epibiosis. *Biofouling*, 32(7), 801–813. <https://doi.org/10.1080/08927014.2016.1198954>
- Padayhag, B. M., Angelou, M., Nada, L., Ivan, J., Baquiran, P., Sison-mangus, M. P., Lourdes, M., Diego-McGlone, S., Cabaitan, P. C., & Conaco, C. (2023). Microbial community structure and settlement induction capacity of marine biofilms developed under varied reef conditions. *Marine Pollution Bulletin*, 193(May), 115–138. <https://doi.org/10.1016/j.marpolbul.2023.115138>

- Page, C. A., Giuliano, C., Meehan, K., Fisher, R., Motti, C. A., Negri, A. P., & Randall, C. J. (2023). Varied effects of *Lobophora* chemistry on settlement of larvae from five coral genera. *Marine Ecology Progress Series*, 717, 17–35. <https://doi.org/10.3354/meps14380>
- Paix, B., Carriot, N., Barry-Martinet, R., Greff, S., Misson, B., Briand, J. F., & Culioli, G. (2020). A multi-omics analysis suggests links between the differentiated surface metabolome and epiphytic microbiota along the thallus of a Mediterranean seaweed holobiont. *Frontiers in Microbiology*, 11(March), 1–18. <https://doi.org/10.3389/fmicb.2020.00494>
- Paix, B., Othmani, A., Debroas, D., Culioli, G., & Briand, J. F. (2019). Temporal covariation of epibacterial community and surface metabolome in the Mediterranean seaweed holobiont *Taonia atomaria*. *Environmental Microbiology*, 21(9), 3346–3363. <https://doi.org/10.1111/1462-2920.14617>
- Palmer, C. V. (2018). Immunity and the coral crisis. *Communications Biology*, 1(1), 1–7. <https://doi.org/10.1038/s42003-018-0097-4>
- Parrot, D., Blümel, M., Utermann, C., Chianese, G., Krause, S., Kovalev, A., Gorb, S. N., & Tasdemir, D. (2019). Mapping the surface microbiome and metabolome of brown seaweed *Fucus vesiculosus* by amplicon sequencing, integrated metabolomics and imaging techniques. *Scientific Reports*, 9(1), 1–17. <https://doi.org/10.1038/s41598-018-37914-8>
- Paul, V. J., Kuffner, I. B., Walters, L. J., Ritson-Williams, R., Beach, K. S., & Becerro, M. A. (2011). Chemically mediated interactions between macroalgae *Dictyota spp.* and multiple life-history stages of the coral *Porites astreoides*. *Marine Ecology Progress Series*, 426, 161–170. <https://doi.org/10.3354/meps09032>
- Payri, C. E., & Naim, O. (1982). Variations entre 1971 et 1980 de la biomasse et de la composition des populations de macroalgues sur le récif corallien de Tiahura. *Algologie*, III(3), 229–240.
- Peixoto, R. S., Sweet, M., Villela, H. D. M., Cardoso, P., Thomas, T., Voolstra, C. R., Høj, L., & Bourne, D. G. (2021). Coral Probiotics: Premise, Promise, Prospects. *Annual Review of Animal Biosciences*, 9, 265–288. <https://doi.org/10.1146/annurev-animal-090120-115444>
- Pereira, L. B., Palermo, B. R. Z., Carlos, C., & Ottoboni, L. M. M. (2017). Diversity and antimicrobial activity of bacteria isolated from different Brazilian coral species. *FEMS Microbiology Letters*, 364(16), 1–8. <https://doi.org/10.1093/femsle/fnx164>
- Pereira, R. C., Bianco, É. M., Bueno, L. B., De Oliveira, M. A. L., Pamplona, O. S., & Da Gama, B. A. P. (2010). Associational defense against herbivory between brown seaweeds. *Phycologia*, 49(5), 424–428. <https://doi.org/10.2216/09-84.1>
- Pereira, R. C., Donato, R., Teixeira, V. L., & Cavalcanti, D. N. (2000). Chemotaxis and chemical defenses in seaweed susceptibility to herbivory. *Revista Brasileira de Biologia*, 60(3), 405–414. <https://doi.org/10.1590/S0034-71082000000300005>
- Pérez-Rosales, G., Brandl, S. J., Chancerelle, Y., Siu, G., Martinez, E., Parravicini, V., & Hédouin, L. (2021). Documenting decadal disturbance dynamics reveals archipelago-

- specific recovery and compositional change on Polynesian reefs. *Marine Pollution Bulletin*, 170(June). <https://doi.org/10.1016/j.marpolbul.2021.112659>
- Pernice, M., Raina, J. B., Rådecker, N., Cárdenas, A., Pogoreutz, C., & Voolstra, C. R. (2020). Down to the bone: the role of overlooked endolithic microbiomes in reef coral health. *ISME Journal*, 14(2), 325–334. <https://doi.org/10.1038/s41396-019-0548-z>
- Petersen, L. E., Moeller, M., Versluis, D., Nietzer, S., Kellermann, M. Y., & Schupp, P. J. (2021). Mono- and multispecies biofilms from a crustose coralline alga induce settlement in the scleractinian coral *Leptastrea purpurea*. *Coral Reefs*, 40(2), 381–394. <https://doi.org/10.1007/s00338-021-02062-5>
- Petersen, L., Kellermann, M. Y., & Schupp, P. J. (2020). Secondary metabolites of marine microbes: from natural products chemistry to chemical ecology. In *YOUMARES 9 - The Oceans: Our Research, Our Future*, (pp. 159–180).
- Petras, D., Koester, I., Silva, R. Da, Stephens, B. M., Haas, A. F., Nelson, C. E., Kelly, L. W., Aluwihare, L. I., & Dorrestein, P. C. (2017). High-resolution liquid chromatography tandem mass spectrometry enables large scale molecular characterization of dissolved organic matter. *Frontiers in Marine Science*, 4(December), 1–14. <https://doi.org/10.3389/fmars.2017.00405>
- Pita, L., Rix, L., Slaby, B. M., Franke, A., & Hentschel, U. (2018). The sponge holobiont in a changing ocean: from microbes to ecosystems. *Microbiome*, 6(1), 46. <https://doi.org/10.1186/s40168-018-0428-1>
- Pluskal, T., Castillo, S., Villar-Briones, A., & Orešič, M. (2010). MZmine 2: Modular framework for processing, visualizing, and analyzing mass spectrometry-based molecular profile data. *BMC Bioinformatics*, 11(1), 1–11. <https://doi.org/10.1186/1471-2105-11-395>
- Pogoreutz, C., Oakley, C. A., Rådecker, N., Cárdenas, A., Perna, G., Xiang, N., Peng, L., Davy, S. K., Ngugi, D. K., & Voolstra, C. R. (2022). Coral holobiont cues prime *Endozoicomonas* for a symbiotic lifestyle. *ISME Journal*, 16(8), 1883–1895. <https://doi.org/10.1038/s41396-022-01226-7>
- Pogoreutz, C., Rådecker, N., Cárdenas, A., Gärdes, A., Wild, C., & Voolstra, C. R. (2018). Dominance of *Endozoicomonas* bacteria throughout coral bleaching and mortality suggests structural inflexibility of the *Pocillopora verrucosa* microbiome. *Ecology and Evolution*, 8(4), 2240–2252. <https://doi.org/10.1002/ece3.3830>
- Pogoreutz, C., & Ziegler, M. (2023). Trends in Microbiology Frenemies on the reef? Resolving the coral – *Endozoicomonas* association. *Trends in Microbiology*, 1–13. <https://doi.org/10.1016/j.tim.2023.11.006>
- Pollock, F. J., McMinds, R., Smith, S., Bourne, D. G., Willis, B. L., Medina, M., Thurber, R. V., & Zaneveld, J. R. (2018). Coral-associated bacteria demonstrate phyllosymbiosis and cophylogeny. *Nature Communications*, 9(1), 1–13. <https://doi.org/10.1038/s41467-018-07275-x>

- Pratte, Z. A., Longo, G. O., Burns, A. S., Hay, M. E., & Stewart, F. J. (2018). Contact with turf algae alters the coral microbiome: contact versus systemic impacts. *Coral Reefs*, 37(1), 1–13. <https://doi.org/10.1007/s00338-017-1615-4>
- Price, J. T., McLachlan, R. H., Jury, C. P., Toonen, R. J., Wilkins, M. J., & Grottoli, A. G. (2023). Long-term coral microbial community acclimatization is associated with coral survival in a changing climate. *PLoS ONE*, September, 1–20. <https://doi.org/10.1371/journal.pone.0291503>
- Price, N. (2010). Habitat selection, facilitation, and biotic settlement cues affect distribution and performance of coral recruits in French Polynesia. *Oecologia*, 163(3), 747–758. <https://doi.org/10.1007/s00442-010-1578-4>
- Pujalte, M. J., Lucena, T., Ruvira, M. A., Arahal, D. R., & Macián, M. C. (2014). The family Rhodobacteraceae. In E. Rosenberg, E. F. DeLong, S. Lory, E. Stackebrandt, & F. Thompson (Eds.), *The Prokaryotes: Alphaproteobacteria and Betaproteobacteria* (Vol. 9783642301, pp. 439–512). Springer Berlin Heidelberg. https://doi.org/10.1007/978-3-642-30197-1_377
- Putnam, H. M., & Gates, R. D. (2015). Preconditioning in the reef-building coral *Pocillopora damicornis* and the potential for trans-generational acclimatization in coral larvae under future climate change conditions. *Journal of Experimental Biology*, 218(15), 2365–2372. <https://doi.org/10.1242/jeb.123018>
- Quigley, K. M., Willis, B. L., & Bay, L. K. (2016). Maternal effects and symbiodinium community composition drive differential patterns in juvenile survival in the coral *Acropora tenuis*. *Royal Society Open Science*, 3(10). <https://doi.org/10.1098/rsos.160471>
- Quinlan, Z. A., Bennett, M., Arts, M. G. I., Levenstein, M., Flores, D., Tholen, H. M., Tichy, L., Juarez, G., Haas, A. F., Chamberland, V. F., Kelly, R., Latijnhouwers, W., Vermeij, M. J. A., Johnson, A. W., Marhaver, K. L., Kelly, L. W., & Kelly, L. W. (2023). Coral larval settlement induction using tissue-associated and exuded coralline algae metabolites and the identification of putative chemical cues. *Proceedings of the Royal Society B: Biological Sciences*, 290, 1–11.
- Quinlan, Z. A., Ritson-Williams, R., Carroll, B. J., Carlson, C. A., & Nelson, C. E. (2019). Species-specific differences in the microbiomes and organic exudates of crustose coralline algae influence bacterioplankton communities. *Frontiers in Microbiology*, 10(November), 1–11. <https://doi.org/10.3389/fmicb.2019.02397>
- Quinn, R. A., Hartmann, A. C., D'Auriac, I. G., Quistad, S. D., Dorrestein, P. C., Lim, Y. W., Smith, J. E., Sandin, S., Haas, A., Little, M., Rohwer, F., Benler, S., & Vermeij, M. J. A. (2016). Metabolomics of reef benthic interactions reveals a bioactive lipid involved in coral defence. *Proceedings of the Royal Society B: Biological Sciences*, 283(1837), 20161485. <https://doi.org/10.1098/rspb.2016.1485>
- Quinn, T. P., Erb, I., Richardson, M. F., & Crowley, T. M. (2018). Understanding sequencing data as compositions: An outlook and review. *Bioinformatics*, 34(16), 2870–2878. <https://doi.org/10.1093/bioinformatics/bty175>

- Rädecker, N., Pogoreutz, C., Voolstra, C. R., Wiedenmann, J., & Wild, C. (2015). Nitrogen cycling in corals: The key to understanding holobiont functioning? *Trends in Microbiology*, *23*(8), 490–497. <https://doi.org/10.1016/j.tim.2015.03.008>
- Rahelivao, M. P., Gruner, M., Lübken, T., Islamov, D., Kataeva, O., Andriamanantoanina, H., Bauer, I., & Knölker, H. J. (2016). Chemical constituents of the soft corals *Sinularia vanderlandi* and *Sinularia gravis* from the coast of Madagascar. *Organic and Biomolecular Chemistry*, *14*(3), 989–1001. <https://doi.org/10.1039/c5ob02280k>
- Raina, J. B., Dinsdale, E. A., Willis, B. L., & Bourne, D. G. (2010). Do the organic sulfur compounds DMSP and DMS drive coral microbial associations? *Trends in Microbiology*, *18*(3), 101–108. <https://doi.org/10.1016/j.tim.2009.12.002>
- Raina, J.-B., Tapiolas, D., Motti, C. A., Foret, S., Seemann, T., Tebben, J., Willis, B. L., & Bourne, D. G. (2016). Isolation of an antimicrobial compound produced by bacteria associated with reef-building corals. *PeerJ*, *4*, e2275. <https://doi.org/10.7717/peerj.2275>
- Randall, C. J., Negri, A. P., Quigley, K. M., Foster, T., Ricardo, G. F., Webster, N. S., Bay, L. K., Harrison, P. L., Babcock, R. C., & Heyward, A. J. (2020). Sexual production of corals for reef restoration in the Anthropocene. In *Marine Ecology Progress Series* (Vol. 635, pp. 203–232). Inter-Research. <https://doi.org/10.3354/MEPS13206>
- Rasher, D. B., & Hay, M. E. (2010). Chemically rich seaweeds poison corals when not controlled by herbivores. *Proceedings of the National Academy of Sciences*, *107*(21), 9683–9688. <https://doi.org/10.1073/pnas.0912095107>
- Rasher, D. B., Hoey, A. S., & Hay, M. E. (2013). Consumer diversity interacts with prey defenses to drive ecosystem function. *Ecology*, *94*(6), 1347–1358. <https://doi.org/10.1038/mp.2011.182>
- Rasher, D. B., Stout, E. P., Engel, S., Kubanek, J., & Hay, M. E. (2011). Macroalgal terpenes function as allelopathic agents against reef corals. *PNAS*, *108*(43), 17726–17731. <https://doi.org/10.1073/pnas.1108628108/-/DCSupplemental>. www.pnas.org/cgi/doi/10.1073/pnas.1108628108
- Ravi, B. N., & Wells, R. J. (1982a). A series of new diterpenes from the brown alga *Dilophus marginatus* (Dictyotaceae). *Australian Journal of Chemistry*, *35*(1), 129–144. <https://doi.org/10.1071/CH9820129>
- Ravi, B. N., & Wells, R. J. (1982b). New nine-membered ring diterpenes from the brown alga *Dictyota prolificans*. *Australian Journal of Chemistry*, *35*(1), 121–128. <https://doi.org/10.1071/CH9820121>
- Reddy, M. M., Goossens, C., Zhou, Y., Chaib, S., Raviglione, D., Nicolè, F., Hume, B. C. C., Forcioli, D., Agostini, S., Boissin, E., Boss, E., Bowler, C., Vargas, C. De, Douville, E., Flores, M., Furla, Reynaud, S., Sullivan, M. B., Sunagawa, S., ... Banaigs, B. (2023). Multi-omics determination of metabolome diversity in natural coral populations in the Pacific Ocean. *Communications Earth and Environment*, *4*(281), 1–10. <https://doi.org/10.1038/s43247-023-00942-y>

- Reidenbach, M. A., Monismith, S. G., Koseff, J. R., Yahel, G., & Genin, A. (2006). Boundary layer turbulence and flow structure over a fringing coral reef. *Limnology and Oceanography*, 51(5), 1956–1968. <https://doi.org/10.4319/lo.2006.51.5.1956>
- Remple, K. L., Nelson, C. E., Silbiger, N. J., Quinlan, Z. A., Fox, M. D., Kelly, L. W., & Donahue, M. J. (2021). Coral reef biofilm bacterial diversity and successional trajectories are structured by reef benthic organisms and shift under chronic nutrient enrichment. *Npj Biofilms and Microbiomes*, 84. <https://doi.org/10.1038/s41522-021-00252-1>
- Reverter, M., Helber, S. B., Rohde, S., de Goeij, J. M., & Schupp, P. J. (2022). Coral reef benthic community changes in the Anthropocene: Biogeographic heterogeneity, overlooked configurations, and methodology. *Global Change Biology*, 28(6), 1956–1971. <https://doi.org/10.1111/gcb.16034>
- Richmond, R. H. (1981). Energetic considerations in the dispersal of *Pocillopora damicornis* (Linnaeus) planulae. *Proceedings of the 4th International Coral Reef Symposium*, 2(January 1981), 153–156.
- Richmond, R. H. (1987). Energetics, competency, and long-distance dispersal of planula larvae of the coral *Pocillopora damicornis*. *Marine Biology*, 93(4), 527–533. <https://doi.org/10.1007/BF00392790>
- Richmond, R., & Hunter, C. (1990). Reproduction and recruitment of corals: comparisons among the Caribbean, the Tropical Pacific, and the Red Sea. *Marine Ecology Progress Series*, 60(1), 185–203. <https://doi.org/10.3354/meps060185>
- Ritchie, K. B. (2006). Regulation of microbial populations by coral surface mucus and mucus-associated bacteria. *Marine Ecology Progress Series*, 322, 1–14. <https://doi.org/10.3354/meps322001>
- Ritson-Williams, R., Arnold, S., Fogarty, N., Steneck, R. S., Vermeij, M., & Paul, V. J. (2009). New perspectives on ecological mechanisms affecting coral recruitment on reefs. *Smithsonian Contributions to the Marine Sciences*, 38, 437–457. <https://doi.org/10.5479/si.01960768.38.437>
- River, G. F., & Edmunds, P. J. (2001). Mechanisms of interaction between macroalgae and scleractinians on a coral reef in Jamaica. *Journal of Experimental Marine Biology and Ecology*, 261(2), 159–172. [https://doi.org/10.1016/S0022-0981\(01\)00266-0](https://doi.org/10.1016/S0022-0981(01)00266-0)
- Roach, T. N. F., Abieri, M. L., George, E. E., Knowles, B., Naliboff, D. S., Smurthwaite, C. A., Kelly, L. W., Haas, A. F., & Rohwer, F. L. (2017). Microbial bioenergetics of coral-algal interactions. *PeerJ*, 5, e3423. <https://doi.org/10.7717/peerj.3423>
- Roach, T. N. F., Dilworth, J., Christian Martin, H., Jones, A. D., Quinn, R. A., & Drury, C. (2021). Metabolomic signatures of coral bleaching history. *Nature Ecology and Evolution*, 5(4), 495–503. <https://doi.org/10.1038/s41559-020-01388-7>
- Roach, T. N. F., Little, M., Arts, M., Huckeba, J., Haas, A., George, E., Quinn, R., Cobian-Guemes, Naliboff, D. S., Silveira, C. B., Vermeij, M. J., Wegley Kelly, L., Dorrestein, P. C., & Rohwer, F. L. (2020). A multi-omic analysis of in situ coral-turf algal interactions.

- Proceedings of the National Academy of Sciences*, 117(24), 13588–13595. <https://doi.org/10.1073/pnas.1915455117>
- Roach, T. N. F., Matsuda, S. B., Martin, C., Huckeba, G., Huckeba, J., Kahkejian, V., Santoro, E. P., van der Geer, A., Drury, C., & Quinn, R. A. (2023). Single-polyp metabolomics reveals biochemical structuring of the coral holobiont at multiple scales. *Communications Biology*, 6(1), 6–13. <https://doi.org/10.1038/s42003-023-05342-8>
- Robbins, S. J., Singleton, C. M., Chan, C. X., Messer, L. F., Geers, A. U., Ying, H., Baker, A., Bell, S. C., Morrow, K. M., Ragan, M. A., Miller, D. J., Forêt, S., Ball, E., Beeden, R., Berumen, M., Aranda, M., Ravasi, T., Bongaerts, P., Hoegh-Guldberg, O., ... Tyson, G. W. (2019). A genomic view of the reef-building coral *Porites lutea* and its microbial symbionts. *Nature Microbiology*, 4(12), 2090–2100. <https://doi.org/10.1038/s41564-019-0532-4>
- Rocker, M. M., Kenkel, C. D., Francis, D. S., Willis, B. L., & Bay, L. K. (2019). Plasticity in gene expression and fatty acid profiles of *Acropora tenuis* reciprocally transplanted between two water quality regimes in the central Great Barrier Reef, Australia. *Journal of Experimental Marine Biology and Ecology*, 511(November 2018), 40–53. <https://doi.org/10.1016/j.jembe.2018.11.004>
- Rodrigues, L. J., & Padilla-Gamiño, J. L. (2022). Trophic provisioning and parental trade-offs lead to successful reproductive performance in corals after a bleaching event. *Scientific Reports*, 12(1), 1–10. <https://doi.org/10.1038/s41598-022-21998-4>
- Roff, G., Hoegh-Guldberg, O., & Fine, M. (2006). Intra-colonial response to Acroporid “white syndrome” lesions in tabular *Acropora* spp. (Scleractinia). *Coral Reefs*, 25(2), 255–264. <https://doi.org/10.1007/s00338-006-0099-4>
- Roff, G., & Mumby, P. J. (2012). Global disparity in the resilience of coral reefs. *Trends in Ecology and Evolution*, 27(7), 404–413. <https://doi.org/10.1016/j.tree.2012.04.007>
- Rogers, J. S., Maticka, S. A., Chirayath, V., Woodson, C. B., Alonso, J. J., & Monismith, S. G. (2018). Connecting flow over complex terrain to hydrodynamic roughness on a coral reef. *Journal of Physical Oceanography*, 48(7), 1567–1587. <https://doi.org/10.1175/JPO-D-18-0013.1>
- Rohart, F., Gautier, B., Singh, A., & Lê Cao, K. A. (2017). mixOmics: An R package for ‘omics feature selection and multiple data integration. *PLoS Computational Biology*, 13(11), 1–19. <https://doi.org/10.1371/journal.pcbi.1005752>
- Rohwer, F., Seguritan, V., Knowlton, N., & Azam, F. (2002). Diversity and distribution of coral-associated bacteria. *Marine Ecology Progress Series*, 243, 1–10. <https://doi.org/10.1002/14651858.CD007615.pub3>
- Roik, A., Reverter, M., & Pogoreutz, C. (2022). A roadmap to understanding diversity and function of coral reef-associated fungi. *FEMS Microbiology Reviews*, 46(6), 1–26. <https://doi.org/10.1093/femsre/fuac028>

- Rosado, P. M., Leite, D. C. A., Duarte, G. A. S., Chaloub, R. M., Jospin, G., Nunes da Rocha, U., P. Saraiva, J., Dini-Andreote, F., Eisen, J. A., Bourne, D. G., & Peixoto, R. S. (2019). Marine probiotics: increasing coral resistance to bleaching through microbiome manipulation. *ISME Journal*, *13*(4), 921–936. <https://doi.org/10.1038/s41396-018-0323-6>
- Rosales, S. M., Huebner, L. K., Evans, J. S., Apprill, A., Baker, A. C., Becker, C. C., Brandt, M. E., Clark, A. S., Campo, J., Dennison, C. E., Eaton, K. R., Huntley, N. E., Kellogg, C. A., Medina, M., Meyer, J. L., Muller, E. M., Rodriguez-lanetty, M., Salerno, J. L., Schill, W. B., ... Voss, J. D. (2023). A meta-analysis of the stony coral tissue loss disease microbiome finds key bacteria in unaffected and lesion tissue in diseased colonies. *ISME Communications*, February. <https://doi.org/10.1038/s43705-023-00220-0>
- Rosenberg, E., Koren, O., Reshef, L., Efrony, R., & Zilber-Rosenberg, I. (2007). The role of microorganisms in coral health, disease and evolution. *Nature Reviews Microbiology*, *5*(5), 355–362. <https://doi.org/10.1038/nrmicro1635>
- Ross, P. M., Parker, L., & Byrne, M. (2016). Transgenerational responses of molluscs and echinoderms to changing ocean conditions. *ICES J. Mar. Sci.*, *73*, 537–549.
- Rouzé, H., Lecellier, G. J., Saulnier, D., Planes, S., Gueguen, Y., Wirshing, H. H., & Berteaux-Lecellier, V. (2017). An updated assessment of *Symbiodinium spp.* that associate with common scleractinian corals from Moorea (French Polynesia) reveals high diversity among background symbionts and a novel finding of clade B. *PeerJ*, *2017*(1). <https://doi.org/10.7717/peerj.2856>
- Rubio-Portillo, E., Martin-Cuadrado, A. B., Caraballo-Rodríguez, A. M., Rohwer, F., Dorrestein, P. C., & Antón, J. (2020). Virulence as a side effect of interspecies interaction in vibrio coral pathogens. *MBio*, *11*(4), 1–16. <https://doi.org/10.1128/mBio.00201-20>
- Russell, L. (2018). “Emmeans: estimated marginal means, aka least-squares means.” *R package version 1.8.3*.
- Sambrook, K., Hoey, A. S., Andréfouët, S., Cumming, G. S., Duce, S., & Bonin, M. C. (2019). Beyond the reef: The widespread use of non-reef habitats by coral reef fishes. *Fish and Fisheries*, *20*(5), 903–920. <https://doi.org/10.1111/faf.12383>
- Santoro, E. P., Borges, R. M., Espinoza, J. L., Freire, M., Messias, C. S. M. A., Villela, H. D. M., Pereira, L. M., Vilela, C. L. S., Rosado, J. G., Cardoso, P. M., Rosado, P. M., Assis, J. M., Duarte, G. A. S., Perna, G., Rosado, A. S., Macrae, A., Dupont, C. L., Nelson, K. E., Sweet, M. J., ... Peixoto, R. S. (2021). Coral microbiome manipulation elicits metabolic and genetic restructuring to mitigate heat stress and evade mortality. *Science Advances*, *7*(33), 19–21. <https://doi.org/10.1126/sciadv.abg3088>
- Scheffer, M., Carpenter, S., Foley, J. A., Folke, C., & Walker, B. (2001). Catastrophic shifts in ecosystems. *Nature*, *413*(6856), 591.
- Schmid, R., Heuckeroth, S., Korf, A., Smirnov, A., Myers, O., Dyrland, T. S., Bushuiev, R., Murray, K. J., Hoffmann, N., Lu, M., Sarvepalli, A., Zhang, Z., Fleischauer, M., Dührkop, K., Wesner, M., Hoogstra, S. J., Rudt, E., Mokshyna, O., Brungs, C., ... Pluskal, T. (2023).

Integrative analysis of multimodal mass spectrometry data in MZmine 3. *Nature Biotechnology*. <https://doi.org/10.1038/s41587-023-01690-2>

- Schmidt-Roach, S., Miller, K. J., Lundgren, P., & Andreakis, N. (2014). With eyes wide open: A revision of species within and closely related to the *Pocillopora damicornis* species complex (Scleractinia; Pocilloporidae) using morphology and genetics. *Zoological Journal of the Linnean Society*, *170*(1), 1–33. <https://doi.org/10.1111/zoj.12092>
- Schmitt, R. J., Holbrook, S. J., Brooks, A. J., & Adam, T. C. (2021). Evaluating the precariousness of coral recovery when coral and macroalgae are alternative basins of attraction. *Limnology and Oceanography*, 1–13. <https://doi.org/10.1002/lno.11929>
- Schmitt, R. J., Holbrook, S. J., Davis, S. L., Brooks, A. J., & Adam, T. C. (2019). Experimental support for alternative attractors on coral reefs. *Proceedings of the National Academy of Sciences of the United States of America*, *116*(10), 4372–4381. <https://doi.org/10.1073/pnas.1812412116>
- Schmitt, T. M., Lindquist, N., & Hay, M. E. (1998). Seaweed secondary metabolites as antifoulants: Effects of *Dictyota spp.* diterpenes on survivorship, settlement, and development of marine invertebrate larvae. *Chemoecology*, *8*(3), 125–131. <https://doi.org/10.1007/s000490050017>
- Setter, R. O., Franklin, E. C., & Mora, C. (2022). Co-occurring anthropogenic stressors reduce the timeframe of environmental viability for the world’s coral reefs. *PLoS Biology*, *20*(10), 1–12. <https://doi.org/10.1371/journal.pbio.3001821>
- Shannon, P., Markiel, A., Ozier, O., Baliga, Nitin. S., Wang, Jonathan. T., Ramage, D., Amin, N., Schwikowski, B., & Ideker, T. (2003). Cytoscape: A software environment for integrated models. *Genome Research*, *13*(22), 426. <https://doi.org/10.1101/gr.1239303.metabolite>
- Sharp, K. H., Distel, D., & Paul, V. J. (2012). Diversity and dynamics of bacterial communities in early life stages of the Caribbean coral *Porites astreoides*. *ISME Journal*, *6*(4), 790–801. <https://doi.org/10.1038/ismej.2011.144>
- Sharp, K. H., Ritchie, K. B., Schupp, P. J., Ritson-Williams, R., & Paul, V. J. (2010). Bacterial acquisition in juveniles of several broadcast spawning coral species. *PLoS ONE*, *5*(5), 1–6. <https://doi.org/10.1371/journal.pone.0010898>
- Shashar, N., Kinane, S., Jokiel, P. L., & Patterson, M. R. (1996). Hydromechanical boundary layers over a coral reef. *Journal of Experimental Marine Biology and Ecology*, *199*(1), 17–28. [https://doi.org/10.1016/0022-0981\(95\)00156-5](https://doi.org/10.1016/0022-0981(95)00156-5)
- Shearer, T. L., Rasher, D. B., Snell, T. W., & Hay, M. E. (2012). Gene expression patterns of the coral *Acropora millepora* in response to contact with macroalgae. *Coral Reefs*, *31*(4), 1177–1192. <https://doi.org/10.1007/s00338-012-0943-7>
- Shearer, T. L., Snell, T. W., & Hay, M. E. (2014). Gene expression of corals in response to macroalgal competitors. *PLoS ONE*, *9*(12), 1–21. <https://doi.org/10.1371/journal.pone.0114525>

- Siboni, N., Abrego, D., Puill-Stephan, E., King, W. L., Bourne, D. G., Raina, J. B., Seymour, J. R., & Harder, T. (2020). Crustose coralline algae that promote coral larval settlement harbor distinct surface bacterial communities. *Coral Reefs*. <https://doi.org/10.1007/s00338-020-01997-5>
- Silveira, C. B., Cavalcanti, G. S., Walter, J. M., Silva-Lima, A. W., Dinsdale, E. A., Bourne, D. G., Thompson, C. C., & Thompson, F. L. (2017a). Microbial processes driving coral reef organic carbon flow. *FEMS Microbiology Reviews*, *41*(4), 575–595. <https://doi.org/10.1093/FEMSRE/FUX018>
- Silveira, C. B., Gregoracci, G. B., Coutinho, F. H., Silva, G. G. Z., Haggerty, J. M., de Oliveira, L. S., Cabral, A. S., Rezende, C. E., Thompson, C. C., Francini-Filho, R. B., Edwards, R. A., Dinsdale, E. A., & Thompson, F. L. (2017b). Bacterial community associated with the reef coral *Mussismilia braziliensis*'s momentum boundary layer over a diel cycle. *Frontiers in Microbiology*, *8*(MAY), 1–12. <https://doi.org/10.3389/fmicb.2017.00784>
- Singh, A., Shannon, C. P., Gautier, B., Rohart, F., Vacher, M., Tebbutt, S. J., & Cao, K. A. L. (2019). DIABLO: An integrative approach for identifying key molecular drivers from multi-omics assays. *Bioinformatics*, *35*(17), 3055–3062. <https://doi.org/10.1093/bioinformatics/bty1054>
- Slattery, M., & Lesser, M. P. (2014). Allelopathy in the tropical alga *Lobophora variegata* (Phaeophyceae): mechanistic basis for a phase shift on mesophotic coral reefs? *Journal of Phycology*, *50*(3), 493–505. <https://doi.org/10.1111/jpy.12160>
- Smith, H. A., Brown, D. A., Arjunwadkar, C. V., Fulton, S. E., Whitman, T., Hermanto, B., Mastroianni, E., Mattocks, N., Smith, A. K., Harrison, P. L., Boström-Einarsson, L., McLeod, I. M., & Bourne, D. G. (2022). Removal of macroalgae from degraded reefs enhances coral recruitment. *Restoration Ecology*, *30*(7), 0–3. <https://doi.org/10.1111/rec.13624>
- Smith, H. A., Conlan, J. A., Pollock, F. J., Wada, N., Shore, A., Hung, J. Y. H., Aeby, G. S., Willis, B. L., Francis, D. S., & Bourne, D. G. (2020). Energy depletion and opportunistic microbial colonisation in white syndrome lesions from corals across the Indo-Pacific. *Scientific Reports*, *10*(1), 1–14. <https://doi.org/10.1038/s41598-020-76792-x>
- Smith, H. A., Fulton, S. E., McLeod, I. M., Page, C. A., & Bourne, D. G. (2023). Sea-weeding: Manual removal of macroalgae facilitates rapid coral recovery. *Journal of Applied Ecology*, *April*, 1–13. <https://doi.org/10.1111/1365-2664.14502>
- Smith, J. E., Brainard, R., Carter, A., Grillo, S., Edwards, C., Harris, J., Lewis, L., Obura, D., Rohwer, F., Sala, E., Vroom, P. S., & Sandin, S. (2016). Re-evaluating the health of coral reef communities: Baselines and evidence for human impacts across the central pacific. *Proceedings of the Royal Society B: Biological Sciences*, *283*(1822), 1–9. <https://doi.org/10.1098/rspb.2015.1985>
- Smith, J. E., Hunter, C. L., & Smith, C. M. (2010). The effects of top-down versus bottom-up control on benthic coral reef community structure. *Oecologia*, *163*(2), 497–507. <https://doi.org/10.1007/s00442-009-1546-z>

- Smith, J. E., Shaw, M., Edwards, R. A., Obura, D., Pantos, O., Sala, E., Sandin, S. A., Smriga, S., Hatay, M., & Rohwer, F. L. (2006). Indirect effects of algae on coral: Algae-mediated, microbe-induced coral mortality. *Ecology Letters*, 9(7), 835–845. <https://doi.org/10.1111/j.1461-0248.2006.00937.x>
- Sneed, J. M., Sharp, K. H., Ritchie, K. B., & Paul, V. J. (2014). The chemical cue tetrabromopyrrole from a biofilm bacterium induces settlement of multiple Caribbean corals. *Proceedings of the Royal Society B: Biological Sciences*, 281(1786), 1–9. <https://doi.org/10.1098/rspb.2013.3086>
- Sogin, E. M., Putnam, H. M., Anderson, P. E., & Gates, R. D. (2016). Metabolomic signatures of increases in temperature and ocean acidification from the reef-building coral, *Pocillopora damicornis*. *Metabolomics*, 12(4). <https://doi.org/10.1007/s11306-016-0987-8>
- Spalding, M. D., & Brown, B. E. (2015). Warm-water coral reefs and climate change. *Science*, 350(6262), 769–771.
- Spalding, M. D., Ravilious, C., & Green, E. P. (2001). *World Atlas of Coral Reefs* (U. W. C. M. Center, Ed.). University of California Press.
- Speare, K. E., Adam, T. C., Winslow, E. M., Lenihan, H. S., & Burkepile, D. E. (2022). Size-dependent mortality of corals during marine heatwave erodes recovery capacity of a coral reef. *Global Change Biology*, 28(4), 1342–1358. <https://doi.org/10.1111/gcb.16000>
- Spiers, L., & Frazer, T. K. (2023). Comparison of feeding preferences of herbivorous fishes and the sea urchin *Diadema antillarum* in Little Cayman. *PeerJ*, 11, 1–28. <https://doi.org/10.7717/peerj.16264>
- Steen, A. D., Kusch, S., Abdulla, H. A., Cakić, N., Coffinet, S., Dittmar, T., Fulton, J. M., Galy, V., Hinrichs, K. U., Ingalls, A. E., Koch, B. P., Kujawinski, E., Liu, Z., Osterholz, H., Rush, D., Seidel, M., Sepúlveda, J., & Wakeham, S. G. (2020). Analytical and computational advances, opportunities, and challenges in marine organic biogeochemistry in an era of “Omics.” *Frontiers in Marine Science*, 7(September). <https://doi.org/10.3389/fmars.2020.00718>
- Stella, J. S., Jones, G. P., & Pratchett, M. S. (2010). Variation in the structure of epifaunal invertebrate assemblages among coral hosts. *Coral Reefs*, 29(4), 957–973. <https://doi.org/10.1007/s00338-010-0648-8>
- Steneck, R. S., Bellwood, D. R., & Hay, M. E. (2017). Herbivory in the marine realm. In *Current Biology* (Vol. 27, Issue 11, pp. R484–R489). Cell Press. <https://doi.org/10.1016/j.cub.2017.04.021>
- Stewart, H. L. (2006). Morphological variation and phenotypic plasticity of buoyancy in the macroalga *Turbinaria ornata* across a barrier reef. *Marine Biology*, 149(4), 721–730. <https://doi.org/10.1007/s00227-005-0186-z>
- Stewart, H. L. (2008). The role of spatial and ontogenetic morphological variation in the expansion of the geographic range of the tropical brown alga, *Turbinaria ornata*. *Integrative and Comparative Biology*, 48(6), 713–719. <https://doi.org/10.1093/icb/icn028>

- Stewart, H. L., Payri, C. E., & Koehl, M. A. R. (2007). The role of buoyancy in mitigating reduced light in macroalgal aggregations. *Journal of Experimental Marine Biology and Ecology*, 343(1), 11–20. <https://doi.org/10.1016/j.jembe.2006.10.031>
- Stiger, V., Deslandes, E., & Payri, C. E. (2004). Phenolic contents of two brown algae, *Turbinaria ornata* and *Sargassum mangarevense* on Tahiti (French Polynesia): Interspecific, ontogenic and spatio-temporal variations. *Botanica Marina*, 47(5), 402–409. <https://doi.org/10.1515/BOT.2004.058>
- Stiger, V., & Payri, C. E. (1999a). Spatial and seasonal variations in the biological characteristics of two invasive brown algae, *Turbinaria ornata* (Turner) J. Agardh and *Sargassum mangarevense* (Grunow) Setchell (Sargassaceae, Fucales) spreading on the reefs of Tahiti (French Polynesia). *Botanica Marina*, 42(3), 295–306. <https://doi.org/10.1515/BOT.1999.033>
- Stiger, V., & Payri, C. E. (1999b). Spatial and temporal patterns of settlement of the brown macroalgae *Turbinaria ornata* and *Sargassum mangarevense* in a coral reef on Tahiti. *Marine Ecology Progress Series*, 191(May), 91–100. <https://doi.org/10.3354/meps191091>
- Sumner, L. W., Amberg, A., Barrett, D., Beale, M. H., Beger, R., Daykin, C. A., Fan, T. W.-M., Fiehn, O., Goodacre, R., Griffin, J. L., Hankemeier, T., Hardy, N., Harnly, J., Higashi, R., Kopka, J., Lane, A. N., Lindon, J. C., Marriott, P., Nicholls, A. W., ... Viant, M. R. (2007). Proposed minimum reporting standards for chemical analysis. *Metabolomics*, 3(3), 211–221. <https://doi.org/10.1007/s11306-007-0082-2>
- Sun, H. H., Waraszkiewicz, S. M., Erickson, K. L., Finer, J., & Clardy, J. (1977). Dictyoxepin and Dictyolene, two new diterpenes from the marine alga *Dictyota acutiloba* (Phaeophyta). *Journal of the American Chemical Society*, 99(10), 3516–3517. <https://doi.org/10.1021/ja00452a062>
- Sunagawa, S., Desantis, T. Z., Piceno, Y. M., Brodie, E. L., Desalvo, M. K., Voolstra, C. R., Weil, E., Andersen, G. L., & Medina, M. (2009). Bacterial diversity and white Plague disease-associated community changes in the Caribbean coral *Montastraea faveolata*. *ISME Journal*, 3(5), 512–521. <https://doi.org/10.1038/ismej.2008.131>
- Swan, B. K., Tupper, B., Sczyrba, A., Lauro, F. M., Martinez-Garcia, M., González, J. M., Luo, H., Wright, J. J., Landry, Z. C., Hanson, N. W., Thompson, B. P., Poulton, N. J., Schwientek, P., Acinas, S. G., Giovannoni, S. J., Moran, M. A., Hallam, S. J., Cavicchioli, R., Woyke, T., & Stepanauskas, R. (2013). Prevalent genome streamlining and latitudinal divergence of planktonic bacteria in the surface ocean. *Proceedings of the National Academy of Sciences of the United States of America*, 110(28), 11463–11468. <https://doi.org/10.1073/pnas.1304246110>
- Sweet, M. J., Bythell, J. C., & Nugues, M. M. (2013). Algae as reservoirs for coral pathogens. *PLoS ONE*, 8(7). <https://doi.org/10.1371/journal.pone.0069717>
- Sweet, M. J., Croquer, A., & Bythell, J. C. (2011). Bacterial assemblages differ between compartments within the coral holobiont. *Coral Reefs*, 30(1), 39–52. <https://doi.org/10.1007/s00338-010-0695-1>

- Sweet, M., Villela, H., Keller-Costa, T., Costa, R., Romano, S., Bourne, D. G., Cárdenas, A., Huggett, M. J., Kerwin, A. H., Kuek, F., Medina, M., Meyer, J. L., Müller, M., Pollock, F. J., Rappé, M. S., Sere, M., Sharp, K. H., Voolstra, C. R., Zaccardi, N., ... Peixoto, R. (2021). Insights into the cultured bacterial fraction of corals. *MSystems*, 6(3). <https://doi.org/10.1128/msystems.01249-20>
- Szöcs, E., Stirling, T., Scott, E. R., Scharmüller, A., & Schäfer, R. B. (2020). Webchem: An R package to retrieve chemical information from the web. *Journal of Statistical Software*, 93(13). <https://doi.org/10.18637/jss.v093.i13>
- Takeda-Sakazume, A., Honjo, J., Sasano, S., Matsushima, K., Baba, S. A., Mogami, Y., & Hatta, M. (2022). Gravitactic swimming of the planula larva of the coral *Acropora*: characterization of straightforward vertical swimming. *Zoological Science*, 40(1), 44–52. <https://doi.org/10.2108/zs220043>
- Takikawa, M., Uno, K., Ooi, T., Kusumi, T., Akera, S., Muramatsu, M., Meha, H., & Horita, C. (1998). Crenulacetal C, a marine diterpene, and its synthetic mimics inhibiting *Polydora websterii*, a harmful lugworm damaging pearl cultivation. *Chemical Pharmaceutical Bulletin*, 46(3), 462–466.
- Tanaka, A., Hoshino, Y., Nagasato, C., & Motomura, T. (2017). Branch regeneration induced by severe damage in the brown alga *Dictyota dichotoma* (dictyotales, phaeophyceae). *Protoplasma*, 254(3), 1341–1351. <https://doi.org/10.1007/s00709-016-1025-4>
- Tandon, K., Lu, C. Y., Chiang, P. W., Wada, N., Yang, S. H., Chan, Y. F., Chen, P. Y., Chang, H. Y., Chiou, Y. J., Chou, M. S., Chen, W. M., & Tang, S. L. (2020). Comparative genomics: Dominant coral-bacterium *Endozoicomonas acroporae* metabolizes dimethylsulfoniopropionate (DMSP). *ISME Journal*, 14(5), 1290–1303. <https://doi.org/10.1038/s41396-020-0610-x>
- Tanner, J. E. (1995). Competition between scleractinian corals and macroalgae, an experimental investigation of coral growth, survival and reproduction. *Journal of Experimental Marine Biology and Ecology*, 190, 151–168. [https://doi.org/10.1016/S0196-0644\(88\)80272-5](https://doi.org/10.1016/S0196-0644(88)80272-5)
- Tebben, J., Motti, C. A., Siboni, N., Tapiolas, D. M., Negri, A. P., Schupp, P. J., Kitamura, M., Hatta, M., Steinberg, P. D., & Harder, T. (2015). Chemical mediation of coral larval settlement by crustose coralline algae. *Scientific Reports*, 5, 1–11. <https://doi.org/10.1038/srep10803>
- Theophilus, T., Vieira, C., Culioli, G., Thomas, O. P., N'Yeurt, A. D. R., Andréfouët, S., Mattio, L., Payri, C. E., & Zubia, M. (2020). Dictyotaceae (Dictyotales, Phaeophyceae) species from French Polynesia: current knowledge and future research. In *Advances in Botanical Research* (Vol. 95). Elsevier Ltd. <https://doi.org/10.1016/bs.abr.2019.12.001>
- Thompson, F. L., Barash, Y., Sawabe, T., Sharon, G., Swings, J., & Rosenberg, E. (2006). *Thalassomonas loyana* sp. nov., a causative agent of the white plague-like disease of corals on the Eilat coral reef. *International Journal of Systematic and Evolutionary Microbiology*, 56(2), 365–368. <https://doi.org/10.1099/ijs.0.63800-0>

- Thompson, J. R., Rivera, H. E., Closek, C. J., & Medina, M. (2015). Microbes in the coral holobiont: partners through evolution, development, and ecological interactions. *Frontiers in Cellular and Infection Microbiology*, 4(January), 1–20. <https://doi.org/10.3389/fcimb.2014.00176>
- Tisthammer, K. H., Timmins-Schiffman, E., Seneca, F. O., Nunn, B. L., & Richmond, R. H. (2021). Physiological and molecular responses of lobe coral indicate nearshore adaptations to anthropogenic stressors. *Scientific Reports*, 11(1), 1–11. <https://doi.org/10.1038/s41598-021-82569-7>
- Toledo-Hernández, C., & Ruiz-Diaz, C. P. (2014). The immune responses of the coral. *Invertebrate Survival Journal*, 11, 319–328.
- Tout, J., Jeffries, T. C., Petrou, K., Tyson, G. W., Webster, N. S., Garren, M., Stocker, R., Ralph, P. J., & Seymour, J. R. (2015). Chemotaxis by natural populations of coral reef bacteria. *ISME Journal*, 9(8), 1764–1777. <https://doi.org/10.1038/ismej.2014.261>
- Tout, J., Jeffries, T. C., Webster, N. S., Stocker, R., Ralph, P. J., & Seymour, J. R. (2014). Variability in microbial community composition and function between different niches within a coral reef. *Microbial Ecology*, 67(3), 540–552. <https://doi.org/10.1007/s00248-013-0362-5>
- Tran, C., & Hadfield, M. G. (2011). Larvae of *Pocillopora damicornis* (Anthozoa) settle and metamorphose in response to surface-biofilm bacteria. *Marine Ecology Progress Series*, 433(Hadfield 2000), 85–96. <https://doi.org/10.3354/meps09192>
- Trapon, M. L., Pratchett, M. S., & Penin, L. (2011). Comparative effects of different disturbances in coral reef habitats in Moorea, French Polynesia. *Journal of Marine Biology*, 2011, 1–11. <https://doi.org/10.1155/2011/807625>
- Tremblay, P., Weinbauer, M. G., Rottier, C., Guérardel, Y., Nozais, C., & Ferrier-Pagès, C. (2011). Mucus composition and bacterial communities associated with the tissue and skeleton of three scleractinian corals maintained under culture conditions. *Journal of the Marine Biological Association of the United Kingdom*, 91(3), 649–657. <https://doi.org/10.1017/S002531541000130X>
- Trygonis, V., & Sini, M. (2012). PhotoQuad: A dedicated seabed image processing software, and a comparative error analysis of four photoquadrat methods. *Journal of Experimental Marine Biology and Ecology*, 424–425, 99–108. <https://doi.org/10.1016/j.jembe.2012.04.018>
- van de Leemput, I. A., Hughes, T. P., van Nes, E. H., & Scheffer, M. (2016). Multiple feedbacks and the prevalence of alternate stable states on coral reefs. *Coral Reefs*, 35(3), 857–865. <https://doi.org/10.1007/s00338-016-1439-7>
- van der Hooft, J. J. J., Wandy, J., Barrett, M. P., Burgess, K. E. V., & Rogers, S. (2016). Topic modeling for untargeted substructure exploration in metabolomics. *Proceedings of the National Academy of Sciences of the United States of America*, 113(48), 13738–13743. <https://doi.org/10.1073/pnas.1608041113>

- van Duyl, F. C., van Bleijswijk, J. D. L., Wuchter, C., Witte, H. J., Coolen, M. J. L., Bak, R. P. M., Engelmann, J. C., & Nugues, M. M. (2023). Recovery patterns of the coral microbiome after relief of algal contact. *Journal of Sea Research*, *191*(March 2022), 102309. <https://doi.org/10.1016/j.seares.2022.102309>
- van Oppen, M. J. H., & Blackall, L. L. (2019). Coral microbiome dynamics, functions and design in a changing world. *Nature Reviews Microbiology*, *17*(9), 557–567. <https://doi.org/10.1038/s41579-019-0223-4>
- Vega Thurber, R., Burkepile, D. E., Correa, A. M. S., Thurber, A. R., Shantz, A. A., Welsh, R., Pritchard, C., & Rosales, S. (2012). Macroalgae decrease growth and alter microbial community structure of the reef-building coral, *Porites astreoides*. *PLoS ONE*, *7*(9), 1–10. <https://doi.org/10.1371/journal.pone.0044246>
- Vega Thurber, R., Mydlarz, L. D., Brandt, M., Harvell, D., Weil, E., Raymundo, L., Willis, B. L., Langevin, S., Tracy, A. M., Littman, R., Kemp, K. M., Dawkins, P., Prager, K. C., Garren, M., & Lamb, J. (2020). Deciphering coral disease dynamics: integrating host, microbiome, and the changing environment. *Frontiers in Ecology and Evolution*, *8*(November), 1–18. <https://doi.org/10.3389/fevo.2020.575927>
- Vega Thurber, R., Willner-Hall, D., Rodriguez-Mueller, B., Desnues, C., Edwards, R. A., Angly, F., Dinsdale, E., Kelly, L., & Rohwer, F. (2009). Metagenomic analysis of stressed coral holobionts. *Environmental Microbiology*, *11*(8), 2148–2163. <https://doi.org/10.1111/j.1462-2920.2009.01935.x>
- Vermeij, M. J. A., Smith, J. E., Smith, C. M., Vega Thurber, R., & Sandin, S. A. (2009). Survival and settlement success of coral planulae: Independent and synergistic effects of macroalgae and microbes. *Oecologia*, *159*(2), 325–336. <https://doi.org/10.1007/s00442-008-1223-7>
- Vidal-Dupiol, J., Dheilily, N. M., Rondon, R., Grunau, C., Cosseau, C., Smith, K. M., Freitag, M., Adjeroud, M., & Mitta, G. (2014). Thermal stress triggers broad *Pocillopora damicornis* transcriptomic remodeling, while *Vibrio coralliilyticus* infection induces a more targeted immuno-suppression response. *PLoS ONE*, *9*(9). <https://doi.org/10.1371/journal.pone.0107672>
- Vidal-Dupiol, J., Ladrière, O., Destoumieux-Garzón, D., Sautière, P. E., Meistertzheim, A. L., Tambutté, E., Tambutté, S., Duval, D., Fouré, L., Adjeroud, M., & Mitta, G. (2011). Innate immune responses of a scleractinian coral to vibriosis. *Journal of Biological Chemistry*, *286*(25), 22688–22698. <https://doi.org/10.1074/jbc.M110.216358>
- Vieira, C., Engelen, A. H., Guentas, L., Aires, T., Houlbreque, F., Gaubert, J., Serrão, E. A., Clerck, O. De, & Payri, C. E. (2016b). Species specificity of bacteria associated to the brown seaweeds *Lobophora* (Dictyotales, Phaeophyceae) and their potential for induction of rapid coral bleaching in *Acropora muricata*. *Frontiers in Microbiology*, *7*(MAR), 1–13. <https://doi.org/10.3389/fmicb.2016.00316>
- Vieira, C., Thomas, O. P., Culioli, G., Genta-Jouve, G., Houlbreque, F., Gaubert, J., De Clerck, O., & Payri, C. E. (2016a). Allelopathic interactions between the brown algal genus

- Lobophora* (Dictyotales, Phaeophyceae) and scleractinian corals. *Scientific Reports*, 6(March), 1–11. <https://doi.org/10.1038/srep18637>
- Villela, H., Modolon, F., Schultz, J., Ordoñez, N. D., Carvalho, S., Soriano, A. U., & Peixoto, R. S. (2023). Genome analysis of a coral associated bacterial consortium highlights complementary hydrocarbon degradation ability and other beneficial mechanisms for the host. *Scientific Reports*, 13, 1–14. <https://doi.org/10.1038/s41598-023-38512-z>
- Voolstra, C. R., Peixoto, R. S., & Ferrier-Pagès, C. (2023). Mitigating the ecological collapse of coral Effective strategies to preserve coral reef ecosystems. *EMBO Reports*, 1–7. <https://doi.org/10.15252/embr.202356826>
- Vu, I., Smelick, G., Harris, S., Lee, S. C., Weil, E., Whitehead, R. F., & Bruno, J. F. (2009). Macroalgae has no effect on the severity and dynamics of Caribbean yellow band disease. *PLoS ONE*, 4(2). <https://doi.org/10.1371/journal.pone.0004514>
- Wada, N., Hsu, M. T., Tandon, K., Hsiao, S. S. Y., Chen, H. J., Chen, Y. H., Chiang, P. W., Yu, S. P., Lu, C. Y., Chiou, Y. J., Tu, Y. C., Tian, X., Chen, B. C., Lee, D. C., Yamashiro, H., Bourne, D. G., & Tang, S. L. (2022). High-resolution spatial and genomic characterization of coral-associated microbial aggregates in the coral *Stylophora pistillata*. *Science Advances*, 8(27), 1–13. <https://doi.org/10.1126/sciadv.abo2431>
- Walsh, K., Haggerty, J. M., Doane, M. P., Hansen, J. J., Morris, M. M., Moreira, A. P. B., de Oliveira, L., Leomil, L., Garcia, G. D., Thompson, F., & Dinsdale, E. A. (2017). Aurobiomes are present in the water layer above coral reef benthic macro-organisms. *PeerJ*, 5, e3666. <https://doi.org/10.7717/peerj.3666>
- Wang, G., Shuai, L., Li, Y., Lin, W., Zhao, X., & Duan, D. (2008). Phylogenetic analysis of epiphytic marine bacteria on Hole-Rotten diseased sporophytes of *Laminaria japonica*. *Journal of Applied Phycology*, 20(4), 403–409. <https://doi.org/10.1007/s10811-007-9274-4>
- Wang, M., Carver, J. J., Phelan, V. V., Sanchez, L. M., Garg, N., Peng, Y., Nguyen, D. D., Watrous, J., Kapon, C. A., Luzzatto-Knaan, T., Porto, C., Bouslimani, A., Melnik, A. V., Meehan, M. J., Liu, W. T., Crüsemann, M., Boudreau, P. D., Esquenazi, E., Sandoval-Calderón, M., ... Bandeira, N. (2016). Sharing and community curation of mass spectrometry data with Global Natural Products Social Molecular Networking. *Nature Biotechnology*, 34(8), 828–837. <https://doi.org/10.1038/nbt.3597>
- Wang, W., Tang, K., Wang, P., Zeng, Z., Tao Xu, W. Z., Liu, T., Wang, Y., & Wang, X. (2022). The coral pathogen *Vibrio coralliilyticus* kills non-pathogenic holobiont competitors by triggering prophage induction. *Nature Ecology & Evolution*, 6(8), 1132–1144. <https://doi.org/https://doi.org/10.1038/s41559-022-01795-y>
- Wangpraseurt, D., Weber, M., Røy, H., Polerecky, L., de Beer, D., Suharsono, & Nugues, M. M. (2012). In situ oxygen dynamics in coral-algal interactions. *PLoS ONE*, 7(2). <https://doi.org/10.1371/journal.pone.0031192>

- Ward, S. (1995). Two patterns of energy allocation for growth, reproduction and lipid storage in the scleractinian coral *Pocillopora damicornis*. *Coral Reefs*, 14(2), 87–90. <https://doi.org/10.1007/BF00303428>
- Wear, E. K., Wilbanks, E. G., Nelson, C. E., & Carlson, C. A. (2018). Primer selection impacts specific population abundances but not community dynamics in a monthly time-series 16S rRNA gene amplicon analysis of coastal marine bacterioplankton. *Environmental Microbiology*, 20(8), 2709–2726. <https://doi.org/10.1111/1462-2920.14091>
- Weber, L., Armenteros, M., Kido Soule, M., Longnecker, K., Kujawinski, E. B., & Apprill, A. (2020). Extracellular reef metabolites across the protected Jardines de la Reina, Cuba reef system. *Frontiers in Marine Science*, 7(December), 1–17. <https://doi.org/10.3389/fmars.2020.582161>
- Weber, L., Gonzalez-Díaz, P., Armenteros, M., & Apprill, A. (2019). The coral ecosystem: A unique coral reef habitat that fosters coral-microbial interactions. *Limnology and Oceanography*, 64(6), 2373–2388. <https://doi.org/10.1002/lno.11190>
- Weber, L., Soule, M. K., Longnecker, K., Becker, C. C., Huntley, N., & Kujawinski, E. B. (2022). Benthic exometabolites and their ecological significance on threatened Caribbean coral reefs. *ISME Communications*, 2(October 2021), 1–13. <https://doi.org/10.1038/s43705-022-00184-7>
- Webster, F. J., Babcock, R. C., Van Keulen, M., & Loneragan, N. R. (2015). Macroalgae inhibits larval settlement and increases recruit mortality at Ningaloo Reef, Western Australia. *PLoS ONE*, 10(4), 1–14. <https://doi.org/10.1371/journal.pone.0124162>
- Webster, N. S., Smith, L. D., Heyward, A. J., Watts, J. E. M., Webb, R. I., Blackall, L. L., & Negri, A. P. (2004). Metamorphosis of a scleractinian coral in response to microbial biofilms. *Applied and Environmental Microbiology*, 70(2), 1213–1221. <https://doi.org/10.1128/AEM.70.2.1213>
- Wegley Kelly, L., Nelson, C. E., Aluwihare, L. I., Arts, M. G. I., Dorrestein, P. C., Koester, I., Matsuda, S. B., Petras, D., Quinlan, Z. A., & Haas, A. F. (2021). Molecular commerce on coral reefs: Using metabolomics to reveal biochemical exchanges underlying holobiont biology and the ecology of coastal ecosystems. *Frontiers in Marine Science*, 8(July). <https://doi.org/10.3389/fmars.2021.630799>
- Wegley Kelly, L., Nelson, C. E., Petras, D., Koester, I., Quinlan, Z. A., Arts, M. G. I., Nothias, L., Comstock, J., White, B. M., & Hopmans, E. C. (2022). Distinguishing the molecular diversity, nutrient content, and energetic potential of exometabolomes produced by macroalgae and reef-building corals. *Proceedings of the National Academy of Sciences*, 119(5), 1–12. <https://doi.org/10.1073/pnas.2110283119/-/DCSupplemental.Published>
- Wegley Kelly, L., Williams, G. J., Barott, K. L., Carlson, C. A., Dinsdale, E. A., Edwards, R. A., Haas, A. F., Haynes, M., Lim, Y. W., McDole, T., Nelson, C. E., Sala, E., Sandin, S. A., Smith, J. E., Vermeij, M. J. A., Youle, M., & Rohwer, F. (2014). Local genomic adaptation of coral reef-associated microbiomes to gradients of natural variability and anthropogenic stressors. *Proceedings of the National Academy of Sciences of the United States of America*, 111(28), 10227–10232. <https://doi.org/10.1073/pnas.1403319111>

- Wegley, L., Yu, Y., Breitbart, M., Casas, V., Kline, D. I., & Rohwer, F. (2004). Coral-associated Archaea. *Marine Ecology Progress Series*, 273, 89–96. <https://doi.org/10.3354/meps273089>
- Wei, Y., Tong, Y., & Zhang, Y. (2022). New mechanisms for bacterial degradation of sulfoquinovose. *Bioscience Reports*, 42(10), 1–13. <https://doi.org/10.1042/BSR20220314>
- Wibowo, J. T., Ahmadi, P., Rahmawati, S. I., Bayu, A., Putra, M. Y., & Kijjoa, A. (2022). Marine-derived indole alkaloids and their biological and pharmacological activities. *Marine Drugs*, 20(1), 1–39. <https://doi.org/10.3390/md20010003>
- Wichard, T., & Beemelmanns, C. (2018). Role of chemical mediators in aquatic interactions across the Prokaryote–Eukaryote boundary. *Journal of Chemical Ecology*, 44(11), 1008–1021. <https://doi.org/10.1007/s10886-018-1004-7>
- Widner, B., Kido Soule, M. C., Ferrer-González, F. X., Moran, M. A., & Kujawinski, E. B. (2021). Quantification of amine- and alcohol-containing metabolites in saline samples using pre-extraction benzoyl chloride derivatization and Ultrahigh Performance Liquid Chromatography Tandem Mass Spectrometry (UHPLC MS/MS). *Analytical Chemistry*, 93(11), 4809–4817. <https://doi.org/10.1021/acs.analchem.0c03769>
- Wild, C., Rasheed, M., Werner, U., Franke, U., Johnstone, R., & Huettel, M. (2004). Degradation and mineralization of coral mucus in reef environments. *Marine Ecology Progress Series*, 267(February), 159–171. <https://doi.org/10.3354/meps267159>
- Williams, A., Chiles, E. N., Conetta, D., Pathmanathan, J. S., Cleves, P. A., Putnam, H. M., Su, X., & Bhattacharya, D. (2021a). Metabolomic shifts associated with heat stress in coral holobionts. *Science Advances*, 7(1), 1–10. <https://doi.org/10.1126/sciadv.abd4210>
- Williams, A. D., Brown, B. E., Putschim, L., & Sweet, M. J. (2015). Age-related shifts in bacterial diversity in a reef coral. *PLoS ONE*, 10(12), 1–16. <https://doi.org/10.1371/journal.pone.0144902>
- Williams, A., Pathmanathan, J. S., Stephens, T. G., Su, X., Chiles, E. N., Conetta, D., Putnam, H. M., & Bhattacharya, D. (2021b). Multi-omic characterization of the thermal stress phenome in the stony coral *Montipora capitata*. *PeerJ*, 9, e12335. <https://doi.org/10.7717/peerj.12335>
- Woodhead, A. J., Hicks, C. C., Norström, A. V., Williams, G. J., & Graham, N. A. J. (2019). Coral reef ecosystem services in the Anthropocene. *Functional Ecology*, 33(6), 1023–1034. <https://doi.org/10.1111/1365-2435.13331>
- Wright, R. M., Aglyamova, G. V., Meyer, E., & Matz, M. V. (2015). Gene expression associated with white syndromes in a reef building coral, *Acropora hyacinthus*. *BMC Genomics*, 16(1), 1–12. <https://doi.org/10.1186/s12864-015-1540-2>
- Wu, Y. H., Li, G. Y., Jian, S. L., Cheng, H., Huo, Y. Y., Wang, C. S., Shao, Z. Z., & Xu, X. W. (2016). *Croceicoccus pelagius* sp. nov. and *Croceicoccus mobilis* sp. nov., isolated from marine environments. *International Journal of Systematic and Evolutionary Microbiology*, 66(11), 4506–4511. <https://doi.org/10.1099/ijsem.0.001381>

- Yamase, H., Umemoto, K., Ooi, T., & Kusumi, T. (1999). Structures and absolute stereochemistry of five new secospatanes and a spatane isolated from the brown alga *Dilophus okamurai*. *Chemical Pharmaceutical Bulletin*, 6(43), 813–819. <http://www.mendeley.com/research/geology-volcanic-history-eruptive-style-yakedake-volcano-group-central-japan/>
- Yan, Y. (2016). MLmetrics: Machine Learning Evaluation Metrics. *R package version 1.1.1*.
- Yang, F., Mo, J., Wei, Z., & Long, L. (2021). Calcified macroalgae and their bacterial community in relation to larval settlement and metamorphosis of reef-building coral *Pocillopora damicornis*. *FEMS Microbiology Ecology*, 97(1), 1–11. <https://doi.org/10.1093/femsec/fiaa215>
- Yang, L., Tan, R. X., Wang, Q., Huang, W. Y., & Yin, Y. X. (2002). Antifungal cyclopeptides from *Halobacillus litoralis* YS3106 of marine origin. *Tetrahedron Letters*, 43(37), 6545–6548. [https://doi.org/10.1016/S0040-4039\(02\)01458-2](https://doi.org/10.1016/S0040-4039(02)01458-2)
- Zaneveld, J. R., Burkepile, D. E., Shantz, A. A., Pritchard, C. E., McMinds, R., Payet, J. P., Welsh, R., Correa, A. M. S., Lemoine, N. P., Rosales, S., Fuchs, C., Maynard, J. A., & Thurber, R. V. (2016). Overfishing and nutrient pollution interact with temperature to disrupt coral reefs down to microbial scales. *Nature Communications*, 7(May), 1–12. <https://doi.org/10.1038/ncomms11833>
- Zaneveld, J. R., McMinds, R., & Thurber, R. V. (2017). Stress and stability: Applying the Anna Karenina principle to animal microbiomes. *Nature Microbiology*, 2(August). <https://doi.org/10.1038/nmicrobiol.2017.121>
- Zendong, Z., Herrenknecht, C., Abadie, E., Brissard, C., Tixier, C., Mondeguer, F., Séchet, V., Amzil, Z., & Hess, P. (2014). Extended evaluation of polymeric and lipophilic sorbents for passive sampling of marine toxins. *Toxicon*, 91, 57–68. <https://doi.org/10.1016/j.toxicon.2014.03.010>
- Zhang, Y., Yang, Q., Ling, J., Long, L., Huang, H., Yin, J., Wu, M., Tang, X., Lin, X., Zhang, Y., & Dong, J. (2021). Shifting the microbiome of a coral holobiont and improving host physiology by inoculation with a potentially beneficial bacterial consortium. *BMC Microbiology*, 21(1), 1–14. <https://doi.org/10.1186/s12866-021-02167-5>
- Zheng, S., Zhang, Y., Lio, G., Lv, J., Liu, Z., Xu, X., Lingyun, L., & Xu, D. (2017). Glycerolipid profiling of yellow sarson seeds using Ultra High Performance Liquid Chromatography Coupled to Triple Time-of-Flight Mass Spectrometry. *Horticultural Plant Journal*, 3(4), 141–150. <https://doi.org/10.1016/j.hpj.2017.07.002>
- Zhou, G., Tong, H., Cai, L., & Huang, H. (2021). Transgenerational effects on the coral *Pocillopora damicornis* microbiome under ocean acidification. *Microbial Ecology*, 82(3), 572–580. <https://doi.org/10.1007/s00248-021-01690-2>
- Ziegler, M., Grupstra, C. G. B., Barreto, M. M., Eaton, M., BaOmar, J., Zubier, K., Al-Sofyani, A., Turki, A. J., Ormond, R., & Voolstra, C. R. (2019). Coral bacterial community structure responds to environmental change in a host-specific manner. *Nature Communications*, 10(1). <https://doi.org/10.1038/s41467-019-10969-5>

- Ziegler, M., Roik, A., Porter, A., Zubier, K., Mudarris, M. S., Ormond, R., & Voolstra, C. R. (2016). Coral microbial community dynamics in response to anthropogenic impacts near a major city in the central Red Sea. *Marine Pollution Bulletin*, *105*(2), 629–640. <https://doi.org/10.1016/j.marpolbul.2015.12.045>
- Ziegler, M., Seneca, F. O., Yum, L. K., Palumbi, S. R., & Voolstra, C. R. (2017). Bacterial community dynamics are linked to patterns of coral heat tolerance. *Nature Communications*, *8*, 1–8. <https://doi.org/10.1038/ncomms14213>
- Zozoya-Valdès, E., Roth-Schulze, A. J., Egan, S., & Thomas, T. (2017). Microbial community function in the bleaching disease of the marine macroalgae *Delisea pulchra*. *Environmental Microbiology*, *19*(8), 3012–3024.
- Zubia, M., Stiger-Pouvreau, V., Mattio, L., Payri, C. E., & Stewart, H. L. (2020). A comprehensive review of the brown macroalgal genus *Turbinaria* J.V. Lamouroux (Fucales, Sargassaceae). *Journal of Applied Phycology*, *32*(5), 2743–2760. <https://doi.org/10.1007/s10811-020-02188-z>
- Zuo, Z. (2019). Why algae release volatile organic compounds - The emission and roles. *Frontiers in Microbiology*, *10*(March), 1–7. <https://doi.org/10.3389/fmicb.2019.00491>

Résumé substantiel (French)

Chapitre 1 – Introduction et objectifs de thèse

Depuis ces dernières décennies, l'accumulation de perturbations d'origine anthropique a gravement altéré les communautés benthiques des récifs coralliens. Leur dégradation se manifeste par des changements de phase où les macroalgues benthiques remplacent les coraux, espèces fondatrices de cet écosystème. Les macroalgues peuvent altérer la santé de l'holobionte corallien (i.e., hôte corail et son microbiome) et le recrutement des coraux, mettant alors en péril la pérennité des récifs coralliens. Les mécanismes de compétition impliquent des processus par contact direct et par l'intermédiaire de la colonne d'eau où des médiateurs chimiques et microbiens jouent un rôle prépondérant. Si, lors de contacts directs, les molécules allopathiques et les microbes peuvent provoquer nécrose et mortalité chez les coraux, leur diffusion et impacts au-delà de l'espace physique occupé par les algues restent encore méconnus. Ma thèse a eu pour objectif de répondre à deux questions majeures : comment les macroalgues modifient les paysages chimiques et microbiens et quelles sont les conséquences de ces modifications sur la santé de l'holobionte corallien ainsi que sur le recrutement ? En alliant le métabarcoding à la métabolomique non ciblée dans une approche intégrative, mes recherches ont permis de mieux comprendre les conséquences des changements de phase sur le fonctionnement et la résilience des récifs par l'identification des microbes et métabolites impliqués dans la compétition corail-macroalgue.

Cette recherche a utilisé comme modèles d'étude les macroalgues, *Turbinaria ornata* et *Dictyota bartayresiana*, devenues invasives dans le lagon de Mo'orea en Polynésie française. Au cours de ces 4 années de thèse, j'ai entrepris un ambitieux travail de terrain d'un an et demi dont les résultats sous-tendent 3 chapitres ayant permis de : (1) caractériser la composition *in-situ* des paysages chimiques et microbiens associés aux macroalgues et d'explorer l'origine et la diffusion des composés chimiques (Chapitre 2) ; (2) étudier les effets environnementaux and parentaux induits par les algues sur le microbiome des larves coralliennes et le succès du recrutement (Chapitre 3) ; (3) déterminer l'influence relative d'interaction par contact et par l'eau avec les macroalgues (Chapitre 4) sur le métabolome et le microbiome du corail. Le microbiome a été caractérisé par séquençage du gène marqueur 16S rDNA. Les profils métabolomiques ont été obtenus par spectrométrie de masse non ciblée en tandem (LC-MS/MS) puis l'annotation des métabolites a été réalisée à partir de réseaux moléculaires et de méthodes *in-silico*.

Chapitre 2 – Les macroalgues invasives influencent la composition chimique et microbienne des eaux récifales

L'écosystème corallien est un assemblage dynamique d'organismes qui interagissent via des médiateurs chimiques et microbiens. Depuis ces dernières décennies, les perturbations anthropiques ont dramatiquement altéré la structure de ces assemblages où les macroalgues prolifèrent au détriment des coraux. Autour des organismes récifaux existent des sphères uniques de métabolites et microbes constituant des paysages complexes dont la composition commence à peine à être élucidée. Par une approche expérimentale, j'ai évalué comment la présence/absence des macroalgues sur des affleurements récifaux (i.e., bommies) influence la composition chimique et microbienne de deux couches de diffusion, la benthique et la momentum, autour de « bommies » à Mo'orea en Polynésie Française. Dans une démarche intégrative, les données ont permis de mettre en évidence une structuration spatiale à fine échelle des microbes et métabolites selon la dominance de macroalgues et les couches de diffusion. Les eaux associées aux macroalgues étaient enrichies en bactéries opportunistes et potentiellement pathogènes (e.g., Flavobacteriaceae) typiquement associées aux récifs dégradés. Afin d'explorer l'origine et la diffusion des exométabolites (i.e., présents dans l'eau), j'ai extrait les métabolites des tissus et des surfaces des algues, et comparé leurs abondances relatives avec celles des couches de diffusion. Des composés allélopathiques (i.e., terpènes) et organiques caractérisaient les eaux algales, dont certains présentaient des gradients de diffusion. Les covariations de métabolites et microbes associés aux algues ont suggéré une influence de ces métabolites sur la structure des communautés microbiennes planctoniques. Ces résultats ont alors démontré une influence spécifique des macroalgues sur les pools d'exométabolites qui eux-mêmes structurent les communautés microbiennes dans la colonne d'eau. Bien que les communautés benthiques marquent physiquement les paysages des récifs, cette étude illustre qu'elles peuvent aussi générer des paysages chimiques et microbiens complexes jouant des rôles essentiels dans la résilience des récifs coralliens.

Chapitre 3 – Les effets parentaux et environnementaux négatifs des macroalgues sur le recrutement corallien sont liés aux altérations du microbiome des larves coralliennes

La persistance des communautés coralliennes est menacée par les assemblages de macroalgues créant un important goulot démographique dans le recrutement des coraux. L'existence d'effets parentaux et environnementaux induit par la compétition coraux-algues, et leur influence potentiel sur la performance des jeunes stades de vie coralliens via des effets sur

le microbiome larvaire, représentent d'importantes lacunes dans la compréhension des mécanismes par lesquels les macroalgues peuvent entraver la récupération des coraux. En se basant sur le design expérimental du chapitre précédent, cette étude a étudié l'influence des paysages associés aux bommies où les algues étaient présentes ou éliminées sur la diversité et la composition du microbiome des larves et adultes du corail *Pocillopora acuta*, et du substrat benthique. J'ai ensuite évalué l'influence relative des effets parentaux et environnementaux sur les étapes successives du recrutement corallien en exposant réciproquement des larves de coraux issus de deux origines parentales (i.e., bommies sans algues et bommies avec algues) à des conditions environnementales avec ou sans algues. Les assemblages de macroalgues ont entraîné des altérations significatives dans la composition du microbiome des larves de coraux et du substrat benthique. Les larves produites par des parents provenant de bommies dominés par les algues ont présenté une survie significativement plus faible par rapport à celle des larves issues de bommies sans algues, quelles que soient les conditions environnementales. En revanche, les données ont révélé une interaction des effets parentaux et environnementaux réduisant la survie des recrues coralliennes. Dans l'ensemble, ces résultats ont démontré des effets parentaux et environnementaux négatifs dûs aux algues sur le recrutement des coraux, pouvant être liés à des altérations du microbiome chez les jeunes stades de vie.

Chapitre 4 - Les interactions par contact et par l'eau avec une algue allélopathique altèrent le microbiome et métabolome corallien

La prolifération des macroalgues constitue une menace majeure pour la résilience des récifs coralliens. Les macroalgues peuvent affecter les coraux, entraînant des altérations de leur microbiome et métabolome. Cependant, notre compréhension de l'échelle spatiale de ces effets et de l'influence des facteurs environnementaux est limitée. Dans ce dernier chapitre, j'ai conduit une expérience manipulative sur le terrain comparant spécifiquement les effets d'une interaction par contact vs. médiée par l'eau avec l'algue allélopathique *Dictyota bartayresiana* sur le microbiome et métabolome corallien. En plaçant les coraux en amont et en aval de l'algue et en étudiant la composition chimique et microbienne de l'eau à la surface des coraux, j'ai testé l'hypothèse selon laquelle les coraux en amont seraient plus impactés que ceux en aval. Dans une démarche intégrative, similaire à celle du Chapitre 2, ce travail a également eu pour objectif d'étudier les co-variations des microbes et métabolites coralliens afin d'améliorer notre compréhension des réponses biologiques de l'holobionte corallien lors de compétition corail-algue. Les résultats ont montré que les dégradations des tissus de type nécrose et blanchissement n'étaient causées que par un contact direct alors que les deux types ont structuré

distinctement le microbiome et le métabolome des coraux. En particulier, les interactions médiées par l'eau ont entraîné une perte de symbiotes bénéfiques (e.g., *Endozoicomonas*) et un enrichissement de familles bactériennes opportunistes (e.g., Rhodobacteraceae, Hyphomonadaceae), mais dans une moindre mesure par rapport aux interactions par contact. De plus, l'eau de mer près de la surface des coraux en contact direct était caractérisée par une augmentation de microbes opportunistes et une diminution de phototrophes indépendamment de la direction du courant. L'abondance différentielle des métabolites coralliens dans les deux types d'interactions a suggéré un ajustement du métabolisme lipidique pour répondre au coût énergétique de la compétition et à la production de métabolites de défense. Ces résultats contribuent à mettre en évidence les mécanismes chimiques et microbiens associés à la compétition corail-algue.

Chapitre 5 – Discussion générale et perspectives de recherche

Au cours de cette thèse, mes résultats ont mis en évidence l'influence des macroalgues sur la composition chimique et microbienne des eaux à l'échelle d'affleurements coralliens (Chapitre 2). Alors que le microbiome des coraux adultes peut être tolérant aux paysages induits par les macroalgues, mes recherches ont révélé l'existence d'effets parentaux et environnementaux altérant le microbiome des larves et réduisant la survie des jeunes stades de vie (Chapitre 3). Cependant, j'ai pu mettre en évidence des effets médiés par l'eau, à très courte distance des algues (i.e, 2 cm), perturbant le microbiome et métabolome corallien (Chapitre 4). Cette thèse a permis de démontrer que les macroalgues influencent significativement les environnements chimiques et microbiens des récifs coralliens. Les microbes et métabolites associés aux algues jouent un rôle déterminant dans la compétition corail-algue, que celle-ci soit par contact ou médiée par l'eau, compromettant alors la santé de l'holobionte corallien et le succès du recrutement.

Dans cette discussion, je mets en perspectives mes résultats dans le contexte hydrodynamique des récifs lagunaires et je discute de la pertinence des échelles écologiques qui sont testées dans les interactions médiées par l'eau. J'élabore alors sur les patterns microbiens et chimiques intéressants mis en évidence dans ce travail et discute des perspectives de recherche futures vers une compréhension plus mécanistique de la compétition corail-algue. Enfin, j'aborde l'avenir des récifs dominés par les macroalgues en termes de structure et de fonctionnement des récifs, ainsi que dans le contexte du changement climatique et des incitations actuelles à la restauration.

Face à la prolifération extensive des macroalgues sur les récifs coralliens, cette thèse a répondu à la nécessité pressante de mieux comprendre les mécanismes par lesquels les algues peuvent limiter la récupération des coraux. Ce travail a fourni des inventaires détaillés des microbes et des métabolites associés à la compétition corail-algue et a révélé des interactions métabolite-microbe clés. Collectivement, il marque une étape importante dans la compréhension des mécanismes par contact et par l'eau dans lesquels les microbes et métabolites associés aux algues altèrent la santé du corail et le succès de recrutement. Afin d'élucider leurs impacts spécifiques sur la biologie de l'holobionte corallien et leurs contributions au maintien des changements de phase, une étape clé serait de manipuler les microorganismes et métabolites interagissant dans des conditions contrôlées. Ces approches expérimentales bénéficieront de cadres multiomiques et quantitatifs pour décrire les réponses des symbiotes microbiens et de l'hôte corail. Des études sur le terrain dans des conditions écologiques réalistes, en tenant compte de la morphologie du récif, de l'hydrodynamique et des concentrations naturelles de micro-organismes et de métabolites, sont essentielles pour valider les mécanismes proposés. Bien que la réversion des états dominés par les macroalgues soit incertaine, des efforts locaux d'éradication des algues offrent un potentiel pour la récupération des communautés coralliennes. Les microbes et les métabolites étant des composants essentiels des écosystèmes de récifs coralliens, la compréhension de leurs distributions et de leurs fonctions est primordiale pour appréhender et favoriser la résilience de ces écosystèmes très menacés.

Substantial abstract

Chapter 1 – Introduction and thesis outline

In recent decades, the accumulation of anthropogenic disturbances has severely altered benthic communities in coral reefs. Their degradation is characterized by phase shifts where benthic macroalgae replace corals, the foundational species of this ecosystem. Macroalgae can affect the health of the coral holobiont (i.e., coral host and its microbiome) and coral recruitment, thus jeopardizing the persistence of coral reefs. Coral-macroalgae competition involve contact and water-mediated mechanisms where chemical and microbial mediators play a crucial role. While direct contact can lead to necrosis and mortality in corals due to allelopathic molecules and microbes, their diffusion and impacts beyond the physical space occupied by the algae remain poorly understood. Therefore, the aim of my thesis was to address two major questions: how do macroalgae modify chemical and microbial waterscapes, and how these modifications alter coral holobiont health and recruitment? By combining metabarcoding with untargeted metabolomics in an integrative approach, my research has provided a better understanding of the consequences of phase shifts on the functioning and resilience of reefs by identifying the microbes and metabolites involved in coral-macroalgae competition.

This research used as models two invasive macroalgae, *Turbinaria ornata* and *Dictyota bartayresiana*, in the lagoon of Mo'orea in French Polynesia. Over the course of this 4-year thesis, I undertook an ambitious year-and-a-half-long fieldwork, the results of which form the basis of three chapters that allowed me to: (1) characterize the *in-situ* composition of chemical and microbial waterscapes associated with macroalgae and explore the origin and diffusion of algal-derived metabolites (Chapter 2); (2) investigate the existence of macroalgal-induced environmental and parental effects on coral larvae microbiomes and recruitment success (Chapter 3); (3) determine the relative influence of contact vs. water-mediated interaction with an allelopathic macroalga on the coral metabolome and microbiome (Chapter 4). The microbiome was characterized by sequencing of the 16S rDNA marker gene. Metabolomic profiles were obtained by untargeted tandem mass spectrometry (LC-MS/MS), and metabolite annotations were achieved using molecular networks and *in-silico* methods (i.e., GNPS platform and SIRIUS software).

Chapter 2 – Invasive macroalgae shape chemical and microbial waterscapes on coral reefs

The coral reef ecosystem is a dynamic assemblage of organisms interacting through chemical and microbial mediators. Over the past decades, anthropogenic disturbances have

dramatically altered the structure of these assemblages, with macroalgae proliferating at the expense of corals. Unique spheres of metabolites and microbes surround reef organisms, constituting complex waterscapes whose composition is only beginning to be unraveled. Through an experimental approach, I assessed how the removal of macroalgae influenced the chemical and microbial composition of two boundary layers, the benthic and momentum, surrounding coral bommies in Mo'orea, French Polynesia. In an integrative approach, the data revealed a fine-scale spatial structuring of microbes and metabolites according to macroalgal abundance and boundary layers. Waters associated with macroalgae were enriched in opportunistic and potentially pathogenic bacteria (e.g., Flavobacteriaceae) typically associated with degraded reefs. To explore the origin and diffusion of exometabolites (i.e., present in the water), I extracted metabolites from algal tissues and surfaces and compared their relative abundance in the boundary layers. Allelopathic (e.g., terpenoids) and labile organic compounds characterized algal waters, with some exhibiting diffusion gradients. Covariations of algal-associated metabolites and microbes suggest that these algal-derived metabolites structure planktonic bacterial communities. Altogether, these results pinpoint macroalgae-specific influence on exometabolite pools, which in turn structure microbial communities in the water column. While benthic communities physically mark underwater landscapes, this study illustrated that they can also generate complex chemical and microbial waterscapes playing essential roles in the structure and resilience of coral reefs.

Chapter 3 – Negative parental and environmental effects of macroalgae on coral recruitment are linked with alterations in the coral larval microbiome

The persistence of coral communities is threatened by macroalgal assemblages, creating a significant demographic bottleneck in coral recruitment. Whether parental and environmental effects exist under coral-algal competition and whether they influence the offspring performance via effects on the larval microbiome represent major knowledge gaps in the comprehension of the mechanisms by which macroalgae may hinder coral recovery. Building upon the experimental design of the previous chapter, this study investigated the influence of waterscapes, associated with bommies where algae were either left untouched or removed, on the diversity and composition of the microbiome of larvae and adults of the coral *Pocillopora acuta*, as well as the surrounding benthic substrate. I then assessed the relative influence of parental and environmental effects on successive stages of coral recruitment by reciprocally exposing coral larvae from two parental origins (i.e., bommies without algae and bommies with algae) to algal-removed and algal-dominated environmental conditions. Dense macroalgal

assemblages led to significant alterations in the microbiome composition of coral larvae and benthic substrates. Larvae produced by parents from bommies dominated by algae exhibited significantly lower survival compared to larvae from algae-removed bommies, irrespective of environmental conditions. In contrast, the data revealed an interaction between parental and environmental effects reducing the survival of coral recruits. Overall, these results demonstrated negative parental and environmental effects of macroalgae on coral recruitment, potentially linked to alterations in the microbiome of early life stages.

Chapter 4 - Contact- and water-mediated interactions with an allelopathic macroalga affect the coral microbiome and metabolome

Macroalgal proliferation constitutes a major threat to coral reef resilience. Macroalgae can affect corals, leading to alterations in their microbiome and metabolome. However, our understanding of the spatial scale of these effects and the influence of environmental factors is limited. In this final chapter, I conducted a manipulative field experiment specifically comparing the effects of contact-mediated vs. water-mediated interactions with the allelopathic alga *Dictyota bartayresiana* on coral microbiome and metabolome. By placing corals upstream and downstream of the alga and studying the chemical and microbial compositions of near-surface coral waters, I tested the hypothesis that upstream corals would be more impacted than downstream corals. In an integrative approach, similar to Chapter 2, this work also aimed to study the co-variations of coral microbes and metabolites to enhance our understanding of the biological responses of the coral holobiont during coral-algal competition. The results showed that necrosis and bleaching damages were only evident upon direct contact, while both interaction types distinctly structured the microbiome and metabolome of corals. In particular, water-mediated interactions led to a loss of beneficial symbionts (e.g., *Endozoicomonas*) and an enrichment of opportunistic microbes (e.g., Rhodobacteraceae, Hyphomonadaceae), but to a lesser extent compared to contact-mediated interactions. Furthermore, surface seawater near corals in direct contact exhibited an increase in opportunistic microbes and a decrease in phototrophs, regardless of current direction. The differential abundance of coral metabolites in the two types of interactions suggested an adjustment of lipid metabolism to meet the energetic cost of competition and the production of defense metabolites. These results highlight the chemical and microbial mechanisms associated with coral-algal competition.

Chapter 5 - General discussion and research perspectives

This thesis has demonstrated the impact of macroalgae on the microbial and chemical composition of reef waters at the scale of coral bommies (Chapter 2). While the microbiome of adult corals may be insensitive to macroalgal-induced waterscapes, my research revealed the existence of parental and environmental effects altering coral larval microbiome and reducing the survival of early coral life stages (Chapter 3). Furthermore, I demonstrated water-mediated effects on adult corals at a very short distance (i.e., 2 cm) from the allelopathic alga *Dictyota bartayresiana* disrupting the coral microbiome and metabolome (Chapter 4). Overall this thesis underscores a strong impact of macroalgal assemblages on the chemical and microbial environments of coral reefs. Microbes and metabolites associated with algae play a crucial role in coral-algal competition, whether by contact or water mediation, compromising coral holobiont health and recruitment success.

I have discussed my results in the light of the hydrodynamic context on lagoonal reefs and the ecologically relevant scales and methods under which water-mediated interactions were tested. I, then, elaborated on interesting microbial and chemical patterns highlighted in this work and discuss future research avenues towards a more mechanistic understanding of coral-algal competition. Finally, I have explained how my results can give insights into the future of macroalgal-dominated reefs in terms of reef resilience, as well as in the context of climate change and current restoration incentives.

Facing the extensive macroalgal proliferation on coral reefs, this thesis responded to the pressing need to better understand the mechanisms by which macroalgae can effectively limit coral recovery. This work provided detailed inventories of microorganisms and metabolites associated with coral-algal competition and revealed key microbe-metabolite interactions. Collectively, it marked an important step in the understanding of the contact and water-mediated mechanisms by which macroalgal-associated microbes and metabolites alter coral health and recruitment success. To further elucidate their specific impacts on coral holobiont biology and their contributions in maintaining phase shifts, a key step would be to manipulate interacting microbes and metabolites under controlled conditions. Such experimental approaches should be coupled with multiomic and quantitative frameworks to describe microbial and host responses. Field-base studies under realistic ecological conditions, taking into account reef morphology, hydrodynamics and the natural concentrations of microbes and metabolites will be essential to validate the proposed mechanisms. Although evidence for reversing macroalgal-dominated states is limited, local eradication efforts offer potential for coral recovery. Microbes and metabolites are essential components of coral reef ecosystems and understanding their

distributions and functions will be paramount for apprehending and enhancing the resilience of these highly threatened ecosystems.

Appendices

Appendix 1: Manuscript “Congruent trophic pathways underpin global coral reef food webs”
<https://doi.org/10.1073/pnas.2100966118>

Pozas-Schacre, C., Casey, J. M., Brandl, S. J., Kulbicki, M., Harmelin-Vivien, M., Strona, G., & Parravicini, V. (2021). Congruent trophic pathways underpin global coral reef food webs. *Proceedings of the National Academy of Sciences*, 118(39), e2100966118

Congruent trophic pathways underpin global coral reef food webs

Chloé Pozas-Schacre^{a,b,1}, Jordan M. Casey^{a,b,c}, Simon J. Brandl^{a,b,c,d}, Michel Kulbicki^e, Mireille Harmelin-Vivien^f, Giovanni Strona^{g,2}, and Valeriano Parravicini^{a,b,1,2}

^aParis Sciences et Lettres Université Paris: Ecole Pratique des Hautes Etudes-Université de Perpignan Via Domitia-Centre National de la Recherche Scientifique, Unité de Service et de Recherche 3278 Centre de Recherches Insulaires et Observatoire de l'Environnement, Université de Perpignan, 66860 Perpignan, France; ^bLaboratoire d'Excellence “CORAIL,” 66860 Perpignan, France; ^cDepartment of Marine Science, Marine Science Institute, University of Texas at Austin, Port Aransas, TX 78373; ^dFondation pour la Recherche sur la Biodiversité, Centre for the Synthesis and Analysis of Biodiversity, 34000 Montpellier, France; ^eUnité Mixte de Recherche Entropie, Labex Corail, Institut de Recherche pour le Développement, Université de Perpignan, 66860 Perpignan, France; ^fInstitut Méditerranéen d'Océanologie, Unité Mixte 110 Aix-Marseille Université, Centre National de la Recherche Scientifique/Institut National des Sciences de l'Univers, Institut pour la Recherche et le Développement, 13288 Marseille, France; and ^gDepartment of Biological and Environmental Sciences, University of Helsinki, 00014 Helsinki, Finland

Edited by M. Aaron MacNeil, Dalhousie University, Halifax, Canada, and accepted by Editorial Board Member James A. Estes July 28, 2021 (received for review January 25, 2021)

Ecological interactions uphold ecosystem structure and functioning. However, as species richness increases, the number of possible interactions rises exponentially. More than 6,000 species of coral reef fishes exist across the world's tropical oceans, resulting in an almost innumerable array of possible trophic interactions. Distilling general patterns in these interactions across different bioregions stands to improve our understanding of the processes that govern coral reef functioning. Here, we show that across bioregions, tropical coral reef food webs exhibit a remarkable congruence in their trophic interactions. Specifically, by compiling and investigating the structure of six coral reef food webs across distinct bioregions, we show that when accounting for consumer size and resource availability, these food webs share more trophic interactions than expected by chance. In addition, coral reef food webs are dominated by dietary specialists, which makes trophic pathways vulnerable to biodiversity loss. Prey partitioning among these specialists is geographically consistent, and this pattern intensifies when weak interactions are disregarded. Our results suggest that energy flows through coral reef communities along broadly comparable trophic pathways. Yet, these critical pathways are maintained by species with narrow, specialized diets, which threatens the existence of coral reef functioning in the face of biodiversity loss.

food web | coral reef | interaction network

Our planet's ecosystems are underpinned by a remarkable diversity of species and their complex ecological interactions, which govern energy and nutrient fluxes across multiple trophic levels (1). As anthropogenic pressures reduce local biodiversity worldwide (2–4) either through severe decreases in abundance or complete local extinctions, the effects of these losses can propagate through ecological networks and induce unexpected ecosystem-scale changes (5–8). Understanding, predicting, and possibly averting such cascading processes requires detailed knowledge of how pairwise species interactions (e.g., predator–prey, host–parasite, and plant–animal interactions) scale up to the complex structure typical of ecological networks. Although the field of network ecology has burgeoned in the last two decades (e.g., refs. 9 and 10), the effort to identify species interactions has been unevenly distributed across ecosystems. Since the number of ecological links increases exponentially with species richness, hyperdiverse systems such as tropical rainforests or coral reefs pose particularly strong challenges to researchers seeking to quantify ecological interactions across entire ecosystems (11).

Tropical ecosystems are highly diverse, disproportionately threatened, and critically important from an ecological and societal perspective (12). Among them, coral reefs produce and recycle a remarkable amount of biomass, supporting the livelihoods

of over 500 million people worldwide (13). The invaluable productivity of reefs is mediated by a tremendous number of interactions across multiple trophic levels (14–16), and most of this complexity, especially pertaining to cryptic organisms (17), remains largely unresolved (18). In contrast, large, mobile fishes are the most intensively studied reef taxa due to their conspicuousness, functional importance, and commercial value (19). Several large datasets exist that quantify fish-centric, trophic interactions based on the visual inspection of fish gut contents (20–24). Yet large-scale evaluations of reef trophic structure is typically performed using categorical, qualitative trophic guilds as proxies (25–28), while quantitative analyses of detailed trophic networks have been restricted to modeling simplified food webs (29–31) or to analyses within a single region (32, 33). Since global analyses on reef fish communities highlight marked variation in the representation of different body size classes (28) and trophic guilds (34) across bioregions, historical and biogeographic factors may have also favored the emergence of multiple trophic organizations across global coral reefs. However, the lack of holistic, large-scale analyses of coral reef food webs based on empirical data prevents

Significance

Species loss can weaken the trophic interactions that underpin ecosystem functioning. Coral reefs are the world's most diverse marine ecosystem, harboring interaction networks of extraordinary complexity. We show that, despite this complexity, global coral reef food webs are governed by a suite of highly consistent energetic pathways, regardless of regional differences in biodiversity. All networks are characterized by species with narrow dietary preferences, arranged into distinct groups of predator–prey interactions. These characteristics suggest that coral reef food webs are robust to the loss of prey resources but vulnerable to local extinctions of consumer species.

Author contributions: C.P.-S., J.M.C., G.S., and V.P. designed research; C.P.-S., J.M.C., S.J.B., G.S., and V.P. performed research; M.K. and M.H.-V. contributed new reagents/analytic tools; C.P.-S., G.S., and V.P. analyzed data; and C.P.-S., J.M.C., S.J.B., M.K., M.H.-V., G.S., and V.P. wrote the paper.

The authors declare no competing interest.

This article is a PNAS Direct Submission. M.A.M. is a guest editor invited by the Editorial Board.

Published under the PNAS license.

¹To whom correspondence may be addressed. Email: valeriano.parravicini@ephe.psl.eu or pozaschloe@gmail.com.

²G.S. and V.P. contributed equally to this work.

This article contains supporting information online at <https://www.pnas.org/lookup/suppl/doi:10.1073/pnas.2100966118/-DCSupplemental>.

Published September 20, 2021.

Appendix 2: Manuscript « Delineating reef fish trophic guilds with global gut content data synthesis and phylogeny »
<https://doi.org/10.1371/journal.pbio.3000702>

Parravicini, V., Casey, J. M., Schittekatte, N. M., Brandl, S. J., **Pozas-Schacre, C.**, Carlot, J., Edgar, G.J., Graham, N.A., Harmelin-Vivien, M., Kulbicki, M. and Strona, G & Stuart-Smith, R. D. (2020). Delineating reef fish trophic guilds with global gut content data synthesis and phylogeny. *PLoS Biology*, 18(12), e3000702.

PLOS BIOLOGY

METHODS AND RESOURCES

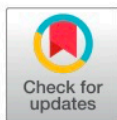
Delineating reef fish trophic guilds with global gut content data synthesis and phylogeny

Valeriano Parravicini^{1,2*}, Jordan M. Casey^{1,2,3}, Nina M. D. Schittekatte^{1,2}, Simon J. Brandl^{1,2,3,4}, Chloé Pozas-Schacre^{1,2}, Jérémy Carlot^{1,2}, Graham J. Edgar⁵, Nicholas A. J. Graham⁶, Mireille Harmelin-Vivien⁷, Michel Kulbicki⁸, Giovanni Strona⁹, Rick D. Stuart-Smith⁴

1 PSL Université Paris: EPHE-UPVD-CNRS, USR 3278 CRIOBE, Université de Perpignan, Perpignan, France, **2** Laboratoire d'Excellence "CORAIL," Perpignan, France, **3** Department of Marine Science, University of Texas at Austin, Marine Science Institute, Port Aransas, Texas, United States of America, **4** Centre for the Synthesis and Analysis of Biodiversity (CESAB), Institut Bouisson Bertrand, Montpellier, France, **5** Institute for Marine and Antarctic Studies, University of Tasmania, Hobart, Tasmania, Australia, **6** Lancaster Environment Centre, Lancaster University, Lancaster, United Kingdom, **7** Aix-Marseille Université, Institut Méditerranéen d'Océanologie, CNRS/INSU, Marseille, France, **8** UMR Entropie, LabEx Corail, IRD, Université de Perpignan, Perpignan, France, **9** University of Helsinki, Department of Bioscience, Helsinki, Finland

✉ These authors contributed equally to this work.

* valeriano.parravicini@ephe.psl.eu



OPEN ACCESS

Citation: Parravicini V, Casey JM, Schittekatte NMD, Brandl SJ, Pozas-Schacre C, Carlot J, et al. (2020) Delineating reef fish trophic guilds with global gut content data synthesis and phylogeny. *PLoS Biol* 18(12): e3000702. <https://doi.org/10.1371/journal.pbio.3000702>

Academic Editor: Pedro Jordano, Estacion Biologica de Doñana CSIC, SPAIN

Received: February 13, 2020

Accepted: December 3, 2020

Published: December 28, 2020

Copyright: © 2020 Parravicini et al. This is an open access article distributed under the terms of the [Creative Commons Attribution License](https://creativecommons.org/licenses/by/4.0/), which permits unrestricted use, distribution, and reproduction in any medium, provided the original author and source are credited.

Data Availability Statement: All methods are described within the paper and its [Supporting Information](#) files. The data and the R code are available at the GitHub repository https://github.com/valerianoparravicini/Trophic_Fish_2020.

Funding: This research was funded by the BNP Paribas Foundation (Reef Services Project) and the French National Agency for Scientific Research (ANR; REEF LUX Project; ANR-17-CE32-0006). This research is product of the SCORE-REEF group funded by the Centre de Synthèse et d'Analyse sur

Abstract

Understanding species' roles in food webs requires an accurate assessment of their trophic niche. However, it is challenging to delineate potential trophic interactions across an ecosystem, and a paucity of empirical information often leads to inconsistent definitions of trophic guilds based on expert opinion, especially when applied to hyperdiverse ecosystems. Using coral reef fishes as a model group, we show that experts disagree on the assignment of broad trophic guilds for more than 20% of species, which hampers comparability across studies. Here, we propose a quantitative, unbiased, and reproducible approach to define trophic guilds and apply recent advances in machine learning to predict probabilities of pairwise trophic interactions with high accuracy. We synthesize data from community-wide gut content analyses of tropical coral reef fishes worldwide, resulting in diet information from 13,961 individuals belonging to 615 reef fish. We then use network analysis to identify 8 trophic guilds and Bayesian phylogenetic modeling to show that trophic guilds can be predicted based on phylogeny and maximum body size. Finally, we use machine learning to test whether pairwise trophic interactions can be predicted with accuracy. Our models achieved a misclassification error of less than 5%, indicating that our approach results in a quantitative and reproducible trophic categorization scheme, as well as high-resolution probabilities of trophic interactions. By applying our framework to the most diverse vertebrate consumer group, we show that it can be applied to other organismal groups to advance reproducibility in trait-based ecology. Our work thus provides a viable approach to account for the complexity of predator–prey interactions in highly diverse ecosystems.

Bulleri, F., Pozas-Schacre, C., Bischoff, H., Bramanti, L., Gasc, J., & Nugues, M. M. (2022). Compounded effects of sea urchin grazing and physical disturbance on macroalgal canopies in the lagoon of Moorea, French Polynesia. *Marine Ecology Progress Series*, 697, 45-56.

Vol. 697: 45–56, 2022 http://dx.doi.org/10.3354/meps14137	MARINE ECOLOGY PROGRESS SERIES Mar Ecol Prog Ser	Published September 22
--	---	------------------------

Compounded effects of sea urchin grazing and physical disturbance on macroalgal canopies in the lagoon of Moorea, French Polynesia

Fabio Bulleri^{1,*}, Chloé Pozas-Schacre^{2,3}, Hugo Bischoff^{3,4}, Lorenzo Bramanti⁵,
Stephanie D'agata⁶, Julien Gasc^{2,3}, Maggy M. Nugues^{2,3}

¹Dipartimento di Biologia, Università di Pisa, CoNISMa, Via Derna 1, 56126 Pisa, Italy

²PSL Université Paris: EPHE-UPVD-CNRS, USR 3278 CRIOBE, Université de Perpignan, 66860 Perpignan, France

³Laboratoire d'Excellence Corail, 66860 Perpignan, France

⁴PSL Université Paris: EPHE-UPVD-CNRS, USR 3278 CRIOBE BP 1013, 98729 Papetoai, Moorea, French Polynesia

⁵Sorbonne Université, CNRS, Laboratoire d'Ecogéochimie des Environnements Benthiques, LECOB,
66650 Banyuls-sur-Mer, France

⁶ENTROPIE (IRD, University of La Reunion, CNRS, University of New Caledonia, Ifremer), 97400 Saint-Denis,
La Reunion c/o IUEM, 29280 Plouzané, France

ABSTRACT: Release from herbivory is a factor underpinning coral replacement by macroalgae. Once macroalgae have achieved dominance, shifts back to the coral-dominated state can be hindered by stabilizing feedbacks. Thus, restoring herbivore assemblages alone can be insufficient to trigger coral recovery. However, herbivores could control macroalgal recovery in the aftermath of physical disturbances removing macroalgae. Diadematid urchins at Moorea (French Polynesia) have collapsed in the last decade. By means of a manipulative field experiment, we tested the interactive effects of physical disturbance and increased diadematid densities on macroalgae inside the lagoon. Massive *Porites* colonies, referred to as 'bommies', were assigned to 3 different macroalgal removal treatments (removal of stipes and fronds of the canopy-forming macroalgae *Turbinaria ornata* and *Sargassum pacificum*, total removal of erect macroalgae or untouched) and exposed to 3 different urchin densities (absent, low [~ 0.5 ind. m^{-2}], and intermediate [~ 1 ind. m^{-2}]). After 1 yr, sea urchins had no effect on the covers of *S. pacificum* and *T. ornata* when macroalgal canopies were left untouched. Urchins could control the recovery of *S. pacificum* on total macroalgal removal bommies, but not that of *T. ornata*. However, urchins, even when at intermediate densities, did not generate major changes in the structure of benthic assemblages on experimental bommies. Our study indicates that a moderate increase in diadematid densities is unlikely to reduce the extent of macroalgal stands in Moorea back reefs unless associated with the recovery of other herbivore guilds able to remove adult macroalgae (i.e. browsers).

KEY WORDS: Coral reefs · Macroalgae · *Turbinaria ornata* · *Sargassum pacificum* · Sea urchins · Disturbance · French Polynesia

Resale or republication not permitted without written consent of the publisher

1. INTRODUCTION

Coral reefs worldwide are threatened by multiple anthropogenic stressors, often resulting in a shift in dominance from corals to macroalgae (Done 1992, McManus & Polsenberg 2004, Hughes et al. 2007,

Norstrom et al. 2009). Coral's ability to recover following mass mortalities due to extreme events, such as heatwaves, cyclones or predator outbreaks, appears to be reduced under weak grazing intensity and enhanced nutrient loading (Mumby & Steneck 2008, Graham et al. 2015; but see Szmant 2002). When con-

*Corresponding author: fabio.bulleri@unipi.it

© Inter-Research 2022 · www.int-res.com

Appendix 4: Scientific vulgarization on the chemical and microbial effects of macroalgae on coral recruitment (text in French).

<https://www.cnrseditions.fr/catalogue/ecologie-environnement-sciences-de-la-terre/etonnants-recifs/>

Pozas-Schacre C, Nugues M.M. 2021. Quand les larves de coraux ont du flair. Dans Hédouin, L. (Dir.), *Etonnants récifs* (p. 213-217). CNRS Editions Paris. ISBN: 978-2-271-13910-8

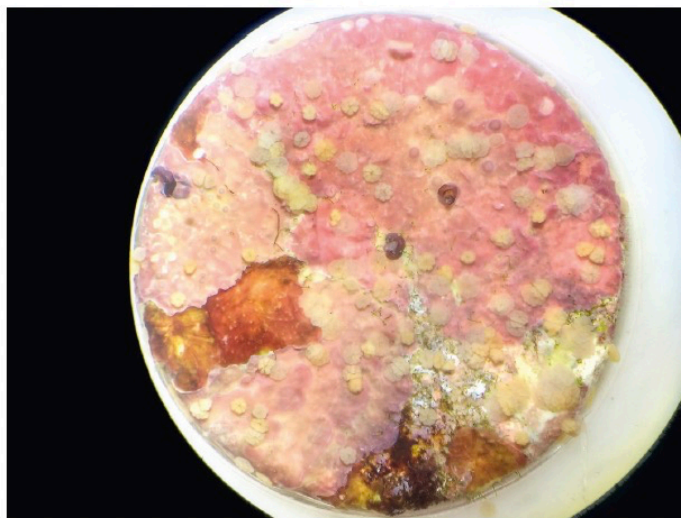
The title can be translated as “When coral larvae follow their nose”. This text was written for the 50-year anniversary book of the CRIOBE. Here, I introduced coral reproduction modes and presented the chemical and microbial effects macroalgae can have on coral recruitment

Quand les larves de coraux ont du flair

Chloé Pozas-Schacre & Maggy Nugues

Pour déjouer tous les pièges que leur réservent les macro-algues, les jeunes larves en quête d'un nouveau récif sont dotées de capacités étonnantes de détection. Commence alors une aventure semée d'embûches dont elles ne sortent pas toujours vainqueurs.

Vous connaissez l'histoire, les enfants quittent (enfin...) leurs parents pour explorer le monde et trouver éventuellement un endroit qui leur plaît pour y vivre leur nouvelle vie. Les larves de coraux, dites « planula », doivent également s'émanciper et ce rapidement après leur naissance. Les jeunes



Observation de la métamorphose des larves coralliennes sur de petits plots préconditionnés dans le milieu naturel pendant 6 mois. Photo Camille Vizon.

RÉSUMÉ

L'accumulation des perturbations environnementales a profondément altéré les communautés benthiques des récifs coralliens, où les macroalgues remplacent souvent les coraux. Ces changements de phase sont favorisés par une compétition intense des algues, limitant la récupération des communautés coralliennes. Si, lors de contacts directs, les molécules allopathiques et les microbes des algues peuvent provoquer la mortalité des coraux, leurs diffusions et leurs impacts au-delà de l'espace physique occupé par les algues demeurent encore largement méconnus. Cette thèse a eu pour objectif de répondre à deux questions majeures : comment les macroalgues modifient les paysages chimiques et microbiens et en quoi ces modifications altèrent la santé de l'holobionte corallien et son recrutement? En manipulant la présence/absence de macroalgues, cette thèse a permis de mettre en évidence une structuration spatiale à fine échelle des microbes et métabolites selon l'abondance de macroalgues et les couches de diffusion (i.e., couches benthique et momentum). Les eaux autour des algues étaient enrichies en bactéries opportunistes, potentiellement pathogènes, et molécules toxiques (i.e., diterpènes). Ces recherches ont ensuite montré que l'exposition aux macroalgues pouvait altérer le microbiome des larves coralliennes (*Pocillopora acuta*) et impacter négativement la survie des larves et recrues, au travers d'effets parentaux et environnementaux. L'influence relative des effets par contact vs. médiés par l'eau (i.e., 2 cm) sur l'holobionte corallien a été testée en utilisant l'algue allélopathique *Dictyota bartayresiana*. Chaque type d'interaction a perturbé distinctement le microbiome et métabolome corallien suggérant un ajustement du métabolisme lipidique pour répondre au coût énergétique de la compétition et à la production de métabolites de défense. En combinant métabarcoding et métabolomique non ciblée, ce travail de thèse a permis de décrire l'identité et la distribution des microbes et métabolites associés à la compétition corail-algues afin de mieux comprendre la conséquence des changements de phase sur la résilience des récifs coralliens.

MOTS-CLÉS

Récifs coralliens, compétition corail-algue, microbiome, métabolome, recrutement corallien, multiomique, holobionte

ABSTRACT

On coral reefs, the cumulative impact of human-driven stressors has resulted in a replacement of the dominant benthic members where phase-shifts from coral to macroalgal dominance prevail. The persistence of macroalgae is favored by an intense competition against corals, limiting the recovery of coral communities. Upon contact, macroalgae can vector allelochemicals and microbes causing necrosis and coral mortality, yet their diffusion and impacts beyond the space that algae physically occupy remain unclear. This thesis aimed to address two major questions: how macroalgae modify chemical and microbial waterscapes, and how they impact coral holobiont health and recruitment. By manipulating the presence/absence of macroalgae, this thesis revealed a fine-scale spatial structuring of microbes and metabolites according to macroalgal abundance and boundary layers (i.e., benthic and momentum). Algal-associated waters were enriched with opportunistic bacteria, potentially pathogenic, and toxic molecules (i.e., diterpenes). This research demonstrated that exposure to macroalgae alter the microbiome of coral larvae (*Pocillopora acuta*) and negatively impact larval and recruit survival through interacting parental and environmental effects. The relative influence of contact vs. water-mediated (i.e., 2 cm) effects on coral microbiome and metabolome was specifically tested using the allelopathic alga *Dictyota bartayresiana*. Each type of interaction distinctly disturbed the coral microbiome and metabolome, suggesting an adjustment in lipid metabolism to meet the energetic cost of competition and the production of defense metabolites. By combining metabarcoding and non-targeted metabolomics, this thesis has described the identity and distribution of microbes and metabolites associated with coral-algae competition, providing a better understanding of the consequences of phase shifts on the resilience of coral reefs.

KEYWORDS

Coral reefs, coral-algal competition, microbiome, metabolome, coral recruitment, multiomic, holobiont